



Universiteit
Leiden
The Netherlands

Targeting for success: mechanistic insights into microRNA-based gene therapy for Huntington disease

Sogorb Gonzalez, M.

Citation

Sogorb Gonzalez, M. (2023, February 9). *Targeting for success: mechanistic insights into microRNA-based gene therapy for Huntington disease*.

Retrieved from <https://hdl.handle.net/1887/3515739>

Version: Publisher's Version

License: [Licence agreement concerning inclusion of doctoral thesis in the Institutional Repository of the University of Leiden](#)

Downloaded from: <https://hdl.handle.net/1887/3515739>

Note: To cite this publication please use the final published version (if applicable).

Targeting for success:
Mechanistic insights into microRNA-based gene
therapy for Huntington disease

Marina Sogorb González

PhD Thesis, Leiden University, February 2023

Targeting for success: Mechanistic insights into microRNA-based gene therapy for Huntington disease

ISBN: 978-94-6469-209-9

Cover design: Stefanie van den Herik

Layout: Marina Sogorb González.

Printing: ProefschriftMaken

Copyright © 2023, Marina Sogorb González. All rights reserved. No part of this thesis may be reproduced in any form or by any means without written permission of the author.

The research described in this thesis was performed and funded by UniQure B.V. The printing of this thesis was financially supported by VectorY B.V.

Targeting for success:
Mechanistic insights into microRNA-based
gene therapy for Huntington disease

Proefschrift

ter verkrijging van
de graad van doctor aan de Universiteit Leiden,
op gezag van rector magnificus prof.dr.ir. H. Bijl,
volgens besluit van het college voor promoties
te verdedigen op donderdag 9 februari 2023
klokke 13:45 uur

door

Marina Sogorb González

geboren te Burgos, Spanje
in 1992

Promotor: Prof. Dr. S.J. van Deventer
Co-promotor: Dr. P. Konstantinova VectorY B.V
Dr. M. Evers uniQure B.V

Leden promotiecommissie:

Prof. Dr. A.J. Rabelink
Dr. J. Wijnholds
Prof. Dr. E. A. J. Reits Amsterdam UMC
Prof. Dr. H. H. Kampinga Groningen UMC
Dr. Y. Shakalisava Universiteit Leiden

Table of contents

Chapter 1	General Introduction – Targeting for success: Mechanistic insights into HTT-lowering therapies for Huntington disease	7
Chapter 2	Exon 1-targeting miRNA reduces the pathogenic exon 1 HTT protein generated by aberrant splicing in Huntington disease mice	29
Chapter 3	Widespread and sustained target engagement in Huntington disease minipigs upon intrastriatal microRNA-based gene therapy	55
Chapter 4	Secreted therapeutics: Monitoring durability of microRNA-based gene therapies in the central nervous system	87
Chapter 5	Beyond transduction: Cross-corrective silencing of AAV-based gene therapy through functional transfer of engineered microRNAs	121
Chapter 6	General discussion and future perspectives	145
Appendix	English Summary Nederlandse Samenvatting Resumen en Español List of abbreviations Curriculum vitae List of publications Acknowledgements	159

Chapter

1

Targeting for success: Mechanistic insights into HTT- lowering therapies for Huntington disease

**Marina Sogorb-Gonzalez^{1,2}, Pavlina Konstantinova²,
Sander van Deventer^{1,2}**

¹ Department of Gastroenterology and Hepatology, Leiden
University Medical Center, The Netherlands

² Department of Research, VectorY B.V, Amsterdam, The
Netherlands

Abstract

Gene therapy is emerging as a potential treatment for untreatable neurodegenerative diseases. Huntington Disease (HD) is the most common inherited neurodegenerative disease caused by a trinucleotide repeat expansion in the huntingtin (HTT) gene, giving rise to a toxic mutant HTT (mHTT) protein. The well-defined monogenic cause makes HD a good target for gene therapy approaches and several novel therapeutics are being developed with the aim of reducing the production of the mHTT. In view of recent failures of some therapeutics to translate into patient benefit, it is essential to precisely understand the pathogenic mechanisms that are currently targeted as well as the mechanism of action of the HTT-lowering therapies in development. We here review our current understanding of the molecular pathology of HD, how to specifically target the critical pathogenic mechanisms and how to determine therapeutic efficacy. Finally, we discuss the current challenges for HTT-lowering therapies and the ongoing advances of gene therapy treatments to overcome these therapeutic limitations.

Introduction

Huntington Disease (HD) is an ultimately lethal, genetic neurodegenerative disease that typically manifests in adulthood with motor, cognitive and psychological symptoms. Symptomatic onset is characterized by the appearance of chorea and muscle rigidity, often preceded or accompanied by neuropsychiatric symptoms like depressed mood, mania, irritability and psychosis (Ross *et al.*, 2014). HD is dominantly inherited and is the most common genetic disease affecting the central nervous system (CNS) with a prevalence of 1 to 9 in 100.000 people, depending on the ethnicity and population (Rawlins *et al.*, 2016). Symptomatic therapies are used to treat motor and psychological symptoms and may have a temporary beneficial effect on motor function and quality of life (Bachoud-Lévi *et al.*, 2019). Unfortunately, despite decades of research and ongoing clinical trials, there is still no established treatment to attenuate the natural course of this devastating disease.

HD is caused by a trinucleotide CAG repeat expansion in exon 1 of the huntingtin (*HTT*) gene (MacDonald *et al.*, 1993). Individuals who inherit ≥ 40 CAG repeats will develop HD given a normal lifespan, with longer repeats resulting in earlier age of onset. Expansions with 36-39 CAG repeats are considered alleles with reduced penetrance. The expanded CAG repeat sequence results in the transcription of a mutant form of huntingtin protein (mHTT) containing an expanded polyglutamine (polyQ) tract in the N-terminal domain. This long polyglutamine tract confers a toxic gain-of-function to the mHTT protein which has been associated with neuronal dysfunction mechanisms including transcriptional dysregulation, proteasome overload, excitotoxicity, mitochondria and synaptic dysfunction, and eventually, cell death (Jimenez-Sanchez *et al.*, 2017; Tabrizi *et al.*, 2020).

The fact that mHTT is expressed since birth and in all tissues, but only becomes pathological in adulthood and initially in striatal neurons, raises the question whether mHTT, or other potentially related mechanisms, are the main driver of HD pathology (Jimenez-Sanchez *et al.*, 2017). Moreover, the CAG length-dependent age of onset also suggests that the relationship between mHTT protein and HD pathogenesis might be more complex. These considerations have become relevant in view of the recent finding that therapies exclusively reducing the mHTT protein have not achieved the expected therapeutic benefits (Kingwell, 2021).

Hence, understanding the different mechanistic aspects of HD pathology and disease-modifying approaches will forward the development of successful therapies. In this chapter, we introduce the current knowledge in the field, as well as therapeutic limitations related to HD pathology, drug modalities and measurements of efficacy, with special focus on HTT-lowering therapies. For this, the field has been categorized into the following questions (**Figure 1**):

- **WHAT?**: Which pathological mechanisms contribute to HD and what is the most promising target to stop neurodegeneration and HD progression?
- **HOW?**: Which currently available technologies are the most suitable to target these mechanisms?
- **WHERE?**: Which brain regions do we need to target to achieve significant therapeutic effect and which technologies can accomplish this?
- **HOW GOOD?**: Which models and outcomes are used to measure efficacy for successful translation to patients? Which new markers should be developed for gene therapy studies?
- **HOW BAD?**: What are the toxicities and immunogenic responses associated with the treatment?

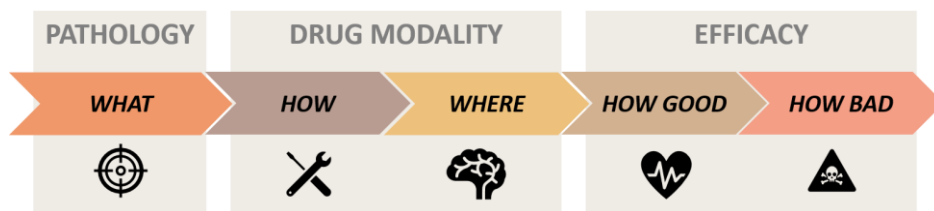


Figure 1: Important questions to investigate the disease pathology and potential targets, properties of current drug modalities, and outcomes of efficacy and safety with the goal to develop successful therapies for HD and other neurodegenerative diseases.

WHAT? – Pathological molecular mechanisms in HD

Despite its monogenic cause, HD pathology is not fully understood and curative therapies are not yet available. A better understanding of the pathological mechanisms leading to the gradual loss of striatal neurons and the midlife onset of symptoms will enable the development of novel therapeutic approaches.

Initially, it was generally accepted that the expression and aggregation of mHTT was the direct toxic molecular driver of HD pathogenesis and early studies in post-mortem patients identified mHTT inclusions in the striatum and cortex as the pathological hallmark of HD (DiFiglia, 1997). At the same time, the first genetic mouse models demonstrated that the incorporation of a long CAG expansion in *HTT* homologous mouse gene or the expression of mHTT cDNA sequences also led to mHTT inclusions, neuronal death and HD-like phenotype in mice (Mangiarini *et al.*, 1996; Menalled *et al.*, 2002). These studies supported the toxic gain-of function of mHTT and the hypothesis that the prevention of mHTT aggregate formation should be a promising therapeutic strategy for treatment of HD. During the last therapies (Wild and Tabrizi, 2017, Tabrizi *et al.*, 2019a; Marxreiter *et al.*,

2020). However, the lack of efficacy of some of such approaches raised concerns about the notion that mHTT constitutes a valid therapeutic target (Kingwell, 2021).

The CAG repeat expansion does have consequences for neuronal biology that extend beyond the production of mHTT aggregates (Tabrizi *et al.*, 2020; Heinz *et al.*, 2021). These include somatic DNA repeat instability, formation of aberrant spliced toxic transcripts and nuclear RNA foci, sequestration of proteins involved in transcriptional regulation and impairment of proteasome function, among others. Recent research has investigated the contribution of these processes as potential drivers of the striatum-selective and age-dependent pathogenesis.

The expanded CAG repeat is unstable and undergoes a progressive increase in length throughout patient's life, process known as somatic instability (Swami *et al.*, 2009). Somatic instability occurs in a tissue-specific manner in HD patients, with striatal neurons undergoing a dramatic mutation length increase up to >1000 CAG repeats (Kennedy *et al.*, 2003). A novel mouse model of somatic instability with uninterrupted CAG repeats (BAC-CAG model) showed significant correlations between somatic instability in the striatum and nuclear mHTT aggregation with the onset of behavioral impairments and other molecular phenotypes (transcriptomic dysregulation and reactive gliosis) which closely resemble HD clinical pathology (Gu *et al.*, 2022). In addition, GWAS studies identified genes involved in DNA mismatch repair (MMR) as contributors of somatic instability disease and worse HD outcomes in HD patients (Lee *et al.*, 2015; Ciosi *et al.*, 2019; Roy *et al.*, 2021). Altogether, these studies support the hypothesis that somatic instability, leading to CAG repeat expansions greatly exceeding the germ-line number, contributes to the onset and progression of striatum-selective pathology in HD.

Not all mHTT protein species are equally pathogenic, and increased somatic CAG expansion in striatal neurons is considered to contribute to the production of the highly toxic exon 1 HTT (HTTex1) fragment through aberrant splicing. Mutant *HTT* pre-mRNA undergoes incomplete splicing of exon1 to exon 2 resulting in the production of a short HTTex1 protein (Sathasivam *et al.*, 2013). Furthermore, in an HD patient's tissue, this mis-spliced HTT transcript can be detected (Neueder *et al.*, 2017). The severe toxicity induced by HTTex1 has been demonstrated in different HD animal models and indeed the fastest progressing HD mouse model is based on the overexpression of HTTex1 fragment (Mangiarini *et al.*, 1996; Barbaro *et al.*, 2015). Phenotype onset correlates with levels of HTTex1 splicing in mouse models with similar CAG repeats (Franich *et al.*, 2019). Importantly, the suppression of HTTex1 expression in a conditional model was able to reverse aggregate formation and motor decline (Yamamoto *et al.*, 2000), suggesting that HTTex1 reduction is beneficial for therapeutic efficacy in HD. Longer CAG repeats correlate with increased aberrant splicing and HTTex1 levels (Neueder *et al.*, 2018) and therefore

1
toxic HTTex1 formation is expected to occur first in neurons that display somatic expansions, such as striatal neurons (Kennedy *et al.*, 2003). For these reasons, it is currently thought that lowering levels of HTTex1 protein will have a greater therapeutic benefit than exclusively targeting the full-length mHTT. Unfortunately, most of the current therapies in preclinical and clinical studies are based on genetic approaches that target sequences downstream exon 1 and therefore are not expected to reduce the translation of the HTTex1 protein.

In conclusion, novel molecular findings, such as somatic instability, CAG repeat expansions and increased generation of toxic HTTex1 fragments, open the door to new therapeutic approaches in HD. In particular, HD pathogenesis is now thought to be a two-step event (presumably including CAG length expansions and HTTex1 production) rather than a result of direct full-length mHTT-induced toxicity (Neueder *et al.*, 2017). According to this model, somatic CAG repeat instability that first accumulates in striatal neurons during the patient's pre-symptomatic years, and not the congenital number of CAG repeats, would trigger the formation of toxic drivers, such as HTTex1, up to a cell type-specific lethal threshold that results in the neurodegeneration of vulnerable cells and disease manifestation (Neueder *et al.*, 2017; Pinto *et al.*, 2020) (**Figure 2**). Consequently, therapies that stop somatic instability or reduce the levels of toxic HTTex1 fragments, ideally in striatal neurons in early disease state, may be potential treatments for HD patients.

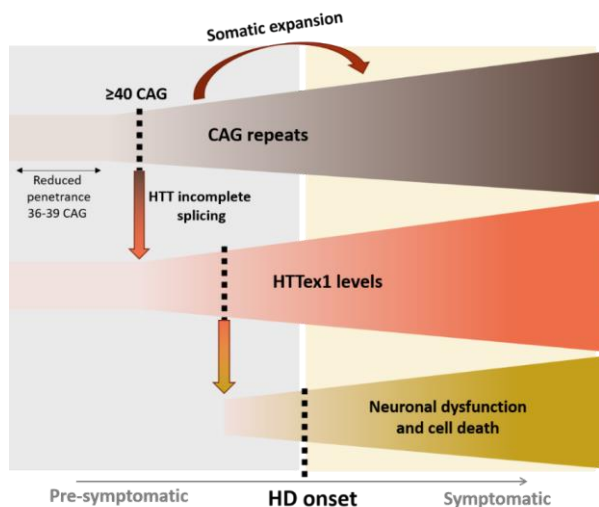


Figure 2: Two-step model of HD pathogenesis. Based on this model CAG expansions, which increase via somatic instability (step 1), induce and accelerate the formation of the pathogenic HTTex1 fragment by aberrant splicing (step 2) up to a threshold level in which induces neuronal dysfunction and cell death during pre-symptomatic phase. Dotted lines represent the “threshold level” that induces the next process.

HOW? - HTT-targeting therapeutic modalities

As a consequence of a better understanding of HD pathology, current therapeutic approaches have shifted from symptomatic to molecular disease-modifying treatments. With the aim to reduce mHTT-induced toxicity, molecular treatments have been used to edit, silence or reduce mHTT expression and protein translation (Tabrizi *et al.*, 2019a; Leavitt *et al.*, 2020; Marxreiter *et al.*, 2020). The efficacy of each of these HTT-lowering approaches would mainly depend on where the intervention targets the HTT pathway: DNA, RNA or protein (Wild and Tabrizi, 2017). The most advanced HTT-targeting therapies are illustrated in **Table 1**.

- **DNA-targeting treatments:** DNA-targeting therapeutics would be ideal to address all aspects of CAG-induced toxicities. Although challenging, these technologies aim at either removing the mutated gene or inhibiting the transcription. The two technologies in development include zinc finger protein (ZFP) and the novel CRISPR-Cas9 (Yang *et al.*, 2017; Zeitler *et al.*, 2019). Both approaches are gene therapy products mediated by the expression of therapeutic proteins delivered by viral vectors.

- **RNA-targeting treatments:** RNA-targeting approaches are the only genetic therapies that have been tested in clinical trials to date. These treatments aim at inducing *mHTT* mRNA degradation, consequently resulting in reduction of mHTT protein and aggregates. Three molecular therapeutics have been used: antisense oligonucleotides (ASO) (Carroll *et al.*, 2011; Kordasiewicz *et al.*, 2012, Tabrizi *et al.*, 2019a), RNAi interference molecules (microRNA (miRNA), small interfering RNA (siRNA) and short hairpin RNA (shRNA)) (Rodriguez-Lebron *et al.*, 2005; McBride *et al.*, 2011; Miniarikova *et al.*, 2016; Alterman *et al.*, 2019), and small molecules (Bhattacharyya *et al.*, 2021). The various approaches importantly differ in their therapeutic efficacy, CNS target area coverage and durability. Importantly, and often overlooked, is the fact that the mRNA target sequence critically determines the lowering of aberrantly-spliced mHTT transcripts, such as HTTex1 (Sathasivam *et al.*, 2013). Therapies targeting sequences downstream of exon 1 will generally not affect the production of HTTex1, despite lowering the full-length mHTT protein.

- **Protein-targeting modalities:** These include the direct targeting of mHTT with intracellular antibodies (Southwell *et al.*, 2009), the modulation of degradation pathways such as autophagy and proteasome (Soares *et al.*, 2019), and the inhibition of proteolytic cleavage to reduce toxic N-terminal fragments (except for HTTex1 fragment) (Wellington *et al.*, 2000).

Table 1: Most advanced HTT-targeting therapies for HD.

Sponsor	Drug name	Clinical status	WHAT? (Target)	HOW?	WHERE? (injection route)	Reference
ASO & siRNA						
Ionis/Roche	Tominersen /RO7234292	Phase 1b/2 Phase 3 – <i>Suspended – lack of efficacy</i>	RNA (Target: <i>HTT</i> exon 36)	ASO	Intrathecal	(Kordasiewicz et al., 2012, Tabrizi et al., 2019) NCT03761849
Wave Life Sciences	WVE-120101	Phase 1b/2a- <i>Suspended – lack of efficacy</i>	RNA (Target: mHTT SNP)	ASO	Intrathecal	NCT04617847 NCT04617860
	WVE-003	Phase 1b-2a- recruiting	RNA (Target: mHTT SNP)	ASO	Intrathecal	NCT05032196
Alnylam	ALN-HTT	Preclinical	RNA (Target: <i>HTT</i> exon 1)	siRNA (cholesterol- conjugated)	Intracerebroventricular	(DiFiglia et al., 2007)
Atalanta		Preclinical	RNA (Target: 3' UTR)	siRNA (divalent- siRNA)	Intrastriatal	(Alterman et al., 2019)
Biomarin/Vico		Preclinical	RNA (Target: CAG repeat)	ASO		(Datson et al., 2017)
Nanjing University, China		Preclinical	RNA (Target: <i>HTT</i> exon 1)	Exosome- mediated siRNA	Intravenous	(Wu et al., 2018)

Continuation Table 1

Sponsor	Drug name	Clinical status	WHAT? (Target)	HOW?	WHERE? (injection route)	Reference
Gene therapy approaches (ZFP, CRISPR and miRNA)						
Takeda/Sangamo	TAK-686	Preclinical	DNA – CAG repeat	AAV-ZFP	Intraparenchymal	(Zeitler <i>et al.</i> , 2019)
Imperial college London		Preclinical	DNA – CAG repeat	AAV-ZFP	Intraparenchymal (striatum)	(Garriga-Canut <i>et al.</i> , 2012)
Emory university		Preclinical	DNA – CAG repeat	AAV-CRISPR/Cas9	Intraparenchymal	(Yang <i>et al.</i> , 2017)
uniQure	AMT-130 (AAV-miHTT)	Phase 1b/2 - Ongoing	RNA (Target: <i>HTT</i> exon 1)	AAV5-miRNA (pre-miR-451)	Intraparenchymal (striatum)	(Miniarikova <i>et al.</i> , 2016) NCT04120493
Voyager	VV-HTT01	Phase 1b – Recruiting	RNA (Target: <i>HTT</i> exon 2)	AAV1-miRNA (pre-miR-30)	Intraparenchymal Putamen-thalamus	(Stanek <i>et al.</i> , 2014) NCT04885114
Spark		Preclinical	RNA (Target: <i>HTT</i> exon 52)	AAV1-miRNA (pre-miR-30)	Intraparenchymal: Putamen	(McBride <i>et al.</i> , 2011)
University of Massachusetts		Preclinical	RNA (Target: <i>HTT</i> exon 48)	AAV9-miRNA (pre-miR-155)	Intraparenchymal (Striatum and cortex)	(Pfister <i>et al.</i> , 2017)
Small molecules						
PTC therapeutics	PTC518	Preclinical	RNA - Splicing modulator	Small molecule	Oral	Bhattacharyya <i>et al.</i> abstract at HSG 2021
Novartis	Branaplam	Phase 1	RNA – Splicing modulator	Small molecule	Oral	(Keller <i>et al.</i> , 2022)
Others						
Triplet therapeutics	TTX-3360	Preclinical/IND	<i>MSH3</i> gene (DNA damage repair)	ASO	Intracerebroventricular (ICV)	Antonijevic <i>et al.</i> presentation at EHDN 2021 meeting

Gene therapy for HD

1

Gene therapy was proposed as a therapeutic tool 30 years ago to deliver genetic material to cells with the aim to alter gene expression (Friedmann, 1992). The DNA material is delivered using a carrier (vector), most commonly based on an adeno-associated virus (AAV), and is then transcribed utilizing the cell's own machinery resulting in continuous expression of the therapeutic transgene. Depending on the nature of the transgene, gene therapy can be used to correct defective genes by introducing a functional copy, to silence mutant alleles using RNAi or to deliver gene-editing technologies (Piguet *et al.*, 2017; Papanikolaou and Bosio, 2021). In HD, the molecular therapeutics tested in a gene therapy modality include the expression of HTT-targeting miRNAs and shRNAs (Rodriguez-Lebron *et al.*, 2005; Miniarikova *et al.*, 2016), CAG-targeting ZFP and CRISPR-Cas9 molecules (Yang *et al.*, 2017; Zeitler *et al.*, 2019), and mHTT-targeting intrabodies (Southwell *et al.*, 2009). The main advantage of gene therapy for brain diseases is that a single administration in affected brain areas, although invasive, can potentially result in long-term correction of disease pathology and lifelong treatment.

WHERE? - Therapeutic coverage of affected brain areas in HD

A basic principle in drug development is that the therapeutic drug should distribute to the diseased target tissues. HD pathology is characterized by intranuclear and cytoplasmic insoluble aggregates of mHTT in neuronal cells (DiFiglia, 1997), and medium spiny neurons (MSN) in the striatum are the primary affected neurons in early-stage HD. Indeed the characteristic pathology in HD patients comprise striatal atrophy and enlargement of the lateral ventricles (Hobbs *et al.*, 2010). As the disease progresses, the loss of neurons extends to other areas, including the deep layer cortical neurons and substantia nigra (Rosas *et al.*, 2006; Tabrizi *et al.*, 2009) and by end stage, typically more than 30% of the brain mass is lost (De La Monte *et al.*, 1988). Therefore, therapeutics targeting HD molecular disease-causing mechanisms, need to effectively distribute to the striatum, and secondarily to other brain areas, in order to achieve a fully effective outcome (Wang *et al.*, 2014). For CNS diseases, the complex brain anatomy and the blood brain barrier (BBB) protection of the brain result in a limited drug distribution which is considered one of the major challenges in the development of treatments for brain diseases. It also has become apparent that results obtained in small animal models often do not translate well to large animals and humans (Eaton and Wishart, 2017).

Three different routes of administration can be used to delivery therapeutics in the brain: intravenous, intrathecal and intraparenchymal (Hocquemiller *et al.*, 2016). Currently,

only the last ensures sufficient delivery of DNA oligonucleotides, siRNAs or gene therapy vectors to deep brain structures such as the striatum. Stereotactic intraparenchymal administration is invasive and cumbersome and the approach would only be suitable for single-dosed approaches with long-term effects such as gene therapeutics (Samaranch *et al.*, 2017). The delivery of various mHTT-lowering RNAi strategies into the striatum, or cerebral ventricles was associated with the reduction of mHTT aggregation and behavioral improvement in HD animal models (Rodriguez-Lebron *et al.*, 2005; DiFiglia *et al.*, 2007; Stanek *et al.*, 2014; Miniarikova *et al.*, 2017; Didiot *et al.*, 2018; Spronck *et al.*, 2019).

The toxicity of misfolded pathogenic proteins and fragments can spread throughout the brain by seeding protein aggregation in recipient cells. Spreading of mHTT between cells is evident from in vitro and animal experiments showing that mHTT aggregate transmission between neurons contributes to HD pathology (Pecho-Vrieseling *et al.*, 2014; Jeon *et al.*, 2016; Ananbeh *et al.*, 2021). One of the mechanisms of intercellular transfer is mediated by the secretion and dissemination of mHTT within extracellular vesicles (EV) (Jeon *et al.*, 2016). EVs are a heterogenous group of nanovesicles, including exosomes and microvesicles, that contain important biological cargos such as cellular miRNAs, long non-coding RNAs, proteins, lipids and DNA (Valadi *et al.*, 2007). Molecular therapies might be able to distribute between affected neuronal cells in the same manner as pathological proteins such as mHTT contributing to improve therapeutic efficacy as disease advances.

HOW GOOD and HOW BAD? – Measuring efficacy and safety of HTT-lowering treatments

In order to assess the therapeutic success of potential treatments it is important to establish a panel of outcomes for both positive and negative effects that are critical for disease progression. Outcomes of efficacy (“how good”) include measurements of target engagement, functional improvement and translational biomarkers predictive of the disease advancement (**Figure 3**). For HTT-lowering therapies, on-target lowering efficacy has been assessed in preclinical studies by measuring the reduction of FL-mHTT protein levels and mHTT aggregates within affected CNS regions. For this, numerous in vitro cultures and animal models have been used, including large transgenic models such as HD transgenic minipigs (Baxa *et al.*, 2013; Howland and Munoz-Sanjuan, 2014; Miniarikova *et al.*, 2018). Since brain biopsies are too invasive, it is not feasible to measure lowering efficacy directly in patients’ brain. The levels of mHTT (FL-mHTT) in cerebral spinal fluid (CSF) were proposed as markers of on-target efficacy in patients’ CNS and have been used in the first clinical trials (Tabrizi *et al.*, 2019). However, it is not clear to which extent the concentrations of mHTT in the CSF reflect the concentrations of mHTT in deep brain areas, or instead and most likely,

they reflect concentrations in spinal cord and cortex, according to the unsuccessful clinical trial with intrathecal infusion of ASOs (Tabrizi *et al.*, 2019). Another biofluid markers commonly used in brain diseases is the concentrations of neurofilament light chain (NfL), a general marker of neuroaxonal damage, in the CSF (Byrne *et al.*, 2018). NfL levels is a good predictor of disease onset, but does not correlated with symptom progression after symptom onset (Byrne *et al.*, 2018; Parkin *et al.*, 2021). Therefore, it is not clear whether it could be a suitable biomarker for response to neuroprotective treatments (Tabrizi *et al.*, 2019). It is important to mention, that although ideal due to their recent contribution in HD pathogenesis, measurements of HTT_{ex1} production or somatic instability in biofluids have not been assessed yet. Measuring these events is challenging since levels are low and first changes mainly take place in striatal neurons.

Other studied biomarkers for early prediction of therapeutic outcomes include volumetric measures by structural magnetic resonance imaging (MRI) (Wilson *et al.*, 2018). In HD patients, striatal volume was identified as the best variable to track longitudinal progression (Abeyasinghe *et al.*, 2021). Hence, monitoring volumetric changes may provide a more reliable measurement of therapeutic improvement. Moreover, imaging motor tracts in thalamus and striatum, first susceptible areas to degeneration, may help to determine timing of treatment and efficacy in pre-manifest patients (Rosas *et al.*, 2006; Zeun *et al.*, 2022).

Safety is a major aspect of drug development, especially for gene targeting therapies which can induce unwanted off-target downregulation of other genes (**Figure 3**). For vector-based gene therapeutics, due to their persistent and irreversible nature, evaluation of long-term HTT-lowering effects as well as potential off-target effects is important (Murlidharan *et al.*, 2014; Keskin *et al.*, 2019). Moreover, pre-existing neutralizing antibodies and AAV-induced immune responses may contribute to treatment durability and patient safety. Most HTT-lowering therapies are non-allele-selective and the potential toxicity of long-term wild-type HTT (wtHTT) lowering is a major safety concern (Kaemmerer and Grondin, 2019). A whole set of preclinical studies, together with first clinical trial, indicates that partial lowering of wtHTT up to a certain extend is well-tolerated for at least 7 months in humanized HD mice (Caron *et al.*, 2020), 6 months in NHP (Grondin *et al.*, 2012) and 4 months in HD patients (Tabrizi *et al.*, 2019)

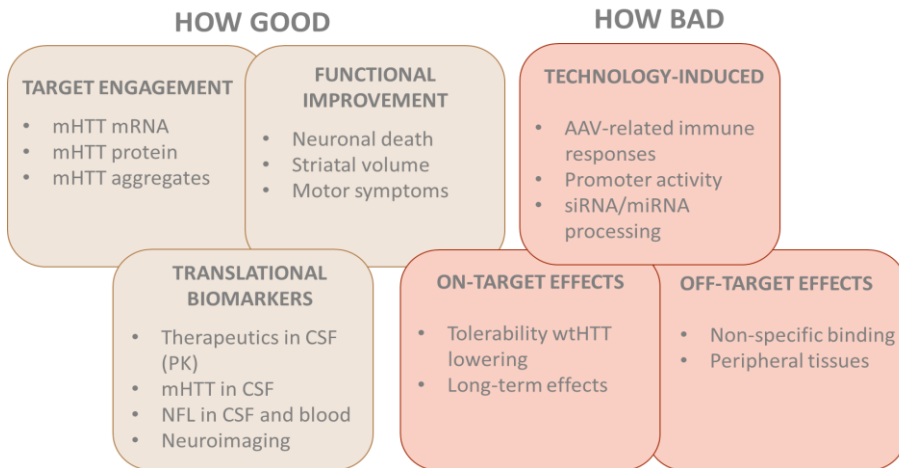


Figure 3: Measurements of efficacy (“how good”) and safety (“how bad”) for HTT-lowering therapies.

Conclusion

During the last decades, great efforts have led to the development and clinical testing of potential therapeutics for the treatment of HD. However, we are not there yet. Altogether, this mechanistic overview of molecular drivers of HD pathology, current therapeutic modalities and outcomes of efficacy illustrates critical requirements and remaining challenges to achieve therapeutic success. Potentially therapeutic approaches should aim to target the most toxic species in the most affected brain areas. For instance, the reduction of HTTex1 fragments or the suppression of somatic instability, rather than the lowering of full-length mHTT protein alone, are suggested as superior targets to effectively stop disease onset and progression. Next, therapeutic targeting should be preferentially and evenly achieved in earlier and most affected brain areas (i.e striatum) and cells, and secondly in other brain areas in line with disease progression. Finally, development of sensitive indicators of early disease changes are needed to correctly assess these therapies in slow progressing HD patients.

Scope of the thesis

Although HD has a well-defined monogenic cause and promising HTT-lowering therapies are being tested in clinical trials, mechanism of action studies can reveal relevant information about effective targets and outcomes required for successful translation into patients. One of the most advanced HTT lowering therapies for HD is a micro(mi)RNA-based gene therapy which consists of an engineered miRNA targeting the exon 1 sequence of HTT (miHTT) and delivered by adeno-associated virus (AAV) into neuronal striatal cells (AAV-miHTT). AAV-miHTT treatment has previously demonstrated efficacy and safety in reducing mutant HTT protein and rescuing HD phenotype in several HD murine models (Miniarikova *et al.*, 2016, 2017; Spronck *et al.*, 2019; Caron *et al.*, 2020), in transgenic minipigs (Evers *et al.*, 2018) and in HD patient-derived cells (Keskin *et al.*, 2019). However, mechanism of action studies are still limited.

The work in this thesis describes novel mechanistic features of AAV-miHTT treatment for HD, including the targeting of different HTT species, the therapeutic spread between neuronal cells and the development of translational biomarkers to monitor its effect in the affected brain regions.

In **Chapter 2** describes the reduction of highly toxic exon 1 HTT fragments, as well as full-length mutant HTT, in the brain of HD mouse models by AAV-miHTT.

Chapter 3 describes the widespread and sustained lowering efficacy of AAV-miHTT in disease-relevant regions in a large brain in HD transgenic minipigs, and the potential of using biofluids markers to determine vector expression and efficacy in the clinic.

Chapter 4 and **5** describe a novel mechanism of secretion and dissemination of engineered miRNAs mediated by extracellular vesicles (EV). Circulating engineered miRNAs in biofluids were used as sources of pharmacokinetic markers to monitor durability of miRNA therapeutics in the brain of non-human primates. Moreover, the uptake of EV-enriched engineered miRNAs by neighboring cells resulted in gene silencing in recipient cells, indicating therapeutic spread beyond AAV transduction.

Chapter 6 provide a general discussion of the main findings on the thesis and its implications for gene therapies for HD and other neurodegenerative diseases.

In the light of the work of this thesis, we support the reduction of HTTex1 fragment, the persistent efficacy in most affected brain areas, and mechanisms that improve therapeutic spread to all affected cells, as processes that potentially contribute to the successful treatment of HD patients.

References

- Abeyasinghe PM, Long JD, Razi A, Pustina D, Paulsen JS, Tabrizi SJ, et al. Tracking Huntington's Disease Progression Using Motor, Functional, Cognitive, and Imaging Markers. *Mov Disord* 2021; 36: 2282–92.
- Alterman JF, Godinho BMDC, Hassler MR, Ferguson CM, Echeverria D, Sapp E, et al. A divalent siRNA chemical scaffold for potent and sustained modulation of gene expression throughout the central nervous system. *Nat Biotechnol* 2019; 37: 884–94.
- Ananbeh H, Vodicka P, Kupcova Skalnikova H. Emerging Roles of Exosomes in Huntington's Disease. *Int J Mol Sci* 2021; 22.
- Bachoud-Lévi AC, Ferreira J, Massart R, Youssov K, Rosser A, Busse M, et al. International guidelines for the treatment of Huntington's disease. *Front Neurol* 2019; 10: 1–18.
- Barbaro BA, Lukacsovich T, Agrawal N, Burke J, Bornemann DJ, Purcell JM, et al. Comparative study of naturally occurring Huntingtin fragments in *Drosophila* points to exon 1 as the most pathogenic species in Huntington's disease. *Hum Mol Genet* 2015; 24: 913–25.
- Baxa M, Hruska-Plochan M, Juhas S, Vodicka P, Pavlok A, Juhasova J, et al. A transgenic minipig model of Huntington's Disease. *J Huntingtons Dis* 2013; 2: 47–68.
- Bhattacharyya A, Trotta CR, Narasimhan J, Wiedinger KJ, Li W, Effenberger KA, et al. Small molecule splicing modifiers with systemic HTT-lowering activity. *Nat Commun* 2021 121 2021; 12: 1–12.
- Byrne LM, Rodrigues FB, Johnson EB, Wijeratne PA, De Vita E, Alexander DC, et al. Evaluation of mutant huntingtin and neurofilament proteins as potential markers in Huntington's disease. *Sci Transl Med* 2018; 10.
- Caron NS, Southwell AL, Brouwers CC, Cengio LD, Xie Y, Black HF, et al. Potent and sustained huntingtin lowering via AAV5 encoding miRNA preserves striatal volume and cognitive function in a humanized mouse model of Huntington disease. *Nucleic Acids Res* 2020; 48: 36–54.
- Carroll JB, Warby SC, Southwell AL, Doty CN, Greenlee S, Skotte N, et al. Potent and selective antisense oligonucleotides targeting single-nucleotide polymorphisms in the Huntington disease gene / allele-specific silencing of mutant huntingtin. *Mol Ther* 2011; 19: 2178–85.
- Ciosi M, Maxwell A, Cumming SA, Hensman Moss DJ, Alshammari AM, Flower MD, et al. A genetic association study of glutamine-encoding DNA sequence structures, somatic CAG expansion, and DNA repair gene variants, with Huntington disease clinical outcomes. *EBioMedicine* 2019; 48: 568–80.
- Datson NA, González-Barriga A, Kourkouta E, Weij R, Van De Giessen J, Mulders S, et al. The expanded CAG repeat in the huntingtin gene as target for therapeutic RNA modulation throughout the HD mouse brain. *PLoS One* 2017; 12
- Didiot MC, Ferguson CM, Ly S, Coles AH, Smith AO, Bicknell AA, et al. Nuclear Localization of Huntingtin mRNA Is Specific to Cells of Neuronal Origin. *Cell Rep* 2018; 24: 2553–2560.e5.
- DiFiglia M. Aggregation of Huntingtin in Neuronal Intranuclear Inclusions and Dystrophic Neurites in Brain. *Science* (80-) 1997; 277: 1990–3.
- DiFiglia M, Sena-Esteves M, Chase K, Sapp E, Pfister E, Sass M, et al. Therapeutic silencing of mutant huntingtin with siRNA attenuates striatal and cortical neuropathology and behavioral deficits. *Proc Natl Acad Sci U S A* 2007; 104: 17204–9.
- Eaton SL, Wishart TM. Bridging the gap: large animal models in neurodegenerative research. *Mamm Genome* 2017; 28: 324–37.

- Evers MM, Miniarikova J, Juhas S, Vallès A, Bohuslavova B, Juhasova J, et al. AAV5-miHTT Gene Therapy Demonstrates Broad Distribution and Strong Human Mutant Huntingtin Lowering in a Huntington's Disease Minipig Model. *Mol Ther* 2018; 26: 2163–77.
- Franich NR, Hickey MA, Zhu C, Osborne GF, Ali N, Chu T, et al. Phenotype onset in Huntington's disease knock-in mice is correlated with the incomplete splicing of the mutant huntingtin gene. *J Neurosci Res* 2019; 97: 1590–605.
- Friedmann T. A brief history of gene therapy. *Nat Genet* 1992; 2: 93–8.
- Garriga-Canut M, Agustín-Pavón C, Herrmann F, Sánchez A, Dierssen M, Fillat C, et al. Synthetic zinc finger repressors reduce mutant huntingtin expression in the brain of R6/2 mice. *Proc Natl Acad Sci U S A* 2012; 109: E3136–45.
- Grondin R, Kaytor MD, Ai Y, Nelson PT, Thakker DR, Heisel J, et al. Six-month partial suppression of Huntingtin is well tolerated in the adult rhesus striatum. *Brain* 2012; 135: 1197–209.
- Gu X, Richman J, Langfelder P, Wang N, Zhang S, Bañez-Coronel M, et al. Uninterrupted CAG repeat drives striatum-selective transcriptionopathy and nuclear pathogenesis in human Huntingtin BAC mice. *Neuron* 2022; 110: 1–20.
- Heinz A, Nabariya DK, Krauss S. Huntingtin and Its Role in Mechanisms of RNA-Mediated Toxicity. *Toxins (Basel)* 2021; 13
- Hobbs NZ, Barnes J, Frost C, Henley SMD, Wild EJ, Macdonald K, et al. Onset and progression of pathologic atrophy in Huntington disease: a longitudinal MR imaging study. *AJNR Am J Neuroradiol* 2010; 31: 1036–41.
- Hocquemiller M, Giersch L, Audrain M, Parker S, Cartier N. Adeno-Associated Virus-Based Gene Therapy for CNS Diseases. *Hum Gene Ther* 2016; 27: 478–96.
- Howland DS, Munoz-Sanjuan I. Mind the gap: models in multiple species needed for therapeutic development in Huntington's disease. *Mov Disord* 2014; 29: 1397–403.
- Jeon I, Cicchetti F, Cisbani G, Lee S, Li E, Bae J, et al. Human - to - mouse prion - like propagation of mutant huntingtin protein. *Acta Neuropathol* 2016; 132: 577–92.
- Jimenez-Sanchez M, Licitra F, Underwood BR, Rubinsztein DC. Huntington's disease: Mechanisms of pathogenesis and therapeutic strategies. *Cold Spring Harb Perspect Med* 2017; 7: 1–22.
- Kaemmerer WF, Grondin RC. The effects of huntingtin-lowering: what do we know so far? *Degener Neurol Neuromuscul Dis* 2019; 9: 3.
- Keller, CG, Shin, Y, Monteys, AM et al. An orally available, brain penetrant, small molecule lowers huntingtin levels by enhancing pseudoexon inclusion. *Nat Commun* 2022; 13, 1150.
- Kennedy L, Evans E, Chen C-M, Craven L, Detloff PJ, Ennis M, et al. Dramatic tissue-specific mutation length increases are an early molecular event in Huntington disease pathogenesis. *Hum Mol Genet* 2003; 12: 3359–67.
- Keskin S, Brouwers CC, Sogorb-Gonzalez M, Martier R, Depla JA, Vallès A, et al. AAV5-miHTT Lowers Huntingtin mRNA and Protein without Off-Target Effects in Patient-Derived Neuronal Cultures and Astrocytes. *Mol Ther - Methods Clin Dev* 2019; 15: 275–84.
- Kingwell K. Double setback for ASO trials in Huntington disease. *Nat Rev Drug Discov* 2021; 20: 412–3.

1
Kordasiewicz HB, Stanek LM, Wancewicz EV, Mazur C, McAlonis MM, Pytel KA, et al. Sustained Therapeutic Reversal of Huntington's Disease by Transient Repression of Huntingtin Synthesis. *Neuron* 2012; 74: 1031–44.

De La Monte SM, Vonsattel JP, Richardson EP. Morphometric demonstration of atrophic changes in the cerebral cortex, white matter, and neostriatum in Huntington's disease. *J Neuropathol Exp Neurol* 1988; 47: 516–25.

Leavitt BR, Kordasiewicz HB, Schobel SA. Huntingtin-Lowering Therapies for Huntington Disease: A Review of the Evidence of Potential Benefits and Risks. *JAMA Neurol* 2020; 77: 764–72.

Lee JM, Wheeler VC, Chao MJ, Vonsattel JPG, Pinto RM, Lucente D, et al. Identification of Genetic Factors that Modify Clinical Onset of Huntington's Disease. *Cell* 2015; 162: 516–26.

MacDonald ME, Ambrose CM, Duyao MP, Myers RH, Lin C, Srinidhi L, et al. A novel gene containing a trinucleotide repeat that is expanded and unstable on Huntington's disease chromosomes. *Cell* 1993; 72: 971–83.

Mangiarini L, Sathasivan K, Seller M, Cozens B. Exon1 of the HD gene expanded. *Cell* 1996; 87: 493–506.

Marxreiter F, Stemick J, Kohl Z. Huntingtin lowering strategies. *Int J Mol Sci* 2020; 21

McBride JL, Pitzer MR, Boudreau RL, Dufour B, Hobbs T, Ojeda SR, et al. Preclinical Safety of RNAi-Mediated HTT Suppression in the Rhesus Macaque as a Potential Therapy for Huntington's Disease. *Mol Ther* 2011; 19: 2152–62.

Menalled LB, Sison JD, Wu Y, Olivieri M, Li X-J, Li H, et al. Early Motor Dysfunction and Striosomal Distribution of Huntingtin Microaggregates in Huntington's Disease Knock-In Mice. 2002

Miniarikova J, Evers MM, Konstantinova P. Translation of MicroRNA-Based Huntingtin-Lowering Therapies from Preclinical Studies to the Clinic. *Mol Ther* 2018; 26: 947–62.

Miniarikova J, Zanella I, Huseinovic A, van der Zon T, Hanemaaijer E, Martier R, et al. Design, Characterization, and Lead Selection of Therapeutic miRNAs Targeting Huntingtin for Development of Gene Therapy for Huntington's Disease. *Mol Ther - Nucleic Acids* 2016; 5: e297.

Miniarikova J, Zimmer V, Martier R, Brouwers CC, Pythoud C, Richetin K, et al. AAV5-miHTT gene therapy demonstrates suppression of mutant huntingtin aggregation and neuronal dysfunction in a rat model of Huntington's disease. *Gene Ther* 2017; 24: 630–9.

Murlidharan G, Samulski RJ, Asokan A. Biology of adeno-associated viral vectors in the central nervous system. *Front Mol Neurosci* 2014; 7

Neueder A, Dumas AA, Benjamin AC, Bates GP. Regulatory mechanisms of incomplete huntingtin mRNA splicing. *Nat Commun* 2018; 9

Neueder A, Landles C, Ghosh R, Howland D, Myers RH, Faull RLM, et al. The pathogenic exon 1 HTT protein is produced by incomplete splicing in Huntington's disease patients. *Sci Rep* 2017; 7

Papanikolaou E, Bosio A. The Promise and the Hope of Gene Therapy. *Front genome Ed* 2021; 3

Parkin GM, Corey-Bloom J, Snell C, Castleton J, Thomas EA. Plasma neurofilament light in Huntington's disease: A marker for disease onset, but not symptom progression. *Parkinsonism Relat Disord* 2021; 87: 32–8.

Pecho-Vrieseling E, Rieker C, Fuchs S, Bleckmann D, Esposito MS, Botta P, et al. Transneuronal propagation of mutant huntingtin contributes to non-cell autonomous pathology in neurons. *Nat Neurosci* 2014; 17: 1064–72.

Pfister EL, Chase KO, Sun H, Kennington LA, Conroy F, Johnson E, et al. Safe and Efficient Silencing with a Pol II, but Not a Pol III, Promoter Expressing an Artificial miRNA Targeting Human Huntingtin. *Mol Ther Nucleic Acids* 2017; 7: 324–34.

Piguet F, Alves S, Cartier N. Clinical Gene Therapy for Neurodegenerative Diseases: Past, Present, and Future. *Hum Gene Ther* 2017; 28: 988–1003.

Pinto RM, Arning L, Giordano J V., Razghandi P, Andrew MA, Gillis T, et al. Patterns of CAG repeat instability in the central nervous system and periphery in Huntington's disease and in spinocerebellar ataxia type 1. *Hum Mol Genet* 2020; 29: 2551–67.

Rawlins MD, Wexler NS, Wexler AR, Tabrizi SJ, Douglas I, Evans SJW, et al. The prevalence of huntington's disease. *Neuroepidemiology* 2016; 46: 144–53.

Rodriguez-Lebron E, Denovan-Wright EM, Nash K, Lewin AS, Mandel RJ. Intrastriatal rAAV-mediated delivery of anti-huntingtin shRNAs induces partial reversal of disease progression in R6/1 Huntington's disease transgenic mice. *Mol Ther* 2005; 12: 618–33.

Rosas HD, Tuch DS, Hevelone ND, Zaleta AK, Vangel M, Hersch SM, et al. Diffusion tensor imaging in presymptomatic and early Huntington's disease: Selective white matter pathology and its relationship to clinical measures. *Mov Disord* 2006; 21: 1317–25.

Ross CA, Aylward EH, Wild EJ, Langbehn DR, Long JD, Warner JH, et al. Huntington disease: Natural history, biomarkers and prospects for therapeutics. *Nat Rev Neurol* 2014; 10: 204–16.

Roy JCL, Vitalo A, Andrew MA, Mota-Silva E, Kovalenko M, Burch Z, et al. Somatic CAG expansion in Huntington's disease is dependent on the MLH3 endonuclease domain, which can be excluded via splice redirection. *Nucleic Acids Res* 2021; 49: 3907–18.

Samaranch L, Blits B, San Sebastian W, Hadaczek P, Bringas J, Sudhakar V, et al. MR-guided parenchymal delivery of adeno-associated viral vector serotype 5 in non-human primate brain. *Gene Ther* 2017; 24: 253–61.

Sathasivam K, Neueder A, Gipson TA, Landles C, Benjamin AC, Housman DE, et al. Aberrant splicing of HTT generates the pathogenic exon 1 protein in Huntington disease. *PNAS* 2013; 110: 2366–70.

Soares TR, Reis SD, Pinho BR, Duchon MR, Oliveira JMA. Targeting the proteostasis network in Huntington's disease. *Ageing Res Rev* 2019; 49: 92–103.

Southwell AL, Ko J, Patterson PH. Intrabody Gene Therapy Ameliorates Motor, Cognitive, and Neuropathological Symptoms in Multiple Mouse Models of Huntington's Disease. *J Neurosci* 2009; 29: 13589–602.

Spronck EA, Brouwers CC, Vallès A, de Haan M, Petry H, van Deventer SJ, et al. AAV5-miHTT Gene Therapy Demonstrates Sustained Huntingtin Lowering and Functional Improvement in Huntington Disease Mouse Models. *Mol Ther - Methods Clin Dev* 2019; 13: 334–43.

Stanek LM, Sardi SP, Mastis B, Richards AR, Treleaven CM, Taksir T, et al. Silencing mutant huntingtin by adeno-associated virus-mediated RNA interference ameliorates disease manifestations in the YAC128 mouse model of Huntington's disease. *Hum Gene Ther* 2014; 25: 461–74.

Swami M, Hendricks AE, Gillis T, Massood T, Mysore J, Myers RH, et al. Somatic expansion of the Huntington's disease CAG repeat in the brain is associated with an earlier age of disease onset. *Hum Mol Genet* 2009; 18: 3039–47.

Tabrizi SJ, Flower MD, Ross CA, Wild EJ. Huntington disease: new insights into molecular pathogenesis and therapeutic opportunities. *Nat Rev Neurol* 2020; 16: 529–46.

Tabrizi SJ, Ghosh R, Leavitt BR. Huntingtin Lowering Strategies for Disease Modification in Huntington's Disease. *Neuron* 2019; 101: 801–19.

Tabrizi SJ, Langbehn DR, Leavitt BR, Roos RA, Durr A, Craufurd D, et al. Biological and clinical manifestations of Huntington's disease in the longitudinal TRACK-HD study: cross-sectional analysis of baseline data. *Lancet Neurol* 2009; 8: 791–801.

Tabrizi SJ, Leavitt BR, Landwehrmeyer GB, Wild EJ, Saft C, Barker RA, et al. Targeting Huntingtin Expression in Patients with Huntington's Disease. *N Engl J Med* 2019; 380: 2307–16.

Valadi H, Ekström K, Bossios A, Sjöstrand M, Lee JJ, Lötvall JO. Exosome-mediated transfer of mRNAs and microRNAs is a novel mechanism of genetic exchange between cells. *Nat Cell Biol* 2007; 9: 645–59.

Wang N, Gray M, Lu XH, Cantle JP, Holley SM, Greiner E, et al. Neuronal targets for reducing mutant huntingtin expression to ameliorate disease in a mouse model of Huntington's disease. *Nat Med* 2014; 20: 536–41.

Wellington CL, Singaraja R, Ellerby L, Savill J, Roy S, Leavitt B, et al. Inhibiting Caspase Cleavage of Huntingtin Reduces Toxicity and Aggregate Formation in Neuronal and Nonneuronal Cells. *J Biol Chem* 2000; 275: 19831–8.

Wild EJ, Tabrizi SJ. Therapies targeting DNA and RNA in Huntington's disease. *Lancet Neurol* 2017; 16: 837–47.

Wilson H, Dervenoulas G, Politis M. Structural Magnetic Resonance Imaging in Huntington's Disease. *Int Rev Neurobiol* 2018; 142: 335–80.

Wu T, Yu M, Zhang L, Chen X, Pei Z. I02 Systemic injection of exosomal sirna significantly reduced huntingtin expression in transgenic mice of huntington's disease. *J Neurol Neurosurg Psychiatry* 2018; 89: A88–9.

Yamamoto A, Lucas JJ, Hen R. Reversal of neuropathology and motor dysfunction in a conditional model of Huntington's disease. *Cell* 2000; 101: 57–66.

Yang S, Chang R, Yang H, Zhao T, Hong Y, Kong HE, et al. CRISPR/Cas9-mediated gene editing ameliorates neurotoxicity in mouse model of Huntington's disease. *J Clin Invest* 2017; 127

Zeitler B, Froelich S, Marlen K, Shivak DA, Yu Q, Li D, et al. Allele-selective transcriptional repression of mutant HTT for the treatment of Huntington's disease. *Nat Med* 2019; 25: 1131–42.

Zeun P, McColgan P, Dhollander T, Gregory S, Johnson EB, Papoutsis M, et al. Timing of selective basal ganglia white matter loss in premanifest Huntington's disease. *Neuroimage (Amst)* 2022; 33: 102927.

Chapter

2

Exon 1-targeting miRNA reduces the pathogenic exon 1 HTT protein generated by aberrant splicing in Huntington disease

Marina Sogorb-Gonzalez^{1,2}, Fanny Mariet¹, Christian Landles³, Steffi Jonk¹, Anouk Stam¹, Nicholas Caron⁴, Michael R Hayden⁴, Pavlina Konstantinova¹, Sander van Deventer^{1,2}, Gillian Bates³, Astrid Vallès^{1*}, Melvin Evers^{1*}

¹Department of Research & Development, uniQure biopharma B.V., Amsterdam, The Netherlands

²Department of Gastroenterology and Hepatology, Leiden University Medical Center, Leiden, The Netherlands

³ Huntington's Disease Centre, Department of Neurodegenerative Disease and UK Dementia Research Institute at UCL, Queen Square Institute of Neurology, UCL, Queen Square, WC1N 3BG, UK

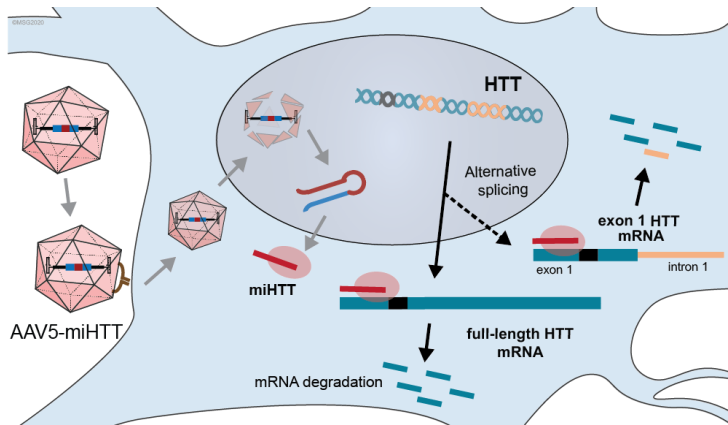
⁴ Centre for Molecular Medicine and Therapeutics, Department of Medical Genetics, University of British Columbia, Vancouver, Canada.

*These authors contributed equally

Manuscript in preparation.

Abstract

Huntington disease (HD) is a fatal neurodegenerative disease caused by a trinucleotide repeat expansion in exon 1 of the huntingtin gene (HTT) resulting in gain-of-function toxicity and cell death. Despite its monogenic cause, HD pathology is highly complex and increasing evidence indicates that, besides the mutant full-length HTT protein, exon 1 HTT (HTTex1) fragments generated by aberrant splicing are highly prone to aggregate and contribute to HD pathology. This finding suggests that reducing the expression of HTTex1 transcripts might achieve a greater therapeutic benefit than targeting only the full-length mutant HTT and conversely, strategies that exclusively target full-length HTT might not prevent HD pathogenesis. We have developed an engineered microRNA targeting *HTT* exon 1 sequence (miHTT) and delivered via adeno-associated serotype 5 virus (AAV5). Preclinical studies with AAV5-miHTT demonstrated efficacy in several rodent and large animal models by reducing full-length HTT mRNA and protein and rescuing HD phenotypes. In this study, we evaluated the ability of AAV5-miHTT to reduce the levels of aberrantly spliced HTTex1 mRNA and protein in the brain of two mouse models of HD (transgenic Q175 knock-in mice and humanized Hu128/21 mice). Polyadenylated HTTex1 mRNA and HTTex1 protein were detected in the striatum and cortex of Q175 knock-in mice, but not in wildtype mice. Intrastratial administration of AAV5-miHTT resulted in dose-dependent levels of mature miHTT microRNA in cortical brain regions, accompanied by significant lowering of both full-length HTT and HTTex1 mRNA expression at two months post-injection. Mutant HTT and HTTex1 protein levels were also significantly reduced in striatum and cortex of Q175 knock-in and humanized Hu128/21 mice at two and four months, respectively, after AAV5-miHTT treatment. These results demonstrate that AAV5-miHTT gene therapy is an efficient approach to lower both full-length HTT and the highly pathogenic HTTex1 levels, and support the added therapeutic benefit of exon 1-targeting therapeutics for HD.



Introduction

Huntington disease (HD) is a fatal genetic, neurodegenerative disease that manifests as a progressive motor, cognitive and behavioral disorder. HD is caused by an expansion of ≥ 36 CAG repeats in exon 1 of the *huntingtin* gene (*HTT*) (MacDonald *et al.*, 1993). This CAG expansion is translated into a polyglutamine (polyQ) tract within the N-terminal domain of the HTT protein. Similar to other related polyQ neurodegenerative disorders, the extended polyQ tract confers a toxic gain-of-function resulting in protein aggregation and neuronal death (Takahashi *et al.*, 2010; Stoyas and La Spada, 2018). Large intracellular aggregates, known as inclusion bodies, have been found throughout post-mortem brains and are considered the main pathological hallmark of HD (Gutekunst *et al.*, 1999; Arrasate and Finkbeiner, 2012), suggesting that prevention of mutant huntingtin aggregates could be a promising therapeutic strategy for the treatment of HD. During the last decade, this hypothesis has led to the development and clinical testing of several HTT lowering therapies (Wild and Tabrizi, 2017, Tabrizi *et al.*, 2019a; Marxreiter *et al.*, 2020). Antisense oligonucleotides (ASOs), RNA interference (RNAi) compounds and zinc finger transcriptional repressors (ZFTRs) aim at reducing the levels of mutant HTT protein and toxic aggregation in the affected areas of the brain (Harper *et al.*, 2005, Rodriguez-Lebron *et al.*, 2005; Kordasiewicz *et al.*, 2012; Miniarikova *et al.*, 2016; Zeitler *et al.*, 2019).

Increasing evidence indicates that, besides the mutant full-length HTT protein, small N-terminal fragments containing extended polyQ tracts also form toxic aggregates and significantly contribute to HD pathology (Mangiarini *et al.*, 1996; Schilling *et al.*, 1999; Tanaka *et al.*, 2006; Landles *et al.*, 2010; Vieweg *et al.*, 2021). Among those, the smallest HTT fragment identified as a exon 1 HTT protein (HTTex1) displayed the highest toxicity by a strong propensity to form nuclear aggregates and a reduction of motor function and lifespan in *Drosophila* (Barbaro *et al.*, 2015; Chongtham *et al.*, 2020). In rodents, HTTex1-expressing mouse models display the most severe phenotype (Mangiarini *et al.*, 1996), although the suppression of HTTex1 expression in a conditional model was able to reverse aggregate formation and motor decline (Yamamoto *et al.*, 2000), suggesting that HTTex1 reduction is beneficial for therapeutic efficacy in HD.

It has recently been demonstrated that in the context of HD, HTT pre-mRNA can undergo CAG-dependent aberrant splicing of exon 1 to exon 2 resulting in the production of the pathogenic HTTex1 protein (Sathasivam *et al.*, 2013; Neueder *et al.*, 2017). This mis-splicing event is caused by abnormal binding of splicing factor SRSF6 to the expanded CAG repeat resulting in activation of cryptic polyadenylation signal within intron 1 and transcription of exon 1 – intron 1 polyadenylated mRNA (*HTTex1*) (Neueder *et al.*, 2018). Analogous to the sequence in the correctly spliced full-length HTT mRNA, the additional intron 1 sequence starts with a base pair that completes the codon for a proline residue,

2 followed by a stop codon (TGA). As a consequence, the short *HTTex1* transcript is translated into the pathogenic HTTex1 protein composed of the same amino acids as the N-terminus in the full-length protein. Although low levels of mis-splicing ratio and *HTTex1* transcripts have been found in adult-onset HD patients (Neueder *et al.*, 2018), steady accumulation of highly toxic HTTex1 is believed to contribute to disease onset and progression of HD. Since HTT aberrant splicing is CAG-dependent, expansion of CAG repeats throughout patient's life via somatic instability is expected to increase HTTex1 production and consequently cause accelerated neurodegeneration (Swami *et al.*, 2009). This hypothesis is part of the two-step model of HD pathogenesis in which somatic CAG repeat instability throughout patient's pre-symptomatic years, and not the congenital number of CAG repeats, triggers the increase production of toxic drivers, such as HTTex1, up to a cell type-specific lethal threshold that results in the neurodegeneration of vulnerable cells and disease manifestation. (Neueder *et al.*, 2017; Pinto *et al.*, 2020).

RNA-targeting approaches designed to lower the full-length mutant HTT protein may not necessarily reduce intracellular levels of the highly toxic HTTex1 protein. In fact, most HD therapeutics in development use ASOs or RNAi technologies that target sequences downstream the exon 1 and therefore they are unlikely to reduce the translation of the HTTex1 protein. We have developed an engineered miRNA targeting *HTT* exon 1 sequence (miHTT), delivered via adeno-associated serotype 5 virus (AAV5) (Miniarikova *et al.*, 2016). Briefly, this approach is based on a AAV5-delivered DNA construct encoding for engineered pri-miRNA hairpins, which are processed into mature miHTT molecules and loaded into RNAi silencing complex (RISC) for recognition and binding to target sequence, resulting in translational repression or enzymatic cleavage of target mRNA (Miniarikova *et al.*, 2016). Proof-of-concept studies have demonstrated that intrastriatal administration of AAV5-miHTT is safe and results in long-term lowering of full-length mutant HTT protein in HD rodents (Miniarikova *et al.*, 2016, 2017; Spronck *et al.*, 2019; Caron *et al.*, 2020), as well as in large animal models (Evers *et al.*, 2018; Spronck *et al.*, 2021; Valles *et al.*, 2021), reducing disease severity and progression. In the current study, we evaluated the ability of AAV5-miHTT to reduce the levels of HTTex1 transcripts in the brain of two mouse models of HD (transgenic Q175 knock-in mice and humanized Hu128/21 mice). Intrastriatal injection of AAV5-miHTT caused a dose-dependent lowering of both full-length HTT and HTTex1 mRNA and protein levels in striatum and cortex of these HD mouse models, demonstrating that, apart from full-length HTT, AAV5-miHTT effectively also reduces the highly pathogenic HTTex1 protein in HD.

Results

Mis-spliced *HTTex1* transcripts are expressed in the cortex of Q175 KI mice.

In order to investigate the target engagement of aberrantly spliced *HTTexon1* transcript by our therapeutic AAV5-miHTT approach, an animal model which closely mimics the genetic context and HTT alternative splicing in HD patients is required. We selected the zQ175 knock-in (Q175 KI) mouse model of HD, a well-validated model for evaluation of therapeutic interventions, as well as for *HTTex1* protein analysis (Papadopoulou *et al.*, 2019; Spronck *et al.*, 2019). In Q175 KI mice, exon 1 and part of intron 1 sequences of murine huntingtin *Hdh* have been replaced with a human *HTT* exon 1 sequence carrying 188 CAG repeats (Menalled *et al.*, 2012) (**Figure 1A**). Heterozygous Q175 KI mice contain a chimeric human-mouse expanded HTT allele, which is subjected to alternative splicing (Sathasivam *et al.*, 2013; Papadopoulou *et al.*, 2019), and a wild-type murine allele.

First, to evaluate the levels of polyadenylated *HTTex1* transcripts in Q175 KI mice, molecular assays were performed with RNA isolated from brain cortex (Sathasivam *et al.*, 2013). 3'RACE-PCR (rapid amplification of cDNA ends) together with intron 1 HTT primers showed the exclusive presence of polyadenylated short *HTTex1* mRNA in the cortex of Q175 KI, but not wild-type (WT) from the same background strain (**Figure 1B**). The sequence of the intron1-containing amplified product was verified by Sanger sequencing (data not showed). End-point PCR with primers for the exon 1 – intron 1 boundary confirmed the presence of *HTTex1* in the cortex of Q175 KI, and its absence in WT littermates (**Figure 1C**). *FL-Htt* transcripts, detected with primers that spanned exon 1-exon 2 junction, were identified in both Q175 KI and WT mice (**Figure 1C**).

To quantify the expression of *HTTex1* transcript, a quantitative PCR (qPCR) was performed with 4 different sets of primers. Levels of *FL-Htt* were determined with primers spanning exon 1-2 and exon 64-65 junction respectively, while *HTTex1* transcript was selectively quantified by amplifying sequences within intron 1 (upstream of cryptic polyA site) and human exon1-intron 1 (**Figure 1D** and **Figure 1E**). A significant reduction in *FL-Htt* mRNA was detected in Q175 KI mice as compared to WT mice when normalized to three housekeeping genes (**Figure 1D**) (Exon 1-2 unpaired t-test **** $p < 0.001$. Exon 64-65 unpaired t-test *** $p = 0.003$). This could be due to mis-splicing of mutant HTT mRNA (Papadopoulou *et al.*, 2019). Consistent with end-point PCR, we quantified high levels of *HTTex1* transcript in the cortex on Q175 KI mice, but not in WT mice (**Figure 1E**) (Intron 1, unpaired t-test **** $p < 0.0001$; human exon1-intron1, unpaired t-test **** $p < 0.0001$). All together, these results obtained by different qualitative and quantitative assays confirmed the presence of mis-spliced polyadenylated *HTTexon1* mRNA in the context of HD in the brain of Q175 KI mice.

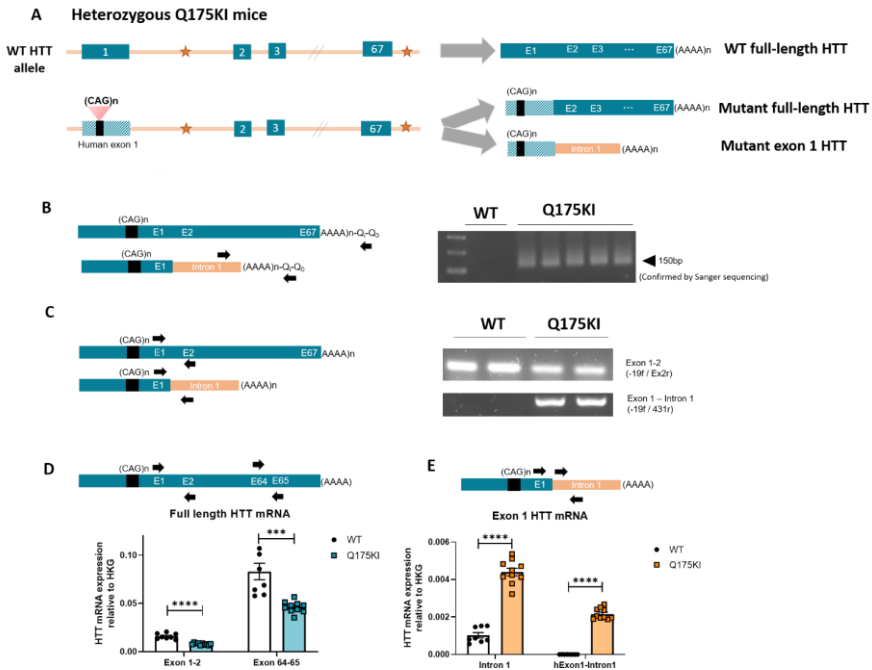


Figure 1. Detection of aberrantly spliced *HTT* exon 1 transcript in Q175 KI mice. **A)** Schematic representation of WT HTT allele and chimeric mutant HTT allele in heterozygous Q175 KI mice. **B)** 3'RACE RT-PCR together with intron 1 HTT primers showed the presence of polyadenylated short mRNA in Q175 KI brain cortex, but not in WT mice. **C)** Detection of polyadenylated *HTT* exon 1 mRNA in the cortex of Q175 KI mice by oligodT RT-PCR assay. Spliced exon 1-exon2 transcripts were detected in frontal cortex of both WT and Q175 KI mice, while exon 1-intron 1 product was only detected in Q175 KI mice, but not in WT. **D)** Relative expression of *FL-HTT* in the frontal cortex of Q175 KI mice and WT detected by TaqMan qPCR with primer-probe sets exon 1-2 (unpaired t-test **** $p < 0.001$) and exon 64-65 (unpaired t-test **** $p = 0.003$). **E)** Relative expression of *HTT* exon 1 mRNA in cortical tissue of Q175 KI and WT mice detected by TaqMan qPCR with primer-probe sets Intron 1 (unpaired t-test **** $p < 0.0001$) and human exon 1-intron 1 (unpaired t-test **** $p < 0.0001$). D-E) Bars show mean \pm SEM.

HTT_{ex1} protein is present in the striatum and cortex of Q175 KI mice

Polyadenylated *HTT*_{ex1} mRNA is translated into an HTT_{ex1} protein, which is prone to aggregate and is considered the most toxic species in HD (Barbaro *et al.*, 2015; Chongtham *et al.*, 2020). Quantification of exon 1 HTT protein was performed by Homogeneous Time Resolved Fluorescence (HTRF) with MW8 antibody specific for HTT exon 1 carboxy-terminal epitope that is present in HTT_{ex1} protein but not in full-length HTT protein (Landles *et al.*, 2010). Combinations of different antibodies were used to specifically measure the

expression of mutant HTT, FL-HTT and aggregated HTTex1 in both Q175 KI and WT mice at 7 months of age (Landles *et al.*, 2021). Significantly higher levels of mutant HTT protein and HTTex1 protein were detected in the striatum and cortex of Q175 KI mice, when compared to background levels in WT mice (**Figure 2A** and **Figure 2B**). However, there was no significant difference between the levels of FL-HTT protein, demonstrating that comparable HTT expression is found in HD and WT mice (**Figure 2C**). Aggregated HTTex1 protein, measured with an antibody against the human polyproline region in the mutant HTT, was detected in Q175 KI mice, but not in WT mice (**Figure 2D**). Overall, levels of all mutant HTT protein species were significantly higher in striatum, the most affected brain region in HD, than in cortex. These results confirm the presence of aberrantly spliced HTTex1 protein in the brain in Q175 KI mice at 7 months of age.

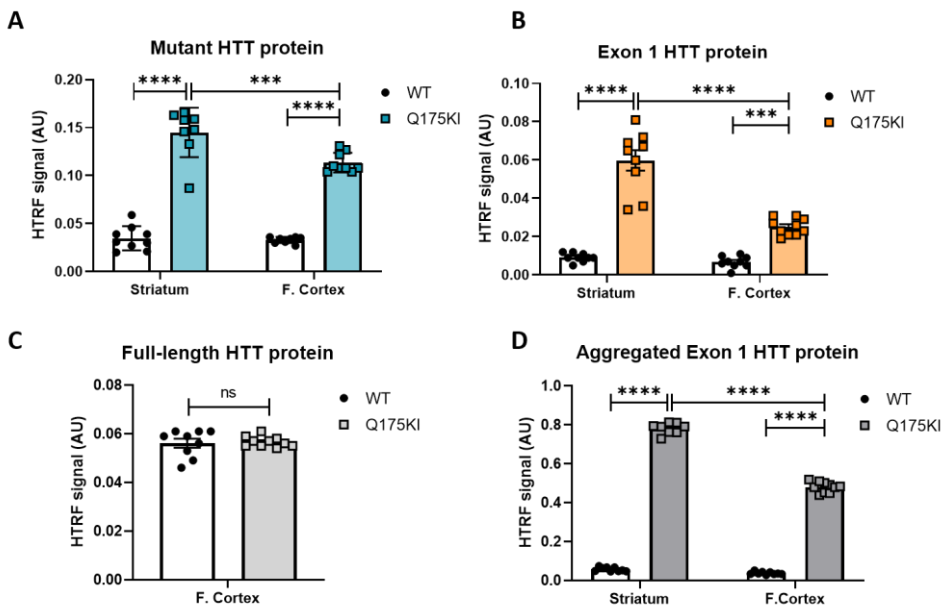


Figure 2. Detection of HTTex1 protein and other HTT protein species in Q175 KI mice. **A)** Levels of soluble human mutant HTT protein in striatum and frontal cortex of WT and Q175 KI mice measured by HTRF with 2B7 and 4C9 antibodies and represented as mean with SEM (one-way ANOVA, Tukey's multiple comparisons test, *** $p=0.009$, **** $p<0.001$). **B)** Levels of soluble HTTex1 protein in striatum and frontal cortex of WT and Q175 KI mice measured by HTRF with 2B7 and MW8 antibodies, and represented as mean with SEM (one-way ANOVA, Tukey's multiple comparisons test, **** $p<0.001$). **C)** Levels of soluble full-length HTT protein in frontal cortex of WT and Q175 KI mice measured by HTRF with MAB5490 and MAB2166 antibodies and represented as mean with SEM (unpaired-test, ns $p=0,7613$). **D)** Levels of aggregated HTTex1 protein in striatum and frontal cortex of WT and Q175 KI mice measured by HTRF with 4C9 and MW8 antibodies and represented as mean with SEM (one-way ANOVA, Tukey's multiple comparisons test, **** $p<0.001$). A-D) Bars show mean \pm SEM.

AAV5-miHTT administration results in dose-dependent expression of exon1-targeting miHTT in Q175 KI mice

2

The discovery that toxic HTT_{ex1} protein is generated by aberrant splicing suggests that, depending on *HTT* target sequence, RNA-targeted therapeutic approaches designed to lower the levels of HTT may not necessarily reduce intracellular levels of the highly toxic HTT_{ex1} protein. However, approaches targeting HTT within exon 1 sequence, such as AAV-miHTT (**Figure 3A**) (Miniarikova *et al.*, 2017), could result in the lowering of the toxic HTT_{ex1} protein and therefore would have a therapeutic advantage compared to strategies that only lower the mutant FL-HTT. To investigate the efficacy of AAV5-miHTT to lower the toxic HTT_{ex1} protein in vivo, Q175 KI mice were bilaterally intrastriatally injected at the age of 5 months with AAV5-miHTT at a low and a high dose, or formulation buffer (vehicle) as control (N=10 per group) (**Figure 3B** and **Figure 3C**). Two months after AAV5-miHTT treatment, mice were sacrificed, and brain areas were separately dissected for analysis of transgene expression and protein lowering. Due to the small volume, striata were used for protein analysis exclusively, while other areas from left and right hemisphere were used for protein and RNA analysis, respectively. Distribution and transduction efficiency of AAV5-miHTT treatment was determined by measuring the expression of mature miHTT transgene by RT-qPCR in the frontal cortex, caudal cortex and hippocampus. A significant dose-dependent increase in mature miHTT molecules was measured in the left frontal cortex, caudal cortex and hippocampus of Q175 KI mice at 2 months post-injection (**Figure 3D-3F**) (N=10, one-way ANOVA, Tukey's multiple comparisons test, *** $p < 0.005$, **** $p < 0.0001$). The low dose showed average 5×10^5 molecules/ μg RNA, whereas high-dose animals had levels of average 7×10^6 molecules/ μg RNA in frontal cortex. Since the cortex was not the direct target of AAV5-miHTT administration, transgene levels in cortical areas indicates that AAV5 vector was actively distributed by axonal transport via cortico-striatal pathways (Samaranch *et al.*, 2017). A comparable spread of the vector from striatum (injection area) to cortical areas has been previously shown in mice and large animals (Samaranch *et al.*, 2017; Evers *et al.*, 2018; Spronck *et al.*, 2019, 2021; Caron *et al.*, 2020; Valles *et al.*, 2021). Based on our previous studies using comparable doses of AAV-miHTT (Spronck *et al.*, 2019; Caron *et al.*, 2020), miHTT levels in striatum are expected to be approximately 8 times higher than in frontal cortex.

Exon 1-targeting miRNA reduces pathogenic exon 1 HTT protein

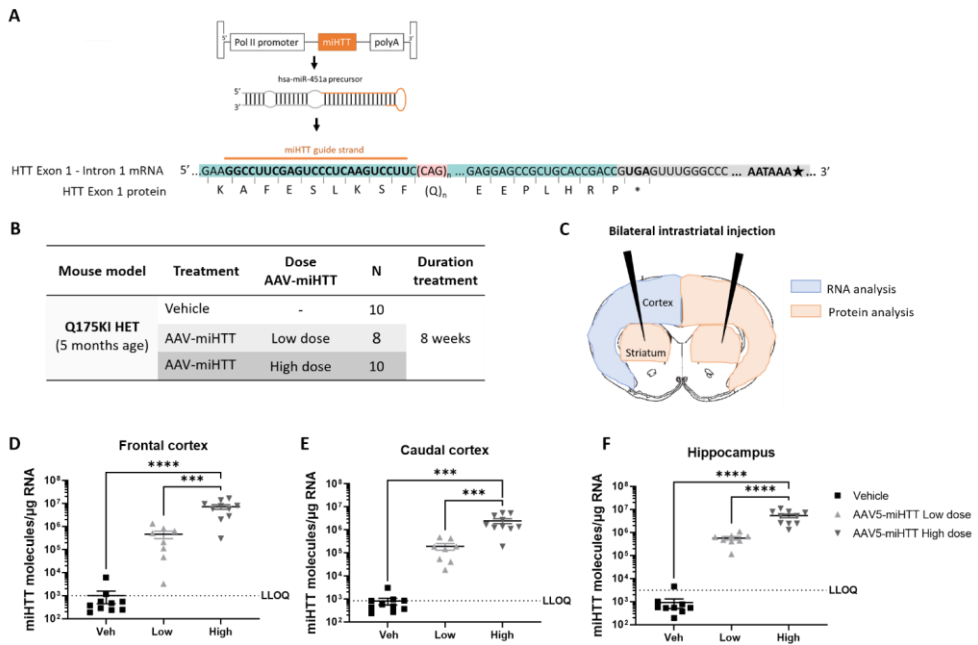


Figure 3. Intrastratial administration of AAV5-miHTT results in dose-dependent expression of exon 1-targeting miHTT. **A)** Graphic representation of AAV5-delivered expression cassette including Pol II promoter, exon 1-targeting miHTT transgene and polyA signal. Transgene is processed into pre-miRNA hairpin with same structure as has-miR-451 precursor, and then processed into a miHTT guide strand which is complementary to HTT exon 1 sequence upstream CAG repeat expansion. **B)** Experimental setup showing Q175 KI mice used in the study with the different dose groups and duration of treatment. **C)** Representation of bilateral intrastratial injection and collection of color-coded brain tissues for RNA and protein analysis. **D-F)** miHTT transgene expression in (D) frontal cortex, (E) caudal cortex and (F) hippocampus from the left hemisphere determined by custom TaqMan RT-qPCR and represented as miHTT molecules/ug RNA (mean with SEM) per dose group (one-way ANOVA, Tukey's multiple comparisons test, *** $p < 0.005$, **** $p < 0.001$). D-F) Graphs show mean \pm SEM.

AAV5-miHTT treatment results in efficient lowering of FL-HTT and HTT_{ex1} species in Q175 KI mice

2

In order to evaluate the efficacy of our AAV5-miHTT to reduce the pathogenic HTT_{ex1} we assessed both RNA and protein levels of HTT_{ex1}. RNA extracted from frontal cortex, together with primers spanning exon 1-2 and exon 64-65 junction were used to determine levels of *FL-Htt* mRNA, while primers within intron 1 and human exon1-intron1 junction were used for quantification of *HTT_{ex1}* mRNA (**Figure 1**, **Figure 4A** and **4B**). Two months after intrastriatal administration of AAV5-miHTT, we detected a 20% significant reduction of *FL-Htt* mRNA in the frontal cortex of high-dose treated mice compared to vehicle group (**Figure 4A**). Moreover, AAV5-miHTT treatment resulted in significant dose-dependent lowering of *HTT_{ex1}* transcript in the frontal cortex, up to 15% and 35% reduction with low and high dose of AAV5-miHTT, respectively (**Figure 4B**).

To quantify the levels of HTT_{ex1} protein at 2 months post-treatment, striatum and frontal cortex tissues from Q175 KI were lysed and subjected to HTRF with specific antibodies and protein levels of soluble mutant HTT, soluble HTT_{ex1}, aggregated HTT_{ex1} and murine FL-HTT were measured accordingly (**Figure 4C-4F**). Levels of mutant HTT species in AAV5-miHTT treated mice were analyzed as relative to levels in vehicle group and WT mice (background). High-dose AAV5-miHTT treatment resulted in a significant 45% and 28% reduction of soluble mutant HTT in striatum and frontal cortex, respectively (**Figure 4C**). Similarly, we detected a significant lowering of soluble HTT_{ex1} in striatum (36% knockdown) and cortex (24% knockdown) (**Figure 4D**). High-dose AAV5-miHTT treatment also resulted in a up to 20% dose-dependent lowering of aggregated HTT_{ex1} protein in striatum, but not in cortex (**Figure 4E**). In general, and consistent with intrastriatal delivery of AAV5-miHTT, we observed a significantly higher magnitude of HTT_{ex1} lowering in the striatum compared to the cortex. Since the miHTT was designed to exclusively target the human sequence (within mutant allele in Q175 mice) and not the murine sequence due to sequence mismatches, we did not expect, nor observed, a significant reduction of total full-length HTT protein in Q175 mice (**Figure 4F**).

Correlation analysis showed an inverse trend between miHTT levels in striatum and cortex in which higher levels of miHTT molecules resulted in stronger reduction of soluble HTT_{ex1} protein (Pearson correlation, $p = 0.2405$) (**Figure 4G**). Lack of statistical significance could be due to the fact that RNA and protein were measured in tissues from different hemispheres. When comparing the lowering efficacy of HTT_{ex1} in striatum and cortex, we observed a positive significant correlation between both brain areas (Pearson correlation, $**p = 0.0066$), demonstrating the widespread efficacy of AAV5-miHTT treatment in most affected brain areas (**Figure 4H**). All together, these results demonstrate

that the intrastriatal administration of AAV5-miHTT, in addition to lowering the full-length HTT, is an effective approach to reduce the toxic HTT_{ex1} protein in the brain of HD mice.

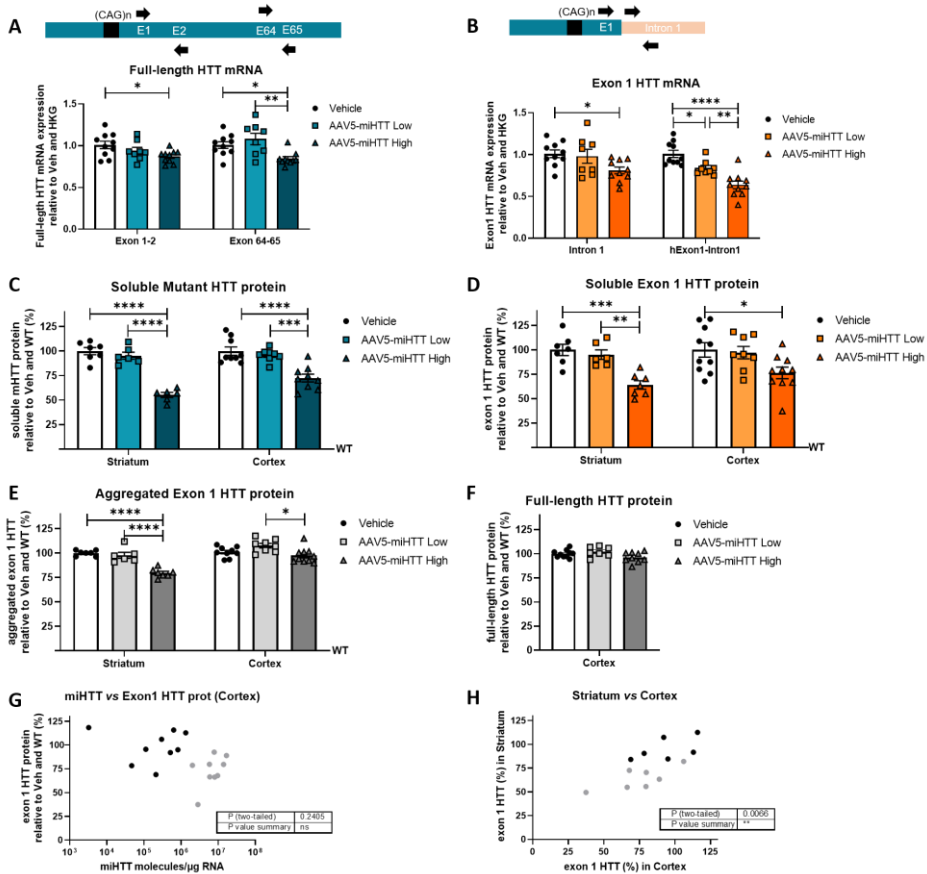


Figure 4. AAV5-miHTT shows dose-dependent lowering of full-length HTT and HTT_{ex1} mRNA and protein in Q175 KI mice at 2 months post-injection. **A)** Expression level of *FL-HTT* mRNA in right frontal cortex of AAV5-miHTT treated mice relative to vehicle group. **B)** Expression level of *HTT_{exon1}* mRNA in right frontal cortex of AAV5-miHTT treated mice relative to vehicle group. **C)** Levels of soluble mutant HTT protein in striatum and cortex of AAV5-miHTT treated mice relative to vehicle group and WT mice. **D)** Levels of HTT_{ex1} HTT protein in striatum and cortex of AAV5-miHTT treated mice relative to vehicle group and WT mice. **E)** Levels of aggregated HTT_{ex1} HTT protein in striatum and cortex of AAV5-miHTT treated mice relative to vehicle group and WT mice. **F)** Levels of full-length HTT protein in frontal cortex of AAV5-miHTT treated mice relative to vehicle group. **G)** Correlation analysis (Pearson's correlation) between levels of miHTT molecules/μg RNA (right frontal cortex) and relative HTT_{ex1} protein expression (left frontal cortex) **H)** Correlation analysis (Pearson's correlation) between HTT_{ex1} protein expression in left frontal cortex vs. striatum. A-F) Bars represent mean ± SEM; Statistics: one-way ANOVA, Tukey's multiple comparison's test, *p<0.05, **p<0.005, ***p<0.0005, ****p<0.0001). G and H) Each point represents an individual measurement per mice; statistics: Pearson's correlation test).

Potent suppression of HTT_{ex1} protein in humanized Hu128/21 mice upon AAV5-miHTT treatment

2

To further validate the lowering of HTT_{ex1} by AAV5-miHTT treatment in a different model, we selected the humanized Hu128/21 mouse model of HD (Caron *et al.*, 2020). Hu128/21 mice express two full-length human HTT transgenes heterozygous for the HD mutation (128CAG and 21CAG repeats) on the *Hdh*^{-/-} background (Southwell *et al.*, 2017). In a previous study we investigated the long-term tolerability and efficacy of AAV5-miHTT in Hu128/21 mice (Caron *et al.*, 2020). Following AAV5-miHTT striatal administration at 1 month of age, we reported a dose-dependent expression of miHTT, and a potent dose-dependent lowering of both wild-type and mutant FL-HTT in the striatum (up to 90%) and cortex (up to 60%) at 4 and 7 months post-injection (Caron *et al.*, 2020). AAV5-miHTT treatment ameliorated the loss of striatal volume and cognitive function in Hu128/21 mice. In this study we investigated the target engagement of HTT_{ex1} by AAV5-miHTT in Hu128/21 mice, that exclusively express human huntingtin sequences. We quantified HTT_{ex1} protein in both striatum and cortex of Hu128/21 at 4 months following intrastriatal administration of three increasing doses of AAV5-miHTT (**Figure 5A**). We measured a strong reduction of HTT_{ex1} with all doses of AAV5-miHTT in both the striatum (**Figure 5B**) and the cortex (**Figure 5C-D**) at 4 months post-injection (Two-way ANOVA treatment $p < 0.0001$, brain region 0.5989, interaction $p = 0.4224$). These data confirm the consistent efficacy of AAV5-miHTT treatment to reduce the highly pathogenic HTT_{ex1} protein in HD mice carrying human *HTT* gene.

A

Mouse model	Treatment	Dose AAV-miHTT	N	Duration treatment
Hu128/21 (2 months age)	Vehicle	-	7	4 months
	AAV5-miHTT	Low dose	7	
	AAV5-miHTT	Mid dose	7	
	AAV5-miHTT	High dose	7	

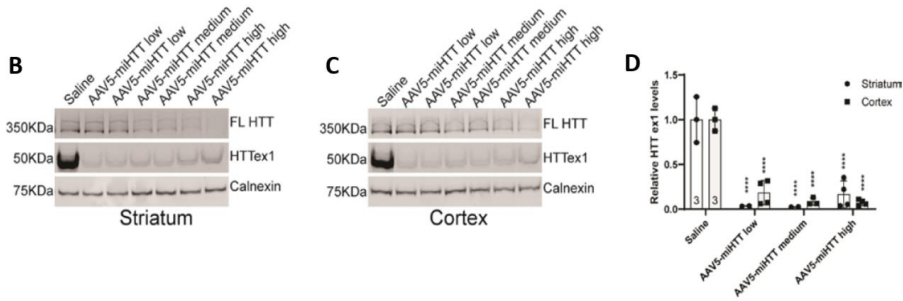


Figure 5: AAV5-miHTT treatment lowers levels of HTTex1 protein in Hu128/21 mice. A) Overview of study design from Caron *et al.* (Caron *et al.*, 2020). **B-C)** Western blots demonstrating HTTex1 lowering with AAV5-miHTT in the (B) striatum and (C) cortex at 4 months post-injection. Full length huntingtin lowering was also demonstrated on the same blots for reference. **D)** Quantification of relative HTTex1 levels in the striatum and cortex with increasing doses of AAV5-miHTT (Two-way ANOVA treatment $p < 0.0001$, brain region $p = 0.5989$, interaction $p = 0.4224$. Sidak's multiple comparison test **** $p < 0.0001$. N=24). Bars represent mean \pm SEM.

Discussion

The work presented here demonstrates that targeting the exon 1 sequence of HTT with an AAV5-delivered engineered miRNA is an effective approach to suppress both the mutant FL-HTT protein and the pathogenic HTTex1 fragment in the brain of HD mice. These results are an important extension of our previous studies which showed that intrastriatal delivery of AAV5-miHTT treatment resulted in widespread expression throughout the brain and that AAV5-miHTT caused a significant dose-dependent reduction of mutant HTT protein in HD iPSC-derived neurons, HD mice, HD transgenic minipigs and nonhuman primates (Miniarikova *et al.*, 2017; Evers *et al.*, 2018; Spronck *et al.*, 2019, 2021; Caron *et al.*, 2020; Valles *et al.*, 2021). This, together with the long-term HTT expression, the favorable safety profile, and the beneficial prevention of neurological phenotypes, supported the initiation

2 of AAV5-miHTT therapy in a phase I/II clinical trial in HD patients. (<https://clinicaltrials.gov/NCT04120493>). We have previously reported that AAV5-miHTT treatment lowered the expression of HTT_{ex1} protein in R6/2 mice (Spronck *et al.*, 2019), a transgenic mouse with an expanded human HTT exon 1 sequence (Mangiarini *et al.*, 1996), and improved median survival of R6/2 mice up to 4 weeks (Spronck *et al.*, 2019). However, the finding of HTT_{ex1} generation by aberrant splicing by Sathasivam *et al.* raised the question whether the therapeutic efficacy of AAV5-miHTT would be the same in an HD-associated splicing context (Sathasivam *et al.*, 2013). To our knowledge, this is the first study that demonstrates the efficacy of a HTT lowering-based treatment to successfully reduce the pathogenic HTT_{ex1} generated by alternative splicing *in vivo*, adding great therapeutic value to the AAV5-miHTT gene therapy for HD. In contrast to most nucleic-acid-based approaches that have been designed to treat HD, AAV5-miHTT targets exon 1 sequence, thereby lowering both HTT_{ex1} as well as FL-HTT.

In this study we used two mouse models of HD, the transgenic Q175 KI mice and the humanized Hu128/21 mice. In both mouse models, we observed a significant reduction of the toxic HTT_{ex1} protein with comparable doses of AAV5-miHTT, with the effect being strikingly larger in Hu128/21 mice. These results could be due to differences in splicing ratio, the analytical methods used and/or increasing levels of accumulation due to somatic instability. In Q175 KI, aberrant splicing ratio and levels of HTT_{ex1} mRNA and protein detected at 7 months of age were in concordance with previous studies (Sathasivam *et al.*, 2013; Neueder *et al.*, 2017; Landles *et al.*, 2021). HTT_{ex1} levels were also significantly higher in striatum than in frontal cortex, the former being the main affected brain area in HD patients (Reiner *et al.*, 1988; Landles *et al.*, 2021). As we have reported previously (Valles *et al.*, 2021), higher striatal miHTT expression was accompanied by greater HTT lowering when compared to cortical areas. Moreover, AAV5-miHTT treatment resulted in reduction of HTT_{ex1} aggregates, previously shown to significantly increase over time in Q175 KI mouse brains (Landles *et al.*, 2021). In Hu128/21 mice, we did not measure the levels of HTT_{ex1} mRNA due to the lack of sample material and therefore we did not assess the splicing ratio in the current study. Previous studies have reported high levels of HTT_{ex1} transcripts and protein in other human HTT mouse models, YAC128 and BACHD (Sathasivam *et al.*, 2013), which were used to generate the Hu128/21 mouse model in a *Hdh*^{-/-} background (Southwell *et al.*, 2017). In our study, high levels of HTT_{ex1} protein were detected in striatum and cortex of non-treated Hu128/21 mice by western blot, a less accurate method of quantification than HTRF. Nonetheless, in two independent HD mouse models and using two different analytical methods, AAV5-miHTT treatment caused a significant lowering of both FL-HTT and HTT_{ex1} HTT in the striatum and cortex of both mouse models of HD. In Hu128/21 mice treated at 1 month of age, AAV5-miHTT administration resulted in a dose-dependent lowering of FL-HTT (Caron *et al.*, 2020), together with a practically complete

suppression of HTT_{ex1} protein at all doses. Since the HTT_{ex1} lowering efficacy is calculated as relative to levels in non-treated mice, and not to levels prior treatment, the potent HTT_{ex1} reduction could represent a prevention of HTT_{ex1} accumulation during 4 months of treatment, even at low doses of AAV5-miHTT.

The generation of HTT_{ex1} transcripts by aberrant splicing has been shown to occur in a CAG repeat length-dependent manner (Sathasivam *et al.*, 2013; Neueder *et al.*, 2017, 2018). Hence, in contrast to FL-HTT protein, levels of the pathogenic HTT_{ex1} may increase and accumulate over time if CAG repeat length expands via somatic instability as is known to occur in HD patients (Swami *et al.*, 2009). We did not measure somatic CAG repeat instability in the brain of Q175 KI and Hu128/21 mice, but uninterrupted repeat regions of CAG repeats, such as in YAC128 mice (Pouladi *et al.*, 2012a), are more prone to expand via somatic instability, causing an increase HTT_{ex1} production over time. Further studies are needed to investigate whether the efficacy of AAV5-miHTT to reduce HTT_{ex1} is robust upon somatic CAG expansion instability. To answer those questions, treatments need to be performed at different time points relative to the development of HD pathology in the brain.

Preliminary data have shown that lowering of FL-HTT by ASOs, results in reduction of somatic expansion of both *HTT* and *ATXN2* CAG tracts in the liver of HD mice (Coffey *et al.*, 2020), suggesting that HTT protein plays a role in regulating somatic instability occurring at several repeat expanded loci. Moreover, genome-wide association studies have identified DNA mismatch repair (MMR) genes required for somatic stability as key genetic modifiers of HD of disease onset (Lee *et al.*, 2015; Goold *et al.*, 2019; Iyer and Pluciennik, 2021). Several studies have demonstrated suppression of CAG expansion by targeting MMR genes *in vitro* and *in vivo* models of HD (Pinto *et al.*, 2020; Roy *et al.*, 2021), proposing a potential treatment for HD and other repeat expansion disorders (Maiuri *et al.*, 2019). In general, these studies suggest that HTT lowering and DNA repair-targeting approaches may indirectly slow down the production of the pathogenic HTT_{ex1} by suppressing somatic CAG expansions. Although these approaches could slow down the disease progression if applied in early stages of the disease, they would not be expected to prevent the slow but steady accumulation of the highly toxic HTT_{ex1} fragment.

Most current disease-modifying therapies for HD are based on HTT lowering technologies (Tabrizi *et al.*, 2019b; Leavitt *et al.*, 2020). However, lack of efficacy with intrathecal infusion of ASO have raised the concern about the potential of HTT lowering therapies as a treatment for HD (Kingwell, 2021). One important hurdle that all HTT-lowering interventions need to overcome is the effective delivery of therapeutics to the deep brain areas such as striatum, characterized by high levels of HTT_{ex1} aggregation and neurodegeneration. Importantly, the data reported in the current study indicate that the location of the target sequence within the HTT gene can also contribute to discrepancies in

therapeutic efficacy between drug candidates. Lowering of FL-HTT by targeting sequences distant from the CAG-containing exon 1 might not prevent the generation of highly toxic aberrantly spliced HTT species. Hence, when designing therapeutic HTT lowering strategies for HD, the target sequence should be chosen to reduce not only the full-length protein, but also the pathogenic HTTex1 protein. Engineered miRNAs targeting sequences close to the repeat expansion have also been effective in other CAG-repeat expansion disorders, such as spinocerebellar ataxin 3 (SCA3) (Martier *et al.*, 2019).

In conclusion, our data demonstrate that exon 1-targeting miRNA delivered by AAV5 is an effective approach to reduce the levels of the pathogenic HTTex1 fragment in an HD-associated splicing context. These results, together with all previous studies demonstrating the efficacy and safety of AAV5-miHTT in preclinical studies, support continued clinical development of AAV5-miHTT gene therapy in HD patients. Therapeutics that target the exon 1 HTT sequence address several primary causes of HD pathology and progression – the mutant FL-HTT, the pathogenic HTTex1 fragment and the correction of somatic CAG repeat instability – suggesting that they could achieve a greater efficacy for the treatment of HD.

Material and methods

AAV5-miHTT gene therapy

The AAV5 vector carrying the miHTT cassette was produced using a baculovirus-based AAV production system (uniQure, Amsterdam, the Netherlands) as described previously (Lubelski *et al.*, 2014). The miRNA expression cassette comprising the miRNA sequence targeting HTT exon 1 sequence driven by the chimeric chicken-beta actin promoter (Miniarikova *et al.*, 2016), was inserted into an AAV vector genome backbone flanked by two intact non-coding AAV2 inverted terminal repeats (ITR).

Q175 KI mice injection and tissue collection

The Q175 KI HD mouse model was generated by spontaneous expansion of the human-mouse chimeric Q140 line (Heikkinen *et al.*, 2012; Menalled *et al.*, 2012). Q175 KI contains a human-mouse chimeric HTT gene composed of mouse 5'UTR and 28bp of exon 1, followed by the remaining exon 1 sequence of human origin containing around 188 CAG repeats, 10bp of human intron 1, with 94bp of mouse intron 1 deleted. Heterozygous Q175 KI mice have a chimeric human-mouse expanded HTT allele and a wild-type murine allele. Wild type mice and heterozygous Q175 KI were treated at 5 months of age by stereotaxic bilateral intrastriatal injection under inhalation anaesthesia, followed by 8-weeks observation period before sacrifice. All mice were injected with 4 µl of solution per site using aseptic surgical procedures. The WT control group was injected with formulation buffer,

and treated mice were injected with two ascending doses of AAV-miHTT: low dose (5.2×10^9 genome copies/mouse) or high dose (1.3×10^{11} genomes copies/mouse). After treatment, mice were kept at room temperature on a normal light cycle with free access to chow (Lab Diet) and drinking water provided through the cage rack system. After 2 months of treatment, mice were sacrificed by Avertin overdose. Mouse brains were extracted immediately following euthanasia and micro-dissected on ice. Striatum, both hemispheres of cortex and cerebellum regions were collected and stored at -80°C until analysis.

Hu128/21 mice injection AAV5-miHTT delivery and tissue collection

The efficacy of AAV5-miHTT treatment was also investigated in the Hu128/21 mouse model of HD (Southwell *et al.*, 2017). Hu128/21 mice were generated by intercrossing YAC128 and BAC21 models of HD with the *Hdh*^{-/-} background (Slow *et al.*, 2003, Pouladi *et al.*, 2012b). Experiments were performed with the approval of the Animal Care Committee at the University of British Columbia (A16-030). As previously published (Caron *et al.*, 2020), mice were anesthetized with isoflurane and placed into a stereotaxic frame. After a midline incision was made, a dental drill was used to make bilateral burr holes at 0.8 mm anterior and 1.8 mm lateral to Bregma. A Hamilton syringe with 30 gauge needle (Hamilton, Reno, NV) was pre-loaded with 3 μl of sterile saline and then with 2 μl of AAV5-miHTT solution diluted to the appropriate titre in sterile saline. The needle was lowered to 3.5 mm below the surface and AAV5-miHTT injected at 0.5 $\mu\text{l}/\text{min}$ using an UltraMicroPump with Micro4 controller (World Precision Instruments). The needle was left in place for 5 min and then withdrawn slowly. At 4-month after injection, mice were sacrificed, and brains were removed and placed on ice for 1 min to increase tissue rigidity. Brains were subsequently microdissected and striata and cortices regions were preserved in RNAlater (Ambion) overnight at 4°C and then stored at -80°C until use (Caron *et al.*, 2020).

RNA isolation, reverse transcription (RT), PCR and quantitative RT-PCR

Total RNA was isolated from crushed brain tissue using a Direct-zolTM RNA MiniPrep kit (Zymo Research) according to the manufacturer's protocol. The DNase treatment and the reverse transcription were performed using the Maxima First Strand cDNA Synthesis Kit (Thermo Fisher, K1671). Briefly, 200 ng of total RNA was treated with 1 μl of 10X dsDNase Buffer and 1 μl of dsDNase for 5 min at 37°C . Then, RNA was reverse transcribed with 4 μl of 5X Reaction Mix, 2 μl of Maxima enzyme Mix and 4 μl of DEPC-treated water. After the RT reaction, the cDNA was diluted 1:5 in DEPC-treated water.

All PCRs were carried out using the Platinum Green Hot system (PlatinumTM Green Hot Start PCR Master Mix (2X), InvitrogenTM, 13001012). Each PCR contained 5 μl of 2X Platinum, 2 μl of 5X GC enhancer, each 0.2 μl of 1000 μM primers, 2 μl cDNA template and water to 10 μl . PCR protocols were as follow: 1 cycle 98°C for 3 min, 35 cycles 98°C for 15 sec, 59°C

for 20 sec, 72°C for 30 sec, 1 cycle 72°C for 5 min. The product was migrated in 2 % Agarose Gel contained SYBR™ Safe DNA Gel Stain (6 µL/100 mL of buffer, Invitrogen™) diluted in 0.5 TAE Buffer (Tris base, acetic acid, EDTA) for 2h at 75V. Bands were excised from the gel, the DNA was purified with the GeneJET Gel Extraction Kit (Thermo Fisher™, K0691), and sequenced by BaseClear B.V. (Leiden). Primer and probe sequences and combinations are in **Table 1-3**.

Quantitative RT-PCR (qRT-PCR) was performed using TaqMan Universal Master Mix II (Thermo Fisher™) and specific primers and probes for detection of HTT mRNA species (**Table 1-3** and (Sathasivam *et al.*, 2013)). For all the primer-probe sets, the concentration was 30 µM primers + 6 µM probe. Each RT-qPCR contained 5 µL of TaqMan Universal Master Mix II with UNG, 0.5 µl of primer-probe mix (0.15 µL of each 100 µM primers, 0.03 µL of 100 µM probes), 4 µL of cDNA template and water to 10 µL. qPCR protocol was a follow: 1 cycle 95°C for 20 sec, 40 cycles 95°C for 3 sec, 60°C for 30 sec. Results were normalized to the expression level of three housekeeping genes (GAPDH, Atp5b, Ubc) measured with 7500 Software v2.3. Expression levels were quantified by Pfaffl's method, calculating the GeoMean of mentioned HKG.

Table 1: Primer and probe sequences for Q175 KI. All primers were purchased at Eurofins Genomics and probes at Applied Biosystems. Fw: forward, rv: reverse, p: probe, Tm: temperature melting.

Name	Sequence (5' to 3')	Position start/end in bp (start from HTT exon 1)	Size (nt)	Assay	Tm (°C)
-19 fw	AGGAACCGCTGCACCGA	348 – 364	17	PCR	57.6
Ex2 fw					
Ex2 p	AGAAAGACCGTGTGATCATTGTCTAACAAATATGTGA	21022 – 21058	37	qPCR	
Ex2 rv	CTGAGAGACTGTGCCACAATGTT	21060 – 21082	23	PCR, qPCR	60.6
135 fw	CTTGCGGGGTCTCTGGC	501 – 517	17	qPCR	60
200 rv	TCAGCGAGTCCCTGGCTG	549 – 566	18	qPCR	60.5
155 p	CCTCAGAGGAGACAGAGCCGGGTCA	521 – 545	25	qPCR	

Table 2: TaqMan Gene expression assays for detection of FL-Htt and mouse HKG expression. These assays were purchased at Applied Biosystems (Thermo Fisher Scientific).

Gene targeted	Number
HTT Exon 64-65	Mm01213820_m1
GAPDH	Mm99999915_g1
Atp5b	Mm01160389_g1
Ubc	Mm01198158_m1

Table 3: Set of specific primers used for the qPCR for Q175 KI mice. Fw: forward, rv: reverse, p: probe.

Region	Primers
Exon 1-2	-19 fw / Ex2 rv / Ex2 p
Intron 1	135 fw / 200 rv / 155 p

OligodT reverse transcription and 3'RACE-PCR

DNase treatment was performed as described above and RNA was reverse transcribed with anchored-oligonucleotide(18dT)-tailed primer (QT 3'RACE, Integrated DNA Technologies). A total of 200 ng of total RNA was treated with 4 μ L of 5 Reverse Transcription Buffer, 1 μ L of 10 mM dNTP solution (Thermo Fisher™), 2 μ L of 0.1 M DTT, 0.5 μ L of 100 ng/ μ L QT primer, 0.25 μ L of 40 U/ μ L RNasin (RNasin® Ribonuclease Inhibitors Plus, Promega), 200 U of Superscript IV RT (SuperScript™ IV Reverse Transcriptase kit, Invitrogen™) and water up to 20 μ L. The reaction mix was incubated as follows: 1 h at 42°C, 10 min at 50°C and 15 min at 70°C. Then the cDNA was digested with 1.5 U of RNaseH (Thermo Fisher™) and incubated for 20 min at 37°C.

The Rapid Amplification of cDNA Ends (3'RACE) was performed according to Sathasivam et al, 2013 (Sathasivam *et al.*, 2013). Each 3'RACE consisted of 2 rounds of amplification by PCR with gene-specific primers (Table 4). Each 3'RACE contained 1ul of non-diluted cDNA, 5 μ L of 5X buffer, 2 μ L of 25 mM MgCl₂ solution, 0.5 μ L of 10 mM dNTP solution, each 0.05 μ L of 100 μ M primers, 0.125 μ L of GoTaq and water to 25 μ L. First 3'RACE round was performed with primers Q₀ and 571f w, 5X uncolored buffer, as follows: 1 cycle for 2 min at 94°C, 10 cycles for 15 sec at 94°C, 25 sec at 59°C, 2 min at 72°C, 30 cycles for 15 sec at 94°C, 20 sec at 59°C, 1 min 45 sec at 72°C, 1 cycle for 6 min at 72°C. Second 3'RACE round was performed with primers Q_i and 622 fw, 5X green buffer, as follow: 1 cycle for 2 min at 94°C, 35 cycles for 15 sec at 94°C, 20 sec at 62°C, 1 min at 72°C, 1 cycle for 6 min at 72°C.

Table 4: Primer sequences for 3'RACE. All primers were purchased at Eurofins Genomics. fw: forward, Tm: melting temperature.

Name	Sequence	Position start/end in bp (start from HTT Intron 1)	Size (nucleotides)	Tm (°C)
Q _T 3'RACE	CCAGTGAGCAGAGTGA CGAGGACTCGAGCTCAA GCTTTTTTTTTTTTTTTTTT	polyA tails	52	66.9
Q ₀	CCAGTGAGCAGAGTGA CG	/	18	58
Q _i	GAGGACTCGAGCTCAA GC	/	18	58
571 fw	AACCAGGTTTTAAGCAT AGCCAGA	571 – 594	24	59
622 fw	AGTTGGATGAGTTGTAT TTGTCAAGTACAT	622 – 651	30	61

FL-HTT and HTTex1 protein quantification by HTRF

Protein lysates from left frontal cortex and striata from mice were prepared according to Landles et al. 2021 (Landles *et al.*, 2021). Briefly, 10% (w/v) total protein homogenate was prepared in ice-cold buffer 1% Triton-X-100 in phosphate-buffered saline (PBS) with complete protease inhibitor cocktail tablets (Roche), and homogenized in a Fast-Prep-24 instrument (MP Biomedical). For protein aggregates, 10 µl crude lysate was used, whereas for soluble proteins, 10 µl of supernatant was used after brief centrifugation at 3500×g for 10 min. All samples were run in triplicates. For HTRF assay, a ratio of 1 ng donor (terbium cryptate) to 20 ng acceptor (Alexa-488 for 4C9 and d2 for all other antibodies) was added per well in 5 µl HTRF detection buffer (50 mM NaH₂PO₄, 0.2 M KF, 0.1% bovine serum albumin and 0.05% Tween-20) with complete protease inhibitor cocktail tablets (Roche). Plates were incubated at room temperature for 1.5h, before signal detection using EnVision (Perkin Elmer) plate reader.

Statistical analysis

Statistical analysis was performed with GraphPad Prism 9 software. Using unpaired t-test, Pearson's correlation and one-way ANOVA, with Tukey's or Sidak's multiple comparison's *post hoc* tests as indicated. Graphs were arranged using GraphPad Prism 9. P-values less than 0.05 were considered statistically significant (*ns* non-significant, *p<0.05, **p<0.005, ***p<0.0005, ****p<0.0001).

References

- Arrasate M, Finkbeiner S. Protein aggregates in Huntington's disease. *Exp Neurol* 2012; 238: 1–11.
- Barbaro BA, Lukacsovich T, Agrawal N, Burke J, Bornemann DJ, Purcell JM, et al. Comparative study of naturally occurring Huntingtin fragments in *Drosophila* points to exon 1 as the most pathogenic species in Huntington's disease. *Hum Mol Genet* 2015; 24: 913–25.
- Caron NS, Southwell AL, Brouwers CC, Cengio LD, Xie Y, Black HF, et al. Potent and sustained huntingtin lowering via AAV5 encoding miRNA preserves striatal volume and cognitive function in a humanized mouse model of Huntington disease. *Nucleic Acids Res* 2020; 48: 36–54.
- Chongtham A, Bornemann DJ, Barbaro BA, Lukacsovich T, Agrawal N, Syed A, et al. Effects of flanking sequences and cellular context on subcellular behavior and pathology of mutant HTT. *Hum Mol Genet* 2020; 29: 674–88.
- Coffey S, Andrew M, Ging H, Hamilton J, Flower M, Kovalenko M, et al. Huntingtin lowering reduces somatic instability at CAG-expanded loci. *bioRxiv* 2020; preprint
- Evers MM, Miniarikova J, Juhas S, Vallès A, Bohuslavova B, Juhasova J, et al. AAV5-miHTT Gene Therapy Demonstrates Broad Distribution and Strong Human Mutant Huntingtin Lowering in a Huntington's Disease Minipig Model. *Mol Ther* 2018; 26: 2163–77.
- Goold R, Flower M, Moss DH, Medway C, Wood-Kaczmar A, Andre R, et al. FAN1 modifies Huntington's disease progression by stabilizing the expanded HTT CAG repeat. *Hum Mol Genet* 2019; 28: 650–61.
- Gutekunst CA, Li SH, Yi H, Mulroy JS, Kuemmerle S, Jones R, et al. Nuclear and neuropil aggregates in Huntington's disease: Relationship to neuropathology. *J Neurosci* 1999; 19: 2522–34.
- Harper SQ, Staber PD, He X, Eliason SL, Martins IH, Mao Q, et al. RNA interference improves motor and neuropathological abnormalities in a Huntington's disease mouse model. *Proc Natl Acad Sci U S A* 2005; 102: 5820–5.
- Heikkinen T, Lehtimäki K, Vartiainen N, Puoliväli J, Hendricks SJ, Glaser JR, et al. Characterization of Neurophysiological and Behavioral Changes, MRI Brain Volumetry and 1H MRS in zQ175 Knock-In Mouse Model of Huntington's Disease. *PLoS One* 2012; 7: e50717.
- Iyer RR, Pluciennik A. DNA Mismatch Repair and its Role in Huntington's Disease. *J Huntingtons Dis* 2021; 10: 75–94.
- Kingwell K. Double setback for ASO trials in Huntington disease. *Nat Rev Drug Discov* 2021; 20: 412–3.
- Kordasiewicz HB, Stanek LM, Wancewicz EV, Mazur C, McAlonis MM, Pytel KA, et al. Sustained Therapeutic Reversal of Huntington's Disease by Transient Repression of Huntingtin Synthesis. *Neuron* 2012; 74: 1031–44.
- Landles C, Milton RE, Jean A, McLarnon S, McAteer SJ, Taxy BA, et al. Development of novel bioassays to detect soluble and aggregated Huntingtin proteins on three technology platforms [Internet]. *Brain Commun* 2021; 3.
- Landles C, Sathasivam K, Weiss A, Woodman B, Moffitt H, Finkbeiner S, et al. Proteolysis of Mutant Huntingtin Produces an Exon 1 Fragment That Accumulates as an Aggregated Protein in Neuronal Nuclei in Huntington Disease. *J Biol Chem* 2010; 285: 8808–23.
- Leavitt BR, Kordasiewicz HB, Schobel SA. Huntingtin-Lowering Therapies for Huntington Disease: A Review of the Evidence of Potential Benefits and Risks. *JAMA Neurol* 2020; 77: 764–72.

Chapter 2

Lee JM, Wheeler VC, Chao MJ, Vonsattel JPG, Pinto RM, Lucente D, et al. Identification of Genetic Factors that Modify Clinical Onset of Huntington's Disease. *Cell* 2015; 162: 516–26.

Lubelski J, Hermens W, Petry H. Insect Cell-Based Recombinant Adeno-Associated Virus Production: Molecular Process Optimization. *Bioprocess J* 2014; 13: 6–11.

MacDonald ME, Ambrose CM, Duyao MP, Myers RH, Lin C, Srinidhi L, et al. A novel gene containing a trinucleotide repeat that is expanded and unstable on Huntington's disease chromosomes. *Cell* 1993; 72: 971–83.

Maiuri T, Suart CE, Hung CLK, Graham KJ, Barba Bazan CA, Truant R. DNA Damage Repair in Huntington's Disease and Other Neurodegenerative Diseases. *Neurotherapeutics* 2019; 16: 948–56.

Mangiarini L, Sathasivan K, Seller M, Cozens B. Exon1 of the HD gene expanded. *Cell* 1996; 87: 493–506.

Martier R, Sogorb-Gonzalez M, Stricker-Shaver J, Hübener-Schmid J, Keskin S, Klima J, et al. Development of an AAV-Based MicroRNA Gene Therapy to Treat Machado-Joseph Disease. *Mol Ther - Methods Clin Dev* 2019; 15: 343–58.

Marxreiter F, Stemick J, Kohl Z. Huntingtin lowering strategies [Internet]. *Int J Mol Sci* 2020; 21.

Menalled LB, Kudwa AE, Miller S, Fitzpatrick J, Watson-Johnson J, Keating N, et al. Comprehensive Behavioral and Molecular Characterization of a New Knock-In Mouse Model of Huntington's Disease: ZQ175. *PLoS One* 2012; 7.

Miniarikova J, Zanella I, Huseinovic A, van der Zon T, Hanemaaijer E, Martier R, et al. Design, Characterization, and Lead Selection of Therapeutic miRNAs Targeting Huntingtin for Development of Gene Therapy for Huntington's Disease. *Mol Ther - Nucleic Acids* 2016; 5: e297.

Miniarikova J, Zimmer V, Martier R, Brouwers CC, Pythoud C, Richetin K, et al. AAV5-miHTT gene therapy demonstrates suppression of mutant huntingtin aggregation and neuronal dysfunction in a rat model of Huntington's disease. *Gene Ther* 2017; 24: 630–9.

Neueder A, Dumas AA, Benjamin AC, Bates GP. Regulatory mechanisms of incomplete huntingtin mRNA splicing [Internet]. *Nat Commun* 2018; 9.

Neueder A, Landles C, Ghosh R, Howland D, Myers RH, Faull RLM, et al. The pathogenic exon 1 HTT protein is produced by incomplete splicing in Huntington's disease patients. *Sci Rep* 2017; 7: 1–10.

Papadopoulou AS, Gomez-Paredes C, Mason MA, Taxy BA, Howland D, Bates GP. Extensive Expression Analysis of Htt Transcripts in Brain Regions from the zQ175 HD Mouse Model Using a QuantiGene Multiplex Assay. *Sci Rep* 2019; 9: 1–10.

Pinto RM, Arning L, Giordano J V., Razghandi P, Andrew MA, Gillis T, et al. Patterns of CAG repeat instability in the central nervous system and periphery in Huntington's disease and in spinocerebellar ataxia type 1. *Hum Mol Genet* 2020; 29: 2551–67.

Pouladi MA, Stanek LM, Xie Y, Franciosi S, Southwell AL, Deng Y, et al. Marked differences in neurochemistry and aggregates despite similar behavioural and neuropathological features of Huntington disease in the full-length BACHD and YAC128 mice. *Hum Mol Genet* 2012; 21: 2219–32.

Reiner A, Albin RL, Anderson KD, D'Amato CJ, Penney JB, Young AB. Differential loss of striatal projection neurons in Huntington disease. *Proc Natl Acad Sci U S A* 1988; 85: 5733–7.

Rodriguez-Lebron E, Denovan-Wright EM, Nash K, Lewin AS, Mandel RJ. Intrastratial rAAV-mediated delivery of anti-huntingtin shRNAs induces partial reversal of disease progression in R6/1 Huntington's disease transgenic mice. *Mol Ther* 2005; 12: 618–33.

Roy JCL, Vitalo A, Andrew MA, Mota-Silva E, Kovalenko M, Burch Z, et al. Somatic CAG expansion in Huntington's disease is dependent on the MLH3 endonuclease domain, which can be excluded via splice redirection. *Nucleic Acids Res* 2021; 49: 3907–18.

Samaranch L, Blits B, San Sebastian W, Hadaczek P, Bringas J, Sudhakar V, et al. MR-guided parenchymal delivery of adeno-associated viral vector serotype 5 in non-human primate brain. *Gene Ther* 2017; 24: 253–61.

Sathasivam K, Neueder A, Gipson TA, Landles C, Benjamin AC, Housman DE, et al. Aberrant splicing of HTT generates the pathogenic exon 1 protein in Huntington disease. *PNAS* 2013.

Schilling G, Becher MW, Sharp AH, Jinnah HA, Duan K, Kotzuc JA, et al. Intracellular inclusions and neuritic aggregates in transgenic mice expressing a mutant N-terminal fragment of huntingtin. *Hum Mol Genet* 1999; 8: 397–407.

Slow EJ, van Raamsdonk J, Rogers D, Coleman SH, Graham RK, Deng Y, et al. Selective striatal neuronal loss in a YAC128 mouse model of Huntington disease. *Hum Mol Genet* 2003; 12: 1555–67.

Southwell AL, Skotte NH, Villanueva EB, Østergaard ME, Gu X, Kordasiewicz HB, et al. A novel humanized mouse model of Huntington disease for preclinical development of therapeutics targeting mutant huntingtin alleles. *Hum Mol Genet* 2017; 26: ddx021.

Spronck EA, Brouwers CC, Vallès A, de Haan M, Petry H, van Deventer SJ, et al. AAV5-miHTT Gene Therapy Demonstrates Sustained Huntingtin Lowering and Functional Improvement in Huntington Disease Mouse Models. *Mol Ther - Methods Clin Dev* 2019; 13: 334–43.

Spronck EA, Vallès A, Lampen MH, Montenegro-Miranda PS, Keskin S, Heijink L, et al. Intra-striatal administration of AAV5-MIHTT in non-human primates and rats is well tolerated and results in MIHTT transgene expression in key areas of huntington disease pathology. *Brain Sci* 2021; 11: 1–18.

Stoyas CA, La Spada AR. The CAG–polyglutamine repeat diseases: a clinical, molecular, genetic, and pathophysiologic nosology. In: *Handbook of Clinical Neurology*. Elsevier B.V.; 2018. p. 143–70

Swami M, Hendricks AE, Gillis T, Massood T, Mysore J, Myers RH, et al. Somatic expansion of the Huntington's disease CAG repeat in the brain is associated with an earlier age of disease onset. *Hum Mol Genet* 2009; 18: 3039–47.

Tabrizi SJ, Ghosh R, Leavitt BR. Huntingtin Lowering Strategies for Disease Modification in Huntington's Disease. *Neuron* 2019; 101: 801–19.

Takahashi T, Katada S, Onodera O. Polyglutamine diseases: Where does toxicity come from? What is toxicity? Where are we going? *J Mol Cell Biol* 2010; 2: 180–91.

Tanaka Y, Igarashi S, Nakamura M, Gafni J, Torcassi C, Schilling G, et al. Progressive phenotype and nuclear accumulation of an amino-terminal cleavage fragment in a transgenic mouse model with inducible expression of full-length mutant huntingtin. *Neurobiol Dis* 2006; 21: 381–91.

Valles A, Evers MM, Stam A, Gonzalez MS, Brouwers C, Tornero CV, et al. Widespread and sustained target engagement in Huntington's disease minipigs upon intra-striatal microRNA-based gene therapy [Internet]. *Sci Transl Med* 2021; 13.

Vieweg S, Mahul-Mellier A-L, Ruggeri FS, Riguet N, Deguire SM, Chiki A, et al. Towards deciphering the Nt17 code: How the sequence and conformation of the first 17 amino acids in Huntingtin regulate the aggregation, cellular properties and neurotoxicity of mutant Httex1. *bioRxiv* 2021: 2021.02.15.431207.

Wild EJ, Tabrizi SJ. Therapies targeting DNA and RNA in Huntington's disease. *Lancet Neurol* 2017; 16: 837–47.

Chapter 2

Yamamoto A, Lucas JJ, Hen R. Reversal of neuropathology and motor dysfunction in a conditional model of Huntington's disease. *Cell* 2000; 101: 57–66.

Zeitler B, Froelich S, Marlen K, Shivak DA, Yu Q, Li D, et al. Allele-selective transcriptional repression of mutant HTT for the treatment of Huntington's disease. *Nat Med* 2019; 25: 1131–42.

2

Chapter 3

Widespread and Sustained Target Engagement in Huntington Disease Minipigs upon Intrastratial MicroRNA-Based Gene Therapy

Astrid Vallès^{1†*}, Melvin M. Evers^{1†*}, Anouk Stam¹, **Marina Sogorb-Gonzalez**¹, Cynthia Brouwers¹, Carlos Vendrell-Tornero¹, Seyda Acar-Broekmans¹, Lieke Paerels¹, Jiri Klima³, Bozena Bohuslavova³, Roberta Pintauro², Valentina Fodale², Alberto Bresciani², Roman Liscak⁴, Dusan Urgosik⁴, Zdenek Starek⁵, Michal Crha⁶, Bas Blits¹, Harald Petry¹, Zdenka Ellederova³, Jan Motlik³, Sander van Deventer¹ and Pavlina Konstantinova¹

¹Department of Research & Development, uniQure B.V., Amsterdam, The Netherlands

²Department of Translational Biology, IRBM, Pomezia, Italy

³Institute of Animal Physiology and Genetics, Libechev, Czech Republic

⁴Department of Stereotactic Radioneurosurgery, Prague, Czech Republic

⁵Interventional Cardiac Electrophysiology, Brno, Czech Republic

⁶Small Animal Clinic, Veterinary and Pharmaceutical University, Brno, Czech Republic

† These authors contributed equally

Science Translational Medicine (2021); 13(588).

Abstract

Huntingtin (HTT)-lowering therapies hold promise to slow-down neurodegeneration in Huntington disease (HD). Here, we assessed the translatability and long-term durability of recombinant adeno-associated viral vector serotype 5 expressing a microRNA targeting human HTT (rAAV5-miHTT) administered by magnetic resonance imaging (MRI)-guided convention-enhanced delivery (CED) in transgenic HD (tgHD) minipigs. rAAV5-miHTT (1.2×10^{13} gc/brain) was successfully administered into the striatum (bilaterally in caudate and putamen), using age-matched untreated animals as controls. Widespread brain biodistribution of vector DNA was observed, with the highest concentration in target (striatal) regions, thalamus and cortical regions. Vector DNA presence and transgene expression were similar at 6- and 12-months post-administration. Expression of miHTT strongly correlated with vector DNA, with a corresponding reduction of mutant HTT (mHTT) protein of more than 75% in injected areas, and 30-50% lowering in distal regions. Translational pharmacokinetic and pharmacodynamic measures in cerebrospinal fluid (CSF) were largely in line with the effects observed in the brain. CSF miHTT expression was detected up to 12 months, with CSF mHTT protein lowering of 25-30% at 6- and 12-months post-dosing. This study demonstrates widespread biodistribution, strong and durable efficiency of rAAV5-miHTT in disease-relevant regions in a large brain, and the potential of using CSF analysis to determine vector expression and efficacy in the clinic.

Introduction

Huntington Disease (HD) is a devastating autosomal dominant neurodegenerative disorder caused by an extended CAG repeat in exon 1 of the huntingtin (HTT) gene, with progressive development of psychiatric, motor and cognitive symptoms (1). Neuropathology in HD precedes disease (motor) onset, especially in striatal regions, and extends throughout the brain with disease progression (2). At present, only symptomatic treatments are available, which do not address the primary pathology nor slow-down disease progression (3). Because of this high unmet need, efforts have been made to develop disease-modifying approaches for HD, many of these in clinical development or entering soon (4). HTT-lowering therapies are of particular interest, as they are conceived to knock-down the expression of the disease causative gene (5). Most of these therapies in clinical development for HD are based on the use of antisense oligonucleotides (ASOs), targeting specific regions of the HTT transcript, thereby reducing HTT mRNA and protein expression (6). Typically, ASOs are administered intrathecally on a periodical basis to ensure steady-state concentrations of the therapeutic agent (7). Based on pre-clinical studies, the expectations are that intrathecally administered ASOs efficiently reach the spinal cord and superficial brain regions (cortex), and less efficiently penetrate into deep brain regions such as caudate nucleus, unless higher doses are used (8). Nonetheless, results on cerebrospinal fluid (CSF) biomarkers show promise for HTT lowering ASOs (7), for which different trials are ongoing (ClinicalTrials.gov identifiers: NCT03761849, NCT03225833, NCT03225846). A recent study with divalent siRNAs injected into the CSF, showed sustained HTT lowering throughout the brain, holding promise for less repetitive injections and wider biodistribution of therapeutic agents (9).

In contrast to ASOs and siRNAs, adeno-associated viral vector (AAV) gene therapies for HD can be administered locally into the brain region of interest, after which they expand to interconnected regions through retrograde and anterograde transport, depending on the AAV serotype used (10). A single administration is presumed to be sufficient to ensure long-term persistence of the therapeutic transgene, especially in non-dividing cells such as neurons (11, 12). Local administration of rAAV5 was shown to result in preferential neuronal (both NeuN+ and DARPP32+) and astrocytic transduction (13, 14). AAV-based HTT-lowering therapies are in pre-clinical phases (15-19) or entering clinical development in the case of rAAV5-miHTT (ClinicalTrials.gov identifier: NCT04120493). rAAV5-miHTT is a recombinant AAV-based gene therapy expressing an engineered microRNA specifically designed to bind to HTT exon 1 (20), resulting in lowering of both wild type and mutant HTT mRNA. This approach has demonstrated efficacy and safety in in vitro models as well as in small and large animal studies, without off-target effects (20-25), supporting transition to clinical investigation. To ensure precise administration and spread of the AAV, a thorough

evaluation of the surgical approach envisaged for the clinic, in relation to the resulting biodistribution and long-term persistence in a large brain is of crucial importance. In addition, adequate translational measures to evaluate the safety, efficacy and durability of rAAV-mediated HTT lowering in patients are much needed. Efficacy and durability aspects were addressed in the present study, using minipigs as a model.

Minipigs have a good similarity to humans in terms of brain structure, cerebral blood supply and immune responses (26) and we have previously reported in the utility of tgHD minipigs to evaluate different routes of administration of rAAV5-miHTT (23). This large animal model of HD expresses a transgene encoding the first 548 amino acids of HTT with 124 glutamines under the control of the human HTT promoter (27), with relatively slow and mild phenotype development shown so far (28-32), making this model suitable for translational purposes. In the current study we have applied clinically translatable MRI-guided convention-enhanced delivery (CED) of rAAV5-miHTT in the tgHD minipig model and assessed long-term rAAV5-miHTT vector biodistribution, target engagement and HD biofluid biomarkers. The caudate nucleus and putamen were chosen as surgical target regions, as the primary affected regions in HD and with relevant connections to cortical areas, which are affected later in the disease (2). For longitudinal evaluation of biomarkers in cerebrospinal fluid (CSF), mutant (m)HTT and neurofilament light chain (NFL) were chosen as disease-specific measures as both increase with disease progression in humans (33), and miHTT as a measure for rAAV5-miHTT expression.

We here report on the feasibility, precision and efficacy of MRI-guided CED of rAAV5-miHTT in caudate and putamen of tgHD minipigs, leading to strong, sustained and brain-widespread vector distribution, human HTT protein lowering and associated biomarker changes. These results support the translational value of these measures and the continuation of rAAV5-miHTT into the clinic as promising HD-modifying agent.

Results

Successful dosing and target acquisition in caudate and putamen of tgHD minipigs using MRI-guided convection-enhanced delivery

rAAV5-miHTT encodes an engineered miRNA embedded into the human miR-415a precursor, targeting exon1 of human HTT (5' of the CAG expansion repeat) (Supplementary Figure 1A). Upon transduction, episomal expression of rAAV5-miHTT should ensure continued supply of miHTT, leading to HTT protein lowering (Supplementary Figure 1B). For HTT lowering approaches to be successful in patients, especially for gene therapy approaches where a single administration should be sufficient, it is crucial to obtain information on long-term efficacy and brain biodistribution after a single administration in a large brain. To this end, the tgHD minipig model of HD was chosen, using the same target structures and surgical approach as envisaged for the clinic. Young (4- to 6-month old, when sinus formation is not yet developing) tgHD minipigs were used. Naïve (untreated) age-matched tgHD animals were used as controls.

To increase translatability of our study, we applied an administration protocol as close as possible to the one envisaged for the clinic. Intracranial MRI-guided convection-enhanced delivery (CED) was used to administer rAAV5-miHTT in the caudate and putamen of tgHD minipigs. This is the first time that this surgical protocol for gene therapy delivery is used in this model. All sixteen tgHD minipigs used in the surgical part of the study were successfully infused into the putamen and nucleus caudate. The two striatal structures were chosen as they are key to the pathology of HD and have relevant connections to cortical regions impacted at later disease stages (2). Surgical planning was undertaken using the Renishaw neuroinspire software. Each subject was implanted bilaterally with a total of four catheters – one in each putamen and each caudate nucleus, receiving 100µl of 3x10¹³ gc/mL rAAV5-miHTT per catheter using the Renishaw neuroinspire planning software and drug delivery system. Gadoteriol (ProHance, 2mM) was used as a contrast agent to visualize the filling of the target structures (**Figure 1**). To confirm target acquisition, a final MR image was taken, and guiding tubes and catheters were removed ten minutes after infusion. A summary of the target acquisition is presented in **Table 1**. In general, the accuracy of the preplanning and subsequent administration was high, with a total of 60 out of 64 catheters correctly placed. The target structures (nucleus caudate and putamen) were effectively reached and correctly infused as evaluated by the target region fill with the contrast agent. The 4 unsuccessful injections (out of 64 total injections) were due to minor reflux in two cases (left putamen of animals T38 and T41), a broken Luer connection in one case (right putamen of animal T31) and a high in-line pressure due to a suture that had tied up the tubing in the last case (left caudate of animal T70). No safety issues related to the surgical

approach were observed in any of the animals throughout the experimental period, as evaluated by daily general observation, weekly body weight, and blood hematology parameters (Supplemental File S1). One TgHD minipig was sacrificed one-month post injection due to complications during CSF collection, not related to administration procedure or drug product. Hence, we demonstrate the feasibility of the MRI-guided CED surgical approach for therapeutic delivery in tgHD minipigs, with a high rate of precision of both target acquisition and structure fill in caudate and putamen.

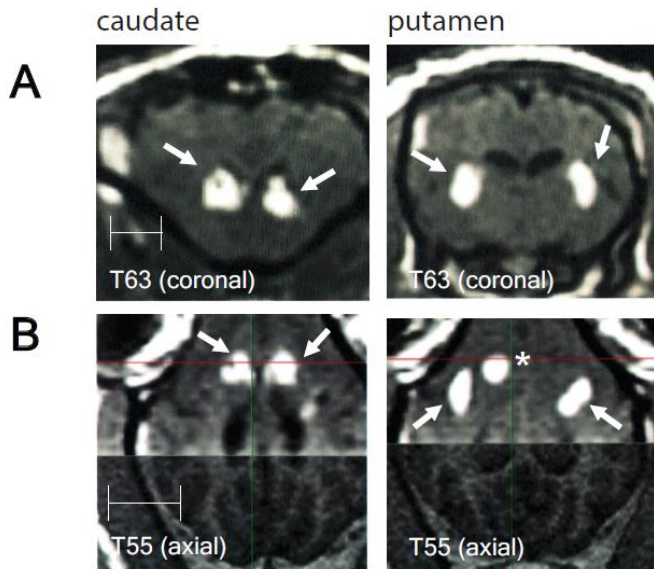


Figure 1. Surgical delivery of rAAV5-miHTT to caudate and putamen in tgHD minipigs. Representative coronal and axial images are shown, as well as target structure fill indicated with arrows. **(A)** Coronal view of bilateral injections in caudate (left) and putamen (right) in animal T63. **(B)** Axial view of bilateral injections in caudate (left) and putamen (right) in animal T55; part of the fill of the caudate can also be observed (indicated by *). Scale bar: 1 cm.

Table 1. Summary of target acquisition in TgHD minipigs

Subject ID	Weight (kg)	Sex	Left		Right	
			Putamen	Caudate	Putamen	Caudate
T29	30	F	OK	OK	OK	OK [#]
T41	32	M	Minor reflux	OK [#]	OK	OK
T39	32	M	OK	OK	OK	OK [#]
T45	25	F	OK	OK	OK	OK
T31	25	F	OK	OK	Failed	OK
T51	25	F	OK	OK	OK	OK
T55	15	F	OK	OK	OK	OK
T62	12	F	OK [#]	OK	OK	OK
T34	35	M	OK [#]	OK [#]	OK	OK [#]
T38	25	F	Minor reflux	OK	OK	OK
T58	22	F	OK	OK	OK	OK
T63	12	F	OK	OK	OK [#]	OK
T70	36	F	OK [#]	Failed	OK	OK
T73	36	F	OK [#]	OK	OK	OK
T87	17	M	OK	OK	OK [#]	OK
T93	17	F	OK	OK	OK	OK [#]

[#] Test material formulation distribution outside the injected structure

Widespread vector DNA distribution in the tgHD minipig brain, comparable at 6- and 12-months post-administration of rAAV5-miHTT

To evaluate the biodistribution and long-term durability of rAAV5-miHTT in the tgHD minipig brain after MRI-guided CED, different interim sacrifices were planned at 6 months and 12 months. At 6 months, three animals were sacrificed, the brains were dissected and a total of n=27 brain tissue punches were analyzed per animal, whereas of four animals n=85 punches per animal were analyzed at 12 months (Supplementary Figure 2). Brain punches were subdivided for assessment of transduction (DNA isolation), transgene expression (RNA isolation) and target engagement (protein analysis). Vector transduction was observed throughout the brain of rAAV5-miHTT injected animals, both at 6- and 12-months post-injection, with peak concentrations in target regions (caudate, putamen), limbic areas (amygdala), cortical regions, and thalamus (**Figure 2A**, Supplementary Figure 3). The highest concentrations ranged between 10^6 - 10^7 vector genome (VG) copies/ μ g DNA,

whereas the lowest concentrations, observed in pons and cerebellum, were generally just above the lower limit of quantification (LLOQ; 5×10^3 VG copies/ μg DNA). Relatively high concentrations (with respect to the LLOQ) were observed in white matter regions (in the range of 10^5 VG copies/ μg DNA). Vector DNA concentrations in the different brain regions were highly comparable at 6- and 12 months post-administration, indicating sustained rAAV5-miHTT vector persistence. In spinal cord, vector DNA concentrations were mostly below LLOQ (**Figure 2B**).

Because of the importance of reaching not only target regions (caudate nucleus, putamen) but also other regions that show neurodegeneration at later stages of the disease, such as cerebral cortex, we performed a more extensive analysis of cortical vector transduction at 12 months (**Figure 2C**). The highest transduction was observed in cortical regions closer to the target areas, such as the insular and perirhinal/retrosplenial cortices (on average 10^6 VG copies/ μg DNA), followed by somatomotor, and temporal cortices ($>10^5$ VG copies/ μg DNA), and visual, cingulate, somatosensory, prefrontal and motor cortices ($>10^4$ VG copies/ μg DNA).

With this extensive analysis of vector DNA distribution across the whole brain, we show that a one-time local injection of rAAV5-miHTT in caudate and putamen in a large HD animal model leads to strong and persistent transduction of and beyond target areas, covering all key brain regions that are affected at the different stages of HD.

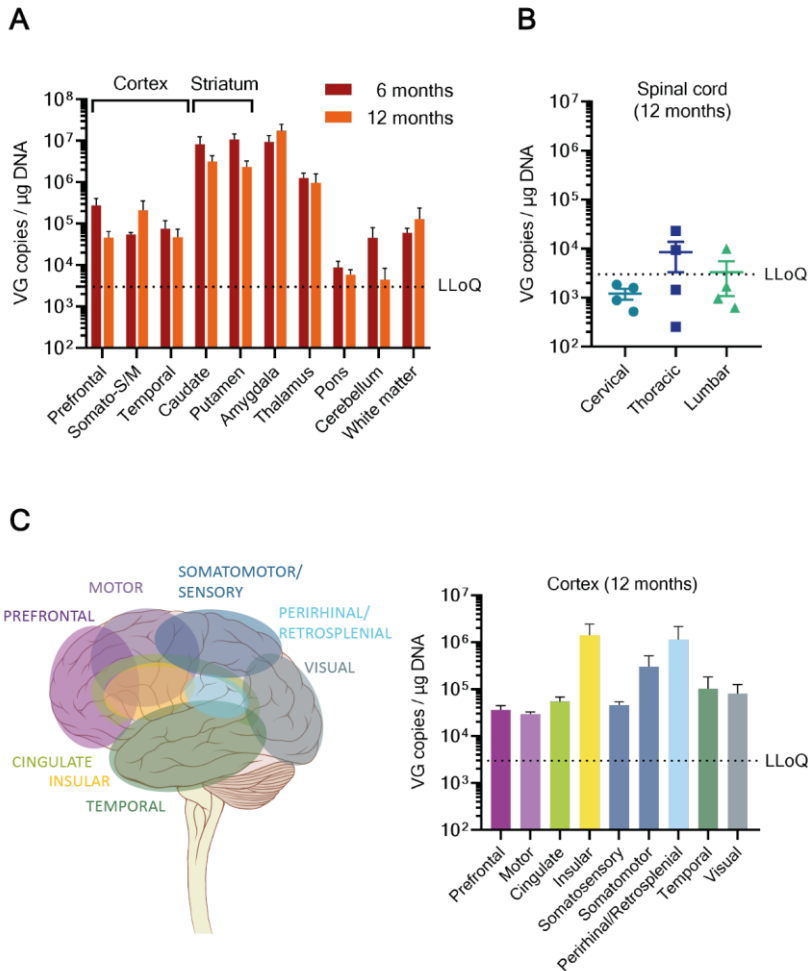


Figure 2. Vector transduction in different brain and spinal cord regions of rAAV5-miHTT injected animals. (A) Transduction in different brain areas at 6 (blue bars) and 12 (red bars) months post-injection were determined by QPCR and indicated in vector genome (VG) copies per μg of genomic DNA. **(B)** Transduction in cervical, thoracic and lumbar regions of the spinal cord at 12 months post-injection ($n=4$ animals/group). **(C)** Detailed view of transduction in cortical subregions 12 months post-rAAV5-miHTT. The cortical regions are color-coded in the drawing, and corresponding concentrations (in VG/ μg genomic DNA) are displayed in the bar graph. Bars represent average \pm SEM; LLoQ: lower limit of quantification.

High precision processing and therapeutic miRNA expression at 1-year post rAAV5-miHTT administration

Next to vector DNA biodistribution, expression of the therapeutic microRNA was determined. Quantification of mature miHTT was performed at 12 months, in the same brain regions as for vector DNA. In line with the observed transduction pattern, mature miHTT RNA molecules were detected in all analyzed brain areas from animals treated with rAAV5-miHTT, except for a small number of individual samples (<10 of approximately 170) in which miHTT expression was at or below the LLoQ (**Figure 3A**). Because the miHTT detection method is specific for the active mature guide strand, its sustained expression validates the correct mechanism of action of rAAV5-miHTT from AAV cell entry, nuclear import, primary miHTT expression to accurate processing. Accordingly, a highly significant correlation of miHTT expression with vector DNA concentration was observed (Pearson $r = 0.8963$, $p < 0.0001$) (**Figure 3B**).

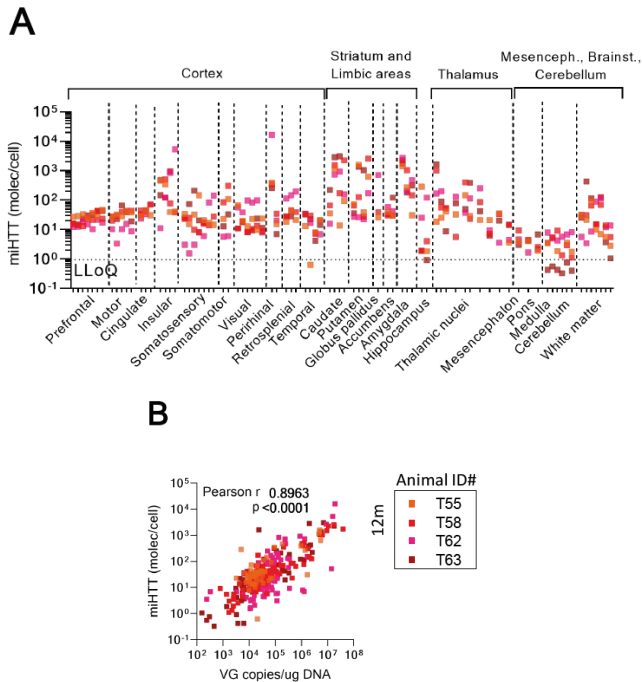


Figure 3. Brain-wide expression of mature miHTT at 12 months post-rAAV5-miHTT administration generally correlates with vector DNA concentration. (A) Mature miHTT concentrations in brain regions were determined using a specific Taqman RT- QPCR assay. Shown are the results for $n=4$ animals (T55, T58, T62 and T63, individually color-coded), per brain region (each dot represents the average results of one punch). *LloQ: lower limit of quantification.*

Strong and widespread mHTT protein lowering after one-time rAAV5-miHTT administration into the caudate and putamen

To evaluate the effect of miHTT on human mHTT protein lowering, all brain regions, at 6 and 12 months, were analyzed using the same method used to quantify human mHTT in CSF of patients with HD (34, 35). Sustained mHTT protein lowering was observed in most areas of the brain (**Figure 4A**), at 6 and 12 months after rAAV5-miHTT MRI-guided CED (**Figure 4B**). The analysis at 12 months post-rAAV5-miHTT administration, with the more extensive brain sampling, demonstrated sustained lowering of mHTT protein in all brain areas measured, except in the cerebellum. The most pronounced mHTT protein lowering was observed in putamen (average 84% lowering; 95%CI [65-104]), caudate (average 79% lowering; 95%CI [65-94]) and amygdala (average 78% lowering; 95%CI [44-112]), followed by thalamus (average 56% lowering; 95%CI [44-68]) and prefrontal cortex (average 44% lowering; 95%CI [37-51]). Although still significant, a less pronounced mHTT protein lowering was obtained in pons ($p < 0.05$) and white matter regions ($p < 0.005$), in line with vector DNA and miHTT expression. In the somatosensory-, somatomotor- and visual-cortex, mHTT lowering did not reach statistical significance ($0.05 < p < 0.1$). We observed a significant global correlation between mHTT protein lowering (in % from control) and miHTT expression in brain (Supplementary Figure 4, Pearson $r = -0.2957$, $p < 0.0001$). The analysis of miHTT and mHTT protein concentration in tgHD minipigs supports the potential of an exceptionally widespread and pronounced effect of rAAV5-miHTT therapy to lower mHTT extensively across a large brain.

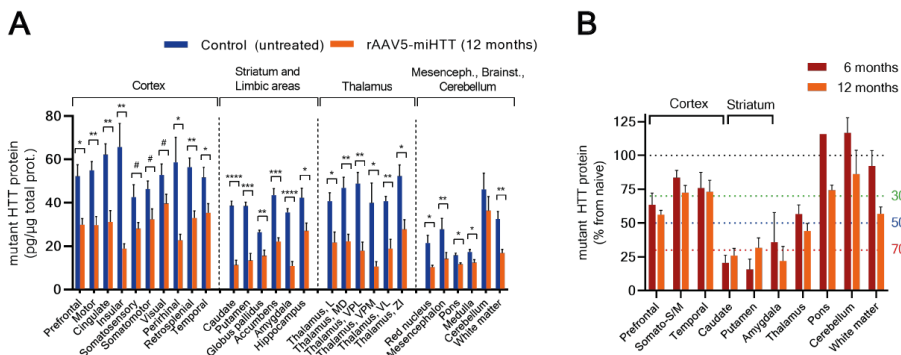


Figure 4. Sustained mHTT protein lowering across the entire tgHD minipig brain. (A) mHTT protein concentrations were determined in several brain areas, in control (untreated) and rAAV5-miHTT treated animals at 12 months post-injection. **(B)** mHTT protein lowering at 6 (blue bars) and 12 (red bars) months post injection. Bars represent average \pm SEM; statistics: two-tailed t-test, corrected $p \# < 0.1$, * < 0.05 , ** < 0.005 , *** < 0.0005 , **** < 0.0001 .

Successful detection of miHTT in cerebrospinal fluid up to one year after one-time intracranial administration allows translational monitoring of the therapeutic agent

As clinical translatable efficacy markers are notoriously challenging in central nervous system (CNS) disorders, due to the inaccessibility to the brain, the use of large (disease-modeling) animals are key as they allow for longitudinal collection of biofluids in which candidate biomarkers can be assessed. Given that endogenous microRNAs can be detected in the CSF (36), we hypothesized that our therapeutic microRNA *miHTT* would also be present in CSF after intracranial rAAV5-*miHTT* administration. Indeed, whereas *miHTT* was undetectable in CSF pre-dose, CSF *miHTT* concentrations were detected from the first time point studied (3 months post-injection), with sustained concentrations up to 12 months post-injection (**Figure 5A**).

Having shown that the active therapeutic molecule can be readily detectable in CSF indicating long-term durability of rAAV5-*miHTT* expression, we moved on to assess candidate HD biomarkers in CSF. Two of the most studied biofluid biomarkers to follow disease progression and therapeutic efficacy in HD are mHTT protein and NFL (37). As such, expression of both mHTT protein and NF-L was assessed in tgHD minipigs before treatment and at different timepoints after rAAV5-*miHTT* administration.

mHTT lowering in the striatum is partially reflected by mHTT lowering in CSF

First, we assessed mHTT protein in the CSF of control (naïve) tgHD animals. A longitudinal age-dependent increase in CSF mHTT protein concentrations was observed (**Figure 5B**), which was confirmed by analysis of additional CSF samples from a previous study in older tgHD minipigs (23) (**Fig. S5A**). The 2B7-MW1 Singulex assay used for mHTT protein quantification is known to be dependent on (i) polyQ length (the longer the polyQ stretch, the higher the signal) and (ii) mHTT protein fragment length (the shorter the fragment, the higher the signal) (34, 35). The observed age-dependent increase could not be attributed to an increase in polyQ repeat with age of these animals, as somatic CAG repeat instability does not occur in this model given the presence of CAA interruptions in the DNA sequence (27). To exclude that the age-dependent increase in mHTT was due to mHTT protein fragmentation, samples were run with an alternative assay (2B7-2166, total HTT assay) which shows neither polyQ nor fragment dependency. Although this is a less sensitive assay, a good correlation between both assays was obtained (**Fig. S5B**), suggesting that the increase in mHTT protein concentration with age in tgHD minipigs is a

concentration-dependent effect, and not due to any assay-related issues secondary to differences in polyQ length or fragment size.

Similar to control (naïve) tgHD animals, rAAV5-miHTT animals demonstrated an age-dependent increase in CSF mHTT concentration (**Figure 5B**). However, a significant treatment effect on CSF mHTT was observed over time and mHTT levels in rAAV5-miHTT animals were lower than in age-matched naïve controls, from 3 months post-treatment ($p < 0.05$) (see **Table S1** for details on the statistical analysis). When compared to non-treated controls, CSF mHTT protein concentration was lower at 6- (27% lowering, 95%CI [3-51]) and 12-months (22% lowering, 95%CI [-5-49]) post-treatment (**Figure 5C**).

Transient increase CSF NFL after rAAV5-miHTT which normalizes by 3 months post-injection

Having determined mHTT lowering in CSF after one-time intracranial administration of rAAV5-miHTT, we analyzed NF-L as an additional biomarker which is linked both to efficacy and safety. There were no differences in NFL expression between wild-type and tgHD minipigs at 6 months of age, nor in a separate cohort of animals of increasing ages (up to 4 years old) (**Fig. S6**). Although this precluded us from assessing phenotypic improvement caused by rAAV5-miHTT, it still allowed us to assess the response of NFL to the administration procedure (**Figure 5D-E**). Following surgery, CSF NFL transiently increased (14- and 28-days post-injection) ($p < 0.0001$). CSF NFL concentration in rAAV5-miHTT animals declined from 3 months onward ($p < 0.001$), being comparable to those of naïve tgHD controls from 6 months on.

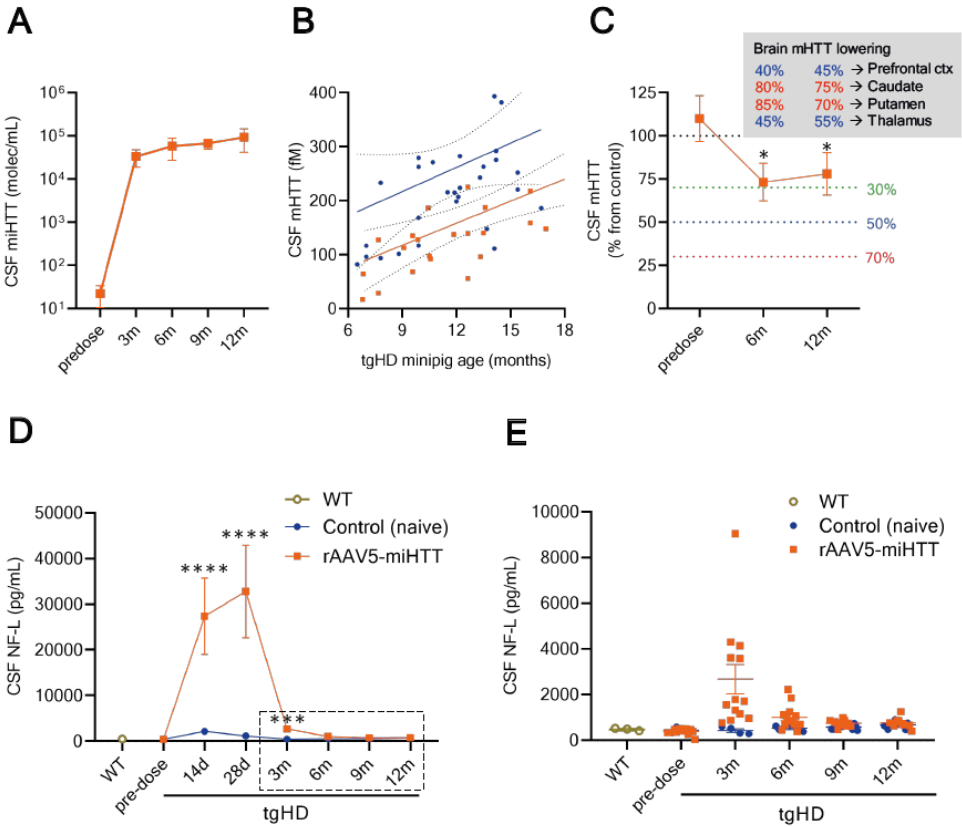


Figure 5. Biomarker measures in CSF of tgHD minipigs. (A) Therapeutic transgene miHTT concentration in CSF of rAAV5-miHTT injected animals (orange squares, representing average \pm SEM) from 3 up to 12 months post-injection. (B) mHTT protein in CSF from control (blue dots) and rAAV5-miHTT (orange squares) tgHD minipigs according to age (in months); each point represents an individual measurement per animal; only data points from 3-months post-injection are displayed. Solid lines represent the best-fit line (linear regression), with their corresponding 95% confidence intervals indicated (dotted curves). (C) CSF mHTT protein lowering in rAAV5-miHTT animals expressed as percentage from age-matched controls; overlaying the graph, the panel indicates percentage lowering in different brain regions. * $p < 0.05$. (D) CSF NF-L (as average \pm SEM) over time following rAAV5-miHTT injection; dotted square indicates data zoomed-in in (E), with individual CSF NF-L values at pre-dose and from 3 months post-injection. Statistics: two-tailed *t*-test, corrected p *** < 0.0005 , **** < 0.0001 .

Discussion

The therapeutic potential of rAAV5-miHTT has been demonstrated in different HD rodent models (21, 22, 24). To support successful transition of CNS gene therapies into the clinic, studies in large animal models are of high importance (15, 23). Critical issues for clinical translation include clinically feasible and precise delivery to target regions, potential of treatment efficacy in a larger brain, and availability of biomarkers for early prediction of therapeutic outcome. One of the key questions that is relevant for all HTT silencing therapies, is whether the striatum and cortex, the main areas affected in the disease, are effectively targeted in a large brain. We now show the feasibility and efficacy of MRI-guided CED for intracranial rAAV5-miHTT administration, resulting in coverage of relevant brain regions, long-term and well tolerated expression and target engagement. In addition, we evaluated the response of relevant candidate biomarkers in CSF to the therapeutic intervention.

In HD, neuropathology is not restricted to caudate and putamen as the initially affected regions, but extends to other areas with disease progression (2), especially cortical regions. Therapeutic coverage of all affected brain regions is considered essential. Targeted administration using CED has been shown to enhance the distribution of therapeutics in the brain parenchyma (38), also in pigs (39). Our first study in tgHD minipigs compared different surgical target regions (putamen, thalamus) to evaluate short-term efficacy of rAAV5-miHTT (23). Here we showed a detailed view of the dimensions of rAAV5-miHTT spread in a large brain, with substantial transduction in virtually all regions examined, except for brainstem and cerebellum, two regions that are not largely affected in HD (2). Our data suggest that thalamic injection might not be needed to achieve cortical coverage, which would avoid risks of direct injection in a sensitive relay station. The occurrence of thalamic calcification following complete HTT ablation (40), also suggests that thalamic administration should preferentially be avoided.

AAV-based gene therapies administered locally in specific brain regions extend to other brain regions based on transport of the virus through neuronal tracts. This is highly dependent on factors such as (i) surgical target region and (ii) AAV serotype (41). The present study supports the use of AAV5, based on its ability for retrograde and anterograde transport (41, 42), as vector for CNS disorders where a relatively wide coverage is needed. When compared to other AAV serotypes, AAV5 transduces neuronal populations at much greater efficiency (43), and shows the highest cortical spread in non-human primates (NHPs) (44-46), and mice (47, 48). One of the contributing factors leading to a greater spread of AAV5 and other serotypes (such as AAV1, AAV8 and AAV9), in contrast to AAV2 and AAV6, is the lack of heparin sulfate proteoglycan binding or binding to other AAV entry factors such as GPR108 (49, 50). In addition, AAV5 transduces both neurons and astrocytes (13, 51),

which has recently been shown to be required for phenotypic rescue in HD mice (16), in line with neurons and astrocytes being implicated in HD pathology (52).

Consistent with the broad pattern of transduction, we observed broad transgene expression and mHTT protein lowering, independently of regional differences in mHTT concentration, not only in the areas that showed substantial transduction, but also in areas with low concentrations of vector DNA. One hypothesis is that miHTT could be sorted into extracellular vesicles (EVs), leading to further spread of the active therapeutic molecule to neighboring cells, independently of neuronal connections. This is a plausible possibility given that miHTT is enclosed into the miR-451 backbone, and miR-451 has been shown to be enriched in EVs (53, 54). The combined effects of viral vector chosen, engineered miRNA design and potential contribution of EV-mediated spread of miHTT, are believed to contribute to the robust and sustained mHTT protein lowering by rAAV5-miHTT. Several other artificial miRNAs targeting human mHTT have been reported, but only few of those have been tested in large animal models (55). One of these, engineered into the miR-155 backbone and delivered via AAV9 (18) has been tested in HD sheep and showed a local transduction pattern (56, 57). Similar results were reported for other microRNA-based approaches in NHPs (55, 58, 59), delivered via AAV1 and AAV2, with effects restricted to striatum. Following intrathecal administration in NHP, HTT-targeting ASOs show an opposite pattern of HTT lowering, with predominant effects in cortex and spinal cord (8) and less anticipated lowering in deep brain regions (such as the caudate and putamen) affected earlier in HD (7).

An important aspect of gene therapies is the durability of expression, and in the CNS, long-lasting effects are expected. Indeed, we observed a similar degree of (ongoing) expression at 6- and 12-months post-administration, in line with rodent data (22, 60, 61). Striatal administration of AAV2 resulted in at least 8 years of transgene persistence in NHPs (62) and over 4 years in humans (63). As many aspects can influence long-term transgene expression (for example, DNA construct, promoter), we will continue to monitor animals remaining in the current study cohort. This will also allow us to assess potential phenotypic improvement in tgHD minipigs, with a disease phenotype expected to manifest at 4.5-6 years of age (32).

Early efficacy measures that allow prediction of beneficial therapeutic responses are much needed in slow progressive neurodegenerative diseases (33, 37). In HD, mHTT and NFL in CSF hold most promise to follow up disease progression and predict therapeutic response (33, 37). CSF mHTT expression in tgHD minipigs increased with age, which could not be attributed to technical issues, nor to somatic instability, absent in this model (27). The rapid rate of increase of CSF mHTT at this young age was unexpected, and may be attributed to neurodevelopment, although more data would be needed to support this

view. So far, this strong age effect has not been described in patients with HD (35, 37, 64), although longitudinal studies are still ongoing (hdclarity.net, 37). We found a 25-30% lowering of mHTT protein in CSF of tgHD minipigs after treatment with rAAV5-miHTT, durable up to 1-year post administration. Hence, when compared to the 70-85% lowering observed in the striatum, and the 40-45% lowering in the cortex, CSF mHTT concentrations underestimate parenchymal silencing induced by rAAV5-miHTT. The origin of CSF mHTT is still largely unknown, although preclinical studies suggest about 60% to be originating from CNS sources (64). However, the specific contributions of superficial (cortical) versus deep (striatum, thalamus) brain regions, and of tissues close to CSF collection (such as the lumbar spinal cord) are still to be elucidated. Because of this, although CSF mHTT concentrations have been proposed as a pharmacodynamic marker for ASO therapies (7, 8), its value for mHTT-silencing gene therapies remains to be determined, as well as its correlation (or lack thereof) with potential therapeutic effects. The present data in tgHD minipigs indicate that CSF mHTT concentrations underestimate the magnitude of parenchymal mHTT silencing induced by rAAV5-miHTT, urging the need of additional biomarkers for gene-therapy based HTT-lowering approaches.

NFL concentrations increase in the CSF of patients with neurodegenerative diseases, including HD (35, 65). Elevated NFL concentrations in the CSF and plasma of HD mutation carriers correlate with disease severity and with different measures of disease progression (66). Although NFL is used as a treatment response marker in other neurological diseases (67-70), no treatment response of NFL to potential disease-modifying drugs in HD has been evaluated preclinically, nor has it been observed in clinical trials so far (7). Recent clinical trials have reported a prolonged and dose-dependent elevation of NFL after intrathecal ASO administration (7), especially with high frequency of administration, and to a much lesser extent with longer intervals between dosing (71). In fact, the lack of HD-like phenotype in young tgHD minipigs in the current study precluded the evaluation of CSF NFL as a treatment response marker. The transient elevation of CSF NFL observed after injection was expected and can be attributed to the neurosurgery itself and local viral load as we have previously observed transient elevations in CSF cytokines after AAV5 brain administration in tgHD minipigs (23). Following the procedure NFL concentrations returned to baseline between 3- and 6-months post-surgery and did not increase during the rest of the study period. This is a similar profile to the CSF NFL profile observed in humans after deep brain stimulation (72). Hence, neither the neurosurgical approach, the exposure of the brain to rAAV5, the expression of the therapeutic miRNA nor the silencing of mutant huntingtin induced a long-term increase of NFL.

The pharmacokinetics of AAV-delivered miRNA-based therapies pose important challenges. As a specific pharmacokinetic marker of rAAV5-miHTT expression, we assessed the presence and persistence of mature miHTT in CSF of tgHD minipigs at different time

points after striatal administration. Our data indicate that it is possible to reliably detect miHTT in CSF from 3 up to 12 months post-injection, making this a suitable pharmacokinetic marker, and a true translational measure of long-term durability of rAAV5-miHTT.

The major limitation of this study is the use of untreated animals as controls, instead of a sham treatment group. This additional control would have been helpful in interpreting the results related to surgery itself, independently of the therapeutic construct, especially concerning disease CSF biomarkers (mHTT and NFL) which have been shown to respond to surgical trauma (23, 72). Group comparisons (rather than longitudinal analyses) were needed because the unexpectedly rapid rise in CSF mHTT, but would have been ideally done with respect animals receiving surgery, and this data should therefore be interpreted with caution. The results of NFL indicate that this would have been of more relevance shortly after surgery, and less from 3-6 months post-surgery. Other limitations are the use of young animals, and lack of disease-related phenotype at this age, making the bridging difficult between animal model and patients with manifest HD, currently the main target population of HTT lowering trials. Also, whether the same distribution would occur in adult animals, would need to be established. An additional limitation is the use of a single high dose for treatment, instead of different doses (low, mid, high). The dose used in the present study, causing profound (80-90%) mHTT lowering in target regions, is not the targeted translatable dose for the clinic. Considering the non-allele-selectivity of the approach, a target lowering of 50% would be considered adequate to avoid potential harmful effects of lowering wild type HTT as complete suppression of HTT may not be desirable because of its vital cellular functions (reviewed in 73). As shown previously (23), the target porcine HTT sequence has two mismatches with miHTT, and therefore this tgHD model is not adequate to assess long-term HTT lowering tolerability. A final limitation is the lack of cell-specific analyses in tissue. Use of laser capture methods to determine the effects in different cell types, would be of added value, and can be considered for future studies.

Altogether, the results of this ongoing study indicate that intrastriatal CED delivery of rAAV5-miHTT results in pronounced, widespread and persistent silencing of mHTT in all brain areas that are known to be affected in HD. CSF mHTT concentrations underestimated silencing in the relevant deep brain areas and the current data do not support their use as a reliable biomarker for therapeutic efficacy, at least for intrastriatal gene therapy approaches. In contrast, mature CSF miHTT concentrations can be used as pharmacokinetic measure to monitor the expression and durability of rAAV5-miHTT delivery to the brain. These data, together with separate large animal GLP toxicology studies, support the further clinical development of the rAAV5-miHTT program into the clinic and shed light into the value of candidate biomarkers to follow-up efficacy.

Materials and Methods

Study design

The general study design is shown in **Table S2**. A total of $n=31$ animals were used in the study, with males and females equally distributed between groups. No sample size calculation was performed. Controls (naïve control group) did not receive any surgery or treatment ($n=15$). The treatment group (rAAV5-miHTT treated) received MRI-guided CED of rAAV5-miHTT ($n=16$). Animals were randomly distributed between control and treatment groups; rAAV5-miHTT treatment was administered without blinding. Control and treatment groups were randomly subdivided for interim sacrifices at 6 months ($n=3-4$ animals/group), 12 months ($n=4$ animals per group) or beyond 24 months post-surgery ($n=8$ animals/group). The present study presents data obtained up to 12 months post-surgery (animals beyond 24 months are still in in-life phase).

Animals

All components of this study were carried out in accordance with the Institutional Animal Care and Use Committee of Institute of Animal Physiology and Genetics, v.v.i. according to current Czech regulations. Male and female Libechov tgHD Göttingen minipigs (27) ($n=31$), ranging between 4-8 months of age at the beginning of the study, were used. The animals were screened for serum total and neutralizing rAAV5-antibodies before the start of the study, as previously described (74), selecting only animals considered seronegative (neutralizing antibody titers lower than 1:50 at baseline). Animals were housed under standard conditions of light and temperature (20 °C), with ad libitum access to food and water, and monitored daily for their general health status.

Vector design and production

cDNA encoding the miHTT cassette was packaged into rAAV5 by a baculovirus-based rAAV production system (uniQure) as described earlier (75, 76). The design and characterization of rAAV5-miHTT has been described previously (20). The complete transcription unit was flanked by two non-coding AAV-derived inverted terminal repeats, and expression was driven by a combination of the cytomegalovirus early enhancer element and chicken β -actin promoter (CAG promoter). The expression cassettes were inserted in a recombinant baculovirus vector by homologous recombination and clones were selected by plaque purification. The recombinant baculovirus containing the cassettes were further amplified and clones screened for best production and stability by PCR and qPCR. To generate AAV5, baculovirus infections on insect cells with recombinant baculoviruses was performed encoding rep for replication and packaging, cap-5 for the AAV5 capsid and the expression cassette. After viral particle assembled, prep purification was performed with AVB Sepharose high-performance affinity medium (GE Healthcare) using AKTA Explorer

purification system (GE Healthcare) and titer was determined by qPCR with specific primer-probe combinations against the CAG promoter.

MRI-guided delivery of rAAV5-miHTT

Pre-scan, surgery and MRI-guided CED drug delivery was performed using Renishaw pre-clinical drug delivery system. Briefly, animals were appropriately anesthetized as previously described (23) and placed in prone position in the MRI-compatible minipig fixation frame (Renishaw). After ensuring function of health monitoring systems the animal was placed into the MRI scanner. Prior to scanning, a fiducial arc (Renishaw) was attached to the frame. T1-weighted anatomical scan(s) with sufficient anatomical resolution were carried out with a cardio-coil in a 1.5 Tesla MRI. After finalizing scan(s), animals were transferred to the surgery room for cannula implantation.

Before surgery, the fiducial arc from the fixation frame was replaced by a stereotactic frame. Using the precise coordinates from the prescan MRI, one burr hole per catheter was drilled. A total of 4 catheters were implanted bilaterally using a frontal approach, two catheters targeting the caudate nuclei and putamen on either side of the brain. After implantation, the frame was removed from the fixation frame and the animal transferred to the MRI for CED of 3×10^{13} vector genomes (vg)/mL (final dose of 1.2×10^{13} vg/brain) of rAAV5-miHTT mixed with a contrast agent (ProHance 2 mM, 1:500) (Bracco International B.V.). Infusions were carried out simultaneously over approximately 30 minutes with a starting infusion rate of $1 \mu\text{L}/\text{min}$ gradually increasing to a maximum rate of $3 \mu\text{L}/\text{min}$. Real-time MRI scans were performed repeatedly during infusion and infusion rates were changed if there was any infusion flowback. The infusion was stopped when the target volume of $100 \mu\text{L}$ per in each of the four target brain areas was achieved. A final MRI scan was performed to document the filling of the target area. After infusion the guides and cannulas were carefully removed, the wound was closed up and the animal was allowed to recover in a warmed environment.

Blood and CSF sampling

Blood samples were collected from the ear vein, both for hematology (EDTA) and clinical blood chemistry (heparin) and processed, accordingly. To obtain plasma, the blood was centrifuged twice 10 min at 1500 G at 4°C , aliquoted and stored at -80°C .

CSF samples of approximately 3 mL were taken via lumbar puncture, under anesthesia (intramuscular TKX mixture: Tiletamin 4 mg/kg, Zolazepam 4 mg/kg, Ketamin 5 mg/kg and Xylazin 1 mg/kg; 1ml TKX mixture per 10-15kg body weight). All CSF processing was done on ice, within 15 minutes of collection. CSF was centrifuged at $2000 \times g$ for 10 min at 4°C to remove cells and preserve cell integrity, supernatant was aliquoted in polypropylene tubes, snap-frozen and stored at -80°C .

Necropsy and brain tissue dissection

Euthanasia was performed using pentobarbital sodium intravenous injection, 100 mg/kg and followed by a bilateral thoracotomy. Animals were transcardially perfused with 500-1000 mL of heparinized PBS. The entire brain was carefully removed from the skull, placed into a brain matrix and coronally sliced into 3-4 mm blocks. The blocks were organized sequentially and identified with roman numbers as depicted in **Fig. S2**. In brains from the 6 months interim sacrifice, approximately n=54 brain punches of 4 mm in diameter from the uneven numbered slices were taken and individually stored in cryovials at -80°C until further use. Before biomolecular analysis, tissue punches from a single hemisphere (n=27 punches/animal) were cut into small pieces on dry ice, mixed, divided into four aliquots and stored at -80°C for subsequent use. In brains from the 12 months interim sacrifice, approximately n=170 brain punches of 4 mm in diameter were collected from all slices. The punches from a single hemisphere (n=85 punches/animal) were directly cut into small pieces, mixed, divided into four aliquots and stored at -80°C for subsequent use.

DNA isolation and determination of vector genome copies

For DNA isolation, one brain punch aliquot was used with the DNeasy 96 Blood and Tissue kit (Qiagen), following the manufacturer's instructions. Primers and probe specific for the polyA tail of the rAAV5-miHTT vector were used to amplify a specific target region of the vector with Taqman QPCR. The amount of vector DNA was calculated from a plasmid standard curve, which was taken along on the same plate. Results were reported as VG copies per µg of genomic DNA.

RNA isolation and determination of miHTT expression in brain tissue

For RNA isolation, one brain punch aliquot was homogenized in TRIzol reagent (Ambion, 15596018, ThermoFisher Scientific) and homogenized using Fast-Prep-24TM 5G (MP Biomedicals). Total RNA was isolated according to manufacturer's protocol (Direct-zol RNA MiniPrep kit, Zymo Research, R2052). To examine miHTT miRNA expression, cDNA was synthesized from isolated total RNA with custom made gene-specific RT primers targeting mature miHTT-24nt using TaqMan MicroRNA Reverse Transcription Kit (Applied Biosystems, ThermoFisher Scientific). A single stranded 24nt-long mature miHTT RNA standard line was taken along. Next, gene-specific TaqMan qPCR was performed with mature miHTT-24nt specific primers and probe using TaqMan Fast Universal PCR Master Mix (Applied Biosystems, ThermoFisher Scientific). Using the mature miHTT-24nt standard line, miHTT molecules per reaction were determined, and the number of miHTT-24nt molecules per cell subsequently calculated.

RNA isolation and determination of miHTT expression in CSF

RNA was isolated from a total of 300 μL minipig CSF using the miRNeasy Serum/Plasma Advanced Kit following manufacturer's protocol (Qiagen). During RNA isolation miR39 spike-in was added at step 4 (simultaneously with RPP buffer) at a concentration of 1.6×10^8 copies/ μL as RNA isolation control. RNA samples were treated with dsDNase (included in Maxima First Strand cDNA synthesis kit, Thermo Scientific, K1672) immediately after isolation.

To measure miRNA expression, RNA samples were retrotranscribed to cDNA with miRNA LNA RT kit and RT-qPCR was performed using miRCURY LNA miRNA PCR Assay kit (Qiagen), cel-miR-39-3p (YP00203952, Qiagen) and custom probes for detection of miHTT. miRNA expression levels were calculated as miHTT molecules/mL CSF based on a standard line performed with synthetic RNA oligos (Integrated DNA Technologies).

Mutant huntingtin (mHTT) protein quantification in brain tissue and CSF

Mutant huntingtin protein quantification in CSF and brain tissue samples was done using an ultrasensitive single molecule counting (SMC) immunossay (Singulex), as described previously (34). Briefly, pulverized tgHD minipig brain samples were homogenized in 170 μL ice cold lysis buffer using a FastPrep-96 tissue homogenizer and stored at -80°C until further testing. Homogenized brain samples or CSF (undiluted) were tested in technical triplicates. All CSF samples were tested for potential blood contamination using a species-independent colorimetric detection kit (Arbor) and following the manufacturer's instructions. Samples above the Hb threshold determined to interfere with the assay, were excluded from subsequent analyses. Final concentration of 15.6 fM to 3800 fM human HTT-Q46, 1-548 was used for quantification. For mutant HTT, the antibodies 2B7 (Novartis) directed against the N-terminal 7-13 amino acids of the huntingtin protein, and MW1 (Caltech) which binds to the expanded polyglutamine repeat, were used. For total HTT, a combination of 2B7 (Novartis) and MAB2166 (Sigma-Aldrich) were used. All analyses were performed at IRBM (Pomezia, Italy).

Neurofilament-light chain quantification in CSF

The UmanDiagnostics NF-light ELISA assay was used to quantify NFL concentrations in tgHD CSF, following the manufacturer's instructions (UmanDiagnostics). Different dilutions of CSF samples were used in order to ensure proper performance within the NFL standard curve. The obtained NF-L concentrations in CSF were expressed in $\mu\text{g/mL}$.

Statistics

Statistical analysis was performed in GraphPad Prism 8.0. Pearson correlation was used for correlation analyses. For comparison between two groups, two-tailed t-test

statistics were used, with multiple testing corrections. Regression analysis with graphical display of confidence intervals (95%CI) was used for the determination of the relationship between mHTT concentrations and age. Statistical analysis of mHTT in CSF was performed in SAS, using an analysis of covariance model (with treatment time, analysis batch and age as covariates). In all cases, the significance level was set to $p < 0.05$.

Acknowledgments: We would like to thank Owen Lewis, Max Wooley and Dave Johnson from Renishaw, for their valuable support during the CED surgical procedure. The authors are grateful to the teams of Process Development and Analytical Development at uniQure for the production and characterization of rAAV5-miHTT, and to Eileen Sawyer and Ellen Broug for critically reading the manuscript. OCS Life Sciences provided support with statistical analysis of CSF mHTT. We are also grateful for the support from the CHDI Foundation, in particular Douglas MacDonald and David Howland.

Funding: Part of this work was supported by PIGMOD Center's sustainability program: National Sustainability Programme, project number LO1609 (Czech Ministry of Education, Youth and Sports) to JM.

Author contributions: Conceptualization: AV, MME, BBI, JM, ZE, HP, SVD, PK; Surgery: BBo, RL, DU, ZS, MC, BBI, ZE, JM; Sample collection: AV, MSG, CB, LP, JK, BB, ZE; Molecular and data analyses: AV, MME, AS, MSG, CB, CVT, SAB, LP, RP, VF, AB; Formal Analysis: AV, MME; Writing: AV; Funding Acquisition: ZE, JM, HP, SVD, PK; Supervision: AV, MME, ZE, JM, PK.

Competing interests: AV, MME, AS, MSG, CB, CVT, SAB, LP, HP, SVD and PK are employees and shareholders at uniQure; ZE, JM and PIGMOD have a collaborative agreement with uniQure. Filed patent applications pertaining to the results presented in this paper include the following: RNAi induced huntingtin gene suppression (WO2016/102664, resulting in at least US 10,174,321, US 10,767,180 and EP 3237618B1), A companion diagnostic to monitor the effects of gene therapy (PCT/EP2019/081759), Method and means to deliver miRNA to target cells (PCT/EP2019/081822) and Targeting misspliced transcripts in genetic disorders (PCT/EP2020/075871); the latter three have not yet published.

Data and materials availability: All data associated with this study are available in the main text or the supplementary materials, and, if required, materials may be available subject to at least an MTA.

References

1. G. P. Bates, R. Dorsey, J. F. Gusella, M. R. Hayden, C. Kay, B. R. Leavitt, M. Nance, C. A. Ross, R. I. Scahill, R. Wetzel, E. J. Wild, S. J. Tabrizi, Huntington disease. *Nat Rev Dis Primers* **1**, 15005 (2015).
2. H. J. Waldvogel, E. H. Kim, L. J. Tippett, J. P. Vonsattel, R. L. Faull, The Neuropathology of Huntington's Disease. *Curr Top Behav Neurosci* **22**, 33-80 (2015).
3. K. J. Wyant, A. J. Ridder, P. Dayalu, Huntington's Disease-Update on Treatments. *Curr Neurol Neurosci Rep* **17**, 33 (2017).
4. C. A. Ross, E. H. Aylward, E. J. Wild, D. R. Langbehn, J. D. Long, J. H. Warner, R. I. Scahill, B. R. Leavitt, J. C. Stout, J. S. Paulsen, R. Reilmann, P. G. Unschuld, A. Wexler, R. L. Margolis, S. J. Tabrizi, Huntington disease: natural history, biomarkers and prospects for therapeutics. *Nat Rev Neurol* **10**, 204-216 (2014).
5. S. J. Tabrizi, R. Ghosh, B. R. Leavitt, Huntingtin Lowering Strategies for Disease Modification in Huntington's Disease. *Neuron* **102**, 899 (2019).
6. P. McColgan, S. J. Tabrizi, Huntington's disease: a clinical review. *Eur J Neurol* **25**, 24-34 (2018).
7. S. J. Tabrizi, B. R. Leavitt, G. B. Landwehrmeyer, E. J. Wild, C. Saft, R. A. Barker, N. F. Blair, D. Craufurd, J. Priller, H. Rickards, A. Rosser, H. B. Kordasiewicz, C. Czech, E. E. Swayze, D. A. Norris, T. Baumann, I. Gerlach, S. A. Schobel, E. Paz, A. V. Smith, C. F. Bennett, R. M. Lane, I.-H. S. S. T. Phase 1-2a, Targeting Huntingtin Expression in Patients with Huntington's Disease. *N Engl J Med* **380**, 2307-2316 (2019).
8. H. B. Kordasiewicz, L. M. Stanek, E. V. Wancewicz, C. Mazur, M. M. McAlonis, K. A. Pytel, J. W. Artates, A. Weiss, S. H. Cheng, L. S. Shihabuddin, G. Hung, C. F. Bennett, D. W. Cleveland, Sustained therapeutic reversal of Huntington's disease by transient repression of huntingtin synthesis. *Neuron* **74**, 1031-1044 (2012).
9. J. F. Alterman, B. Godinho, M. R. Hassler, C. M. Ferguson, D. Echeverria, E. Sapp, R. A. Haraszti, A. H. Coles, F. Conroy, R. Miller, L. Roux, P. Yan, E. G. Knox, A. A. Turanov, R. M. King, G. Gernoux, C. Mueller, H. L. Gray-Edwards, R. P. Moser, N. C. Bishop, S. M. Jaber, M. J. Gounis, M. Sena-Esteves, A. A. Pai, M. DiFiglia, N. Aronin, A. Khvorova, A divalent siRNA chemical scaffold for potent and sustained modulation of gene expression throughout the central nervous system. *Nat Biotechnol* **37**, 884-894 (2019).
10. S. R. Choudhury, E. Hudry, C. A. Maguire, M. Sena-Esteves, X. O. Breakefield, P. Grandi, Viral vectors for therapy of neurologic diseases. *Neuropharmacology* **120**, 63-80 (2017).
11. S. Ingusci, G. Verlengia, M. Soukupova, S. Zucchini, M. Simonato, Gene Therapy Tools for Brain Diseases. *Front Pharmacol* **10**, 724 (2019).
12. Y. Chu, R. T. Bartus, F. P. Manfredsson, C. W. Olanow, J. H. Kordower, Long-term post-mortem studies following neurturin gene therapy in patients with advanced Parkinson's disease. *Brain* **143**, 960-975 (2020).
13. B. L. Davidson, C. S. Stein, J. A. Heth, I. Martins, R. M. Kotin, T. A. Derksen, J. Zabner, A. Ghodsi, J. A. Chiorini, Recombinant adeno-associated virus type 2, 4, and 5 vectors: transduction of variant cell types and regions in the mammalian central nervous system. *Proc Natl Acad Sci U S A* **97**, 3428-3432 (2000).
14. N. S. Caron, A. L. Southwell, C. C. Brouwers, L. D. Cengio, Y. Xie, H. F. Black, L. M. Anderson, S. Ko, X. Zhu, S. J. van Deventer, M. M. Evers, P. Konstantinova, M. R. Hayden, Potent and sustained huntingtin lowering via AAV5 encoding miRNA preserves striatal volume and cognitive function in a humanized mouse model of Huntington disease. *Nucleic Acids Res* **48**, 36-54 (2020).
15. J. Miniarikova, M. M. Evers, P. Konstantinova, Translation of MicroRNA-Based Huntingtin-Lowering Therapies from Preclinical Studies to the Clinic. *Mol Ther* **26**, 947-962 (2018).
16. L. M. Stanek, J. Bu, L. S. Shihabuddin, Astrocyte transduction is required for rescue of behavioral phenotypes in the YAC128 mouse model with AAV-RNAi mediated HTT lowering therapeutics. *Neurobiol Dis* **129**, 29-37 (2019).

17. L. M. Stanek, S. P. Sardi, B. Mastis, A. R. Richards, C. M. Treleaven, T. Taksir, K. Misra, S. H. Cheng, L. S. Shihabuddin, Silencing mutant huntingtin by adeno-associated virus-mediated RNA interference ameliorates disease manifestations in the YAC128 mouse model of Huntington's disease. *Hum Gene Ther* **25**, 461-474 (2014).
18. E. L. Pfister, K. O. Chase, H. Sun, L. A. Kennington, F. Conroy, E. Johnson, R. Miller, F. Borel, N. Aronin, C. Mueller, Safe and Efficient Silencing with a Pol II, but Not a Pol III, Promoter Expressing an Artificial miRNA Targeting Human Huntingtin. *Mol Ther Nucleic Acids* **7**, 324-334 (2017).
19. B. Zeitler, S. Froelich, K. Marlen, D. A. Shivak, Q. Yu, D. Li, J. R. Pearl, J. C. Miller, L. Zhang, D. E. Paschon, S. J. Hinkley, I. Ankoudinova, S. Lam, D. Guschin, L. Kopan, J. M. Cherone, H. B. Nguyen, G. Qiao, Y. Ataei, M. C. Mendel, R. Amora, R. Surosky, J. Laganieri, B. J. Vu, A. Narayanan, Y. Sedaghat, K. Tillack, C. Thiede, A. Gartner, S. Kwak, J. Bard, L. Mrzljak, L. Park, T. Heikkinen, K. K. Lehtimaki, M. M. Svedberg, J. Haggkvist, L. Tari, M. Toth, A. Varrone, C. Halldin, A. E. Kudwa, S. Ramboz, M. Day, J. Kondapalli, D. J. Surmeier, F. D. Urnov, P. D. Gregory, E. J. Rebar, I. Munoz-Sanjuan, H. S. Zhang, Allele-selective transcriptional repression of mutant HTT for the treatment of Huntington's disease. *Nat Med* **25**, 1131-1142 (2019).
20. J. Miniarikova, I. Zanella, A. Huseinovic, T. van der Zon, E. Hanemaaijer, R. Martier, A. Koornneef, A. L. Southwell, M. R. Hayden, S. J. van Deventer, H. Petry, P. Konstantinova, Design, Characterization, and Lead Selection of Therapeutic miRNAs Targeting Huntingtin for Development of Gene Therapy for Huntington's Disease. *Mol Ther Nucleic Acids* **5**, e297 (2016).
21. J. Miniarikova, V. Zimmer, R. Martier, C. C. Brouwers, C. Pythoud, K. Richetin, M. Rey, J. Lubelski, M. M. Evers, S. J. van Deventer, H. Petry, N. Deglon, P. Konstantinova, AAV5-miHTT gene therapy demonstrates suppression of mutant huntingtin aggregation and neuronal dysfunction in a rat model of Huntington's disease. *Gene Ther* **24**, 630-639 (2017).
22. E. A. Spronck, C. C. Brouwers, A. Valles, M. de Haan, H. Petry, S. J. van Deventer, P. Konstantinova, M. M. Evers, AAV5-miHTT Gene Therapy Demonstrates Sustained Huntingtin Lowering and Functional Improvement in Huntington Disease Mouse Models. *Mol Ther Methods Clin Dev* **13**, 334-343 (2019).
23. M. M. Evers, J. Miniarikova, S. Juhas, A. Valles, B. Bohuslavova, J. Juhasova, H. K. Skalnikova, P. Vodicka, I. Valekova, C. Brouwers, B. Blits, J. Lubelski, H. Kovarova, Z. Ellederova, S. J. van Deventer, H. Petry, J. Motlik, P. Konstantinova, AAV5-miHTT Gene Therapy Demonstrates Broad Distribution and Strong Human Mutant Huntingtin Lowering in a Huntington's Disease Minipig Model. *Mol Ther* **26**, 2163-2177 (2018).
24. N. S. Caron, A. L. Southwell, C. C. Brouwers, L. D. Cengio, Y. Xie, H. F. Black, L. M. Anderson, S. Ko, X. Zhu, S. J. van Deventer, M. M. Evers, P. Konstantinova, M. R. Hayden, Potent and sustained huntingtin lowering via AAV5 encoding miRNA preserves striatal volume and cognitive function in a humanized mouse model of Huntington disease. *Nucleic Acids Res*, (2019).
25. S. Keskin, C. C. Brouwers, M. Sogorb-Gonzalez, R. Martier, J. A. Depla, A. Valles, S. J. van Deventer, P. Konstantinova, M. M. Evers, AAV5-miHTT Lowers Huntingtin mRNA and Protein without Off-Target Effects in Patient-Derived Neuronal Cultures and Astrocytes. *Mol Ther Methods Clin Dev* **15**, 275-284 (2019).
26. N. M. Lind, A. Moustgaard, J. Jelsing, G. Vajta, P. Cumming, A. K. Hansen, The use of pigs in neuroscience: modeling brain disorders. *Neurosci Biobehav Rev* **31**, 728-751 (2007).
27. M. Baxa, M. Hruska-Plochan, S. Juhas, P. Vodicka, A. Pavlok, J. Juhasova, A. Miyanojara, T. Nejime, J. Klima, M. Macakova, S. Marsala, A. Weiss, S. Kubickova, P. Musilova, R. Vrtel, E. M. Sontag, L. M. Thompson, J. Schier, H. Hansikova, D. S. Howland, E. Cattaneo, M. DiFiglia, M. Marsala, J. Motlik, A transgenic minipig model of Huntington's Disease. *J Huntingtons Dis* **2**, 47-68 (2013).
28. T. Ardan, M. Baxa, B. Levinska, M. Sedlackova, T. D. Nguyen, J. Klima, S. Juhas, J. Juhasova, P. Smatlikova, P. Vochozkova, J. Motlik, Z. Ellederova, Transgenic minipig model of Huntington's disease exhibiting gradually progressing neurodegeneration. *Dis Model Mech*, (2019).

29. J. Krizova, H. Stufkova, M. Rodinova, M. Macakova, B. Bohuslavova, D. Vidinska, J. Klima, Z. Ellederova, A. Pavlok, D. S. Howland, J. Zeman, J. Motlik, H. Hansikova, Mitochondrial Metabolism in a Large-Animal Model of Huntington Disease: The Hunt for Biomarkers in the Spermatozoa of Presymptomatic Minipigs. *Neurodegener Dis* **17**, 213-226 (2017).
30. M. Rodinova, J. Krizova, H. Stufkova, B. Bohuslavova, G. Askeland, Z. Dosoudilova, S. Juhas, J. Juhasova, Z. Ellederova, J. Zeman, L. Eide, J. Motlik, H. Hansikova, Deterioration of mitochondrial bioenergetics and ultrastructure impairment in skeletal muscle of a transgenic minipig model in the early stages of Huntington's disease. *Dis Model Mech* **12**, (2019).
31. D. Vidinska, P. Vochozkova, P. Smatlikova, T. Ardan, J. Klima, S. Juhas, J. Juhasova, B. Bohuslavova, M. Baxa, I. Valekova, J. Motlik, Z. Ellederova, Gradual Phenotype Development in Huntington Disease Transgenic Minipig Model at 24 Months of Age. *Neurodegener Dis* **18**, 107-119 (2018).
32. M. Baxa, B. Levinska, M. Skrivankova, M. Pokorny, J. Juhasova, J. Klima, J. Klempir, S. Juhas, Z. Ellederova, Longitudinal study revealed motor, cognitive and behavioral decline in transgenic minipig model of Huntington's disease. *Dis Model Mech*, (2019).
33. F. B. Rodrigues, L. M. Byrne, E. J. Wild, Biofluid Biomarkers in Huntington's Disease. *Methods Mol Biol* **1780**, 329-396 (2018).
34. V. Fodale, R. Boggio, M. Daldin, C. Cariulo, M. C. Spiezia, L. M. Byrne, B. R. Leavitt, E. J. Wild, D. Macdonald, A. Weiss, A. Bresciani, Validation of Ultrasensitive Mutant Huntingtin Detection in Human Cerebrospinal Fluid by Single Molecule Counting Immunoassay. *J Huntingtons Dis* **6**, 349-361 (2017).
35. E. J. Wild, R. Boggio, D. Langbehn, N. Robertson, S. Haider, J. R. Miller, H. Zetterberg, B. R. Leavitt, R. Kuhn, S. J. Tabrizi, D. Macdonald, A. Weiss, Quantification of mutant huntingtin protein in cerebrospinal fluid from Huntington's disease patients. *J Clin Invest* **125**, 1979-1986 (2015).
36. M. M. J. van den Berg, J. Krauskopf, J. G. Ramaekers, J. C. S. Kleinjans, J. Prickaerts, J. J. Briede, Circulating microRNAs as potential biomarkers for psychiatric and neurodegenerative disorders. *Prog Neurobiol*, 101732 (2019).
37. L. M. Byrne, F. B. Rodrigues, E. B. Johnson, P. A. Wijeratne, E. De Vita, D. C. Alexander, G. Palermo, C. Czech, S. Schobel, R. I. Scahill, A. Heslegrave, H. Zetterberg, E. J. Wild, Evaluation of mutant huntingtin and neurofilament proteins as potential markers in Huntington's disease. *Sci Transl Med* **10**, (2018).
38. R. H. Bobo, D. W. Laske, A. Akbasak, P. F. Morrison, R. L. Dedrick, E. H. Oldfield, Convection-enhanced delivery of macromolecules in the brain. *Proc Natl Acad Sci U S A* **91**, 2076-2080 (1994).
39. N. U. Barua, M. Woolley, A. S. Bienemann, D. Johnson, M. J. Wyatt, C. Irving, O. Lewis, E. Castrique, S. S. Gill, Convection-enhanced delivery of AAV2 in white matter--a novel method for gene delivery to cerebral cortex. *J Neurosci Methods* **220**, 1-8 (2013).
40. P. Dietrich, I. M. Johnson, S. Alli, I. Dragatsis, Elimination of huntingtin in the adult mouse leads to progressive behavioral deficits, bilateral thalamic calcification, and altered brain iron homeostasis. *PLoS Genet* **13**, e1006846 (2017).
41. L. Samaranch, B. Blits, W. San Sebastian, P. Hadaczek, J. Bringas, V. Sudhakar, M. Macayan, P. J. Pivrotto, H. Petry, K. S. Bankiewicz, MR-guided parenchymal delivery of adeno-associated viral vector serotype 5 in non-human primate brain. *Gene Ther* **24**, 253-261 (2017).
42. M. E. Emborg, S. A. Hurley, V. Joers, P. M. Tromp do, C. R. Swanson, S. Ohshima-Hosoyama, V. Bondarenko, K. Cummisford, M. Sonnemans, S. Hermening, B. Blits, A. L. Alexander, Titer and product affect the distribution of gene expression after intraputamenal convection-enhanced delivery. *Stereotact Funct Neurosurg* **92**, 182-194 (2014).
43. E. A. Markakis, K. P. Vives, J. Bober, S. Leichtle, C. Leranthe, J. Beecham, J. D. Elsworth, R. H. Roth, R. J. Samulski, D. E. Redmond, Jr., Comparative transduction efficiency of AAV vector serotypes 1-6 in the substantia nigra and striatum of the primate brain. *Mol Ther* **18**, 588-593 (2010).
44. A. Gerits, P. Vancraeynest, S. Vreysen, M. E. Laramée, A. Michiels, R. Gijssbers, C. Van den Haute, L. Moons, Z. Debyser, V. Baekelandt, L. Arckens, W. Vanduffel, Serotype-dependent transduction

- efficiencies of recombinant adeno-associated viral vectors in monkey neocortex. *Neurophotonics* **2**, 031209 (2015).
45. I. Diester, M. T. Kaufman, M. Mogri, R. Pashaie, W. Goo, O. Yizhar, C. Ramakrishnan, K. Deisseroth, K. V. Shenoy, An optogenetic toolbox designed for primates. *Nat Neurosci* **14**, 387-397 (2011).
 46. M. A. Colle, F. Piguet, L. Bertrand, S. Raoul, I. Bieche, L. Dubreil, D. Sloothaak, C. Bouquet, P. Moullier, P. Aubourg, Y. Chereil, N. Cartier, C. Sevin, Efficient intracerebral delivery of AAV5 vector encoding human ARSA in non-human primate. *Hum Mol Genet* **19**, 147-158 (2010).
 47. J. M. Taymans, L. H. Vandenberghe, C. V. Haute, I. Thiry, C. M. Deroose, L. Mortelmans, J. M. Wilson, Z. Debyser, V. Baekelandt, Comparative analysis of adeno-associated viral vector serotypes 1, 2, 5, 7, and 8 in mouse brain. *Hum Gene Ther* **18**, 195-206 (2007).
 48. I. Scheyltjens, M. E. Laramee, C. Van den Haute, R. Gijsbers, Z. Debyser, V. Baekelandt, S. Vreysen, L. Arckens, Evaluation of the expression pattern of rAAV2/1, 2/5, 2/7, 2/8, and 2/9 serotypes with different promoters in the mouse visual cortex. *J Comp Neurol* **523**, 2019-2042 (2015).
 49. B. E. Deverman, B. M. Ravina, K. S. Bankiewicz, S. M. Paul, D. W. Y. Sah, Gene therapy for neurological disorders: progress and prospects. *Nat Rev Drug Discov* **17**, 641-659 (2018).
 50. A. M. Dudek, N. Zabaleta, E. Zinn, S. Pillay, J. Zengel, C. Porter, J. S. Franceschini, R. Estelien, J. E. Carette, G. L. Zhou, L. H. Vandenberghe, GPR108 Is a Highly Conserved AAV Entry Factor. *Mol Ther* **28**, 367-381 (2020).
 51. C. Burger, O. S. Gorbatyuk, M. J. Velardo, C. S. Peden, P. Williams, S. Zolotukhin, P. J. Reier, R. J. Mandel, N. Muzyczka, Recombinant AAV viral vectors pseudotyped with viral capsids from serotypes 1, 2, and 5 display differential efficiency and cell tropism after delivery to different regions of the central nervous system. *Mol Ther* **10**, 302-317 (2004).
 52. M. Gray, Astrocytes in Huntington's Disease. *Adv Exp Med Biol* **1175**, 355-381 (2019).
 53. J. Guduric-Fuchs, A. O'Connor, B. Camp, C. L. O'Neill, R. J. Medina, D. A. Simpson, Selective extracellular vesicle-mediated export of an overlapping set of microRNAs from multiple cell types. *BMC Genomics* **13**, 357 (2012).
 54. R. Reshke, J. A. Taylor, A. Savard, H. Guo, L. H. Rhym, P. S. Kowalski, M. T. Trung, C. Campbell, W. Little, D. G. Anderson, D. Gibbings, Reduction of the therapeutic dose of silencing RNA by packaging it in extracellular vesicles via a pre-microRNA backbone. *Nat Biomed Eng* **4**, 52-68 (2020).
 55. M. S. Keiser, H. B. Kordasiewicz, J. L. McBride, Gene suppression strategies for dominantly inherited neurodegenerative diseases: lessons from Huntington's disease and spinocerebellar ataxia. *Hum Mol Genet* **25**, R53-64 (2016).
 56. E. L. Pfister, N. DiNardo, E. Mondo, F. Borel, F. Conroy, C. Fraser, G. Gernoux, X. Han, D. Hu, E. Johnson, L. Kennington, P. Liu, S. J. Reid, E. Sapp, P. Vodicka, T. Kuchel, A. J. Morton, D. Howland, R. Moser, M. Sena-Estevés, G. Gao, C. Mueller, M. DiFiglia, N. Aronin, Artificial miRNAs Reduce Human Mutant Huntingtin Throughout the Striatum in a Transgenic Sheep Model of Huntington's Disease. *Hum Gene Ther* **29**, 663-673 (2018).
 57. J. C. Jacobsen, C. S. Bawden, S. R. Rudiger, C. J. McLaughlan, S. J. Reid, H. J. Waldvogel, M. E. MacDonald, J. F. Gusella, S. K. Walker, J. M. Kelly, G. C. Webb, R. L. Faull, M. I. Rees, R. G. Snell, An ovine transgenic Huntington's disease model. *Hum Mol Genet* **19**, 1873-1882 (2010).
 58. J. L. McBride, M. R. Pitzer, R. L. Boudreau, B. Dufour, T. Hobbs, S. R. Ojeda, B. L. Davidson, Preclinical safety of RNAi-mediated HTT suppression in the rhesus macaque as a potential therapy for Huntington's disease. *Mol Ther* **19**, 2152-2162 (2011).
 59. R. Grondin, M. D. Kaytor, Y. Ai, P. T. Nelson, D. R. Thakker, J. Heisel, M. R. Weatherspoon, J. L. Blum, E. N. Burright, Z. Zhang, W. F. Kaemmerer, Six-month partial suppression of Huntingtin is well tolerated in the adult rhesus striatum. *Brain* **135**, 1197-1209 (2012).
 60. S. E. Leff, S. K. Spratt, R. O. Snyder, R. J. Mandel, Long-term restoration of striatal L-aromatic amino acid decarboxylase activity using recombinant adeno-associated viral vector gene transfer in a rodent model of Parkinson's disease. *Neuroscience* **92**, 185-196 (1999).

61. D. Sondhi, D. A. Peterson, E. L. Giannaris, C. T. Sanders, B. S. Mendez, B. De, A. B. Rostkowski, B. Blanchard, K. Bjugstad, J. R. Sladek, Jr., D. E. Redmond, Jr., P. L. Leopold, S. M. Kaminsky, N. R. Hackett, R. G. Crystal, AAV2-mediated CLN2 gene transfer to rodent and non-human primate brain results in long-term TPP-I expression compatible with therapy for LINCL. *Gene Ther* **12**, 1618-1632 (2005).
62. P. Hadaczek, J. L. Eberling, P. Pivrotto, J. Bringas, J. Forsayeth, K. S. Bankiewicz, Eight years of clinical improvement in MPTP-lesioned primates after gene therapy with AAV2-hAADC. *Mol Ther* **18**, 1458-1461 (2010).
63. G. Mittermeyer, C. W. Christine, K. H. Rosenbluth, S. L. Baker, P. Starr, P. Larson, P. L. Kaplan, J. Forsayeth, M. J. Aminoff, K. S. Bankiewicz, Long-term evaluation of a phase 1 study of AADC gene therapy for Parkinson's disease. *Hum Gene Ther* **23**, 377-381 (2012).
64. A. L. Southwell, S. E. Smith, T. R. Davis, N. S. Caron, E. B. Villanueva, Y. Xie, J. A. Collins, M. L. Ye, A. Sturrock, B. R. Leavitt, A. G. Schrum, M. R. Hayden, Ultrasensitive measurement of huntingtin protein in cerebrospinal fluid demonstrates increase with Huntington disease stage and decrease following brain huntingtin suppression. *Sci Rep* **5**, 12166 (2015).
65. R. Constantinescu, M. Romer, D. Oakes, L. Rosengren, K. Kiebertz, Levels of the light subunit of neurofilament triplet protein in cerebrospinal fluid in Huntington's disease. *Parkinsonism Relat Disord* **15**, 245-248 (2009).
66. L. M. Byrne, F. B. Rodrigues, K. Blennow, A. Durr, B. R. Leavitt, R. A. C. Roos, R. I. Scahill, S. J. Tabrizi, H. Zetterberg, D. Langbehn, E. J. Wild, Neurofilament light protein in blood as a potential biomarker of neurodegeneration in Huntington's disease: a retrospective cohort analysis. *Lancet Neurol* **16**, 601-609 (2017).
67. J. Kuhle, G. Disanto, J. Lorscheider, T. Stites, Y. Chen, F. Dahlke, G. Francis, A. Shrinivasan, E. W. Radue, G. Giovannoni, L. Kappos, Fingolimod and CSF neurofilament light chain levels in relapsing-remitting multiple sclerosis. *Neurology* **84**, 1639-1643 (2015).
68. A. Mellgren, R. W. Price, L. Hagberg, L. Rosengren, B. J. Brew, M. Gisslen, Antiretroviral treatment reduces increased CSF neurofilament protein (NFL) in HIV-1 infection. *Neurology* **69**, 1536-1541 (2007).
69. B. Olsson, L. Alberg, N. C. Cullen, E. Michael, L. Wahlgren, A. K. Kroksmark, K. Rostasy, K. Blennow, H. Zetterberg, M. Tulinius, NFL is a marker of treatment response in children with SMA treated with nusinersen. *J Neurol* **266**, 2129-2136 (2019).
70. J. Kuhle, H. Kropshofer, D. A. Haering, U. Kundu, R. Meinert, C. Barro, F. Dahlke, D. Tomic, D. Leppert, L. Kappos, Blood neurofilament light chain as a biomarker of MS disease activity and treatment response. *Neurology* **92**, e1007-e1015 (2019).
71. S. A. Schobel. (2020).
72. R. Constantinescu, B. Holmberg, L. Rosengren, O. Corneliusson, B. Johnels, H. Zetterberg, Light subunit of neurofilament triplet protein in the cerebrospinal fluid after subthalamic nucleus stimulation for Parkinson's disease. *Acta Neurol Scand* **124**, 206-210 (2011).
73. F. Saudou, S. Humbert, The Biology of Huntingtin. *Neuron* **89**, 910-926 (2016).
74. A. Majowicz, D. Salas, N. Zabaleta, E. Rodriguez-Garcia, G. Gonzalez-Aseguinolaza, H. Petry, V. Ferreira, Successful Repeated Hepatic Gene Delivery in Mice and Non-human Primates Achieved by Sequential Administration of AAV5(ch) and AAV1. *Mol Ther* **25**, 1831-1842 (2017).
75. M. Urabe, C. Ding, R. M. Kotin, Insect cells as a factory to produce adeno-associated virus type 2 vectors. *Hum Gene Ther* **13**, 1935-1943 (2002).
76. C. Unzu, S. Hervas-Stubbs, A. Sampedro, I. Mauleon, U. Mancheno, C. Alfaro, R. E. de Salamanca, A. Benito, S. G. Beattie, H. Petry, J. Prieto, I. Melero, A. Fontanellas, Transient and intensive pharmacological immunosuppression fails to improve AAV-based liver gene transfer in non-human primates. *J Transl Med* **10**, 122 (2012).

Supplementary Tables

Table S1. Statistical analysis of mHTT in CSF of tgHD minipigs (control versus treated).

Type 3 tests of fixed effects				
Effect	Num DF	Den DF	F Value	Pr > F
Treatment	1	28.8	5.64	0.0244
Time	3	44.9	0.79	0.5036
Analysis_batch	1	58.8	14.13	0.0004
Treatment*Time	4	47.9	0.32	0.8634
Contrasts				
Comparison	N	Confidence Interval	P	
Average effect over time	73	0.568 (0.412-0.784)	0.001	
Treatment versus control at T=6 months	73	0.668 (0.449-0.993)	0.046	
Treatment versus control at T=9 months	73	0.551 (0.378-0.803)	0.003	
Treatment versus control at T=12 months	73	0.657 (0.438-0.984)	0.042	

Analysis of covariance model: $\log(\text{AVG mHTT (fM)}) = \text{Treatment} + \text{Time} + \text{Analysis_batch} + \text{Treatment} * \text{Time} + \text{Age_at_collection}$

NOTE: Raw estimates based on the log transformed AVG mHTT (fM) were back transformed, presenting the ratio of treatment versus control with 95% confidence intervals and p-values for the average effect over time and at each time point

Table S2. Study design of intrastriatal microRNA-based gene therapy in tgHD minipigs.

Timepoint	- 7 d	0	7 d	14 d	28 d	3 m o	6 m o	9 m o	12 mo	15 mo	18 mo	21 mo	24 mo	>24 mo* *
TgHD minipigs														
1. Naive 6mo (n = 3)							†							
2. Naive 12mo (n = 4)									†					
3. Naive >24mo (n = 8)														
4. rAAV5miH TT 6mo (n = 3*)							†							
5. rAAV5miH TT 12mo (n = 4)									†					
6. rAAV5miH TT >24mo (n = 8)														
MRI-guided CED (groups 4 to 6)	x													
Blood and CSF collection	x		x	x	x	x	x	x	x	x	x	x	x	x
Sacrifice and brain collection							x		x					

■: in life, †: sacrifice, **: phenotypic follow-up, d: days, mo: months

*Note: Initial group size was n=4, but one animal did not recover from anesthesia during CSF collection at 28d post-injection

Supplementary Figures

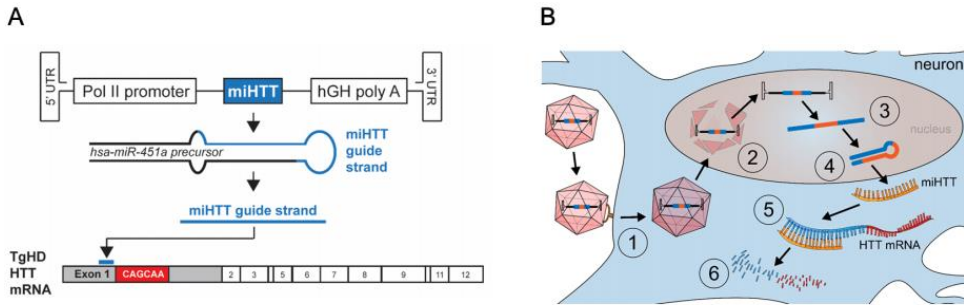


Fig. S1. Design and mechanism of action of rAAV5-miHTT leading to HTT lowering in the cell. (A) The DNA construct is comprised of miHTT, an artificial microRNA in which the guide strand of hs-miR-451a has been modified to specifically target human HTT; miHTT is flanked by a pol II promoter, and a hGH polyA signal at the 5' and 3' ends, respectively, as well as inverted terminal repeats (ITR) at each end. The miHTT guide strand binds 5' from the expanded CAG repeat, therefore targeting human HTT exon 1. In tgHD minipigs, the CAG expansion repeat is regularly interrupted with by CAA to avoid somatic instability in this model. **(B)** The mechanism of action can be described in several steps. (1) Upon parenchymal injection AAV5-miHTT binds to neuronal cell-surface receptors and is internalized. (2) Transport to the nucleus and uncoating of the miHTT transgene which remains mostly episomal. (3) Expression and processing of the miHTT transgene by the endogenous RNA interference machinery; (4) Hairpin structured precursor is transported to the cytoplasm and further processed to mature guide miHTT. No passenger strand is formed, strongly limiting the risk of off-target activity. (5) Mature miHTT is loaded in the RNA-induced silencing complex and binds HTT mRNA. (6) HTT mRNA is cleaved and degraded, resulting in lowering of HTT protein translation.

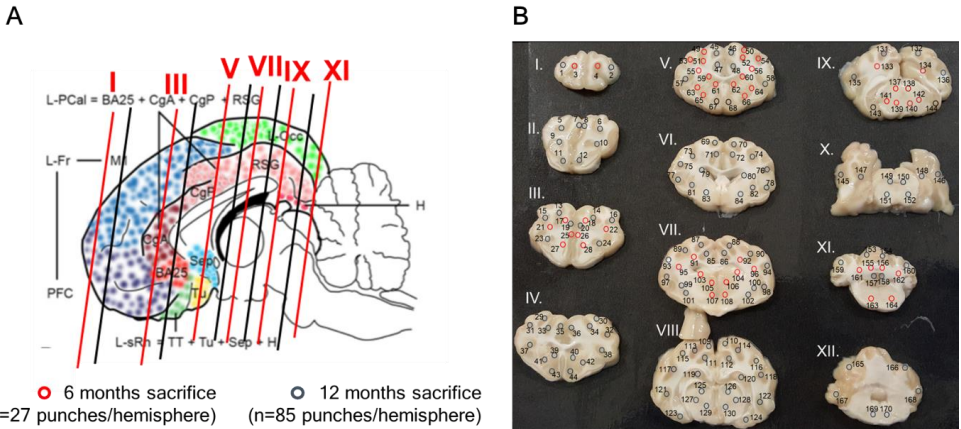


Fig. S2. Brain dissection scheme for bioanalytics. (A) tgHD minipig brains were cut in coronal sections of 4mm thick (12 sections in total, numbered in roman numbers I to XII). Brain regions of interest for bioanalyses were dissected by micropunch, using uneven sections (in the case of 6 months interim sacrifice) or both even and uneven (for 12 months interim sacrifice). (B) Scheme depicting the position of the punches (4 mm in diameter) to dissect brain regions of interest. In red, regions dissected for the 6-month interim sacrifice. In dark blue, additional regions dissected after the 12 months interim sacrifice.

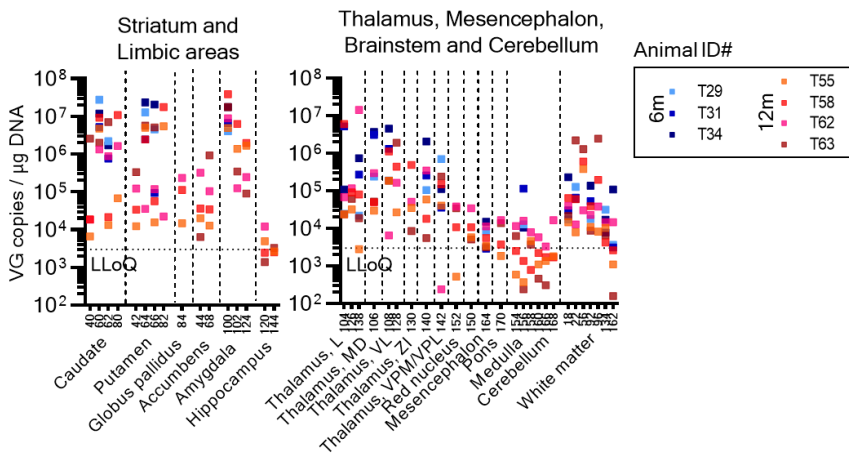


Fig. S3. Vector genome copies in deep brain regions of tgHD minipigs at 6- and 12-months post RAAV5-miHTT administration in caudate and putamen. Concentrations of vector DNA (expressed as vector genome copies/µg genomic DNA) in striatum, limbic areas, thalamus, brainstem and cerebellum, are shown. In blue, animals sacrificed at 6 months (coded T29, T31 and T34). In shades of orange to pink, animals sacrificed at 12 months (coded T55, T58, T62 and T63). Each square represents an individual punch. VG concentrations were above LLOQ in all brain regions, except partly in hippocampus, cerebellum, white matter and individual brainstem nuclei. LLOQ: lower limit of quantification.

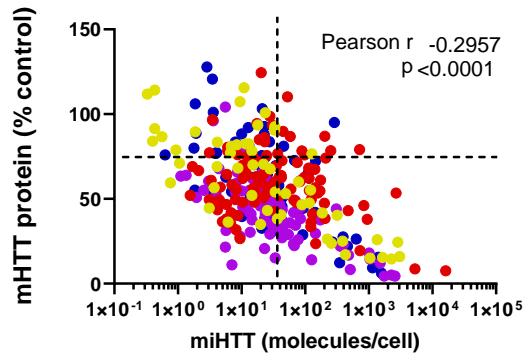


Fig. S4. Correlation between miHTT expression and mHTT protein lowering (as % from control), 12months post rAAV5-miHTT administration. Each color represents one of the 4 animals of the treated group, sacrificed at 12 months post-treatment.

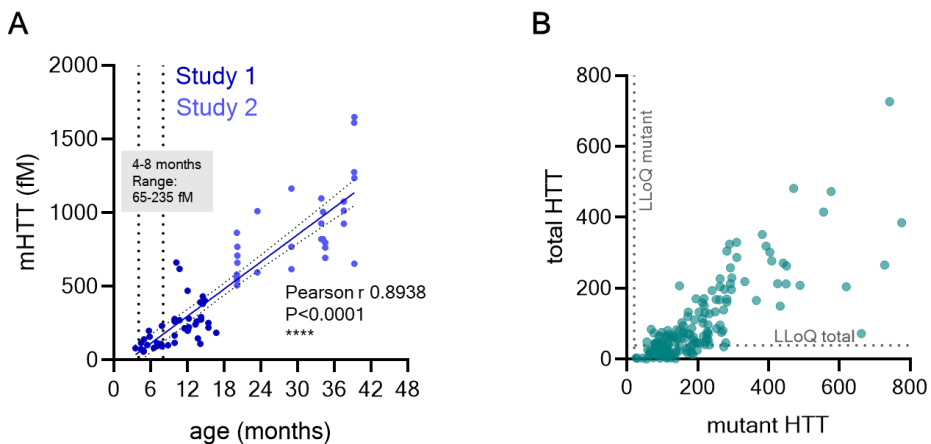


Fig. S5. Huntingtin protein concentrations in CSF of tgHD minipigs increase with age, as determined by two independent immunoassays. (A) Mutant HTT (mHTT) protein concentrations in CSF (expressed in fM) using samples from two independent studies with untreated tgHD minipigs of different ages. **(B)** Quantification of total and mutant HTT using an independent immunoassay. *LLoQ*: lower limit of quantification.

3

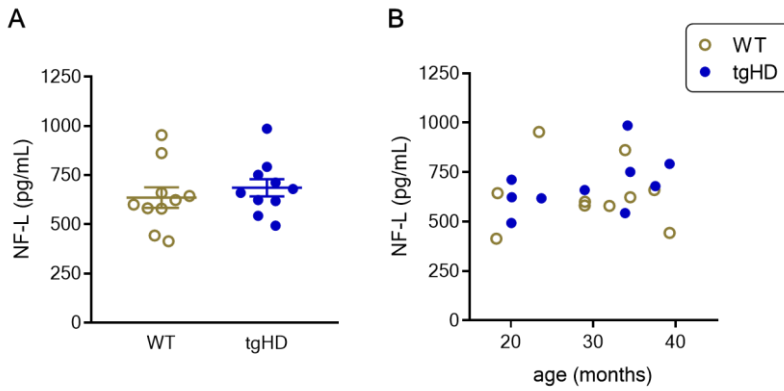


Fig. S6. No differences in CSF neurofilament light chain (NF-L) between wild type (WT) and transgenic HD minipigs (TG) up to 4 years of age. (A) NF-L concentrations in WT and tgHDminipigs and **(B)** CSF NF-L concentration by age in WT and tgHD minipigs.

Chapter

4

Secreted therapeutics: Monitoring durability of microRNA-based gene therapies in the central nervous system

Marina Sogorb-Gonzalez^{1,2}, Carlos Vendrell-Tornero¹,
Jolanda Snapper¹, Anouk Stam¹, Sonay Keskin¹, Jana
Miniarikova^{1,2}, Elisabeth A. Spronck¹, Martin de Haan¹, Rien
Nieuwland³, Pavlina Konstantinova¹, Sander J. van
Deventer^{1,2}, Melvin M. Evers^{1*}, Astrid Vallès^{1*}

¹Department of Research & Development, uniQure Biopharma
N.V., Amsterdam, The Netherlands

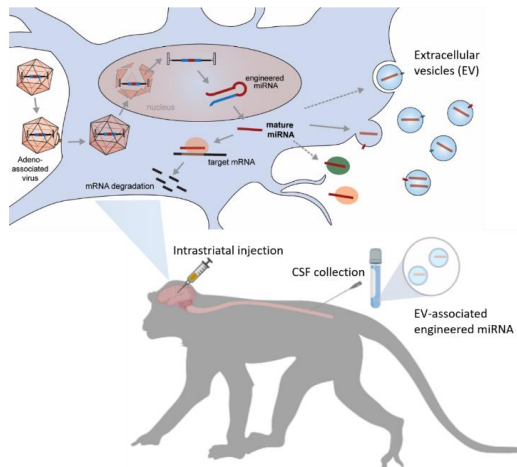
²Department of Gastroenterology and Hepatology, Leiden
University Medical Center, Leiden, The Netherlands

³Laboratory of Experimental Clinical Chemistry, Amsterdam UMC,
University of Amsterdam, Amsterdam, The Netherlands, and
Vesicles Observation Center, Amsterdam UMC, University of
Amsterdam, Amsterdam, The Netherlands

*These authors contributed equally

Abstract

The preclinical development of microRNA-based gene therapies for inherited neurodegenerative diseases is accompanied by translational challenges. Due to the inaccessibility of the brain to periodically evaluate therapy effects, accessible and reliable biomarkers indicative of dosing, durability and therapeutic efficacy in the central nervous system are very much needed. This is particularly important for viral vector-based gene therapies, in which a one-time administration results in long-term expression of active therapeutic molecules in the brain. Recently, extracellular vesicles (EVs) have been identified as carriers of RNA species, including microRNAs, and proteins in all biological fluids, whilst becoming potential sources of biomarkers for diagnosis. In this study, we investigated the secretion and potential use of circulating extracellular miRNAs associated with EVs as suitable sources to monitor the expression and durability of gene therapies in the brain. Neuronal cells derived from induced pluripotent stem cells (iPSCs) were treated with adeno-associated viral vector serotype 5 (AAV5) carrying an engineered microRNA targeting HTT gene (miHTT) or ataxin 3 gene (miATXN3) sequence, the diseases-causing genes of Huntington disease and spinocerebellar ataxia type 3, respectively. After AAV treatment, the secretion of mature engineered microRNA molecules was confirmed, with extracellular microRNA levels correlating with viral dose and cellular microRNA expression in neurons. We further investigated the detection of engineered microRNAs over time in the cerebrospinal fluid of non-human primates after a single intrastriatal injection of AAV5-miHTT. Quantifiable engineered microRNA levels enriched in EVs were detected in the cerebrospinal fluid (CSF) up to two years after brain infusion. Altogether, these results confirm the long-term expression of AAV5-delivered microRNAs and support the use of EV-associated microRNAs as novel translational pharmacokinetic markers in ongoing clinical trials of gene therapies for neurodegenerative diseases.



Introduction

The identification of causal mutations in many neurodegenerative diseases has opened the door to the development of novel disease-modifying therapies. In the case of polyglutamine (polyQ) diseases, caused by inheritance of CAG triplet-repeat expansions, gene silencing approaches are being investigated to lower the presence of toxic polyQ proteins (Boudreau *et al.*, 2011; Keiser *et al.*, 2016; Wild and Tabrizi, 2017; Matos *et al.*, 2018; Miniarikova *et al.*, 2018). Next to the use of antisense oligonucleotides, one of the most advanced lowering strategies is microRNA (miRNA)-based gene therapy (Tabrizi *et al.*, 2019). This approach is based on the design of RNA interference (RNAi) molecules complementary to the mutation-carrying mRNA and inserted into a precursor miRNA (pre-miRNA) backbone. Engineered pre-miRNAs, likewise their endogenous counterparts, are processed into mature ~21 nucleotide miRNA molecules which are incorporated in the RNAi silencing complex (RISC). Activated miRNA-RISC complex binds to target mRNA based on sequence complementarity resulting in translational repression or enzymatic cleavage (Jonas and Izaurralde, 2015). Engineered miRNA-based treatments rely on the administration of an adeno-associated viral (AAV) vector containing an expression cassette of the therapeutic miRNA precursor. The episomal persistence of the viral expression cassette results in a continuous production of the therapeutic agent and long-term gene suppression after one-time administration, bypassing the need of re-administration. Proof-of-concept studies have demonstrated that AAV-delivered miRNAs can be used for safe, effective and durable lowering of toxic mutant proteins in polyQ-related neurodegenerative disorders (McBride *et al.*, 2011; Keiser *et al.*, 2016; Miniarikova *et al.*, 2016; Martier *et al.*, 2019). For Huntington disease (HD), the most common polyQ disorder, infusion of a serotype 5 AAV-delivered miRNA targeting the huntingtin gene (*HTT*) sequence (AAV5-miHTT) resulted in efficient and well-tolerated HTT protein lowering in the brain of different HD animal models (Miniarikova *et al.*, 2016, 2017; Evers *et al.*, 2018; Spronck *et al.*, 2019). Long-term HTT lowering was associated with prevention of neuronal dysfunction and functional improvement in HD mouse models, supporting the Food and Drug Administration (FDA) approval and initiation of a Phase I/II clinical trial in early manifest HD (Clinicaltrials.gov, NCT04120493).

The translation of miRNA-based gene therapies to the clinic is faced with meaningful challenges (Chakraborty *et al.*, 2017; Miniarikova *et al.*, 2018). One of the main obstacles for neurodegenerative diseases is the relative inaccessibility of the central nervous system (CNS). Different routes of administration have been investigated to achieve a wide distribution of viral particles and sufficient expression of engineered miRNA molecules in affected brain regions (Hocquemiller *et al.*, 2016). Studies in non-human primates show that AAV5 infusion in the striatum leads to efficient transduction not only in the primary target

structures, but also in cortical projection areas, which become also affected in HD (Waldvogel *et al.*, 2015; Samaranch *et al.*, 2017). Besides delivery, there is an urgent need to establish accessible biomarkers which are indicative of dosing, safety and efficacy in patients after treatment. This is especially important for AAV-based gene therapy approaches, where a one-time administration results in long-term expression of active therapeutic molecules. Finding reliable translational measurements to monitor vector expression and levels of therapeutic molecules would be an important step towards establishing pharmacokinetic measures to predict efficacy and long-term durability of miRNA-based gene therapies in ongoing and future clinical studies.

Recent evidence has shown that signaling molecules such as proteins, lipids and RNAs can be released from the cells of origin within extracellular vesicles (EVs) (Valadi *et al.*, 2007; Zhang *et al.*, 2015). The term “EVs” includes exosomes, microvesicles and other small vesicles that are released into the extracellular environment by fusion of multivesicular bodies or by direct budding of the plasma membrane. Since they are found in all body fluids, EV profiles and cargos are emerging as clinically useful and non-invasive prognostic biomarker carriers in cancer and brain disorders (Kinoshita *et al.*, 2017; Sheinerman *et al.*, 2017). In the case of neurodegenerative disorders, the trafficking of molecules from the inaccessible CNS to cerebrospinal fluid (CSF) mediated by EVs allows the detection of pathology-related molecules, which remain protected from proteases and nucleases present in the liquid. Numerous studies have reported altered CSF miRNA expression profiles for Alzheimer disease, Parkinson disease and multiple sclerosis (Cogswell *et al.*, 2008; Haghikia *et al.*, 2012; Gui *et al.*, 2015). However, in order to establish reliable biomarkers, it is important to understand that EV loading is not a random process and cellular overexpression does not always imply packaging into EVs. For instance, a recent study identified a set of endogenous miRNAs preferentially released within EVs across different cell types (Guduric-Fuchs *et al.*, 2012). Among those, miR-451a was found to be the most highly EV-enriched miRNAs relative to the cellular levels. Therefore, characterization of preferentially exported molecules and correlation with cellular status is highly relevant.

In this study, we evaluated the secretion of engineered therapeutic miRNAs from neuronal cells via EVs after AAV5 delivery. We further investigated the potential use of extracellular miRNAs in biological fluids as suitable sources for measurements to monitor the long-term durability of active miRNA molecules in the brain after one-time AAV5 administration. For this purpose, we selected two therapeutic miRNAs designed to target huntingtin gene (miHTT) and ataxin 3 gene (miATXN3), the disease-causing genes of HD and spinocerebellar ataxia type 3 (SCA3), respectively, both delivered via AAV5 (AAV5-miHTT and AAV5-miATXN3) (Miniarikova *et al.*, 2016; Martier *et al.*, 2019). Our results show that AAV5-delivered therapeutic miRNA molecules are released from neuronal cells in a dose-

dependent manner in association with EVs and protein complexes. Furthermore, a reliable detection of therapeutic miRNA in biological fluids in non-human primates up to two years after dosing confirms the translational value of extracellular miRNAs to monitor the expression and durability of therapeutic miRNAs directly delivered in the brain. The present findings have important implications for the long-term monitoring of ongoing and future clinical studies of miRNA-based gene therapies for CNS disorders.

Results

Engineered miRNA-based therapeutic candidates for inherited neurodegenerative diseases

In order to validate our hypothesis that engineered miRNAs delivered in the CNS can be detected extracellularly in biological fluids, we first evaluated their secretion from neuronal cells after AAV5-treatment. For this purpose, a neuronal system based on human induced-pluripotent stem cells (iPSCs) from an HD patient was selected. iPSCs were differentiated into neuronal progenitor cells and matured into forebrain-like neuronal cells which were positive for microtubule-associated protein 2 (MAP2) neuronal marker. Glial cells positive for glial fibrillary acidic protein (GFAP) astrocytic marker were also found to a lesser extent (Supplementary Figure 1). We designed two miRNA sequences, both inserted in the pre-miR-451a backbone (Cheloufi *et al.*, 2010) (**Figure 1A**), and incorporated into an AAV5 capsid. One miRNA candidate was designed to target the *HTT* sequence (miHTT) as a potential treatment for HD (Miniarikova *et al.*, 2016). The other miRNA candidate targets ataxin-3 (*ATXN3*) sequence (miATXN3), the disease-causing gene of SCA3 (Martier *et al.*, 2019). After nuclear expression by RNA polymerase II, engineered miRNAs are processed from primary transcripts to hairpin-containing precursors (pre-miRNA). Unlike other miRNAs, pre-miR-451 stem-loop structure is too short to be cleaved by the endoribonuclease Dicer and it is directly processed by protein argonaute-2 (Ago2) into mature miRNA molecules. Mature miRNAs are incorporated in the RISC complex and together bind the target mRNA based on sequence complementarity (Matsuyama and Suzuki, 2019) (**Figure 1B**). The processing of pre-miR-451 engineered miHTT and miATXN3 constructs into mature molecules has been previously determined by RNA sequencing in human and murine models (Keskin *et al.*, 2019; Martier *et al.*, 2019). Moreover, efficacy of both AAV5-miHTT and AAV5-miATXN3 treatment to suppress target genes has been demonstrated in human neuronal cells, brain organoids and animal models achieving successful lowering of HTT and ATXN3 protein, respectively (Miniarikova *et al.*, 2017; Evers *et al.*, 2018; Martier *et al.*, 2019; Depla *et al.*, 2020).

AAV5-delivered therapeutic miRNAs are secreted from human iPSC-derived neurons

Neuronal cells were transduced with three increasing doses of AAV5-miHTT multiplicity of infection (MOI) 1×10^5 , 1×10^6 and 1×10^7 viral particles per cell) or two doses of AAV5-miATXN3 (MOI 1×10^6 and 1×10^7 viral particles per cell). Successful transduction and transgene expression were confirmed by green fluorescent protein (GFP) five days after AAV5-GFP treatment (Supplementary Figure 1). Dose-dependent genome copies (gc) were detected for AAV5-miHTT and AAV5-miATXN3 treatment, with the highest dose generating approximately 1×10^8 gc/ μ g of input gDNA (n=3; **Figure 2A** and **2B**). To quantify the expression levels of engineered miRNAs after AAV5 treatment, we used a method specific for the detection of active mature miRNA (guide strand) based on TaqMan reverse transcription (RT)- quantitative (q)PCR. As expected, higher levels of mature miHTT and miATXN3 molecules were measured in neuronal cells at increasing doses of AAV5 (n=3) (**Figure 2C** and **2D**).

It has been recently established that miRNAs are not exclusively cellular but can be secreted via EVs into peripheral fluids or cell-culture media (Valadi *et al.*, 2007). We first investigated the secretion of pre-miR-451 engineered miRNAs by enriching EVs from the culture media after AAV5 treatment. Due to large culture media volumes and the expected low RNA abundance, a precipitation-based method was used for EV isolation. Total RNA was isolated from the EV-enriched pellet and mature miRNA molecules were quantified by TaqMan qPCR. Increasing levels of extracellular miHTT and miATXN3 molecules were detected in association with EVs secreted from neuronal cells at increasing AAV5 doses (**Figure 2E** and **2F**). Stable levels, up to approximately 1×10^5 miRNA molecules/ml medium were found at 5 and 12 days after one-time AAV5 treatment. In all experiments, we detected comparable levels of endogenous miR-16 miRNA, independent of the dose and time point, confirming the replicable isolation of extracellular miRNAs by this method (Supplementary Figure 2). To validate these results, independent experiments with other doses of AAV5-miHTT were performed (MOI 6.7×10^5 , 6.7×10^6 , 3.33×10^7 viral particles per cell). As previously reported, we observed a steady correlation between AAV5-dose (log10) and relative cellular miHTT expression ($R^2=0.9275$, $p=0.002$) (**Figure 2G**), confirming a dose-dependent transduction and transgene expression in iPSC-derived neurons. Similarly, a strong correlation was observed between AAV5-dose and extracellular miHTT molecules ($R^2=0.8766$, $p=0.006$) (**Figure 2H**), and between cellular transgene expression and extracellular miHTT molecules ($R^2=0.9431$, $p=0.001$) (**Figure 2I**). Since we used a method specific for the active mature miRNA (guide strand), extracellular miRNA content is the result of cellular transgene expression, processing and secretion of AAV5-delivered miRNA.

This confirms that pre-miR-451-derived engineered miRNAs are stably secreted by neuronal cells after AAV5 transgene expression.

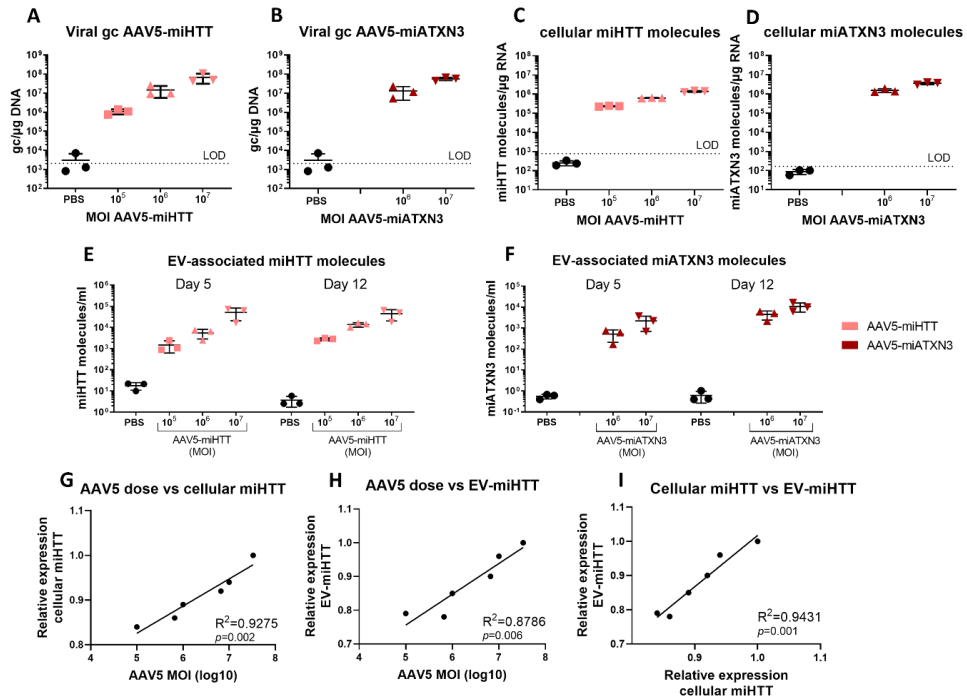


Figure 2. AAV5-delivered therapeutic miRNAs are secreted by iPSC-derived neurons in a dose-dependent manner. (A and B) Dose-dependent transduction of neuronal cells by AAV5-miHTT (A) and AAV5-miATXN3 (B) (n=3 culture plates/group). Results are expressed as AAV5 genome copies/μg DNA (each dot representing independent cell culture and average ± SEM indicated). (C and D) Dose-dependent expression of miHTT (C) and miATXN3 (D) molecules in neuronal cells (n=3 culture plates/group). (E and F) Detection of EV-associated miHTT (E) and miATXN3 (F) molecules secreted from neuronal cells at 5 and 12 days after treatment. (G, H and I) Correlation analysis of AAV5 dose (log₁₀) and relative cellular miHTT expression (G), AAV5 dose (log₁₀) and relative EV-associated miHTT detection (H), and relative cellular miHTT expression and EV-associated miHTT detection (I) (n=6, each dot represents the average value of an independent experiment in triplicates). Linear regression analysis indicating coefficient of determination (R^2) and p-value (p).

Isolation of EVs by precipitation results in co-isolation of other miRNA-bound particles

Precipitation-based isolation of EVs, such as ultracentrifuge or precipitating agents, are among the most widely applied techniques for vesicle isolation. These methods have the advantage to achieve high yield of RNA, yet possibly attributable to co-isolation of RNA-bound proteins including lipoproteins and silencing protein complexes (Karttunen *et al.*, 2019). To investigate the population of particles isolated from cultured media by precipitation, we assessed the presence, size, and morphology of vesicular and non-vesicular species by several methods. Western blot analyses confirmed the detection of exosomal markers (CD63, Alix and TSG-101), microvesicles (calnexin), and RISC complex (Ago2) in EV pellets precipitated from conditioned culture media (**Figure 3A**). In contrast, EV pellets were negative for intracellular marker α -tubulin, confirming the absence or low abundance of apoptotic cell bodies in the samples (**Figure 3A**). Distribution of particles based on size was measured by microfluidic resistive pulse sensing. The highest concentration of particles ranged between 60-80 nm diameter, characteristic of EV populations (**Figure 3B**). Flow cytometry analysis confirmed the presence of vesicles exposing CD63 and CD81, tetraspanins classically used as specific exosomal markers. Moreover, vesicles were also positive for lactadherin, a protein binding to phosphatidylserine, considered one of the best current markers for most EVs (De Rond *et al.*, 2018) (Supplementary Figure 2). Particles with a refraction index (RI) < 1.42 were characterized as EVs, and discriminated from lipoproteins (de Rond *et al.*, 2019). Isotype IgG₁ labeled samples were used as controls and showed low or undetectable levels, confirming the specificity of the signal measured by EV-marker antibodies (Supplementary Figure 2). The morphology of the vesicle population was assessed by transmission electron microscopy (TEM). Vesicle structures in a range size of 100-150 nm were visible in samples from control cells (incubated with formulation buffer) and AAV5-miATXN3 transduced cells, but not in unconditioned culture media (**Figure 3C** and Supplementary Figure 2). Notably, a significant amount of smaller protein complexes was observed in all three conditions, suggesting the presence of soluble proteins in these samples. Taken together, these results show the successful enrichment of EVs by precipitation. However, co-isolation of other protein complexes, likely associated with miRNAs, might influence the detection levels of extracellular miRNAs. To investigate the nature of extracellular miRNAs, we analyzed the effect of RNase A and detergent treatment on the miRNA levels in EV pellets precipitated from neuronal cells. Treatment of EV pellets with RNase A reduced the relative expression levels by 87% for therapeutic miATXN3 and endogenous let-7a levels, yet completely degraded endogenous levels of miR-16 and spike-in cel-miR-39 (**Figure 3D**). However, lysis of vesicles with detergent (Triton X-100) prior to RNase A resulted in complete degradation of miATXN3 and let-7a (**Figure 3D**). These results indicated that when EVs are isolated by

precipitation-based methods, extracellular miATXN3 and endogenous let-7a molecules are only partially present and protected within EVs, and that non-vesicular miRNAs highly contributed to the extracellular levels of miRNA.

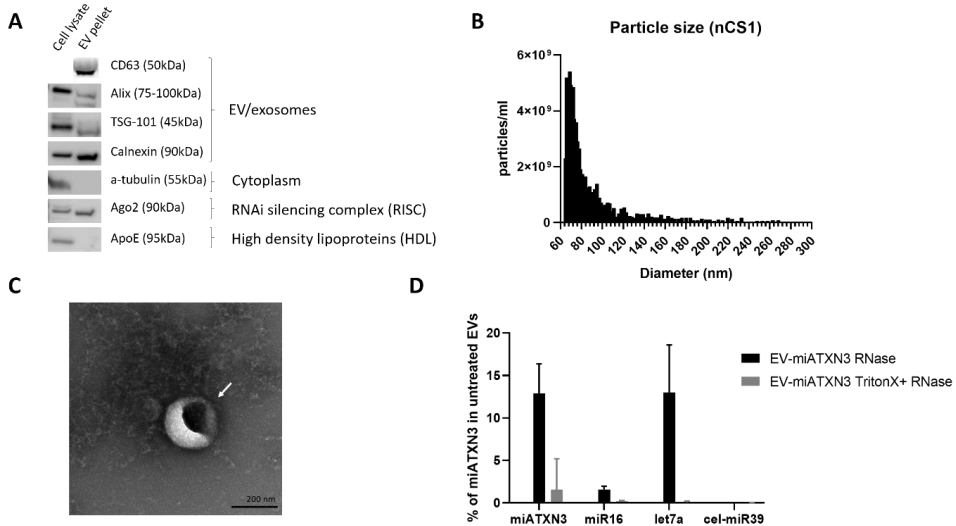


Figure 3. Characterization of EVs isolated from culture media by precipitation. (A) Western-blot analysis of cell lysate (left lane) and EV pellet (right lane) with exosomal markers (CD63, Alix and TSG-101), microvesicles (Calnexin), cytoplasm (a-tubulin), RISC complex (Ago2) and high-density lipoproteins (HDL) (ApoE). (B) Particle size distribution of vesicles measured by microfluidic resistive pulse sensing (MRPS nCS1). (C) Representative image of transmission electron microscopy (TEM) analysis of vesicles precipitated from culture media of AAV5-miATXN3 transduced cells (right). Scale bar 200nm. (D) Relative levels of miATXN3, miR-16, let-7a and spike-in cel-miR39 in EV pellets after RNase treatment (black bars) and TritonX-100 (detergent) together with RNase (grey bars) compared to non-treated EV pellets isolated by precipitation. Bars represent average \pm SEM.

Engineered miRNAs are secreted from neuronal cells in association with EVs and soluble proteins

To better understand the secretion and extracellular features of AAV5-delivered engineered miRNAs, it is important to select an isolation method that achieves higher purification of EVs and separation from protein complexes than precipitating agents. Due to size difference between these particles, efficient separation of EVs from plasma proteins have been achieved by size-exclusion chromatography (SEC) columns in numerous studies (**Figure 4A**) (Böing *et al.*, 2014). Sepharose columns allow for recovery of intact functional vesicles from soluble protein contaminants. In this study, culture media collected from cells transduced with the highest dose of AAV5-miHTT and AAV5-miATXN3 (MOI 1×10^7) was separated in 26 fractions ($n=3$ per condition). After separation, fractions were concentrated by centrifugation filters, followed by RNA isolation. The abundance of mature miHTT and miATXN3 molecules was measured in fractions 2 to 21. Both engineered miRNAs were enriched in the SEC fractions corresponding to EVs (fractions 6-8), as well as in the fractions containing the bulk of proteins, protein complexes, and EVs with a diameter < 70 nm (fractions 14-17; **Figure 4B** and **4C**). Interestingly, endogenous let-7a miRNA was comparably detected in EV- and protein-containing fractions, as opposed to endogenous miR-16, which was only detected in association with protein particles and not within EVs (fig S3). Clean separation of EVs from protein complexes was confirmed by flow cytometry analysis with CD63, CD81 and lactadherin markers. Positive events for all markers were present in a representative EV-containing fraction (fraction 7, Supplementary Figure 3), but significantly less to non-detectable in a protein-containing fraction (fraction 15, Supplementary Figure 3). TEM analysis was used to further visualize and confirm the presence of EVs in fraction 7, as compared to the high amount of protein complexes and absence of EVs in fraction 15 (**Figure 4D**). Altogether, these results confirmed the secretion of engineered miRNAs in association with EVs, which protect them from RNases, as well as with soluble proteins. That being the case, the presence and detection of such secreted therapeutics in biological fluids *in vivo* could be used as translational pharmacokinetics markers for gene therapy.

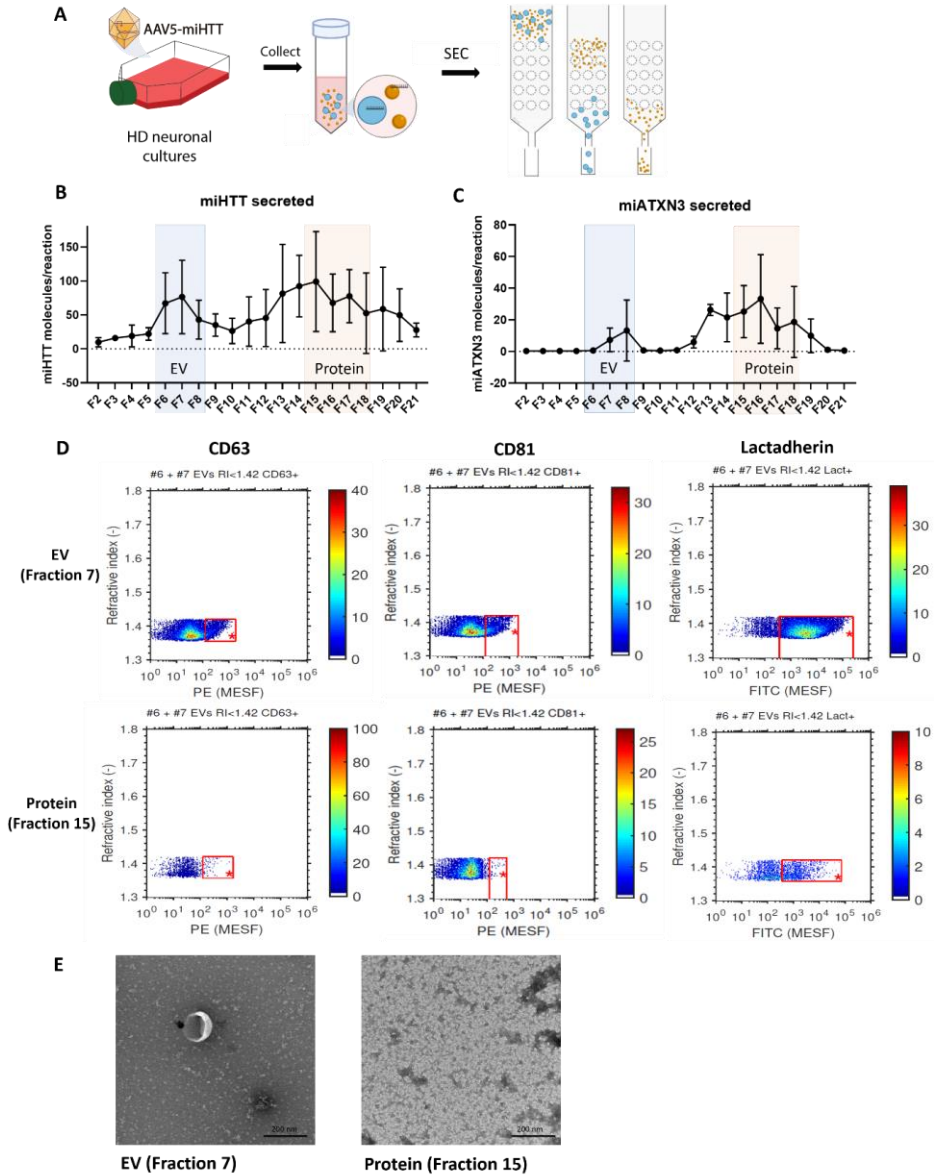


Figure 4. Detection of therapeutic miRNAs associated with EVs and protein complexes secreted from AAV5-treated iPSC-derived neurons. (A) Schematic of AAV5-miRNA transduction of iPSC-derived neurons and isolation of EVs and protein complexes by size exclusion chromatography (SEC). **(B and C)** Detection of miHTT (B) and miATXN3 (C) molecules in different SEC fractions corresponding to EV- (blue) and protein- (orange) containing fractions complexes. **(D)** Flow cytometry analysis of fraction 7 (EV fraction), showing positive signal for CD63, CD81 and lactadherin markers, and of fraction 15 (soluble protein), showing low or no detection signal for CD63, CD81 and lactadherin. **(E)** Representative images of TEM analysis of vesicles isolated by SEC in fraction 7 (left) and abundant proteins in fraction 15 (right). Scale bar 200nm.

Widespread distribution of therapeutic miHTT in non-human primates after intrastriatal treatment with AAV5-miHTT

One of the advantages of miRNA-based lowering gene therapies is the long-term expression after a one-time administration of AAV5 treatment. Monitoring the expression of the active miRNA molecules in accessible biological fluids would add value to dosing, safety and efficacy evaluation in the clinic. In this study, the secretion and successful detection of engineered miRNAs in association within EVs offers the possibility to develop an accessible pharmacokinetic measure for gene therapies injected in the brain. To investigate this, a large animal model is necessary for the appropriate translation of AAV5-miRNA therapeutic spread in a human-like brain size, correspondence to biomarker measures in biofluids, and sampling of sufficient CSF volume to perform these measurements. Therefore, we next assessed the detection and endurance of engineered miRNA molecules in the CSF in non-human primates after one-time intrastriatal administration. The therapeutic candidate for HD, AAV5-miHTT, was intracranially and bilaterally injected in the caudate and putamen, the most affected structures in HD patients (**Figure 5A**). Administration of AAV5-miHTT was performed by guided real-time MRI, which mimics the surgical approach and target region planned in ongoing clinical trial. Animals were injected with AAV5-miHTT at two doses (low and high) as indicated in **Figure 5B** and sacrificed at 6 month (cohort 1) or 24 months (cohort 2).

First, we evaluated the biodistribution and long-term expression of miHTT at six months, and at 24 months after treatment by collection of brain punches across several structures of interest. As expected, the highest level of vector DNA, as well as miHTT molecules were observed in injected areas such as caudate and putamen (striatum) (Supplementary Figure 4 and **Figure 5C**). High levels of viral DNA and miHTT expression were also detected in other deep brain structures, including thalamus and midbrain, and in cortical areas from frontal to occipital lobes (Supplementary Figure 4 and **Figure 5C**). Comparable levels of miHTT expression were found between the two cohorts at 6 months and 24 months. Due to a mismatch between the engineered miHTT and the HTT primate sequence, the lowering efficacy could not be evaluated in these areas. Low to undetectable levels of miHTT molecules were found in peripheral organs including kidney, liver and spleen (**Figure 5C**). This treatment approach shows that a one-time local infusion of AAV5-miHTT is sufficient for widespread and enduring expression of therapeutic miRNAs in the brain of large animals.

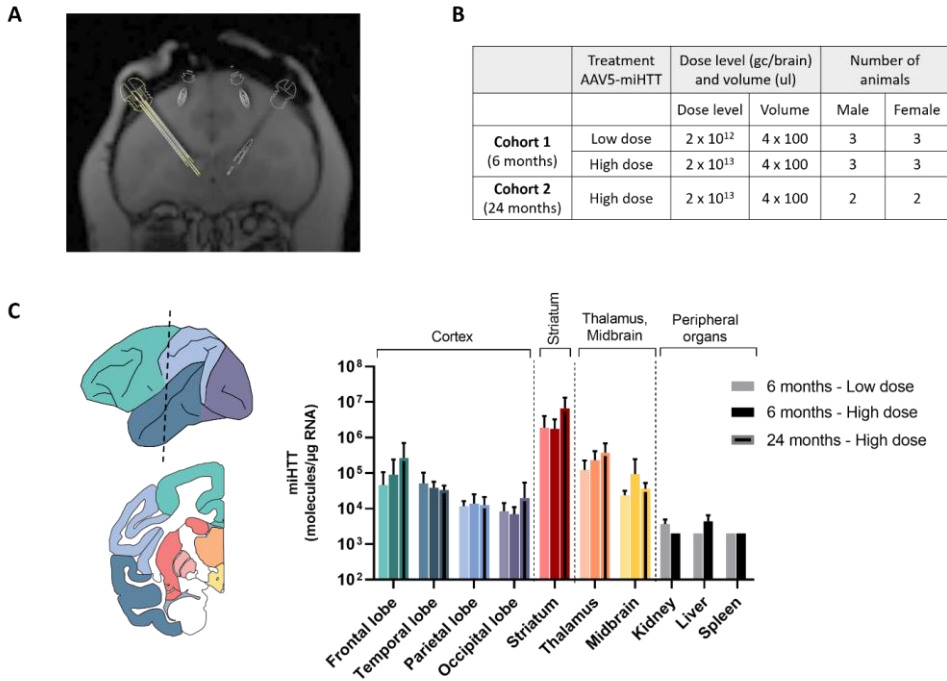


Figure 5. Widespread distribution and expression of miHTT in non-human primates after intrastriatal guided injection. (A) Non-human primate coronal brain section indicating the placement of bilateral injection in caudate and putamen by MRI-guided convention-enhanced delivery (CED). (B) Study design and treatment groups with different doses of AAV5-miHTT. (C) Biodistribution of miHTT expression in different brain areas. Scheme on the left indicates color-coded brain regions, corresponding to the colors on the right graph. Bars represent average \pm SEM of miHTT (molecules/ μ g input RNA).

Detection of EV-associated miHTT molecules in biofluids from non-human primates after intrastriatal treatment with AAV5-miHTT

To validate the potential use of circulating engineered miRNAs as pharmacokinetic markers of AAV5-miRNA gene therapies directly administered into the CNS, we quantified the presence of EV-associated therapeutic miHTT in biological fluids from non-human primates after direct brain infusion of AAV5-miHTT. CSF was collected by lumbar puncture from each animal pre-dose and at months 1, 3, 4.5 and 6 (cohort 1) and 12, 15, 18, 21 and 24 (cohort 2) post-treatment (**Figure 6A**). Total RNA associated with EVs was isolated by a spin column-based method that allows for enrichment of vesicular over non-vesicular RNA (Enderle et al., 2015), using spiked cel-miR-39 miRNA as RNA isolation control (Supplementary Figure 5). High levels of EV-associated miHTT molecules were detected in CSF at 6 months after intrastriatal treatment in cohort 1, and comparable levels up to 24 months in cohort 2 (**Figure 6B**). Levels of EV-associated miHTT molecules were quantified as fold change expression relative to pre-dose or background of the assay. In both cohorts, a comparable and relatively constant miHTT expression in the CSF was measured during the 6-month and 24-month observation period. Despite variations, there were no significant differences of miHTT levels across timepoints. In contrast, viral vector levels in CSF and plasma rapidly declined from day 1, to levels around the lower limit of quantification after four weeks (1 month), and undetectable levels at week 12 (3 months) (**Figure 6C and 6D**). Separation of CSF EVs by SEC confirmed the presence of low levels of miHTT molecules in association with EVs, as well as in protein-enriched fractions (Supplementary Figure 5). In conclusion, these results confirm the detection of circulating EV-associated therapeutic miRNAs in CSF and its potential utility as translational pharmacokinetic markers to monitor the expression and persistence of CNS delivered AAV-miRNA-based gene therapies injected in CNS.

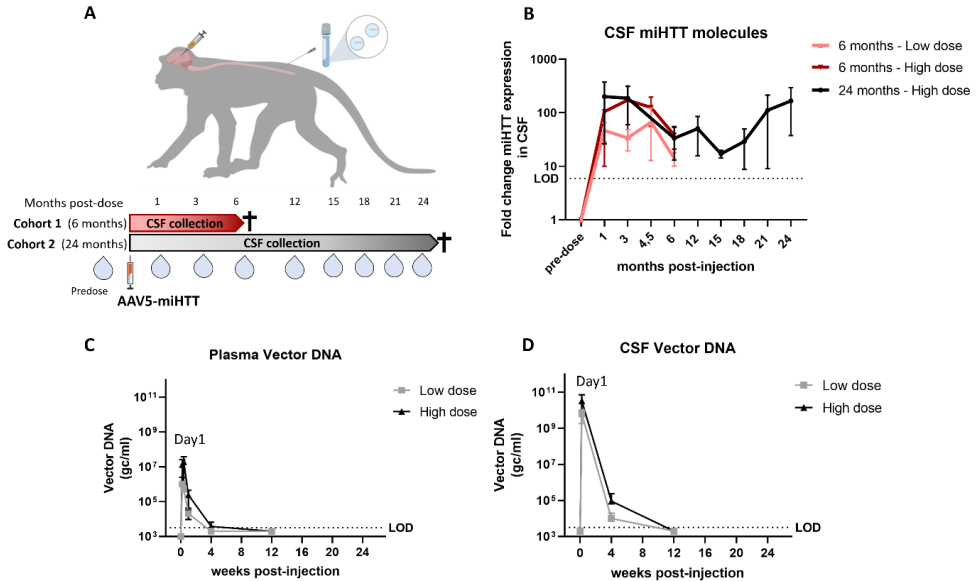


Figure 6. Detection of therapeutic miHTT in CSF at 6 months and 24 months after local brain administration in non-human primates. (A) Scheme of local intrastriatal injection of AAV5-miHTT in non-human primates and longitudinal collection of CSF by lumbar puncture at different time points for cohort 1 and cohort 2. (B) Fold change expression of EV-associated miHTT molecules in the CSF detected by TaqMan qPCR at different time points after striatal treatment up to 6 month in cohort 1 (low dose and high dose, $n_s=6$ per dose group) and 24-months in cohort 2 (high dose, $n_s=4$) (average \pm SEM per time point are indicated). (C and D) Quantification of vector DNA in plasma (C) and CSF (D) at different time points after striatal treatment in cohort 1 with low and high doses of AAV5-miHTT. LOD: Limit of detection.

Discussion

Gene therapy for CNS disorders has faced a number of translational challenges that hamper the establishment of clinically relevant readouts. At this moment, AAV5-miHTT treatment (also known as AMT-130 by uniQure) is entering the clinic and first patients have been successfully injected (Clinicaltrial.gov, NCT04120493). For this and future trials, sensitive measurements reliably reflecting the long-term expression of the therapeutic molecules in the brain are needed. In this study, we demonstrated that engineered miRNA profiles in CSF are suitable pharmacokinetic measurements of AAV-based miRNA therapies directly infused into the brain. We reported for the first time that two different AAV5-delivered therapeutic miRNAs are secreted from diseased neuronal cells in association with EVs, and that the detection of such circulating miRNAs in biofluids is a sensitive indicator of long-term (up to two years) therapeutic expression in the brain. Despite the low protein content of CSF and more invasive sampling compared to plasma, the rapid interchange of molecules between CSF and brain interstitial fluid through the glymphatic system makes the CSF a valuable biofluid for CNS biomarker discovery (Jessen *et al.*, 2015). Moreover, since the blood-brain barrier restricts the passage of large and small molecules in the blood, the quantification of therapeutic miRNAs in the CSF seems to be a more appropriate source for pharmacokinetic measurements specific for CNS. Other studies have focused on the characterization of quantifiable treatment-response biomarkers that correlate with neurodegeneration. Prominent examples of such biomarkers are tau protein and neurofilament light chain, which are suitable general markers for a variety of neurodegenerative disorders (Niemelä *et al.*, 2017; Li *et al.*, 2019). However, due to slow disease progression of neurodegenerative diseases in general, significant changes are difficult to measure over a short period of time in a clinical trial. Development of specific pharmacokinetic markers, such as detection of circulating engineered miRNAs, offers the possibility to monitor the active molecule over time, as well as to understand the relationship between dose, efficacy, and biomarker response.

EVs provide a protective and enriched source of specific bioactive molecules, including RNA, lipids and proteins (Valadi *et al.*, 2007). Next generation sequencing analysis of plasma-derived circulating RNAs suggest that miRNAs are the most abundant EV-associated RNAs (Huang *et al.*, 2013). Interestingly, the cellular miRNA composition generally differs from the EV-enriched miRNA profile, suggesting that cells may utilize sorting mechanisms to regulate the selective packaging of miRNAs into EVs. For instance, specific sequence motifs, chromosomal location, 3' end post-transcriptional modifications and miRNA:target mRNA ratio have been reported to influence the sorting of miRNAs into EVs (Villarroya-Beltri *et al.*, 2013; Koppers-Lalic *et al.*, 2014; Squadrito *et al.*, 2014; Tsang *et al.*, 2017). Differences in secretion profile have also been associated with Ago2-dependent processing

of pre-miRNA backbones (Guduric-Fuchs et al., 2012). In this study, the pre-miR-451a backbone, which follows a dicer-independent non-canonical processing by Ago2 protein (Cheloufi et al., 2010; Herrera-Carrillo and Berkhout, 2017), was selected for the design of our engineered therapeutic miRNAs (miHTT and miATXN3). Despite the different sequence content, the insertion of both engineered miRNA sequences in the pre-miR-451a scaffold resulted in similar secretion profile. Our results support the work by Reshke et al. (Reshke et al., 2020), in which different siRNA were efficiently loaded into EVs when integrated in pre-miR-451 scaffold, but not in pre-miR-16. These studies support the advantage of pre-miR-451 based candidates, not only to deliver safe and efficacious gene therapies, but also for pharmacokinetic and translational extracellular measurements.

A major challenge in the EV research field is the large and not-fully characterized vesicle diversity (Greening and Simpson, 2018). Due to discrepancies and methodological limitations to isolate pure subtype populations, the term “extracellular vesicles” has been encouraged to generally refer to all cell-derived, non-replicable, secreted membrane structures (Théry et al., 2018). This term includes vesicular subtypes with different origins, including endosome-derived exosomes and shedding vesicles released from plasma membrane. In this context, specification and understanding of the strengths and limitations of the selected methods of isolation is crucial for data interpretation (Konoshenko *et al.*, 2018; Théry *et al.*, 2018). In this study, we evaluated the association of therapeutic miRNAs with EVs by using three different methods of isolation. As a first step, a precipitation-based method for tissue culture media was selected for high particle recovery. Cell culture conditions were optimized to assure the isolation of sufficient number of particles for miRNA detection. Characterization of isolated vesicles by imaging and molecular methods showed vesicles of expected size, shape and membrane composition. However, other RNA-containing non-vesicular particles were highly present (Karttunen *et al.*, 2019). To achieve a better purification of EVs from other soluble component, we selected a size-based separation method known as size-exclusion chromatography (SEC) (Böing *et al.*, 2014). Compared to other conventional EV isolation techniques – such as ultracentrifugation and density gradient – SEC has been recommended as a fast and affordable method for good recovery of vesicles larger than 75nm, with almost complete removal of protein contaminants (Coumans *et al.*, 2017). We found detectable levels of therapeutic miRNAs in EV-enriched fractions, but also in protein-containing fractions. Besides lipoproteins and Ago2 protein complexes, which have been remarkably associated with circulating miRNAs (Turchinovich *et al.*, 2011; Vickers *et al.*, 2011), smaller vesicles might also elute in these fractions (Böing *et al.*, 2014; Stranska *et al.*, 2018). Lastly, and due to limited sample availability of CSF, we used a spin column-based method for the direct isolation of RNA from EVs in biofluids (Enderle *et al.*, 2015). By using different methods of isolation, we confirmed the presence of pre-miR-451 engineered miRNAs within EVs, as well as in association with

soluble proteins, in both cultured media and body fluids. These results reflect the importance of purifying and characterizing extracellular miRNA-binding species in order to avoid misinterpretations.

Apart from its value as a source for translational pharmacokinetic measures, the association of therapeutic miRNAs with EVs might have further implications for gene therapies. Vesicular transfer of miRNAs, lipids and misfolded proteins have been described as a novel cell-to-cell communication pathway (Zhang *et al.*, 2015; Zhenwei *et al.*, 2020). Endogenous and viral miRNAs associated with EVs were transferred and delivered into recipient cells by fusion with cell membrane, where they were still functional and lowered the expression of target genes upon transfer (Pegtel *et al.*, 2010; El-Andaloussi *et al.*, 2012). Besides their potential role as novel delivery systems, we also postulate that EVs might contribute to the spread and amplification of AAV-based gene therapies throughout the brain. In other words, efficacy of miRNA-based gene therapy could be extended beyond the initial viral transduction via EV-dependent transfer. New methods to track the uptake and content delivery are necessary to characterize the contribution of EV internalization (Mathieu *et al.*, 2019). Further implications of EV-associated therapeutic miRNAs for successful gene therapies still need to be investigated.

Altogether, our results show the potential of EV-associated artificial miRNAs in CSF as pharmacokinetic markers for monitoring long-term expression of AAV-miRNA gene therapies directly delivered in the brain. The present findings contribute to the better understanding of the transfer of therapeutic miRNAs between cells and body compartments. This knowledge is highly relevant to optimize delivery, therapeutic distribution, dose translation, transgene persistence and efficacy monitoring in the first clinical trial of miRNA-based gene therapies for brain diseases.

Material and methods

Differentiation of forebrain neuronal cultures from human induced pluripotent stem cells (iPSCs)

We selected human iPSC cells from a Huntington Disease (HD) patient containing 71 CAG repeats (ND42229*B, Coriell Institute Stem Biobank, New Jersey, USA). These cells were generated from human HD fibroblasts (GM04281, Coriell Institute Stem Biobank) and reprogrammed with six factors (OCT4, SOX2, KLF4, LMYC, LIN28, shRNA to P53) using episomal vectors. iPSCs were maintained on matrigel coating with mTeSR medium (StemCell Technologies, Vancouver, Canada) for several passages, following the manufacturer's instructions. Karyotype analysis was performed to confirm chromosomal stability before differentiation. Non-differentiated colonies were released using ReLeSR reagent during each passage and split 1:5-20 (StemCell Technologies). For the neural induction, cells were plated onto AggreWell™ 800 plate at day 0 as 3×10^6 cells per well in STEMdiff™ Neural Induction Medium (StemCell Technologies). At day 5, embryoid bodies were formed and replated onto poly-D-lysine/laminin coated 6-well plates. Coating was prepared with poly-D-lysine hydrobromide (0,1 mg/mL) and Laminin from Engelbreth-Holm-Swarm murine (0,1 mg/ml) (Sigma-Aldrich). At day 12, the neuronal rosettes were selected using STEMdiff™ Neural Rosette Selection Reagent (StemCell Technologies) and replated in poly-D-lysine/laminin coated plates. The following day, differentiation of neural progenitor cells was initiated using STEMdiff™ Neuron Differentiation Kit (StemCell Technologies). From day 19, cells were matured using STEMdiff™ Neuron Maturation Kit for a minimum of two weeks (StemCell Technologies). Cell cultures were daily monitored during the whole process.

Vector design and production

The AAV5 vector encoding cDNA of the miHTT cassette was produced using a baculovirus-based AAV production system (uniQure, Amsterdam, the Netherlands) as described previously (Miniarikova *et al.*, 2016). Expression was driven by a combination of the cytomegalovirus early enhancer element and chicken b-actin promoter (CAG), and the transcription unit was flanked by two non-coding AAV-derived inverted terminal repeats.

Transduction iPSC-derived neuronal cultures

Two days after seeding in poly-D-lysine/laminin coated plates (1×10^5 cells), neuronal cells were transduced with three doses of AAV5-miHTT (multiplicity of infection (MOI) 1×10^5 , 1×10^6 and 1×10^7 viral particles per cell, respectively) or two doses of AAV5-miATXN3 (MOI 1×10^6 and 1×10^7 viral particles per cell).

Intrastriatal injection in non-human primates and CSF collection

This study in non-human primates was performed by Covance Preclinical Services in Munster (Germany) in compliance with the German Animal Welfare Act and approved by the local Institutional Animal Care and Use Committee. This study was ethically approved by the Niedersächsisches Landesamt für Verbraucherschutz und Lebensmittelsicherheit (LAVES, permit number AZ 33.19-42502-04-16/2363; Oldenburg, Germany) and the institutional Tierschutzausschuss (IACUC), prior to the initiation of the *in life* phase. Cynomolgus monkeys (*Macaca fascicularis*) aged 2.6-3.5 years, were randomized into two cohorts and kept in live for either 6 months (Cohort 1) or 24 months (Cohort 2). Animals in each cohort were injected with formulation buffer or AAV5-miHTT locally in the caudate and putamen (100 μ l/region) by using magnetic resonance imaging (MRI)-guided convention-enhanced delivery (CED). Animals in cohort 1 were separated in two groups (each group included three males and three females) and received low dose 2×10^{12} gc/brain or high dose 2×10^{13} gc/brain of AAV5-miHTT. Animals in cohort 2 received high dose 2×10^{13} gc/brain of AAV5-miHTT. Several longitudinal CSF samples were taken, namely on pre-dose (day 0), month 1, 3, 4, 5 and 6 (cohort 1) and 12, 15, 18, 21 and 24 (cohort 2). For CSF sample collection, animals were anesthetized with ketamine (10 mg/kg) and dexmedetomidine (0.015 mg/kg). A pencil-point needle for pediatric use was used for CSF withdrawal at level L3 - L6 and the withdrawn volume was substituted with the same volume of artificial CSF. CSF samples (approximately 1 mL) were collected at each time point, centrifuged for 10 min at 2000 x g, 4°C, divided into 2 aliquots (0.5 mL each), snap frozen and stored at - 80°C until further analysis.

Necropsy procedures and tissue collection

Cynomolgus monkeys were sacrificed at 6 months for cohort 1 and 24 months for cohort 2 after AAV5-miHTT administration by sedation with intramuscular injection of ketamine hydrochloride. The brains were carefully removed and coronally sliced into 3mm slices. In total 80 punches were taken from 3mm brains slices across different structures of interest.

RNA/DNA isolation and real-time qPCR

RNA was isolated from neuronal cells and non-human primate brain tissue with Direct-zol™ according to the manufacturer's protocol (Zymo Research; CA, USA). To determine miRNA expression levels, two-step RT-qPCR was performed TaqMan Fast Universal kit (Thermo Scientific, MA, USA), and custom stem-loop primer/probe for detection of miHTT and miATXN3 (Thermo Scientific). Complementary DNA (cDNA) was diluted two-fold in nuclease-free water, of which 4 μ L per reaction were analyzed by TaqMan qPCR. Expression levels of miHTT and miATXN3 were calculated based on a standard line with synthetic RNA

oligos (Integrated DNA Technologies, IA, USA). Expression levels of endogenous miRNAs were measured as internal control, using primer/probe U6 snRNA (001973), hsa-miR-16 (000391), has-miR-21-5p (000397), and cel-miR-39 (000200) from ThermoFisher Scientific.

For viral DNA isolation, neuronal cultures were processed using DNeasy Blood & Tissue Kit (Qiagen, CA, USA) following the manufacturer's protocol. AAV5 vector genome copies were measured by qPCR using SYBR Green (Applied Biosystems, CA, USA) and specific primers against CAG promoter (5'-3' primer sequences: Forward GAGCCGCAGCCATTGC, reverse CACAGATTGGGACAAAGGAAGT). A standard line with expression plasmids was used to calculate the genome copies per microgram of genomic DNA (gDNA).

Isolation of EVs from culture media by precipitation

Medium from transduced neuronal cultures was refreshed every two days, collected on day 5 and day 12 after transduction and centrifuged at 4,000 x g for 15 minutes to remove cells and cell debris. EVs were isolated with a polymer-based precipitation buffer (ExoQuick-TC, System Bioscience, California, USA) according to the manufacturer's protocol. Briefly, 3 mL of ExoQuick buffer was added to 10 mL of conditioned medium, gently mixed, and incubated at 4°C overnight. Next day, EVs were collected at 1,500 x g for 30 minutes and the supernatant was discarded. The residual solution was additionally centrifuged at 1,500 x g for 10 minutes. EV pellets were resuspended in appropriate buffers and stored at -80°C for further experiments. For miRNA detection, EV pellets were resuspended in 300 µL TRIzol (Invitrogen) and RNA content was isolated by using Direct-zol™ (Zymo Research; CA, USA), according to the manufacturer's protocol.

Isolation of EVs from culture media by size-exclusion chromatography

Medium from neuronal cultures was collected and centrifuged at 4,000 x g for 15 minutes to remove cell and cell debris. Separation of EVs from protein complexes (including high-density lipoproteins (HDL)) was achieved by size-exclusion chromatography (SEC) with qEV10 columns (Izon Science; New Zealand). Briefly, after washing the column with PBS, 10 mL of medium was loaded on the column and 26 fractions of 5mL were collected. Every fraction was concentrated to 300 µL by Amicon® Ultra-15 Centrifugal Filter Units (10 kDa molecular weight cut-off) by centrifugation at 4,000 x g for 15 minutes at 4 °C. For miRNA detection, 300 µL TRIzol (Invitrogen) were added to each fraction and RNA content was isolated by using Direct-zol™ (Zymo Research; CA, USA), according to the manufacturer's protocol.

Isolation of EV-associated miRNA from CSF

RNA was isolated from a total of 500 µL CSF, using the exoRNeasy Serum/Plasma kit (Qiagen), as per protocol description, enriching for RNA from EVs. The sample was spiked in

with miR-39, in order to control for possible variations in RNA isolation efficiency. Subsequently, TaqMan-based RT-PCR was carried out with custom stem-loop primers and probes for detection of miHTT and cel-miR-39, using 8 μ L as RNA template. The cDNA was diluted to a final volume of 35 μ L (15 μ L cDNA + 20 μ L RNase free water). Results were expressed as miHTT molecules/mL CSF, corrected for variations in miR-39 spiked in the RNA samples.

Western blotting

EV precipitates were lysed using 100 μ L radioimmunoprecipitation assay (RIPA) buffer (Sigma-Aldrich, St. Louis, MO, USA) supplemented with protein inhibitor cocktail (cOmplete™ ULTRA Tablet; Roche, Basel, Switzerland). Total protein concentration was quantified using a Bradford Protein Assay (Bio-Rad, Hercules, CA, USA) and absorbance was measured at 600 nm on the GloMax Discover System (Promega, Wisconsin, USA). Equal amounts of sample protein (20 μ g) were incubated with β -mercaptoethanol-containing Laemmli buffer at 95 °C for 5 minutes. Proteins were separated using 4-20% Mini-Protean TGX Stain-Free Protein Gel (Bio-Rad). Samples were transferred to polyvinylidene difluoride (PVDF) membranes by Trans-Blot Turbo Transfer system (Bio-Rad) using the “Mixed molecular-weight” protocol (5-150 kDa) at 1.3A, up to 25V for 7 minutes. Blots were incubated with 3% Blotting-Grade blocker (Bio-Rad) in Tris Buffered Saline (TBS) for 1 hour at room temperature, followed by immunoblotting with the selected primary antibody overnight at 4°C (**Table 1**). Chromogenic signals were detected after 2 hours incubation with HRP-conjugated secondary antibodies (Table 1) and 5 min incubation with SuperSignal Pico sensitivity Substrate (Thermo Scientific) using ChemiDoc Touch Gel Imaging System (Bio-Rad).

Table 2: List of primary and secondary antibodies

	Antibodies	Company	Reference	Concentration
EV/exosomes	CD63	System Biosciences	EXOAB-CD63A-1	1:1000
	Alix	Abcam	Ab76608	1:1000
	TSG101	Abcam	Ab30871	1:1000
EV/microvesicles	Calnexin	Abcam	Ab92573	1:20000
Lipoproteins	ApoE	Abcam	Ab58475	1:1000
RISC complex	Ago2	EMD Millipore	07-590-25UG	1:1000
Cytoplasm	α-tubulin	Abcam	Ab7291	1:1000
Secondary HRP antibody	HRP goat anti-rabbit	Abcam	Ab97051	1:20000
	HRP rabbit anti-mouse	Dako	P0260	1:20000

Flow cytometry

Samples were analyzed by APOGEE flow cytometer (Hemel Hempstead, Hertfordshire, UK). EV-containing samples (5 μ L) were incubated with 5 μ L of a solution containing a monoclonal antibody (CD63 or CD81) or lactadherin and diluted with PBS to a final volume of 50 μ L. These samples were incubated in the dark for 15 minutes at room temperature before the addition of 300 μ L PBS. Samples were analyzed for 1 minute by FCM using a FACSCalibur with CellQuest software (BD) at a flow rate of 60 μ L/minute. The detector settings used throughout the experiments and the calculation of EV concentration were as described previously (Böing *et al.*, 2014).

Microfluidic resistive pulse sensing (MRPS)

MRPS (nCS1, Spectradyne LLC, Torrance CA, USA) was used to measure particle size and concentration of all samples. MRPS applies the Coulter Principle, relating the change in electrical impedance of a particle passing through a nanoconstriction to the volume of the particle traversing the nanoparticle tracking analyzer constriction to determine particle size and concentration. All samples were diluted 2-fold or 5-fold in 100 kDa-filtered (Vivaspin) 0.1 % (w/v) bovine serum albumin in Dulbecco's phosphate-buffered saline (DPBS). All samples were measured with a TS-400 cartridge at 4 V. To ensure the particle size distributions were representative of the sample, a minimum of 1,000 particles were counted. Filters were applied based on the recommendations of the manufacturer for the TS-400 cartridge before any data were analyzed to exclude false-positive signals.

Transmission electron microscopy (TEM)

EVs were fixed at room temperature overnight by 0.1% (weight/volume, w/v) paraformaldehyde (Electron Microscopy Sciences, Hatfield, PA). Next, a 200-mesh EM copper grid with formvar coating (Electron Microscopy Sciences) was put on top of a sample (10 μ L) and incubated for 7 minutes at room temperature. The grids were transferred to 1.75% uranyl acetate (w/v) for negative staining. The grid was imaged using a Tecnai 12 transmission electron microscopy (TEM, FEI Company, Eindhoven, The Netherlands), operated at 80 kV. Blind analysis and caption of representative pictures was performed at the Electron Microscopy Centre Amsterdam (EMCA), at Amsterdam Medical Centre (AMC) (Amsterdam, The Netherlands).

Statistics

Mean values were used for statistical analyses. Data are expressed as means \pm SEM. Relationship between viral dose, transgene cellular expression and levels of extracellular EV-associated miRNAs were examined using linear regression analysis. The level of statistical significance was set at $p < 0.05$.

Data availability

The authors confirm that the data supporting the findings of this study are available from the corresponding author on request.

Acknowledgements: The authors are grateful to the team of Process Development and Analytical Development at uniQure for the production and characterization of AAV5-miHTT and AAV5-miATXN3. Special thanks should be given to Jacek Lubelski, Erich Ehlert, Tamar Grevelink, Mark van Veen, and Maroeska Oudshoorn. The authors also thank Ellen Broug, Eileen Sawyer and David Lickorish at uniQure for critically reviewing the manuscript. We are also grateful for the research and technical input to Linda G. Rikkert, Najat Hajji and Chi M. Hau from Laboratory of Experimental Clinical Chemistry at Amsterdam UMC, and to Nicole N. van der Wel and Anita E. Grootemaat for Electron Microscopy analysis at Cellular Imaging core facility of the Amsterdam UMC.

Funding: This research project was funded by uniQure biopharma B.V.

Competing interests: MSG, MME, AV, CVT, JS, AS, SK, EAS, PK, SvD were employees and shareholders at uniQure at the time this work was conducted. MDH has close affiliations with uniQure. Filed patent applications pertaining to the results presented in this paper include the following: WO2016102664 (resulting in at least US 10,174,321 and EP 3237618B1), WO2020104435A1 and, WO2020104469A1.

Data and materials availability: Data associated with this study are available in the main text or the supplementary materials. AAV5-miHTT and AAV5-miATXN3 are proprietary to uniQure and are not available without at least an MTA.

References

- Böing AN, van der Pol E, Grootemaat AE, Coumans FAW, Sturk A, Nieuwland R. Single-step isolation of extracellular vesicles by size-exclusion chromatography. *J Extracell Vesicles* 2014; 3: 1–11.
- Boudreau RL, Rodríguez-Lebrón E, Davidson BL. RNAi medicine for the brain: progresses and challenges. *Hum Mol Genet* 2011; 20: R21-7.
- Chakraborty C, Sharma AR, Sharma G, Doss CGP, Lee SS. Therapeutic miRNA and siRNA: Moving from Bench to Clinic as Next Generation Medicine. *Mol Ther - Nucleic Acids* 2017; 8: 132–43.
- Cheloufi S, Dos Santos CO, Chong MMW, Hannon GJ. A dicer-independent miRNA biogenesis pathway that requires Ago catalysis. *Nature* 2010; 465: 584–9.
- Cogswell JP, Ward J, Taylor IA, Waters M, Shi Y, Cannon B, et al. Identification of miRNA changes in Alzheimer's disease brain and CSF yields putative biomarkers and insights into disease pathways. *J Alzheimers Dis* 2008; 14: 27–41.
- Coumans FAW, Brisson AR, Buzas EI, Dignat-George F, Drees EEE, El-Andaloussi S, et al. Methodological guidelines to study extracellular vesicles. *Circ Res* 2017; 120: 1632–48.
- Depla JA, Sogorb-Gonzalez M, Mulder LA, Heine VM, Konstantinova P, van Deventer SJ, et al. Cerebral Organoids: A Human Model for AAV Capsid Selection and Therapeutic Transgene Efficacy in the Brain. *Mol Ther - Methods Clin Dev* 2020; 18: 167–75.
- El-Andaloussi S, Lee Y, Lakhali-Littleton S, Li J, Seow Y, Gardiner C, et al. Exosome-mediated delivery of siRNA in vitro and in vivo. *Nat Protoc* 2012; 7: 2112–26.
- Enderle D, Spiel A, Coticchia CM, Berghoff E, Mueller R, Schlumpberger M, et al. Characterization of RNA from exosomes and other extracellular vesicles isolated by a novel spin column-based method. *PLoS One* 2015; 10: 1–19.
- Evers MM, Miniarikova J, Juhas S, Vallès A, Bohuslavova B, Juhasova J, et al. AAV5-miHTT Gene Therapy Demonstrates Broad Distribution and Strong Human Mutant Huntingtin Lowering in a Huntington's Disease Minipig Model. *Mol Ther* 2018; 26: 2163–77.
- Greening DW, Simpson RJ. Understanding extracellular vesicle diversity—current status. *Expert Rev Proteomics* 2018; 15: 887–910.
- Guduric-Fuchs J, O'Connor A, Camp B, O'Neill CL, Medina RJ, Simpson DA. Selective extracellular vesicle-mediated export of an overlapping set of microRNAs from multiple cell types. *BMC Genomics* 2012; 13: 357.
- Gui YX, Liu H, Zhang LS, Lv W, Hu XY. Altered microRNA profiles in cerebrospinal fluid exosome in Parkinson disease and Alzheimer disease. *Oncotarget* 2015; 6: 37043–53.
- Haghikia A, Haghikia A, Hellwig K, Baraniskin A, Holzmann A, Décard BF, et al. Regulated microRNAs in the CSF of patients with multiple sclerosis: A case-control study. *Neurology* 2012; 79: 2166–70.
- Herrera-Carrillo E, Berkhout B. Survey and summary: Dicer-independent processing of small RNA duplexes: Mechanistic insights and applications. *Nucleic Acids Res* 2017; 45: 10369–79.
- Hocquemiller M, Giersch L, Audrain M, Parker S, Cartier N. Adeno-Associated Virus-Based Gene Therapy for CNS Diseases. *Hum Gene Ther* 2016; 27: 478–96.
- Huang X, Yuan T, Tschannen M, Sun Z, Jacob H, Du M, et al. Characterization of human plasma-derived exosomal RNAs by deep sequencing. *BMC Genomics* 2013; 14

Jessen NA, Munk ASF, Lundgaard I, Nedergaard M. The Glymphatic System: A Beginner's Guide. *Neurochem Res* 2015; 40: 2583–99.

Jonas S, Izaurralde E. Towards a molecular understanding of microRNA-mediated gene silencing. *Nat Rev Genet* 2015; 16: 421–33.

Karttunen J, Heiskanen M, Navarro-Ferrandis V, Das Gupta S, Lipponen A, Puhakka N, et al. Precipitation-based extracellular vesicle isolation from rat plasma co-precipitate vesicle-free microRNAs. *J Extracell Vesicles* 2019; 8

Keiser MS, Kordasiewicz HB, McBride JL. Gene suppression strategies for dominantly inherited neurodegenerative diseases: lessons from Huntington's disease and spinocerebellar ataxia. *Hum Mol Genet* 2016; 25: R53–64.

Keskin S, Brouwers CC, Sogorb-Gonzalez M, Martier R, Depla JA, Vallès A, et al. AAV5-miHTT Lowers Huntingtin mRNA and Protein without Off-Target Effects in Patient-Derived Neuronal Cultures and Astrocytes. *Mol Ther - Methods Clin Dev* 2019; 15: 275–84.

Kinoshita T, Yip KW, Spence T, Liu FF. MicroRNAs in extracellular vesicles: Potential cancer biomarkers. *J Hum Genet* 2017; 62: 67–74.

Konoshenko MY, Lekchnov EA, Vlassov A V., Laktionov PP. Isolation of Extracellular Vesicles: General Methodologies and Latest Trends. *Biomed Res Int* 2018: 8545347.

Koppers-Lalic D, Hackenberg M, Bijnsdorp I V., van Eijndhoven MAJ, Sadek P, Sie D, et al. Nontemplated nucleotide additions distinguish the small RNA composition in cells from exosomes. *Cell Rep* 2014; 8: 1649–58.

Li Q-F, Dong Y, Yang L, Xie J-J, Ma Y, Du Y-C, et al. Neurofilament light chain is a promising serum biomarker in spinocerebellar ataxia type 3. *Mol Neurodegener* 2019; 14: 39.

Martier R, Sogorb-Gonzalez M, Stricker-Shaver J, Hübener-Schmid J, Keskin S, Klima J, et al. Development of an AAV-Based MicroRNA Gene Therapy to Treat Machado-Joseph Disease. *Mol Ther - Methods Clin Dev* 2019; 15: 343–58.

Mathieu M, Martin-Jaular L, Lavieu G, Théry C. Specificities of secretion and uptake of exosomes and other extracellular vesicles for cell-to-cell communication. *Nat Cell Biol* 2019; 21: 9–17.

Matos CA, Carmona V, Vijayakumar UG, Lopes S, Albuquerque P, Conceição M, et al. Gene therapies for polyglutamine diseases. In: *Advances in Experimental Medicine and Biology*. Springer New York LLC; 2018. p. 395–438

Matsuyama H, Suzuki HI. Systems and Synthetic microRNA Biology: From Biogenesis to Disease Pathogenesis. *Int J Mol Sci* 2019; 21

McBride JL, Pitzer MR, Boudreau RL, Dufour B, Hobbs T, Ojeda SR, et al. Preclinical safety of RNAi-mediated HTT suppression in the rhesus macaque as a potential therapy for Huntington's disease. *Mol Ther* 2011; 19: 2152–62.

Miniarikova J, Evers MM, Konstantinova P. Translation of MicroRNA-Based Huntington-Lowering Therapies from Preclinical Studies to the Clinic. *Mol Ther* 2018; 26: 947–62.

Miniarikova J, Zanella I, Huseinovic A, van der Zon T, Hanemaaijer E, Martier R, et al. Design, Characterization, and Lead Selection of Therapeutic miRNAs Targeting Huntingtin for Development of Gene Therapy for Huntington's Disease. *Mol Ther - Nucleic Acids* 2016; 5: e297.

Miniarikova J, Zimmer V, Martier R, Brouwers CC, Pythoud C, Richetin K, et al. AAV5-miHTT gene therapy demonstrates suppression of mutant huntingtin aggregation and neuronal dysfunction in a

Chapter 4

rat model of Huntington's disease. *Gene Ther* 2017; 24: 630–9.

Niemelä V, Landtblom AM, Blennow K, Sundblom J. Tau or neurofilament light-Which is the more suitable biomarker for Huntington's disease? *PLoS One* 2017; 12

Pegtel DM, Cosmopoulos K, Thorley-Lawson DA, Van Eijndhoven MAJ, Hopmans ES, Lindenberg JL, et al. Functional delivery of viral miRNAs via exosomes. *Proc Natl Acad Sci U S A* 2010; 107: 6328–33.

Reshke R, Taylor JA, Savard A, Guo H, Rhym LH, Kowalski PS, et al. Reduction of the therapeutic dose of silencing RNA by packaging it in extracellular vesicles via a pre-microRNA backbone. *Nat Biomed Eng* 2020; 4: 52–68.

de Rond L, Libregts SFWM, Rikkert LG, Hau CM, van der Pol E, Nieuwland R, et al. Refractive index to evaluate staining specificity of extracellular vesicles by flow cytometry. *J Extracell Vesicles* 2019; 8: 1643671.

De Rond L, Van Der Pol E, Hau CM, Varga Z, Sturk A, Van Leeuwen TG, et al. Comparison of generic fluorescent markers for detection of extracellular vesicles by flow cytometry. *Clin Chem* 2018; 64: 680–9.

Samaranch L, Blits B, San Sebastian W, Hadaczek P, Bringas J, Sudhakar V, et al. MR-guided parenchymal delivery of adeno-associated viral vector serotype 5 in non-human primate brain. *Gene Ther* 2017; 24: 253–61.

Sheinerman KS, Toledo JB, Tsivinsky VG, Irwin D, Grossman M, Weintraub D, et al. Circulating brain-enriched microRNAs as novel biomarkers for detection and differentiation of neurodegenerative diseases. *Alzheimers Res Ther* 2017; 9: 89.

Spronck EA, Brouwers CC, Vallès A, de Haan M, Petry H, van Deventer SJ, et al. AAV5-miHTT Gene Therapy Demonstrates Sustained Huntingtin Lowering and Functional Improvement in Huntington Disease Mouse Models. *Mol Ther - Methods Clin Dev* 2019; 13: 334–43.

Squadrito ML, Baer C, Burdet F, Maderna C, Gilfillan GD, Lyle R, et al. Endogenous RNAs Modulate MicroRNA Sorting to Exosomes and Transfer to Acceptor Cells. *Cell Rep* 2014; 8: 1432–46.

Stranska R, Gysbrechts L, Wouters J, Vermeersch P, Bloch K, Dierickx D, et al. Comparison of membrane affinity-based method with size-exclusion chromatography for isolation of exosome-like vesicles from human plasma. *J Transl Med* 2018; 16

Tabrizi SJ, Ghosh R, Leavitt BR. Huntingtin Lowering Strategies for Disease Modification in Huntington's Disease. *Neuron* 2019; 101: 801–19.

Théry C, Witwer KW, Aikawa E, Alcaraz MJ, Anderson JD, Andriantsitohaina R, et al. Minimal information for studies of extracellular vesicles 2018 (MISEV2018): a position statement of the International Society for Extracellular Vesicles and update of the MISEV2014 guidelines. *J Extracell Vesicles* 2018; 7: 1535750.

Tsang EK, Abell NS, Li X, Anaya V, Karczewski KJ, Knowles DA, et al. Small RNA sequencing in cells and exosomes identifies eQTLs and 14q32 as a region of active export. *G3 Genes, Genomes, Genet* 2017; 7: 31–9.

Turchinovich A, Weiz L, Langheinz A, Burwinkel B. Characterization of extracellular circulating microRNA. *Nucleic Acids Res* 2011; 39: 7223–33.

Valadi H, Ekström K, Bossios A, Sjöstrand M, Lee JJ, Lötvall JO. Exosome-mediated transfer of mRNAs and microRNAs is a novel mechanism of genetic exchange between cells. *Nat Cell Biol* 2007; 9: 645–59.

Vickers KC, Palmisano BT, Shoucri BM, Shamburek RD, Remaley AT. MicroRNAs are transported in plasma and delivered to recipient cells by high-density lipoproteins. *Nat Cell Biol* 2011; 13: 423–35.

Villarroya-Beltri C, Gutiérrez-Vázquez C, Sánchez-Cabo F, Pérez-Hernández D, Vázquez J, Martín-Cofreces N, et al. Sumoylated hnRNPA2B1 controls the sorting of miRNAs into exosomes through binding to specific motifs. *Nat Commun* 2013; 4: 2980.

Waldvogel HJ, Kim EH, Tippett LJ, Vonsattel JPG, Faull RLM. The neuropathology of Huntington's disease. *Curr Top Behav Neurosci* 2015; 22: 33–80.

Wild EJ, Tabrizi SJ. Therapies targeting DNA and RNA in Huntington's disease. *Lancet Neurol* 2017; 16: 837–47.

Zhang J, Li S, Mi S, Li L, Li M, Guo C, et al. Exosome and Exosomal MicroRNA : Trafficking , Sorting , and Function. *Genomics, Proteomics Bioinforma* 2015; 13: 17–24.

Zhenwei Y, Shi M, Stewart T, Ferganut P, Huang Y, Tian C, et al. Reduced oligodendrocyte exosome secretion in multiple system atrophy involves SNARE dysfunction. *Brain* 2020; 143: 1780–97.

Supplementary Figures

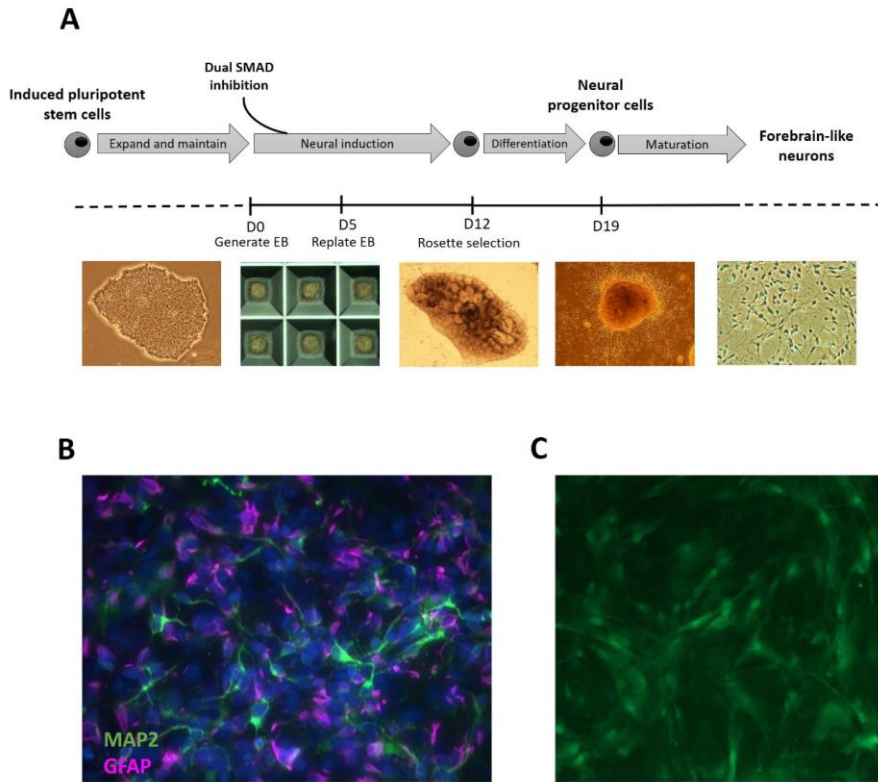


Fig. S1. (A) Differentiation of induced pluripotent stem cells to forebrain-like neurons. (B) Immunocytochemistry of 2-week matured neuronal cultures positive for neuronal (MAP2, green) and astrocytic (GFAP, magenta) markers. DAPI (blue) represents the nucleus of the cells. (C) Transduction of neuronal cultures with AAV5-GFP (high dose). Representative picture of GFP expression at day 5.

Secreted Therapeutics: Monitoring durability of miRNA-based gene therapies in CNS

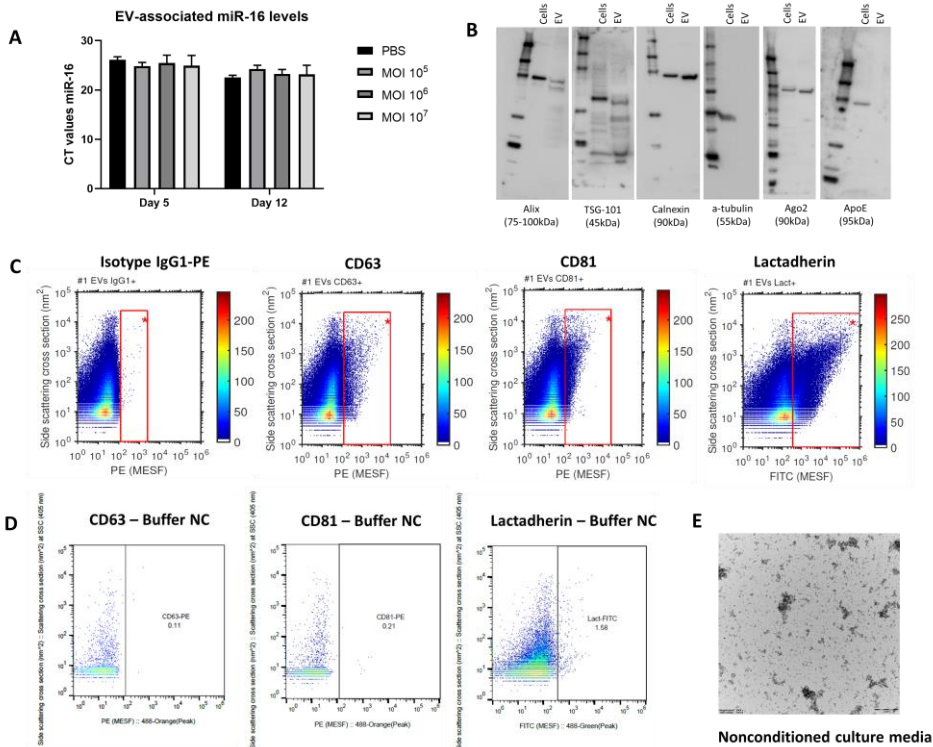


Fig. S2. (A) Quantification of endogenous miR-16 levels in EV pellets isolated by precipitation from culture media of neuronal cells at day 5 and 12. (B) Uncropped western blots from for EV and cell markers from Figure 3. (C) Flow cytometry results raw data. (D) Flow cytometry results of buffers as negative controls (NC) for markers CD63, CD81 and lactadherin. (E) TEM picture of particles isolated from non-conditioned culture media.

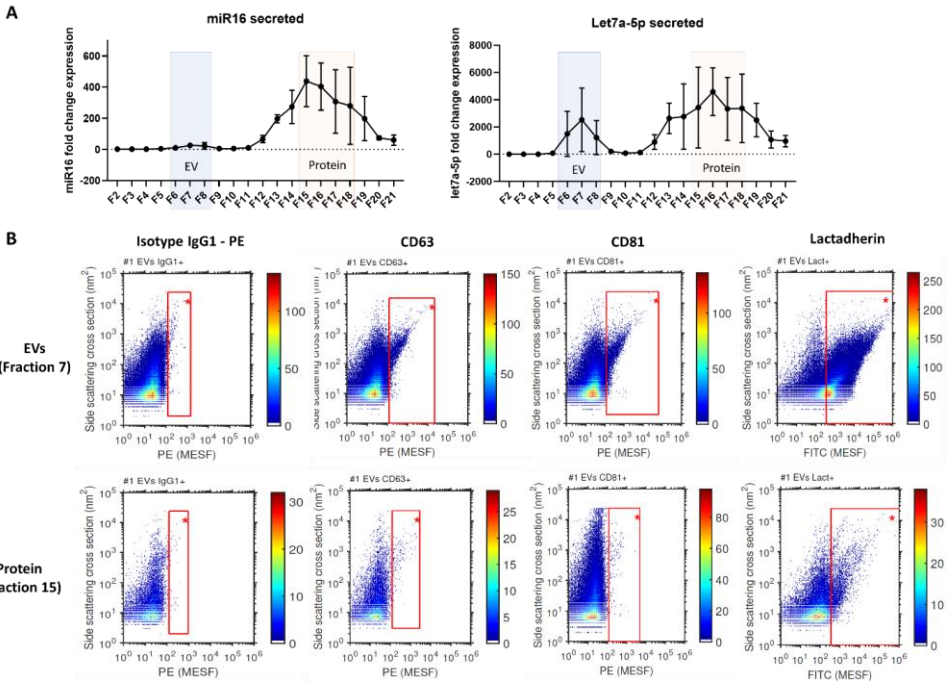


Fig. S3. (A) Quantification of secreted endogenous miR-16 (left) and Let7a-5p (right) miRNAs by TaqMan qPCR in fractions 2-21 separated by SEC from culture media of neuronal cells. (B) Flow cytometry results raw data of a representative EV fraction (fraction 7) and protein fraction (fraction 15).

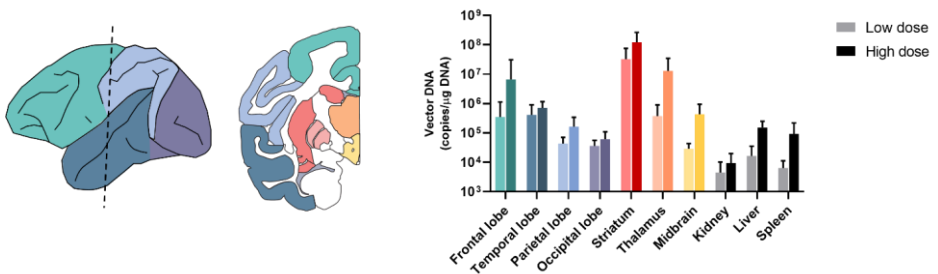


Fig. S4. Transduction of different brain areas of cohort 1 (6 months) represented by vector DNA (copies/ μ g DNA) after intrastriatal injection of AAV5-miHTT (low and high dose). Scheme on the left indicates color-coded brain regions, corresponding to the colors on the right graph. Bars represent average \pm SEM of miHTT (molecules/ μ g input RNA).

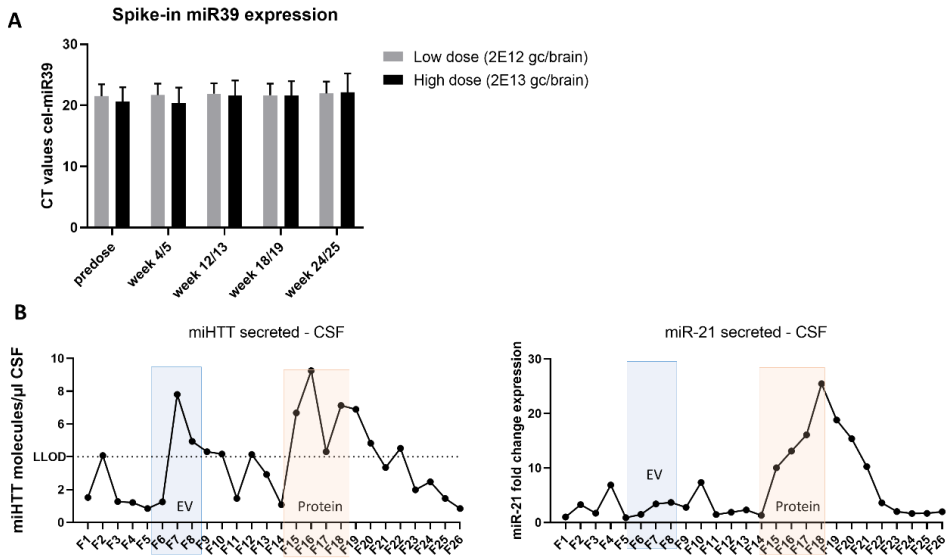


Fig. S5. (A) Quantification of spike-in cel-miR-39 by TaqMan qPCR (CT values) after EV-associated RNA isolation from CSF samples. (B) Quantification of therapeutic miHTT (left) and endogenous miR-21 (right) in fractions 1-26 separated by SEC from CSF samples.

Chapter

5

Beyond transduction: Cross-corrective silencing of gene therapy through functional transfer of engineered microRNAs

**Marina Sogorb-Gonzalez^{1,2}, Astrid Vallès¹, Zdenka
Ellederova³, Jan Motlik³, Melvin Evers¹, Pavlina
Konstantinova¹, Sander van Deventer²**

¹ Department of Research and Development, uniQure biopharma B.V.,
Amsterdam

² Department of Gastroenterology and Hepatology, Leiden University
Medical Center, Leiden, The Netherlands

³ Institute of Animal Physiology and Genetics, Libečov, Czech
Republic

This chapter is integrated in Cells (2022); 11(17):2748

Abstract

Adeno-associated virus (AAV)-based vectors are used to deliver gene therapies to brain cells in order to treat neurodegenerative diseases. Using this delivery technology, expression of the therapeutic transgene is limited to the cells that are primarily transduced by the AAV vector. In large animals, including humans, even the most advanced direct AAV administration technologies, such as intraparenchymal convention-enhanced delivery, will lead to transduction of a limited number of cells within a target brain area. Considering the extent of neuropathology of neurodegenerative diseases affecting most cells and multiple brain regions, widespread therapeutic targeting is needed for sufficient genetic correction. Extracellular vesicles (EV) are secreted nanovesicles that carry specific intracellular cargo and can transfer genetic information upon uptake by neighboring cells. In this study, we investigated the EV-mediated functional transfer of engineered microRNA (miRNA) molecules from AAV-corrected neuronal cells to neighboring cells. To investigate the secretion, uptake and gene-correction efficacy of engineered miRNAs mediated by EVs, we have set up *in vitro* cultures based on the co-culturing of human iPSC-derived neurons. The results demonstrated the transfer of engineered miRNAs and their ability to lower the expression of disease-causing genes upon transfer to recipient cells. Next, we analyzed the distribution of therapeutic miRNA in the brain of minipigs at 12 months after intrastriatal administration. In injected areas and anatomically connected regions, AAV vector DNA levels correlated with miRNA-induced protein lowering effect, while in non-directedly connected brain regions, we observed a mutant protein lowering effect in the presence of low or no vector DNA copies. Altogether our results indicate that AAV-delivered engineered miRNAs can disseminate to neighboring neuronal cells, potentially via EV, where they maintain its therapeutic effect in recipient cells. The spread of miRNA-based gene therapy, presumably mediated by EV, might be an effective mechanism to achieve greater therapeutic effect beyond transduction for gene therapies in neurodegenerative diseases.

Introduction

Huntington disease (HD) and spinocerebellar ataxia type 3 (SCA) are devastating neurodegenerative disorders triggered by triplet expansions in the huntingtin gene (*HTT*) and the ataxin 3 gene (*ATXN3*), respectively (MacDonald *et al.*, 1993; Kawaguchi *et al.*, 1994). The CAG repeat expansion results in the translation of an extended polyglutamine tract in the mutated protein which confers a toxic gain-of-function inducing misfolding and aggregation, cellular toxicity and neurodegeneration (Takahashi *et al.*, 2010). As a promising therapeutic approach for the treatment of HD and SCA, engineered microRNAs (miRNA) delivered by adeno-associated virus (AAV) (AAV-miRNA) have been designed to target the mutant mRNA and reduce the expression of the disease-causing proteins HTT and ATXN respectively (Miniarikova *et al.*, 2016; Martier *et al.*, 2019). Upon delivery of expression cassette into cell nucleus, precursor miRNAs are synthesized and processed into functional mature miRNAs by utilizing the cellular machinery of neuronal cells. Mature miRNAs are then loaded into the multiprotein RNA-induced silencing complex (RISC), which binds to the target mRNA inducing its degradation (Davidson and Boudreau, 2007). The expression of engineered miRNAs targeting *HTT* (miHTT) and *ATXN3* (miATXN3) mRNA transcripts has resulted in reduced levels of toxic mutant proteins in both in vitro and in vivo models (Miniarikova *et al.*, 2016, 2017; Keskin *et al.*, 2019; Martier *et al.*, 2019; Spronck *et al.*, 2019; Caron *et al.*, 2020; Valles *et al.*, 2021). Moreover, preclinical studies demonstrated a reduction of aggregate pathology, preservation of motor function and extension of survival (Miniarikova *et al.*, 2017; Martier *et al.*, 2019; Spronck *et al.*, 2019). In HD and SCA, as well as in most neurodegenerative diseases, the pathology and neuronal loss is initially limited to a defined brain region of selectively vulnerable neurons (Hobbs *et al.*, 2010). However, as disease progresses, broader depositions of pathological aggregates and neuronal dysfunction are found in numerous brain areas contributing to a progressive symptomatic decline. Considering the extent of neuropathology, one of the main challenges for gene therapies targeting the human central nervous system (CNS) is to achieve widespread distribution and sufficient levels of therapeutic molecules in all affected cells and regions of the brain after one-time administration.

Since the expression of therapeutic genes relies on the efficient AAV entry to neuronal cells, initial efforts have focused on optimizing AAV capsids and CNS delivery technologies. Capsid engineering via rational mutagenesis or directed evolution has been used to design vectors more capable of crossing blood-brain barrier, leading to better neuronal transduction after systemic administration (Deverman *et al.*, 2016; Chan *et al.*, 2017). Unfortunately, these results, initially demonstrated in C57BL/6 mice, did not translate to other larger species (Hordeaux *et al.*, 2018; Matsuzaki *et al.*, 2018). The site of injection and the AAV dose can also affect the dissemination of AAVs in the brain (Cearley and Wolfe,

2007, Samaranch *et al.*, 2017). Within the CNS parenchyma, AAVs can be transported from the site of injection via axonal pathways of the CNS connectome resulting in transduction at distal anatomically connected areas (Samaranch *et al.*, 2017). For instance, injection of AAV9 in brain areas with multiple dispersed projections, such as the ventral tegmental area, resulted in better distribution of the therapeutic gene compared to other brain areas with less projections, such as striatum or hippocampus (Cearley and Wolfe, 2007). Other attempts to potentiate AAV diffusion after local delivery in the brain include convection enhanced delivery (CED) via application of pressure differential (Hadaczek *et al.*, 2006), and co-infusion of factors such as heparin or mannitol (Mastakov *et al.*, 2002). Despite all these improvements, and using the best currently available AAV-based technologies, in large animals only a limited percentage of target cells is transduced by AAV vectors (Blits *et al.*, 2010). Therefore, mechanisms that contribute to the widespread diffusion of therapeutics beyond the initially transduced cells would promote removal of intracellular disease-inducing proteins in all affected neuronal cells and eventually prevent disease progression.

In this study, we propose a novel mechanism of dissemination of engineered miRNA therapeutics mediated by extracellular vesicles (EV), termed “*cross-corrective silencing*”. EVs are membrane-delimited particles secreted by all cell types into extracellular space and carry important biological cargos including miRNAs. Circulating EVs are involved in distant inter-cellular communication by internalization in recipient cells, where upon endosomal escape, miRNA activity remains functional (Valadi *et al.*, 2007; Felicetti *et al.*, 2016). EVs are loaded with a selected subset of miRNAs, being miR-451 one of the most highly enriched in EVs compared to cellular levels (Guduric-Fuchs *et al.*, 2012). Moreover, siRNA sequences embedded into pre-miR-451 backbone were robustly packaged into secreted EV (Reshke *et al.*, 2020; Sogorb-Gonzalez *et al.*, 2021).

Here, we investigated functional transfer of engineered miRNAs, embedded into pre-miR-451 backbone, from AAV-corrected neuronal cells to neighboring cells. For this purpose, *in vitro* systems based on human neuronal cells differentiated from induced pluripotent stem cells (iPSC) were used. Following AAV transduction, dose-dependent levels of engineered miRNAs were detected in secreted EV-enriched fractions, which were then added to recipient cells demonstrating that EV-miRNA are taken up by recipient cells. Non-contacting co-culture of AAV-treated neurons together with non-treated cells resulted in gene silencing in both cultures, suggesting that engineered miRNAs remain functional upon internalization. Next, we analyzed the distribution patterns of therapeutic miRNAs in the large brain of minipigs at 12 months after intrastriatal administration of therapeutic AAV-miRNA (Valles *et al.*, 2021). In the injected areas (striatum) and the anatomically connected regions, AAV genomic levels correlated with miRNA-induced protein lowering effect. However, in non-directedly connected brain regions, we observed a mild protein lowering effect in the presence of low or no vector DNA copies, which suggests a spread of

therapeutic efficacy beyond treated cells. Altogether, these results indicate that therapeutic miRNAs spread between neuronal cells, presumably via EV and exert therapeutic silencing of pathogenic proteins upon uptake in neighboring cells. Cross-corrective silencing of engineered miRNAs mediated EV might contribute to achieving widespread efficacy of gene therapeutics in CNS diseases.

Results

AAV-delivered engineered miRNAs are secreted by neuronal cells in a dose-dependent manner

Compared to other cellular miRNAs, miR-451 is one of the most highly packaged miRNAs within EVs (Guduric-Fuchs *et al.*, 2012; Reshke *et al.*, 2020). We hypothesized that engineered therapeutic miRNAs, embedded in a pre-miR-451 backbone, and expressed in neuronal cells might spread between cells in a similar manner as their endogenous counterparts, inducing a therapeutic gene correction in neighboring cells upon uptake (**Figure 1A**). In order to investigate the functional transfer of engineered miRNAs, we first evaluated the secretion levels of miRNAs by neuronal cells upon AAV-mediated expression. For this purpose, iPSC-derived neuronal cells were transduced with increasing doses of two therapeutic miRNAs delivered by AAV serotype 5 (AAV5): “miHTT”, an engineered miRNA designed to target the exon 1 sequence of huntingtin (*HTT*) gene for Huntington disease (HD) (Miniarikova *et al.*, 2016), and “miATXN3”, designed to target the ataxin 3 (*ATXN3*) gene for Spinocerebellar ataxia 3 (SCA3) (Martier *et al.*, 2019). Both engineered miRNAs were embedded in a pre-miRNA-451 scaffold. The processing, expression and efficacy have been previously tested both *in vitro* and in several animal models (Miniarikova *et al.*, 2017; Keskin *et al.*, 2019; Spronck *et al.*, 2019; Caron *et al.*, 2020). Following AAV-mediated transduction of neuronal cells and exhaustive washing, cell supernatants were collected and EV were isolated with an EV-specific precipitation buffer. EV-specificity was confirmed with specific markers and the EV yield was quantified as previously reported in our previous study (Sogorb-Gonzalez *et al.*, 2021). To quantify the intracellular and extracellular expression levels of engineered miRNAs, we used a TaqMan reverse transcription (RT)-quantitative (q)PCR with stem-loop primers specific for each mature miRNA sequence. AAV5-miHTT exposure dose-dependently increased both intracellular and well as extracellular levels of engineered miRNAs. Moreover, levels of intracellular transgene expression positively and significantly correlated with levels of extracellular miHTT enriched in EVs secreted from neuronal cells (**Figure 1B**). Similar results were obtained after transduction of iPSC-derived neuronal cells with AAV5-miATXN3, showing that intracellular

miATXN3 levels significantly correlated with extracellular levels of miATXN3 (**Figure 1C**). Hence, as previously demonstrated by us (Sogorb-Gonzalez *et al.*, 2021), engineered miRNAs expressed by neuronal are sorted and secreted within EVs in a dose-dependent manner.

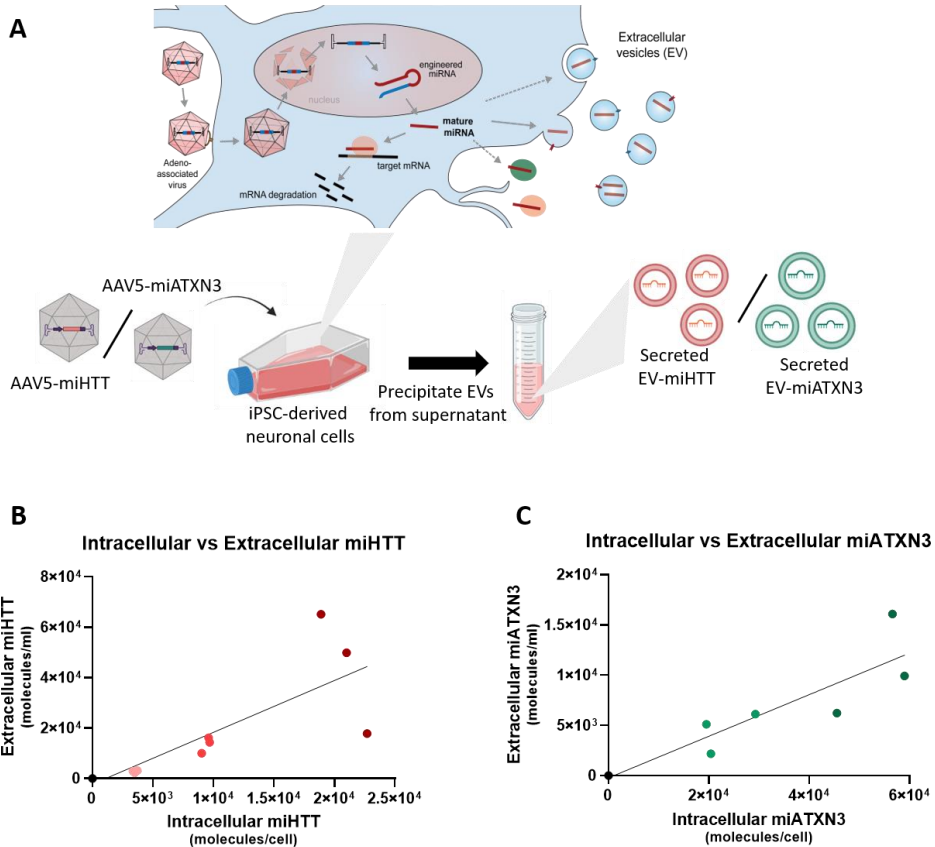


Figure 1. AAV-delivered artificial miRNAs are secreted by neuronal cells. A) Experimental outline shows transduction of iPSC-derived neuronal cells with either AAV5-miHTT or AAV5-miATXN3, collection of supernatant and precipitation of EVs enriched in miHTT and miATXN3 molecules respectively. **B)** Correlation analysis between intracellular miHTT levels (molecules/cell) in neuronal cells upon transduction with three increasing doses of AAV5-miHTT, and extracellular miHTT levels (molecules/ml) in supernatant medium (Simple linear regression, *** $p=0.0014$). **C)** Correlation analysis between intracellular miATXN3 levels (molecules/cell) in neuronal cells upon transduction with two increasing doses of AAV5-miATXN3, and extracellular miATXN3 levels (molecules/ml) in supernatant medium (Simple linear regression, **** $p=0.0006$)

Engineered miRNAs enriched in EVs are taken up by recipient neuronal cells in a dose-dependent manner

To investigate whether engineered miRNAs enriched in EVs can be internalized by neighboring neuronal cells, we exposed non-treated neuronal cells to different concentrations of EVs secreted by AAV-transduced cells. EVs were precipitated from large volumes (1 ml to 10 ml) of supernatant of AAV-transduced neuronal cells with a precipitation buffer and centrifugation. To monitor the EV uptake, EVs were fluorescently tagged with PKH67 lipid-dye and then added to recipient neuronal cells (**Figure 2A**). An overlap between PKH67-EVs and cell membrane of recipient neuronal cells was observed at 24 hours after EV exposure, demonstrating the binding of EV to recipient cells (**Figure 2B**). Next, EVs precipitated from AAV5-miHTT transduced cells (EV-miHTT) and non-treated cells (EV-Ctrl) were added to naïve recipient cells in different concentrations (eg. 1x=1ml, 2x=2ml, 10x=10ml, 20x=20ml and 50x=50ml of supernatant). Since remaining AAV particles could also be enriched within EV fraction (not measured), miHTT levels in recipient cells were measured at 24h, hence prior to any potential transgene expression resulting from AAV contamination. At 24 hours after EV exposure, a dose-dependent increase of the intracellular miHTT concentration was detected in recipient cells (**Figure 2C**). Similarly, exposure of EVs precipitated from AAV5-miATXN3 transduced cells (EV-miATXN3) resulted in increasing levels of miATXN3 in recipient cells. (**Figure 2D**).

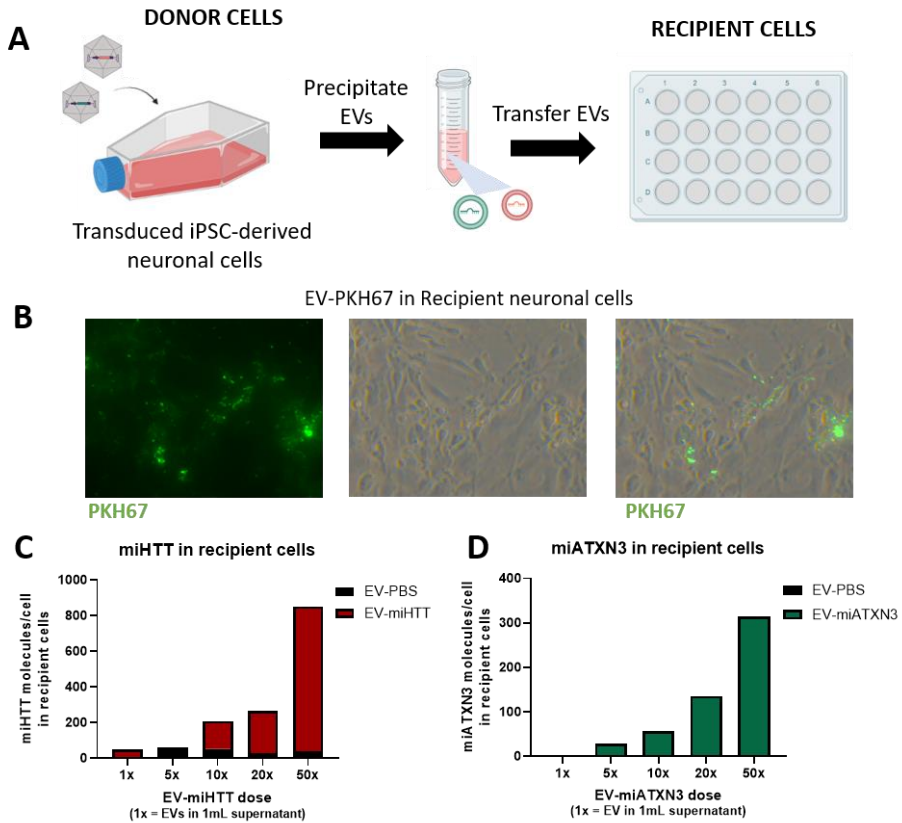


Figure 2. Engineered miRNAs enriched in EVs are taken up by recipient neuronal cells in a dose-dependent manner. **A)** Diagram of transduction of iPSC-derived neuronal cells with either AAV5-miHTT or AAV5-miATXN3, isolation of EVs by precipitation and exposure to recipient neuronal cells for 24 hours. **B)** Representative image of the uptake of PKH67 fluorescently-tagged EVs by recipient neuronal cells at 24h after EV exposure (dose = 20x EV or EV precipitated from 20ml of supernatant). **C)** Levels of engineered miHTT (molecules/cell) in recipient cells at 24 hours after exposure of increasing doses of miHTT-enriched EVs. Dose of “1x” equals amount of EVs present in 1ml supernatant of donor cells prior concentration and EV isolation. **D)** Levels of artificial miATXN3 (molecules/cell) in recipient cells at 24 hours after exposure of increasing doses of miATXN3-enriched EVs. Dose of “1x” equals amount of EVs present in 1ml supernatant of donor cells prior concentration and EV isolation.

Continuous transfer of engineered miHTT from AAV-treated neurons results in significant lowering of target *HTT* mRNA in recipient cells

Next, we investigated whether engineered miRNAs induce the degradation of target mRNA in recipient cells after EV transfer. Since the miRNA levels in recipient cells after one-time transfer were not sufficient to induce significant reduction of target transcript, we set up a cell culture assay that allows for continuous transfer of EV-miRNAs to recipient cells. For this, we used a transwell co-culture system in which AAV5-miHTT transduced “donor” cells were seeded in a transwell insert with a porous membrane and suspended in a standard tissue culture well containing non-treated “recipient” neuronal cells (**Figure 3A**). This system allows for the intercellular exchange of small secreted factors such as EVs while avoiding cell contamination or direct cell-to-cell contact. Two weeks after co-culture, cells within the different compartments were harvested with meticulous care to prevent cross-contamination and vector genomes were quantified in each cell population. We detected high numbers of AAV5 vector genome copies in AAV5-miHTT transduced “donor” cells by qPCR, but not in “recipient” cells or non-treated control cells (n=6) (**Figure 3B**), indicating a lack of viral transfer between donor and recipient cells. Next, levels of full-length *HTT* mRNA were measured by RT-PCR to quantify the efficacy of miHTT to reduce *HTT* expression upon AAV treatment or potential EV transfer. A 30% full-length *HTT* mRNA lowering was detected in AAV5-treated “donor” cells, when normalized to housekeeping gene *GAPDH* and compared to expression levels in control cells (n=6) (**Figure 3C**). Moreover, we measured a 20% *HTT* mRNA reduction in “recipient” cell co-cultured with AAV5-miHTT transduced cells for two weeks, presumably due to continuous transfer of miHTT molecules mediated by EV (**Figure 3C**). In contrast, gene expression levels of *ATXN3* and endogenous housekeeping genes were not affected (data not shown). Therefore, in the absence of vector DNA, a significant specific lowering of *HTT* expression was observed in recipient cells, indicating functional cross-corrective silencing by miHTT transfer.

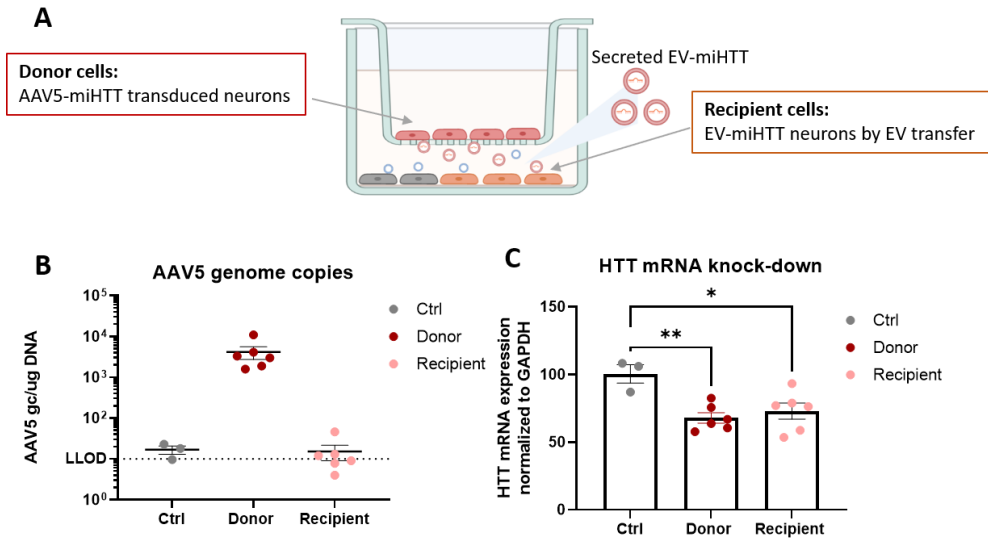


Figure 3. Non-viral continuous transfer of engineered miHTT enriched in EVs results in significant lowering of target *HTT* mRNA in recipient cells. **A)** Diagram of iPSC-derived neuronal cells cultured in a transwell co-culture system in which two cell compartment are separated by a filtered polyester membrane. Donor cells refer to neuronal cells transduced with high dose of AAV5-miHTT, washed and replated in upper compartment to ensure AAV removal. Recipient cells refer to naive neuronal cells seeded in the lower compartment. **B)** Quantification of AAV5 vector DNA levels (gc/μg DNA) in donor cells (AAV5-miHTT transduced) and recipient cells after 2 weeks of co-culture. Control cells are non-treated neuronal cells. Only donor cells had detectable levels of AAV5 genome copies. LLOD: lower limit of detection. **C)** Relative expression levels of target *HTT* mRNA from control cells and normalized to *GAPDH*. Significant lowering of *HTT* mRNA was detected in both donor and recipient cells after 2 weeks of co-culture (ANOVA, Tukey's multiple comparison test, * $p=0.0197$, ** $p=0.0197$). Bars represent mean \pm SEM.

Functional transfer of miATXN3-enriched EVs from transduced neuronal cells to recipient fibroblast cells

To further investigate the functional transfer of engineered miRNAs to neighboring cells, we set up a different non-contacting culture system based on the co-culture of non-chambered slides in a shared culture dish which allows for continuous transfer of secreted particles between two separated cell populations (**Figure 4A**). First, chambered cell culture slides were seeded with iPSC-derived neuronal cells and transduced with AAV5-miATXN3 for 5 days to ensure vector uncoating and transgene miATXN3 expression. To minimize the possibility of remaining AAV particles and subsequent cross-contamination, cells were carefully washed before chamber removal and transfer into the shared culture dish. To increase the transfer ratio, 3x slides containing AAV5-miATXN3 transduced neurons (“donor” cells) were co-cultured together with 1x separate slide containing non-treated fibroblasts (“recipient” cells). After 8 days, cells were separately harvested, and RNA was isolated for gene expression quantification by RT-qPCR. In concordance with previous studies (Martier 2019), neuronal cells directly transduced with AAV5-miATXN3 (“donor” cells) expressed high levels of miATXN3 molecules, up to 5×10^3 molecules/ng RNA (**Figure 4B**). Detectable levels of miATXN3, up to 1×10^2 molecules/ng RNA, were also found in “recipient” fibroblast cells, indicating the transfer and internalization of miATXN3 from AAV5-transduced to non-treated fibroblast cells (**Figure 4B**). As expected, a significant 43% reduction of *ATXN3* expression was detected in directly AAV5-treated neuronal cells ((**Figure 4C**). Moreover, a significant 22% lowering of *ATXN3* expression was also measured in “recipient” fibroblast cells after 8 days of co-culture (**Figure 4C**). In concordance to Figure 3, this data indicates that engineered miATXN3 molecules are transported, presumably within EVs, and taken up by recipient cells, where they maintain their therapeutic property in reducing *ATXN3* expression.

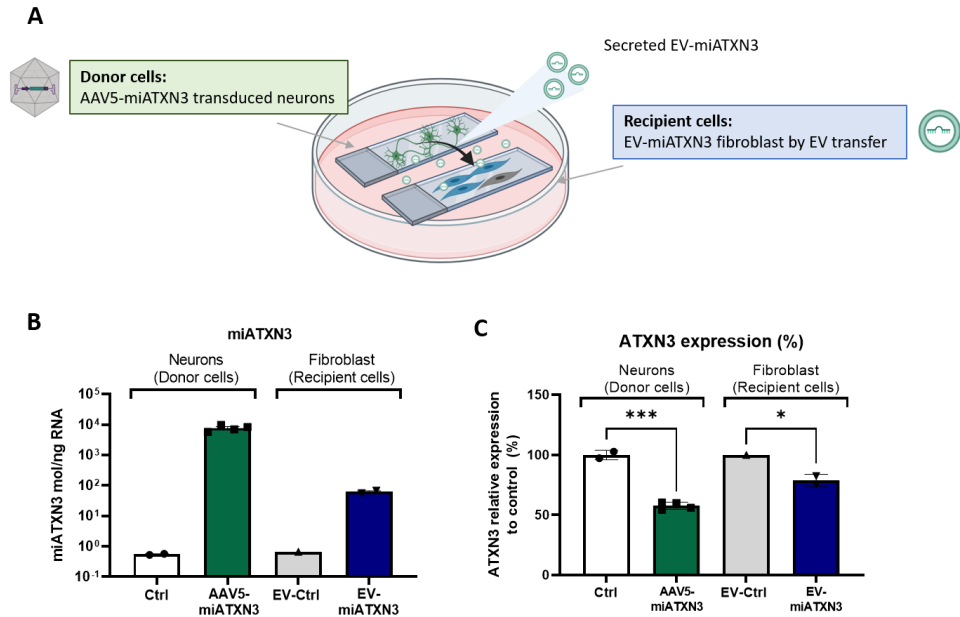


Figure 4. Functional transfer of miATXN3-enriched EVs from transduced neuronal cells to recipient fibroblast cells. **A)** Diagram of cell co-culture of iPSC-derived neuronal cells transduced with AAV5-miATXN3 (donor), and non-treated fibroblast (recipient), seeded in separate slides and co-culture in a tissue culture dish for 8 days. **B)** Quantification of miATXN3 molecules (molecules/ng RNA) in neuronal (donor) and fibroblast cells (recipient). Detectable levels were found in transduced neurons as well as in recipient fibroblast cells, likely due to EV-miATXN3 transfer during co-culture. **C)** Relative expression of target *ATXN3* mRNA compared to non-treated control cells and normalized to *GAPDH*. Significant lowering of *ATXN3* mRNA was detected in both transduced neuronal cells (43% lowering) and recipient fibroblast (22% lowering) after 8 days of co-culture. (ANOVA, Tukey's multiple comparison test, *** $p=0.0002$, * $p=0.0205$). Bars represent mean \pm SEM.

Local AAV5-miHTT infusion in striatum results in widespread distribution and silencing efficacy

The striatum, composed by putamen and caudate, is the first and most affected area in HD patients (Hobbs *et al.*, 2010). The GABAergic medium spiny neurons (MSN) in the striatum receive projections from the cortex and thalamus, known as the “cortico-striatal-thalamic” pathway, as well as from substantia nigra pars compacta (SNc) (Zeun *et al.*, 2022). Striatal neurons send direct and indirect inhibitory projections to the globus pallidus and substantia nigra pars reticulata (**Figure 5B**).

We have previously demonstrated the biodistribution, efficacy and/or safety of AAV5-miHTT in several rodent models (Minarikova *et al.*, 2017; Spronck *et al.*, 2019; Caron *et al.*, 2020), as well as in transgenic HD minipigs and in nonhuman primates (Evers *et al.*, 2018; Spronck *et al.*, 2021; Valles *et al.*, 2021). In these studies, intrastriatal administration of AAV5-miHTT resulted in widespread and persistent levels of vector DNA, miHTT transgene expression and mHTT lowering in the striatum, the main affected area in HD patient. As a consequence of anterograde and retrograde axonal transport of AAV5, vector genomes and *HTT* silencing were found in areas beyond the striatum, including cortex, thalamus, and globus pallidus, important areas also affected in HD. The axonal transport of AAV5 and other serotypes via the CNS circuitry has been previously described and is accepted to contribute to transgene distribution (Sondhi *et al.*, 2005; Cearley and Wolfe, 2007; Salegio *et al.*, 2013).

In a long-lasting study in HD transgenic minipig model (Baxa *et al.*, 2013), AAV5-miHTT striatal infusion resulted in a significant mHTT protein lowering in almost all brain areas (Valles *et al.*, 2021). Surprisingly, in some regions that contained low concentrations of vector DNA, mild reduction of mHTT protein was also observed. Our findings on the functional transfer of miHTT after AAV5-transduction suggested that, besides AAV axonal transport, the widespread mHTT lowering could be a result of EV-mediated spread of miHTT. This hypothesis is supported by the detection of circulating miHTT in the CSF of minipigs, as well as in nonhuman primates, up to two years after brain infusion (Sogorb-Gonzalez *et al.*, 2021; Valles *et al.*, 2021). To further investigate this proposition, we analyzed the spread of vector DNA and mHTT lowering effect in the different brain areas of HD transgenic minipigs at 12 months after AAV5-miHTT treatment. HD transgenic minipigs were treated with 1.2×10^{13} gc of AAV5-miHTT per animal by bilateral injection in the putamen and caudate of each hemisphere (**Figure 5A**). The injection was performed by MRI-guided convention-enhanced delivery (CED) (Valles *et al.*, 2021). At 12 months after treatment, animals were sacrificed and tissues from multiple brain areas collected for molecular analysis. Areas were classified into directly connected and non-directly connected to the striatum according to the main basal ganglia pathways (**Figure 5B**). As expected, high levels of vDNA were measured in injected brain regions (caudate and

putamen) (**Figure 5C**). High vDNA concentrations were also measured in regions known to be directly connected to the striatum (thalamus, nucleus accumbens and cortex), while in non-directly connected areas (brain stem, hippocampus, and cerebellum) vDNA levels were low or below the limit of quantification ($<5 \times 10^3$ gc/ug DNA) (**Figure 5C**). At 12 months after injection, significant region-dependent lowering of mHTT protein was measured in most brain areas with the exception of the cerebellum and spinal cord (data not shown), with an average 84% lowering in putamen (Valles *et al.*, 2021). Correlation analysis showed a general significant negative correlation between mHTT levels (in % from control) and vDNA levels. (Pearson $r = -0.3260$, $p < 0.0001$) (**Figure 5C**). Interestingly, in some areas a significant mild reduction of mHTT protein ($>25\%$ lowering) was observed despite low levels of vector DNA ($<1 \times 10^4$ gc/ug DNA) (blue shadowed area in Figure 5C).

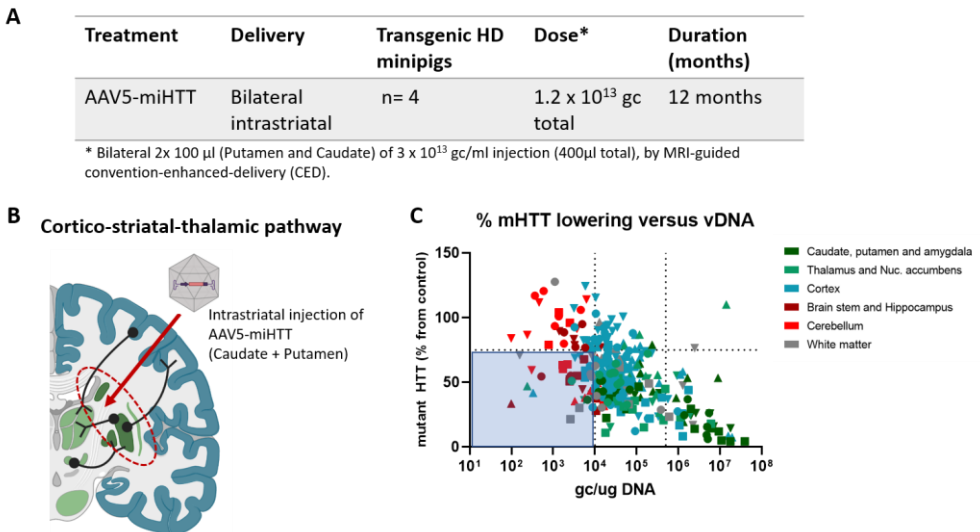


Figure 5. Intrastratial delivery of AAV5-miHTT in transgenic HD minipigs results in widespread HTT lowering, even in regions with low concentrations of vector genomes (Valles *et al* 2020). A) Experimental design of minipig *in vivo* study. Four transgenic minipigs were injected with AAV5-miHTT by MRI-guided CED bilateral intrastratial administration and sacrificed at 12 months post-injection (n=4). **B)** Diagram of injection location in striatum (caudate and putamen) and cortico-striatal-thalamic pathway showing direct connections between striatum (dark green), thalamus, substantia nigra (light green), and cortical areas (blue). **C)** Correlation analysis of mutant HTT protein (as % from non-treated controls) and AAV5 vector genome copies (gc/ μg DNA) in different brain region of tgHD minipigs at 12 months post-injection of AAV5-miHTT in caudate and putamen. A significant negative correlation was obtained (Pearson $r = -0.3260$, $p < 0.0001$). Lines crossing the x-axis indicate the transduction threshold estimated to be needed for efficacy of HTT lowering (1×10^4 gc/ μg DNA) and the minimum levels found in target areas (8×10^5 gc/ μg DNA). The line crossing the y-axis delimitates the efficacy threshold of 75% mutant HTT expression with respect to control. The blue shadowed region delimitates the brain samples with vector DNA levels below the transduction threshold of 1×10^4 gc/ug DNA and mutant HTT protein levels below 75% from control.

Silencing efficacy is detected in distant non-directly connected brain areas

To investigate the contribution of *in vivo* cross-corrective silencing of miHTT between striatum and other directly and non-directly connected brain areas, we performed correlation analyses between vector distribution and HTT lowering for each brain area, depending on the direct or non-direct connections with the striatum. Significant correlations between AAV vDNA levels and mHTT lowering were found in the striatum ($p < 0.0001$) (**Figure 6A**), as well as the in striatal-directly connected areas (thalamus, amygdala, nucleus accumbens and cortical regions) ($p < 0.0001$) (**Figure 6B**). In contrast, non-significant correlation between vDNA levels and mHTT lowering was observed in non-directly-connected areas such as brain stem, hippocampus and cerebellum. In these areas, a substantial number of samples displayed $>25\%$ lowering of mHTT while levels of vDNA measured are considered too low to induce expression of therapeutic levels of miHTT. The same effect was measured when looking into cortical connections. Correlation analysis of cortical subregions showed a significant correlation between striatal-directly-connected cortical areas (prefrontal, motor, insular and perirhinal) ($p = 0.0007$), but not between non-directly connected cortical regions ($p = 0.2831$) (**Figure 6C**). These results indicate that while mHTT lowering might be induced by AAV transduction and axonal transport in directly-connected areas, while in other non-connected areas, reduction of mHTT protein is not explained by AAV levels and therefore, other mechanisms such as EV-spread might contribute to therapeutic lowering in these areas.

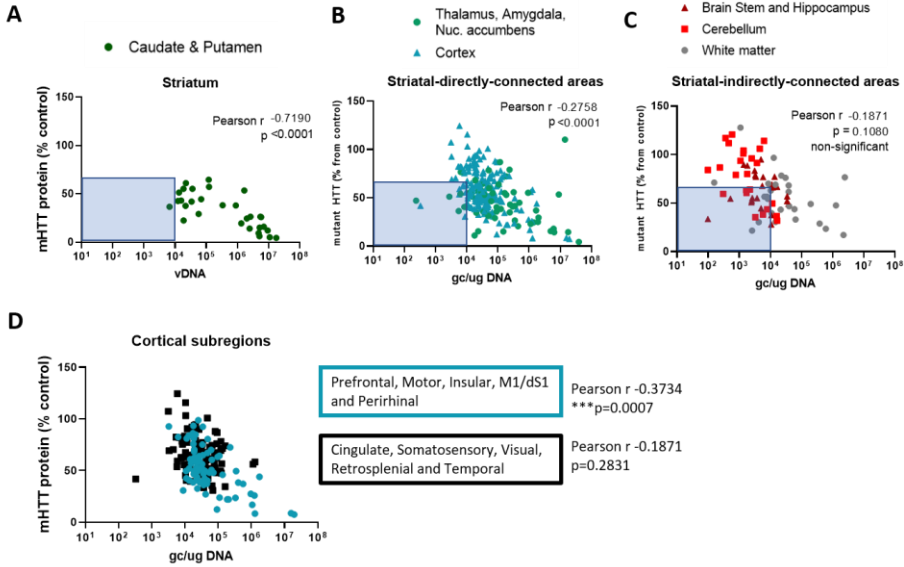


Figure 6. Lowering of mHTT protein in striatal-indirectly-connected brain areas does not correlate with AAV5 transduction levels. A-C) Mutant HTT protein levels (as % from control) in (A) striatum (injected region), (B) regions directly connected to striatum (thalamus, amygdala, nucleus accumbens and cortex) and (C) regions with indirect connections to striatum (brainstem, hippocampus, cerebellum and white matter). Pearson r correlations with AAV5 genome levels (gc/ μ g DNA) led to significant negative correlations in target regions ($r = -0.7190$, **** $p < 0.0001$) and directly connected regions ($r = -0.2758$, **** $p < 0.0001$), but not in regions with indirect connections ($r = -0.1871$, $p = 0.1080$). D) Mutant HTT protein levels (as % from control) in subcortical regions with direct striatal connections (prefrontal, motor, insular somato-motor and perirhinal cortices), and with indirect striatal connections (cingulate, somatosensory, visual, retrosplenial and temporal cortices). Pearson correlations with AAV5 genome levels (gc/ μ g DNA) led to significant negative correlations in directly connected cortical regions ($r = -0.3734$, $p < 0.0007$) but not in subcortical regions with indirect striatal connections ($r = -0.1157$, $p = 0.2831$).

Discussion

The delivery and even biodistribution of therapeutic transgenes to all affected neurons and brain areas is one of the major challenges of gene therapy for neurodegenerative diseases. In HD, sufficient coverage of all striatal neurons, as well as cortical areas and thalamus, is thought to be required for therapeutic efficacy (Wang *et al.*, 2014). We demonstrated that AAV-delivered engineered miRNAs spread beyond treated neuronal cells to secondary neighboring and distant cells, presumably via EV. This mechanism of dissemination or cross-corrective silencing might contribute to the widespread brain distribution and efficacy of a promising AAV-mediated miRNA-based gene therapy for HD.

Previous studies have proposed and exploited the use of EVs as carriers of both endogenous or engineered miRNAs with therapeutic purposes. For instance, EVs collected from healthy donors, or siRNAs loaded in EVs have been studied as potential treatments for several diseases (Alvarez-Erviti *et al.*, 2011; Alexander *et al.*, 2015; Reshke *et al.*, 2020). However, due to their short half-life, repetitive administrations are required for sustained therapeutic effect, a significant disadvantage when targeting CNS diseases. In this study, we propose a novel role of EV as mediators of miRNA transfer inducing cross-corrective silencing. We hypothesized that AAV-transduced cells might become local “factories” of therapeutic engineered miRNAs, which will be then distributed to all affected neighboring cells resulting in an evenly and widely modulation of disease pathology. In order to better understand this process, we investigated the EV-mediated transfer of our therapeutic miRNAs in three distinct steps: (1) EV loading and secretion, (2) uptake by recipient cells and (3) *in vivo* gene-correction upon continuous transfer.

As a first step, we detected dose-dependent levels of engineered miRNAs in EV-enriched fractions after increasing doses of AAV-miRNA treatment, demonstrating the intracellular expression and subsequent secretion of our therapeutic miRNAs. Although these results may appear obvious, profiling studies have showed that EV-enriched miRNAs often differ from parent cells, indicating a regulated loading of miRNAs into EVs while others are retained within the cells (Guduric-Fuchs *et al.*, 2012; Squadrito *et al.*, 2014; Zhang *et al.*, 2015). One of the mechanisms involved in the sorting of miRNAs into EVs include Argonaute-2 (Ago2) protein, an important component of pre-miRNA processing and functional RISC complex (McKenzie *et al.*, 2016). Ago2 is also involved in the processing of pre-miR-451, the only known miRNA which follows a dicer-independent non-canonical processing that relies on slicer activity by Ago2 protein (Cheloufi *et al.*, 2010; Herrera-Carrillo and Berkhout, 2017). Interestingly, miR-451 was consistently the most highly exported miRNA in different cell types (Guduric-Fuchs *et al.*, 2012), supporting the speculation that the efficient EV export of miR-451 is mediated by Ago2. In this study, engineered therapeutic miRNAs (miHTT and miATXN3) were designed by embedding the

target sequence in a pre-miR-451 backbone. After AAV5 mediated delivery into neuronal cells, dose-dependent levels of therapeutic miRNAs were detected in EV-enriched vesicles. These findings are supported by our previous study, in which we detected circulating miHTT molecules in the CSF of minipigs and in nonhuman primates, up to two years after brain infusion (Sogorb-Gonzalez *et al.*, 2021; Valles *et al.*, 2021). This, together with the safe Dicer-independent processing, makes the selection of pri-miR-451 a suitable candidate for the design of miRNA-based therapeutics.

Second, the uptake of EV-enriched engineered miRNAs (miHTT and miATXN3) in recipient cells was demonstrated after one-time exposure with increasing levels of EV. In this experiment, EVs were specifically precipitated from the supernatant of AAV transduced cells and uptake was visualized by PKH67-membrane marker. Different pathways have been reported to mediate the internalization of EVs in recipient cells: clathrin- and caveolin-mediated endocytosis, phagocytosis and direct cell surface membrane fusion (Mulcahy *et al.*, 2014; O'Brien *et al.*, 2020). By silencing specific genes in recipient cells, de Jong *et al.* identified the important role of integrin ITGB1, Rab5 and Rab7 in endosome trafficking (de Jong *et al.*, 2020). The development of new sensitive and quantitative techniques might help to unravel the molecular mechanisms of EV binding and subsequent uptake in different biological systems (Toribio *et al.*, 2019; de Jong *et al.*, 2020). Moreover, the transfer by other potential carriers, such as lipoproteins or Ago2-bound complexes, remains to be investigated (Arroyo *et al.*, 2011).

5 Once inside the cells, miRNAs may either be degraded or remain active and induce gene silencing in recipient cells. To evaluate silencing efficacy upon transfer, we measured target engagement of *HTT* mRNA and *ATXN3* mRNA levels in recipient cells in a co-culture system with AAV-treated cells as donor cells. For this, a non-contacting co-culture that allows for a continuous transfer for 8-15 days was required to ensure sufficient levels of miRNA molecules and subsequent significant silencing in recipient cells. To exclude possible AAV-induced contamination among recipient cells and further characterize the mechanisms of secretion, future studies could include the development of a stable cell line overexpressing the engineered miRNAs as donor cells.

In vivo, in large HD transgenic minipig brains, we detected a widespread lowering effect after intrastriatal infusion, even in areas with low levels of AAV transduction. These findings, together with the *in vitro* functional transfer of engineered miRNAs, suggested that, besides AAV axonal transport, the widespread mHTT lowering could be a result of EV-mediated spread of miHTT. This hypothesis is supported by the detection of circulating miHTT in the CSF of treated animals up to two years after infusion (Sogorb-Gonzalez *et al.*, 2021; Valles *et al.*, 2021). The cross-corrective spread of therapeutic miRNAs after AAV-mediated expression might have some positive consequences for the treatment of HD and

other globally affected neurodegenerative diseases. In the striatum, the injected area, therapeutic miRNA transfer between neighboring neurons will result in a more equal therapeutic effect in all affected cells, instead of a potent lowering in AAV-target cells and no effect in neighboring cells. Hence, the AAV-target cells will become “local factories” of therapeutics to treat neighboring and distant cells. In other regions beyond striatum, affected in a later stage, minor secondary spread mediated by EV will contribute to therapeutic silencing and prevention of disease progression. Lowering of mHTT protein was not detected in spinal cord areas (Valles *et al.*, 2021), indicating that contribution of miRNA is still mild and safe. Moreover, the progression of HD from initially affected brain areas (striatum) to other regions (e.g cortex) is thought to be partially mediated by the EV transfer of mHTT fragments and aggregates (Jeon *et al.*, 2016; Tang, 2018). Assuming that the dissemination of therapeutic miRNAs within EV's would follow the same route as the pathological molecules, this might also contribute to a greater therapeutic effect.

Altogether, our findings indicate that engineered miRNAs embedded in pre-miR-451 scaffold, can be secreted, taken up and able to maintain its therapeutic properties in recipient cells, contributing to inter-cellular transfer and cross-corrective silencing effect in all affected neuronal cells beyond AAV transduction.

Material and methods

AAV production

AAV5 vector encoding cDNA of the miHTT cassette or miATXN3 was packaged into AAV5 by a baculovirus-based AAV production system (uniQure, Amsterdam, The Netherlands) as previously described (Evers *et al.*, 2018; Martier *et al.*, 2019).

Transduction and extracellular Vesicles (EVs) precipitation

Cells were transduced with different doses of AA5-miHTT (3×10^{11} gc, 3×10^{12} gc and 3×10^{13} gc) at MOI 1×10^5 , 1×10^6 and 1×10^7 or AAV5-miATXN (3×10^{12} gc and 3×10^{13} gc) at MOI 1×10^6 and 1×10^7 . Medium from transduced neuronal cultures was refreshed every two days and collected on day 5 and day 12 after transduction, and centrifuged at $3000 \times g$ for 15 min to remove cells and cell debris. The EVs were isolated with ExoQuick-TC (System Bioscience, California, USA) according to manufacturer's protocol. 3 ml of ExoQuick buffer was added to 10 ml of conditioned medium and incubated at 4°C overnight. Next day, the exosomes were collected at $1500 \times g$ for 30 minutes and the supernatant was discarded. The residual solution was additionally centrifuged at $1500 \times g$ for 10 minutes (Sogorb-Gonzalez *et al.*, 2021). The EVs pellets were re-suspended in appropriate buffers and stored at -80°C for further experiments.

Co-culture Transwell system

iPS-derived neuronal cells transduced with 3×10^{13} gc AAV5-miHTT were seeded in Coming® Transwell® polyester membrane cell culture inserts (24 mm, 0.4 μ m pore, Sigma). Naive iPS-derived neurons were seeded 5×10^5 neurons/well in a 6-well plate. At 47 hours after seeding, inserts were placed on top of the wells and cells were cocultured for 2 weeks, refreshing medium every 2 or 3 days. Naive iPSC-derived cells without inserts were used as controls. Cells were harvested separately with Accutase (STEMcell technologies) and divided for further analysis.

Co-culture iPSC-derived neurons and fibroblast in chamber slides

Three-week matured iPSC-derived forebrain neurons from HD patient (Example 1) were plated in 4-well chamber slides in BrainPhys medium (StemCell technologies). Neuronal cells were transduced with a high dose of AAV-miATXN3 (1×10^{12} gc/well) at MOI 2×10^7 . Five days after neuronal transduction, neuronal cells were properly washed, wells removed, and slides were placed into a petri dish (150mm) for co-culturing with non-transduced fibroblast cells. Fibroblast derived from human control individuals were purchased at Coriell repository. Cells were plated in 4 well chamber slides in MEM medium (Thermo Fisher) supplemented with 2 mM L-Glutamine, 15% Fetal Bovine Serum and 1% Penicillin/Streptomycin.

Co-culture system comprised of 3x transduced neuron slides and 1x non-transduced fibroblast slide (ratio 3:1) in MEM medium for 8 days. As a control, 3x non-transduced neurons slides were co-cultured with 1x non-transduced fibroblast slide in MEM medium. As a positive control, fibroblast cells were directly transduced with two doses of AAV-miATXN3 at MOI 1×10^6 and 1×10^8 and maintained for 8 days, likewise to the co-culture system (see Figure 4). Cells were washed, harvested separately and resuspend in 200ul Trizol for RNA purposes, or in 100ul RIPA buffer for protein assays, and stored at -80 C.

Minipig injections and sample collection (adapted from Valles et al. (Valles *et al.*, 2021))

All experiments were carried out according to the guidelines for the care and use of experimental animals and approved by the State Veterinary Administration of the Czech Republic. TgHD minipigs (Baxa *et al.*, 2013) and healthy controls of both sexes, 6 months old, were used. The animals were injected bilaterally into the caudate and putamen with a total of four catheters, one in each putamen and each caudate. Each minipig received 100 μ l of 1.2×10^{13} gc/mL AAV-miHTT per catheter using the Renishaw drug delivery system. At 12 months after injection, n=4 treated animals and n=4 naïve (untreated) controls were sacrificed. From each of these animals, the brains were collected and sliced coronally (4 mm-thick sections) after which a total 170 brain punches of 3mm in diameter were taken bilaterally. Each punch of the left hemisphere was divided in four parts for different

purposes (DNA, RNA, protein or backup). All punches were kept at -80 C until further analysis.

RNA isolation and real-time qPCR

RNA was isolated from cells using Trizol according to the manufacturer's protocol (Invitrogen). To detect engineered miRNA expression levels, RT-qPCR was performed using TaqMan Fast Universal kit (Thermo Scientific), and commercially available primers and probes hsa-miR-16 (000391, Applied Biosystems). Custom-made miHTT primers and probes (assay ID CTXGPY4, Thermo Scientific) and miATXN3 primers and probes (assay ID CTEPRZE, Thermo Scientific), were used. The expression level was normalized to hsa-miR-16 levels. Fold changes of miRNA expression were calculated based on $2^{-\Delta\Delta CT}$ method. miRNA expression was calculated based on a standard line with synthetic RNA oligos.

For the viral vector DNA isolation, neuronal cultures were processed using DNeasy Blood & Tissue Kit (Qiagen, Valencia, CA, USA) following manufacturer's protocol. AAV5 vector genome copies were measured by qPCR reaction using SYBR Green protocol (Applied Biosystems, Foster City, CA, USA) and validated standard line for detection of CAG promoter. Forward primer sequence: GAGCCGCAGCCATTGC and reverse primer sequence: CACAGATTTGGGACAAAGGAAGT. The standard line was used to calculate the genome copies per DNA microgram.

Statistical analysis

Statistical analysis and presented graphs were performed with GraphPad Prism 9 software. Data are expressed as means \pm SEM. Correlation analysis were performed using liner regression analysis and Pearson's correlation as indicated. One-way ANOVA, with Tukey's multiple comparison's *post hoc* tests, was used for group comparison. The level of statistical significance was set at $p < 0.005$ (*ns* non-significant, * $p < 0.05$, ** $p < 0.005$, *** $p < 0.0005$, **** $p < 0.0001$).

References

- Alexander M, Hu R, Runtsch MC, Kagele DA, Mosbrugger TL, Tolmachova T, et al. Exosome-delivered microRNAs modulate the inflammatory response to endotoxin. *Nat Commun* 2015; 6: 7321.
- Alvarez-Erviti L, Seow Y, Yin H, Betts C, Lakhali S, Wood MJA. Delivery of siRNA to the mouse brain by systemic injection of targeted exosomes. *Nat Biotechnol* 2011; 29: 341–5.
- Arroyo JD, Chevillet JR, Kroh EM, Ruf IK, Pritchard CC, Gibson DF, et al. Argonaute2 complexes carry a population of circulating microRNAs independent of vesicles in human plasma. *Proc Natl Acad Sci U S A* 2011; 108: 5003–8.
- Baxa M, Hruska-Plochan M, Juhas S, Vodicka P, Pavlok A, Juhasova J, et al. A transgenic minipig model of Huntington's Disease. *J Huntingtons Dis* 2013; 2: 47–68.
- Blits B, Derks S, Twisk J, Ehlert E, Prins J, Verhaagen J. Adeno-associated viral vector (AAV)-mediated gene transfer in the red nucleus of the adult rat brain: comparative analysis of the transduction properties of seven AAV serotypes and lentiviral vectors. *J Neurosci Methods* 2010; 185: 257–63.
- Caron NS, Southwell AL, Brouwers CC, Cengio LD, Xie Y, Black HF, et al. Potent and sustained huntingtin lowering via AAV5 encoding miRNA preserves striatal volume and cognitive function in a humanized mouse model of Huntington disease. *Nucleic Acids Res* 2020; 48: 36–54.
- Cearley CN, Wolfe JH. A Single Injection of an Adeno-Associated Virus Vector into Nuclei with Divergent Connections Results in Widespread Vector Distribution in the Brain and Global Correction of a Neurogenetic Disease. *J Neurosci* 2007; 27: 9928–40.
- Chan KY, Jang MJ, Yoo BB, Greenbaum A, Ravi N, Wu WL, et al. Engineered AAVs for efficient noninvasive gene delivery to the central and peripheral nervous systems. *Nat Neurosci* 2017; 20: 1172–9.
- Cheloufi S, Dos Santos CO, Chong MMW, Hannon GJ. A dicer-independent miRNA biogenesis pathway that requires Ago catalysis. *Nature* 2010; 465: 584–9.
- Davidson BL, Boudreau RL. RNA Interference: A Tool for Querying Nervous System Function and an Emerging Therapy. *Neuron* 2007; 53: 781–8.
- Deverman BE, Pravdo PL, Simpson BP, Kumar SR, Chan KY, Banerjee A, et al. Cre-dependent selection yields AAV variants for widespread gene transfer to the adult brain. *Nat Biotechnol* 2016; 34: 204–9.
- Evers MM, Miniarikova J, Juhas S, Vallès A, Bohuslavova B, Juhasova J, et al. AAV5-miHTT Gene Therapy Demonstrates Broad Distribution and Strong Human Mutant Huntingtin Lowering in a Huntington's Disease Minipig Model. *Mol Ther* 2018; 26: 2163–77.
- Felicetti F, De Feo A, Coscia C, Puglisi R, Pedini F, Pasquini L, et al. Exosome-mediated transfer of miR-222 is sufficient to increase tumor malignancy in melanoma. *J Transl Med* 2016; 14: 56.
- Guduric-Fuchs J, O'Connor A, Camp B, O'Neill CL, Medina RJ, Simpson DA. Selective extracellular vesicle-mediated export of an overlapping set of microRNAs from multiple cell types. *BMC Genomics* 2012; 13: 357.
- Hadaczek P, Kohutnicka M, Krauze MT, Bringas J, Pivrotto P, Cunningham J, et al. Convection-enhanced delivery of adeno-associated virus type 2 (AAV2) into the striatum and transport of AAV2 within monkey brain. *Hum Gene Ther* 2006; 17: 291–302.
- Herrera-Carrillo E, Berkhout B. Survey and summary: Dicer-independent processing of small RNA duplexes: Mechanistic insights and applications. *Nucleic Acids Res* 2017; 45: 10369–79.

Hobbs NZ, Barnes J, Frost C, Henley SMD, Wild EJ, Macdonald K, et al. Onset and progression of pathologic atrophy in Huntington disease: a longitudinal MR imaging study. *AJNR Am J Neuroradiol* 2010; 31: 1036–41.

Hordeaux J, Wang Q, Katz N, Buza EL, Bell P, Wilson JM. The Neurotropic Properties of AAV-PHP.B Are Limited to C57BL/6J Mice. *Mol Ther* 2018; 26: 664–8.

Jeon I, Cicchetti F, Cisbani G, Lee S, Li E, Bae J, et al. Human - to - mouse prion - like propagation of mutant huntingtin protein. *Acta Neuropathol* 2016; 132: 577–92.

de Jong OG, Murphy DE, Mäger I, Willms E, Garcia-Guerra A, Gitz-Francois JJ, et al. A CRISPR-Cas9-based reporter system for single-cell detection of extracellular vesicle-mediated functional transfer of RNA. *Nat Commun* 2020 111 2020; 11: 1–13.

Kawaguchi Y, Okamoto T, Taniwaki M, Aizawa M, Inoue M, Katayama S, et al. CAG expansions in a novel gene for Machado-Joseph disease at chromosome 14q32.1. *Nat Genet* 1994; 8: 221–8.

Keskin S, Brouwers CC, Sogorb-Gonzalez M, Martier R, Depla JA, Vallès A, et al. AAV5-miHTT Lowers Huntingtin mRNA and Protein without Off-Target Effects in Patient-Derived Neuronal Cultures and Astrocytes. *Mol Ther - Methods Clin Dev* 2019; 15: 275–84.

MacDonald ME, Ambrose CM, Duyao MP, Myers RH, Lin C, Srinidhi L, et al. A novel gene containing a trinucleotide repeat that is expanded and unstable on Huntington's disease chromosomes. *Cell* 1993; 72: 971–83.

Martier R, Sogorb-Gonzalez M, Stricker-Shaver J, Hübener-Schmid J, Keskin S, Klima J, et al. Development of an AAV-Based MicroRNA Gene Therapy to Treat Machado-Joseph Disease. *Mol Ther - Methods Clin Dev* 2019; 15: 343–58.

Mastakov MY, Baer K, Kotin RM, During MJ. Recombinant Adeno-associated Virus Serotypes 2– and 5–Mediated Gene Transfer in the Mammalian Brain: Quantitative Analysis of Heparin Co-infusion. *Mol Ther* 2002; 5: 371–80.

Matsuzaki Y, Konno A, Mochizuki R, Shinohara Y, Nitta K, Okada Y, et al. Intravenous administration of the adeno-associated virus-PHP.B capsid fails to upregulate transduction efficiency in the marmoset brain. *Neurosci Lett* 2018; 665: 182–8.

McKenzie AJ, Hoshino D, Hong NH, Cha DJ, Franklin JL, Coffey RJ, et al. KRAS-MEK Signaling Controls Ago2 Sorting into Exosomes. *Cell Rep* 2016; 15: 978–87.

Miniarikova J, Zanella I, Huseinovic A, van der Zon T, Hanemaaijer E, Martier R, et al. Design, Characterization, and Lead Selection of Therapeutic miRNAs Targeting Huntingtin for Development of Gene Therapy for Huntington's Disease. *Mol Ther - Nucleic Acids* 2016; 5: e297.

Miniarikova J, Zimmer V, Martier R, Brouwers CC, Pythoud C, Richetin K, et al. AAV5-miHTT gene therapy demonstrates suppression of mutant huntingtin aggregation and neuronal dysfunction in a rat model of Huntington's disease. *Gene Ther* 2017; 24: 630–9.

Mulcahy LA, Pink RC, Carter DRF. Routes and mechanisms of extracellular vesicle uptake. *J Extracell Vesicles* 2014; 3

O'Brien K, Breyne K, Ughetto S, Laurent LC, Breakefield XO. RNA delivery by extracellular vesicles in mammalian cells and its applications. *Nat Rev Mol Cell Biol* 2020 2110 2020; 21: 585–606.

Reshke R, Taylor JA, Savard A, Guo H, Rhym LH, Kowalski PS, et al. Reduction of the therapeutic dose of silencing RNA by packaging it in extracellular vesicles via a pre-microRNA backbone. *Nat Biomed Eng* 2020; 4: 52–68.

Salegio EA, Samaranch L, Kells AP, Mittermeyer G, San Sebastian W, Zhou S, et al. Axonal transport of adeno-associated viral vectors is serotype-dependent. *Gene Ther* 2013; 20: 348–52.

Samaranch L, Blits B, San Sebastian W, Hadaczek P, Bringas J, Sudhakar V, et al. MR-guided parenchymal delivery of adeno-associated viral vector serotype 5 in non-human primate brain. *Gene Ther* 2017; 24: 253–61.

Sogorb-Gonzalez M, Vendrell-Tornero C, Snapper J, Stam A, Keskin S, Miniarikova J, et al. Secreted therapeutics: monitoring durability of microRNA-based gene therapies in the central nervous system. *Brain Commun* 2021; 3

Sondhi D, Peterson DA, Giannaris EL, Sanders CT, Mendez BS, De B, et al. AAV2-mediated CLN2 gene transfer to rodent and non-human primate brain results in long-term TPP-I expression compatible with therapy for LINCL. *Gene Ther* 2005 1222 2005; 12: 1618–32.

Spronck EA, Brouwers CC, Vallès A, de Haan M, Petry H, van Deventer SJ, et al. AAV5-miHTT Gene Therapy Demonstrates Sustained Huntingtin Lowering and Functional Improvement in Huntington Disease Mouse Models. *Mol Ther - Methods Clin Dev* 2019; 13: 334–43.

Spronck EA, Vallès A, Lampen MH, Montenegro-Miranda PS, Keskin S, Heijink L, et al. Intrastratial administration of AAV5-MIHTT in non-human primates and rats is well tolerated and results in MIHTT transgene expression in key areas of huntington disease pathology. *Brain Sci* 2021; 11: 1–18.

Squadrito ML, Baer C, Burdet F, Maderna C, Gilfillan GD, Lyle R, et al. Endogenous RNAs Modulate MicroRNA Sorting to Exosomes and Transfer to Acceptor Cells. *Cell Rep* 2014; 8: 1432–46.

Takahashi T, Katada S, Onodera O. Polyglutamine diseases: Where does toxicity come from? What is toxicity? Where are we going? *J Mol Cell Biol* 2010; 2: 180–91.

Tang BL. Unconventional Secretion and Intercellular Transfer of Mutant Huntingtin. *Cells* 2018; 7

Toribio V, Morales S, López-Martín S, Cardeñes B, Cabañas C, Yáñez-Mó M. Development of a quantitative method to measure EV uptake. *Sci Reports* 2019 91 2019; 9: 1–14.

Valadi H, Ekström K, Bossios A, Sjöstrand M, Lee JJ, Lötvall JO. Exosome-mediated transfer of mRNAs and microRNAs is a novel mechanism of genetic exchange between cells. *Nat Cell Biol* 2007; 9: 645–59.

Valles A, Evers MM, Stam A, Gonzalez MS, Brouwers C, Tornero CV, et al. Widespread and sustained target engagement in Huntington's disease minipigs upon intrastratial microRNA-based gene therapy. *Sci Transl Med* 2021; 13: 1–51.

Wang N, Gray M, Lu XH, Cantle JP, Holley SM, Greiner E, et al. Neuronal targets for reducing mutant huntingtin expression to ameliorate disease in a mouse model of Huntington's disease. *Nat Med* 2014; 20: 536–41.

Zeun P, McColgan P, Dhollander T, Gregory S, Johnson EB, Papoutsis M, et al. Timing of selective basal ganglia white matter loss in premanifest Huntington's disease. *Neuroimage (Amst)* 2022; 33: 102927.

Zhang J, Li S, Mi S, Li L, Li M, Guo C, et al. Exosome and Exosomal MicroRNA : Trafficking , Sorting , and Function. *Genomics, Proteomics Bioinforma* 2015; 13: 17–24.

Chapter 6

**General discussion and
future perspectives**

Main findings of this thesis

In order to have clinical benefit, therapies need to address the precise disease-related pathogenic mechanism at the right place and the right time. Focusing on the first two requirements, the work in this thesis aimed to contribute to our understanding of the mechanism of action of adeno-associated virus (AAV)-delivered micro(mi)RNA-based gene therapy (AAV-miRNA) for Huntington's disease.

We proposed and demonstrated four relevant mechanistic aspects related to AAV-miRNA: (1) the lowering of the highly toxic mis-spliced exon 1 HTT fragment (HTTex1) by engineered miRNAs targeting exon 1 sequence, (2) the sustained and widespread lowering of mHTT in large animal model using this approach, (3) the secretion of engineered miRNAs within extracellular vesicles as sources of translational biomarkers to monitor efficacy *in vivo* and (4) the inter-cellular dissemination of engineered miRNAs as a mechanism of therapeutic spread to cover all cells exposed to mHTT toxicity. These data provide a scientific basis for an ongoing clinical trial of the first AAV-miRNA-based gene therapy in HD patients. Above all, this work emphasizes the importance of meticulously investigating and validating the critical molecular pathological drivers of the disease in conjunction with the development of technologies that enable targeting of the majority of the degenerating neurons that cause the disease phenotype.

Below, we summarize these findings and discuss the implications of these novel concepts for the HD field and the potential use of AAV-miRNA gene therapy for other neurodegenerative diseases.

Reducing the toxic exon 1 HTT fragment

The classical view that germ-line CAG repeat expansions directly cause HD through the expression of mutant HTT (mHTT) protein expression has been challenged in recent years. It has now become apparent that somatic instability can cause a dramatic increase of the CAG repeats, and it is thought that this somatic repeat expansion, rather than the germ-line CAG repeat number, may be the driver of the accelerated neurodegeneration observed in many HD patients during mid-life (Swami *et al.*, 2009; Ciosi *et al.*, 2019). There also is ample data supporting the notion that rather than the full-length mutant huntingtin protein, an aberrantly spliced glutamine rich exon-1 fragment drives HD pathology (Sathasivam *et al.*, 2013; Franich *et al.*, 2019). Both observations are likely related, because CAG repeat expansion is known to be correlated to increased generation of aberrantly spliced exon-1 protein fragments (Neueder *et al.*, 2017). These observations have important consequences for the design of HTT lowering therapies.

The finding that HTTex1 is generated by aberrant splicing raised the alarm that nucleic-acid-based approaches currently being developed might not reduce the most toxic fragment, because most compounds target sequences distant from the CAG-containing exon 1 (Sathasivam *et al.*, 2013). The work presented in **Chapter 2** demonstrated that our AAV-delivered engineered miRNA targeting HTT exon 1 sequence (AAV-miHTT) effectively suppressed translation of both the mutant full-length HTT protein and the highly pathogenic HTTex1 fragment. In contrast to most other nucleic-acid-based approaches for HD, AAV5-miHTT targets exon 1 sequence, thereby lowering HTTex1 transcript, as demonstrated in this thesis (**Chapter 2**). To our knowledge, this is the first study that demonstrates the efficacy of a HTT lowering-based treatment to successfully reduce the pathogenic HTTex1 in a HD splicing context, which may be a critical determinant of clinical efficacy. This work also highlights the importance of the choice of the mRNA target sequence as well as considering potential pathogenic splicing events when designing silencing therapeutics for HD and other diseases. Indeed, engineered miRNAs targeting sequences close to the repeat expansion have also been effective in other CAG-repeat expansion disorders, such as spinocerebellar ataxin 3 (SCA3) (Martier *et al.*, 2019).

Apart from exon 1-targeting technologies, other approaches may reduce exposure to toxic polyglutamine species. Antisense-oligonucleotides (ASO) and short hairpin RNA (shRNA) targeting the CAG repeat expansion directly have showed selective lowering of full-length mHTT protein, reduction of RNA foci and are expected to reduce expanded HTTex1 fragments (Evers *et al.*, 2011; Datson *et al.*, 2017; Urbanek *et al.*, 2017; Kotowska-Zimmer *et al.*, 2020) (**Chapter 1**, Table 1). However, these therapies are likely to downregulate the expression of other important CAG-containing genes, leading to off-target adverse effects. Protein-targeting approaches, including intrabodies that target the proline-rich region in

exon 1, have showed reduced HTTex1 aggregation and reduced gene dysregulation, but the efficacy of these approaches in the context of alternative exon-1 splicing is not yet known (Southwell *et al.*, 2009; Amaro and Henderson, 2016).

Exposure to toxic HTTex1 levels may also be prevented by suppressing somatic instability. In contrast to FL-HTT protein, the levels of the pathogenic HTTex1 are CAG length-dependent and correlate with somatic instability in HD transgenic mice (Gu *et al.*, 2022). Hence, CAG expansion in striatal neurons due to somatic instability leads to a greatly increased production of HTTex1, causing cell death and neurodegeneration. Based on this two-step model of HD pathogenesis, blocking somatic instability, when applied in early stages of the disease and in striatal cells, could slow down the disease progression. Since DNA mismatch repair (MMR) genes have been associated with disease severity and somatic instability, initial approaches to silence MMR genes, including MSH3 and MLH3, are investigated (Pinto *et al.*, 2013; Flower *et al.*, 2019; Goold *et al.*, 2019; Roy *et al.*, 2021). Interestingly, lowering of HTT protein can result in suppression of somatic repeat expansion in several genes. Preliminary data have shown that, in the liver of HD mice, lowering of full-length HTT by antisense oligonucleotides, results in reduction of somatic expansion CAG tracts in *HTT* as well as in ataxin 2 (*ATXN2*) genes (Coffey *et al.*, 2020). This suggests that HTT protein itself plays a role in regulating somatic instability occurring at several repeat expanded loci.

Widespread coverage and therapeutic effect in all affected brain regions

6 One important question for all HTT lowering therapies is whether the main brain areas affected in the disease, striatum and cortex, are effectively covered. Biodistribution data obtained in small animals such as mice and rats, poorly translate into larger brains and even non-human primates have much smaller brains than humans (Eaton and Wishart, 2017). In transgenic HD minipigs (Baxa *et al.*, 2013), which have a relatively large brain, we demonstrated that intrastriatal convention-enhanced delivery is an effective and well-tolerated approach to achieve widespread biodistribution and long-lasting mHTT lowering in the disease-relevant areas in a large brain (**Chapter 3**) (Valles *et al.*, 2021). This study was essential for dose finding for the ongoing phase 1b/2 clinical study in HD patients (clinicaltrials.gov, NCT04120493).

The favorable distribution of the vector DNA throughout the brain is likely related to the AAV serotype 5 (AAV5) used in these studies. Compared to other frequently used AAV serotypes, AAV5 has the ability to be transported in a retrograde and anterograde direction

along the neuronal tracts, resulting in a therapeutically relevant coverage of the brain in rodents and in non-human primates (NHP) (Colle *et al.*, 2010; Gerits *et al.*, 2015; Samaranch *et al.*, 2017). Since the striatum is connected to thalamus and cortical regions, high levels of AAV5-delivered therapeutic miRNA were also observed in these connected areas in minipigs after intrastriatal administration (**Chapter 3**), which correlated with mHTT protein lowering effect (**Chapter 5**) (Valles *et al.*, 2021).

In order to achieve global gene correction in CNS and avoid multiple-injection strategies, the injection site and volume are important factors that contribute to AAV spread and maximal efficacy (Cearley and Wolfe, 2007). Although less invasive delivery routes would be preferable, such as intrathecal or intravenous infusions, these currently available options lead to poor coverage of the striatum. For instance, following intrathecal administration in NHP, HTT-targeting ASOs showed an opposite pattern of HTT lowering, with predominant effects in cortex and spinal cord (Kordasiewicz *et al.*, 2012) and much less lowering in deep brain regions (such as the caudate and putamen) which are relevant for HD. Not targeting the right areas might be one of the reasons why trials with ASOs have recently lacked efficacy in early-manifest HD patients (Kingwell, 2021).

Since gene therapy treatments result in steady levels of therapeutic transgene for more than 7 years after one-time dosing (Yuan *et al.*, 2020; Marcó *et al.*, 2021), accessible measurements of durability and efficacy in the brain are needed. In **Chapter 3** we assessed pharmacokinetic and brain damage markers (such as neurofilament light chain, NFL) in plasma and cerebrospinal fluid (CSF) after striatal infusion, demonstrating the persistence as well as the safety of AAV-miHTT approach. These measurements in biofluids importantly contributed to the rationale for the first clinical trial ([clinicaltrials.gov, NCT04120493](https://clinicaltrials.gov/ct2/show/study/NCT04120493)). Unfortunately, HTTex1 targeting could not be assessed in the minipig model since it was generated using HTT cDNA without splicing signals and the animals, that were still relatively young, lacked a disease-related phenotype.

Nonetheless, the results in HD transgenic minipigs, together with separate preclinical studies in iPSC-derived cultures (Keskin *et al.*, 2019), murine models (Miniarikova *et al.*, 2017; Spronck *et al.*, 2019; Caron *et al.*, 2020) and large animal GLP toxicology studies (Spronck *et al.*, 2021) provided strong support for the further development of the AAV5-miHTT program into the clinic and identified candidate biomarkers to assess transgene expression and persistence.

Extracellular vesicles and the concept of cross-corrective silencing

Even the best AAV vectors currently available transduce <30% of target neurons (Blits *et al.*, 2010; Hammond *et al.*, 2017), which may be too low to translate into a clinically meaningful effect in neurodegenerative diseases such as HD. Hence, we have explored technologies to ensure a wider exposure to the miRNA-related mHTT silencing.

Engineered miRNAs are small interfering RNA (siRNA) sequences embedded in a pre-miRNA scaffold, which is then processed in the same manner as their endogenous counterparts (Lam *et al.*, 2015). Engineered miRNAs delivered by AAV are expressed in the nucleus and processed in the cytoplasm of target cells, where they target and degrade complementary mRNA sequences via the activation of RNA-induced silencing complex (RISC) (O'Brien *et al.*, 2018). Endogenous miRNAs have also been found to be enriched in extracellular vesicles (EV) secreted by almost all cell types (Hu *et al.*, 2012). Circulating endogenous miRNAs contained in EVs, are protected from degradation and can be taken up by other cells where they exert their biological function contributing to intercellular communication (Valadi *et al.*, 2007; Li *et al.*, 2019). The work in this thesis demonstrated that AAV-delivered therapeutic engineered miRNAs, expressed and functional within neuronal cells, are secreted within EVs (**Chapter 4**) (Sogorb-Gonzalez *et al.*, 2021) and induce gene lowering in recipient cells upon internalization (**Chapter 5**). These findings have important implications for AAV-miRNA-based gene therapies targeting brain diseases, such as AAV-miHTT for the treatment HD.

Secretion of engineered miRNAs may seem self-evident, but sorting of miRNA into EVs is a highly regulated process leading to a selected subset of cellular miRNAs being loaded into EVs (Zhang *et al.*, 2015). Among those, miR-451 has been reported as one of the most highly enriched in EVs (Guduric-Fuchs *et al.*, 2012). The short-stem miR-451 is the only miRNA which follows a non-canonical dicer-independent processing mediated by argonaute 2 (Ago2) protein (Cheloufi *et al.*, 2010; Herrera-Carrillo and Berkhout, 2017). Phosphorylation of Ago2 is known to affect miRNA sorting, suggesting that the efficient EV export of miR-451 might be mediated by Ago2 (McKenzie *et al.*, 2016). Our engineered therapeutic miRNAs targeting HTT (miHTT) and ataxin 3 (miATXN3) were designed by embedding the complementary target sequence in a pre-miR-451 backbone (Miniarikova *et al.*, 2016; Martier *et al.*, 2019). Extracellular dose-dependent levels of mature miHTT and miATXN3 were detected in EV-enriched fractions secreted by neuronal cells (**Chapter 4**) (Sogorb-Gonzalez *et al.*, 2021). The scaffold-dependent secretion of engineered miRNAs is supported by Reshke *et al.* who showed that pre-miR-451, when compared to preferentially intracellular pre-miR-16, was indeed efficiently loaded in EVs (Reshke *et al.*, 2020). This, together with dicer-independent processing, which results in the absence of a passenger

strand, makes the selection of pre-miR-451 an attractive candidate for the design of miRNA-based therapeutics.

The secretion of EV-protected therapeutic miRNAs into biofluids offers a source of pharmacokinetic biomarkers in CNS diseases. This is especially important for AAV-based gene therapies, where a one-time administration results in long-term expression of active therapeutic molecules in the inaccessible brain. In **chapter 4**, we detected dose-dependent levels of miHTT in the CSF of NHP up to years after AAV-miHTT striatal treatment, supporting the use of engineered miRNA profiles in CSF as useful pharmacokinetic measurements of AAV-based miRNA therapies administered to the brain parenchyma (Sogorb-Gonzalez *et al.*, 2021). These findings are critical for the assessment of transgene expression and persistence in the first clinical trial of AAV-miHTT for HD.

Extracellular vesicles were discovered as intercellular communicators due to the functional transfer of their cargo to neighboring cells (Valadi *et al.*, 2007). The work in this thesis demonstrates that EV-mediated transfer of engineered miRNAs can be used as a novel mechanism of dissemination of gene therapeutics in the brain (**Chapter 5**). We demonstrated that, upon AAV transduction and secretion of the engineered miRNA by neuronal cells, EV-enriched therapeutic miRNAs (miHTT and miATXN3) are internalized by neighboring cells where they remain functional and cause gene silencing of target genes (**Chapter 5**). This innovative “cross-corrective silencing” concept implies that AAV-transduced cells might become local “factories” of therapeutic engineered miRNAs, which can distribute and treat all disease-affected neighboring cells. A similar mechanism of dissemination is widely used for the treatment of lysosomal storage disease, where cross-correction is mediated by the secretion of AAV-expressed enzymes (Kosuga *et al.*, 2000).

For HD and other neurodegenerative diseases, considering the extend of neuropathology in multiple brain regions, the intercellular dissemination of engineered miRNAs might importantly contribute to a meaningful therapeutic effect. Moreover, the progression of neurodegenerative diseases from initially affected brain areas to other regions is known to be partially mediated by the transfer of pathological proteins within EVs (Russo *et al.*, 2012). In HD, the secretion and intercellular transfer of mHTT fragments and aggregates is thought to contribute to neuropathology progression (Pecho-Vrieseling *et al.*, 2014; Jeon *et al.*, 2016). Assuming that the dissemination of therapeutic miRNAs within EV's would follow the same route as the pathological molecules, this might also contribute to a greater cover of affected brain areas.

Concluding remarks and future perspectives

Gene therapies have evolved as a potential treatment for neurodegenerative disease, especially those with a genetically identified mutation such as HD. Compared to other treatments, AAV-based gene therapies offer a lifelong treatment after a one-time administration. The approach investigated in this thesis, AAV-miHTT, was designed to target relevant pathogenic molecules (FL-HTT and Httex1) in the deep structures of the brain (striatum) that are most affected in HD patients. Furthermore, we demonstrated that intrastriatal delivery in a large brain is well-tolerated and results in widespread efficacy, mediated by both axonal transfer (AAV) and inter-cellular transfer via extracellular vesicles. AAV-miHTT is currently being tested in a Phase1b/2 clinical trial in USA and recently in Europe as well (clinicaltrial.gov, NCT04120493). No adverse effects have been observed at one-year follow-up upon AAV-miHTT intrastriatal infusion. Although the efficacy of AAV-miHTT to improve the symptoms and behavioral signs of HD still has to be shown, the findings presented in this thesis demonstrate important mechanistic insights of the treatment, increasing the odds of hopefully reaching therapeutic efficacy for HD patients.

During the last decades, the knowledge in the field of HD has greatly advanced due to the enormous effort from academic, private and clinical teams, leading to the development and testing of potential therapeutics in HD patients. Unfortunately, the lack of efficacy in recent trials have raised concern about the potential of HTT-lowering therapies as a treatment for HD. As reviewed in this thesis, in order to achieve therapeutic success, it is critical to understand the disease pathological aspects as well as the mechanism of action of the therapeutic approach. Therefore, developing therapies should aim at targeting the right species in the right location and moment in time. Novel pathological mechanisms have been described as potential drivers of the disease in early stages, including the tissue-specific somatic instability of the CAG repeat and the consequent formation of toxic fragment and other CAG-dependent processes. In view of these findings, disease-modifying therapies are now shifting to suppressing somatic instability and reducing pathogenic HTT fragments, rather than silencing full-length mHTT. These approaches are expected to better prevent neuronal loss and brain damage hopefully resulting in greater therapeutic effects. As previously indicated, a critical aspect is the timing of treatment. The disease course is characterized by a long pre-symptomatic phase that, in mid adulthood, dramatically progresses into a severe state with progressive neuronal loss. Therefore, early treatment, before irreversible somatic expansion, is likely to achieve better protection. The success of novel therapeutics will hopefully extend to pre-manifest mutation carriers. Future studies should investigate the optimal therapeutic window to ensure clinical benefit.

These concepts regarding the right target, location and timing have important consequences for clinical trials. Development of markers that correlate with levels of pathological drivers and disease progression in affected areas and in early stages are needed to assess efficacy of potential therapeutics. For instance, somatic instability or genetic modifiers such as DNA damage repair genes might become early markers to effectively predict HD progression. The main challenge is that these processes are mainly confined to deep brain structure, especially during early phases of the disease. Therefore, development of markers in accessible biofluids will contribute to advance the treatment of pre-symptomatic carriers. Moreover, recent advances in brain imaging of mHTT aggregates and fragments by positron emission tomography (PET) tracers also offer promising prospects as biomarkers (Prime *et al.*, 2020).

Finally, yet importantly, advances in the treatment HD could be highly valuable to apply to other neurodegenerative diseases. The mechanistic insights of AAV-miRNA-based gene therapy for HD demonstrated in this work will hopefully open the door to the successful and lifelong treatment of other brain diseases.

References

- Amaro IA, Henderson LA. An Intrabody Drug (rAAV6-INT41) Reduces the Binding of N-Terminal Huntingtin Fragment(s) to DNA to Basal Levels in PC12 Cells and Delays Cognitive Loss in the R6/2 Animal Model. *J Neurodegener Dis* 2016; 2016
- Baxa M, Hruska-Plochan M, Juhas S, Vodicka P, Pavlok A, Juhasova J, et al. A transgenic minipig model of Huntington's Disease. *J Huntingtons Dis* 2013; 2: 47–68.
- Blits B, Derks S, Twisk J, Ehlert E, Prins J, Verhaagen J. Adeno-associated viral vector (AAV)-mediated gene transfer in the red nucleus of the adult rat brain: comparative analysis of the transduction properties of seven AAV serotypes and lentiviral vectors. *J Neurosci Methods* 2010; 185: 257–63.
- Caron NS, Southwell AL, Brouwers CC, Cengio LD, Xie Y, Black HF, et al. Potent and sustained huntingtin lowering via AAV5 encoding miRNA preserves striatal volume and cognitive function in a humanized mouse model of Huntington disease. *Nucleic Acids Res* 2020; 48: 36–54.
- Cearley CN, Wolfe JH. A Single Injection of an Adeno-Associated Virus Vector into Nuclei with Divergent Connections Results in Widespread Vector Distribution in the Brain and Global Correction of a Neurogenetic Disease. *J Neurosci* 2007; 27: 9928–40.
- Cheloufi S, Dos Santos CO, Chong MMW, Hannon GJ. A dicer-independent miRNA biogenesis pathway that requires Ago catalysis. *Nature* 2010; 465: 584–9.
- Ciosi M, Maxwell A, Cumming SA, Hensman Moss DJ, Alshammari AM, Flower MD, et al. A genetic association study of glutamine-encoding DNA sequence structures, somatic CAG expansion, and DNA repair gene variants, with Huntington disease clinical outcomes. *EBioMedicine* 2019; 48: 568–80.
- Coffey S, Andrew M, Ging H, Hamilton J, Flower M, Kovalenko M, et al. Huntingtin lowering reduces somatic instability at CAG-expanded loci. *bioRxiv* 2020; preprint
- Colle MA, Piguet F, Bertrand L, Raoul S, Bieche I, Dubreil L, et al. Efficient intracerebral delivery of AAV5 vector encoding human ARSA in non-human primate. *Hum Mol Genet* 2010; 19: 147–58.
- Datson NA, González-Barriga A, Kourkouta E, Weij R, Van De Giessen J, Mulders S, et al. The expanded CAG repeat in the huntingtin gene as target for therapeutic RNA modulation throughout the HD mouse brain. *PLoS One* 2017; 12
- Eaton SL, Wishart TM. Bridging the gap: large animal models in neurodegenerative research. *Mamm Genome* 2017; 28: 324–37.
- Evers MM, Pepers BA, van Deutekom JCT, Mulders SAM, den Dunnen JT, Aartsma-Rus A, et al. Targeting several CAG expansion diseases by a single antisense oligonucleotide. *PLoS One* 2011; 6
- Flower M, Lomeikaite V, Ciosi M, Cumming S, Morales F, Lo K, et al. MSH3 modifies somatic instability and disease severity in Huntington's and myotonic dystrophy type 1. *Brain* 2019; 142: 1876.

Franich NR, Hickey MA, Zhu C, Osborne GF, Ali N, Chu T, et al. Phenotype onset in Huntington's disease knock-in mice is correlated with the incomplete splicing of the mutant huntingtin gene. *J Neurosci Res* 2019; 97: 1590–605.

Gerits A, Vancraeynest P, Vreysen S, Laramée M-E, Michiels A, Gijsbers R, et al. Serotype-dependent transduction efficiencies of recombinant adeno-associated viral vectors in monkey neocortex. *Neurophotonics* 2015; 2: 031209.

Goold R, Flower M, Moss DH, Medway C, Wood-Kaczmar A, Andre R, et al. FAN1 modifies Huntington's disease progression by stabilizing the expanded HTT CAG repeat. *Hum Mol Genet* 2019; 28: 650–61.

Gu X, Richman J, Langfelder P, Wang N, Zhang S, Bañez-Coronel M, et al. Uninterrupted CAG repeat drives striatum-selective transcriptionopathy and nuclear pathogenesis in human Huntington BAC mice. *Neuron* 2022; 110: 1–20.

Guduric-Fuchs J, O'Connor A, Camp B, O'Neill CL, Medina RJ, Simpson DA. Selective extracellular vesicle-mediated export of an overlapping set of microRNAs from multiple cell types. *BMC Genomics* 2012; 13: 357.

Hammond SL, Leek AN, Richman EH, Tjalkens RB. Cellular selectivity of AAV serotypes for gene delivery in neurons and astrocytes by neonatal intracerebroventricular injection. *PLoS One* 2017; 12

Herrera-Carrillo E, Berkhout B. Survey and summary: Dicer-independent processing of small RNA duplexes: Mechanistic insights and applications. *Nucleic Acids Res* 2017; 45: 10369–79.

Hu G, Drescher KM, Chen XM. Exosomal miRNAs: Biological properties and therapeutic potential. *Front Genet* 2012; 3: 56.

Jeon I, Cicchetti F, Cisbani G, Lee S, Li E, Bae J, et al. Human - to - mouse prion - like propagation of mutant huntingtin protein. *Acta Neuropathol* 2016; 132: 577–92.

Keskin S, Brouwers CC, Sogorb-Gonzalez M, Martier R, Depla JA, Vallès A, et al. AAV5-miHTT Lowers Huntingtin mRNA and Protein without Off-Target Effects in Patient-Derived Neuronal Cultures and Astrocytes. *Mol Ther - Methods Clin Dev* 2019; 15: 275–84.

Kingwell K. Double setback for ASO trials in Huntington disease. *Nat Rev Drug Discov* 2021; 20: 412–3.

Kordasiewicz HB, Stanek LM, Wancewicz EV, Mazur C, McAlonis MM, Pytel KA, et al. Sustained Therapeutic Reversal of Huntington's Disease by Transient Repression of Huntingtin Synthesis. *Neuron* 2012; 74: 1031–44.

Kosuga M, Takahashi S, Sasaki K, Li XK, Fujino M, Hamada H, et al. Adenovirus-mediated gene therapy for mucopolysaccharidosis VII: involvement of cross-correction in wide-spread distribution of the gene products and long-term effects of CTLA-4lg coexpression. *Mol Ther* 2000; 1: 406–13.

Kotowska-Zimmer A, Ostrovska Y, Olejniczak M. Universal RNAi Triggers for the Specific Inhibition of Mutant Huntingtin, Atrophin-1, Ataxin-3, and Ataxin-7 Expression. *Mol Ther - Nucleic Acids* 2020; 19: 562–71.

Lam JKW, Chow MYT, Zhang Y, Leung SWS. siRNA Versus miRNA as Therapeutics for Gene Silencing. *Mol Ther - Nucleic Acids* 2015; 4: e252.

Li J, Jiang X, Wang K. Exosomal mirna: An alternative mediator of cell-to-cell communication. *ExRNA* 2019; 1: 1–6.

Marcó S, Haurigot V, Jaén ML, Ribera A, Sánchez V, Molas M, et al. Seven-year follow-up of durability and safety of AAV CNS gene therapy for a lysosomal storage disorder in a large animal. *Mol Ther Methods Clin Dev* 2021; 23: 370–89.

Martier R, Sogorb-Gonzalez M, Stricker-Shaver J, Hübener-Schmid J, Keskin S, Klima J, et al. Development of an AAV-Based MicroRNA Gene Therapy to Treat Machado-Joseph Disease. *Mol Ther - Methods Clin Dev* 2019; 15: 343–58.

McKenzie AJ, Hoshino D, Hong NH, Cha DJ, Franklin JL, Coffey RJ, et al. KRAS-MEK Signaling Controls Ago2 Sorting into Exosomes. *Cell Rep* 2016; 15: 978–87.

Miniarikova J, Zanella I, Huseinovic A, van der Zon T, Hanemaaijer E, Martier R, et al. Design, Characterization, and Lead Selection of Therapeutic miRNAs Targeting Huntingtin for Development of Gene Therapy for Huntington’s Disease. *Mol Ther - Nucleic Acids* 2016; 5: e297.

Miniarikova J, Zimmer V, Martier R, Brouwers CC, Pythoud C, Richetin K, et al. AAV5-miHTT gene therapy demonstrates suppression of mutant huntingtin aggregation and neuronal dysfunction in a rat model of Huntington’s disease. *Gene Ther* 2017; 24: 630–9.

Neueder A, Landles C, Ghosh R, Howland D, Myers RH, Faull RLM, et al. The pathogenic exon 1 HTT protein is produced by incomplete splicing in Huntington’s disease patients. *Sci Rep* 2017; 7

O’Brien J, Hayder H, Zayed Y, Peng C. Overview of microRNA biogenesis, mechanisms of actions, and circulation. *Front Endocrinol (Lausanne)* 2018; 9: 402.

Pecho-Vrieseling E, Rieker C, Fuchs S, Bleckmann D, Esposito MS, Botta P, et al. Transneuronal propagation of mutant huntingtin contributes to non-cell autonomous pathology in neurons. *Nat Neurosci* 2014; 17: 1064–72.

Pinto RM, Dragileva E, Kirby A, Lloret A, Lopez E, St. Claire J, et al. Mismatch Repair Genes Mlh1 and Mlh3 Modify CAG Instability in Huntington’s Disease Mice: Genome-Wide and Candidate Approaches. *PLoS Genet* 2013; 9

Prime ME, Liu L, Lee MR, Khetarpal V, Brown CJ, Johnson PD, et al. Imaging Mutant Huntingtin Aggregates: Development of a Potential PET Ligand. *J Med Chem* 2020; 63: 8608–33.

Reshke R, Taylor JA, Savard A, Guo H, Rhym LH, Kowalski PS, et al. Reduction of the therapeutic dose of silencing RNA by packaging it in extracellular vesicles via a pre-microRNA backbone. *Nat Biomed Eng* 2020; 4: 52–68.

Roy JCL, Vitalo A, Andrew MA, Mota-Silva E, Kovalenko M, Burch Z, et al. Somatic CAG expansion in Huntington’s disease is dependent on the MLH3 endonuclease domain, which can be excluded via splice redirection. *Nucleic Acids Res* 2021; 49: 3907–18.

Russo I, Bubacco L, Greggio E. Exosomes-associated neurodegeneration and progression of Parkinson's disease. *Am J Neurodegener Dis* 2012; 1: 217.

Samaranch L, Blits B, San Sebastian W, Hadaczek P, Bringas J, Sudhakar V, et al. MR-guided parenchymal delivery of adeno-associated viral vector serotype 5 in non-human primate brain. *Gene Ther* 2017; 24: 253–61.

Sathasivam K, Neueder A, Gipson TA, Landles C, Benjamin AC, Housman DE, et al. Aberrant splicing of HTT generates the pathogenic exon 1 protein in Huntington disease. *PNAS* 2013; 110: 2366–70.

Sogorb-Gonzalez M, Vendrell-Tornero C, Snapper J, Stam A, Keskin S, Miniarikova J, et al. Secreted therapeutics: monitoring durability of microRNA-based gene therapies in the central nervous system. *Brain Commun* 2021; 3

Southwell AL, Ko J, Patterson PH. Intrabody Gene Therapy Ameliorates Motor, Cognitive, and Neuropathological Symptoms in Multiple Mouse Models of Huntington's Disease. *J Neurosci* 2009; 29: 13589–602.

Spronck EA, Brouwers CC, Vallès A, de Haan M, Petry H, van Deventer SJ, et al. AAV5-miHTT Gene Therapy Demonstrates Sustained Huntingtin Lowering and Functional Improvement in Huntington Disease Mouse Models. *Mol Ther - Methods Clin Dev* 2019; 13: 334–43.

Spronck EA, Vallès A, Lampen MH, Montenegro-Miranda PS, Keskin S, Heijink L, et al. Intra-striatal administration of AAV5-MIHTT in non-human primates and rats is well tolerated and results in MIHTT transgene expression in key areas of huntington disease pathology. *Brain Sci* 2021; 11: 1–18.

Swami M, Hendricks AE, Gillis T, Massood T, Mysore J, Myers RH, et al. Somatic expansion of the Huntington's disease CAG repeat in the brain is associated with an earlier age of disease onset. *Hum Mol Genet* 2009; 18: 3039–47.

Urbanek MO, Fiszer A, Krzyzosiak WJ. Reduction of Huntington's Disease RNA Foci by CAG Repeat-Targeting Reagents. *Front Cell Neurosci* 2017; 11: 1–13.

Valadi H, Ekström K, Bossios A, Sjöstrand M, Lee JJ, Lötvall JO. Exosome-mediated transfer of mRNAs and microRNAs is a novel mechanism of genetic exchange between cells. *Nat Cell Biol* 2007; 9: 645–59.

Valles A, Evers MM, Stam A, Gonzalez MS, Brouwers C, Tornero CV, et al. Widespread and sustained target engagement in Huntington's disease minipigs upon intra-striatal microRNA-based gene therapy. *Sci Transl Med* 2021; 13: 1–51.

Yuan J, Zhang Y, Liu H, Wang D, Du Y, Tian Z, et al. Seven-Year Follow-up of Gene Therapy for Leber's Hereditary Optic Neuropathy. *Ophthalmology* 2020; 127: 1125–7.

Zhang J, Li S, Mi S, Li L, Li M, Guo C, et al. Exosome and Exosomal MicroRNA: Trafficking, Sorting, and Function. *Genomics, Proteomics Bioinforma* 2015; 13: 17–24.

Appendix



- English Summary
- Nederlandse samenvatting
- Resumen en Español
- List of abbreviations
- Curriculum vitae
- List of publications
- Acknowledgements

English Summary

Huntington Disease (HD) is a fatal neurodegenerative disease caused by a CAG repeat expansion in the exon 1 of the huntingtin (HTT) gene. This mutation is translated into a polyglutamine tract in the mutant HTT protein which confers a toxic gain-of-function inducing aggregation and cell death. Due to its monogenic cause and undeniably polyglutamine-dependent toxicity, mutant HTT protein became the ideal target of choice for many therapies in development.

One of the most advanced HTT lowering approaches is a miRNA-based gene therapy, consisting of an engineered microRNA targeting HTT (miHTT), delivered by adeno-associated virus (AAV), referred from now on as “AAV-miHTT”. The direct administration of AAV-miHTT in the striatum of animal models has demonstrated efficacy in lowering the mutant HTT protein and rescuing HD phenotypes, and safety in toxicology studies in nonhuman primates. However, during the last years, relevant studies in the field have demonstrated that HD pathology is rather complex and new hypothesis are being debated as the cause of onset and progression of the disease. Moreover, the lack of efficacy in first HTT lowering clinical trials suggests that the lowering of the mutant HTT protein might not be sufficient to delay the progression of the disease.

This thesis describes novel mechanistic insights of miRNA-based gene therapies including the targeting of different HTT species, the therapeutic spread between neuronal cells and the development of translational biomarkers to monitor its effect in the affected brain regions.

Chapter 1 is a general introduction to the field of HD and includes an up-to-date comprehensive analysis of the most relevant questions and challenges for the development of successful therapies. We describe *what*, *how*, and *where* to target and treat the disease and the main outcomes to assess the efficacy (*how good*) and toxicity (*how bad*) to ensure optimal translation to patients.

Increasing evidence indicates that, besides the mutant full-length HTT protein, exon 1 HTT (HTT_{ex1}) fragments generated by aberrant splicing are highly prone to aggregate and contribute to HD pathology. Generation of pathogenic HTT_{ex1} highly correlates with CAG repeat expansion and somatic instability and the slow but steady accumulation over time might explain why HD patients develop neurodegeneration and symptoms in adult life. This finding also suggests that reducing the expression of HTT_{ex1} transcripts might achieve a greater therapeutic benefit than targeting only the full-length mutant HTT and conversely, strategies that exclusively target full-length HTT might not prevent HD pathogenesis. In **chapter 2**, we evaluated the ability of AAV5-miHTT to reduce the levels of aberrantly spliced HTT_{ex1} in the brain of two mouse models of HD. Intrastriatal administration of AAV5-miHTT



resulted in dose-dependent significant lowering of both full-length mutant HTT and HTTex1 in striatum and cortex of Q175 knock-in and humanized Hu128/21 mice at two and four months, respectively. These results demonstrate that AAV5-miHTT gene therapy is an efficient approach to lower both full-length HTT and the highly pathogenic HTTex1 levels, and support the added therapeutic benefit of exon 1-targeting therapeutics for HD.

One of the biggest challenges in the treatment of brain diseases is to achieve adequate biodistribution and coverage of all affected brain areas, as well as sustained effect in time. For this, preclinical studies in large animals are important for successful translation into patients. In **chapter 3** we investigated the transability and long-term efficacy of AAV5-miHTT administered in the striatum in transgenic HD minipigs. We demonstrated that direct intrastriatal delivery of AAV-miHTT therapy results in widespread and persistent HTT protein lowering in all brain areas that are known to be affected in up to one year. Potential reliable biomarkers to monitor expression and therapeutic efficacy were also investigated. This study, together with separate toxicology studies, was essential to support the clinical development of AAV5-miHTT into the clinic.

Regarding the mechanism of action of AAV-miHTT, we have proposed a novel mechanism of secretion and dissemination of gene therapeutics mediated by extracellular vesicles (EV). In **chapter 4** we investigated the secretion of engineered miRNAs and its potential use as suitable markers to monitor the expression and durability of gene therapies in the brain. Moreover, measurable engineered miRNA levels enriched in EVs were detected in the CSF of nonhuman primates up to 2 years after intrastriatal infusion. These results support the use of EV-associated miRNAs as novel translational pharmacokinetic markers in ongoing clinical trials of gene therapies for neurodegenerative diseases.

Mechanisms that diffuse therapeutics beyond initially transduced cells might contribute to elimination of intracellular disease-causing proteins in all affected brain cells and regions and eventually prevent disease progression. In **chapter 5**, we investigated the EV-mediated functional transfer of AAV-delivered therapeutic microRNA molecules from AAV-miRNA-corrected neuronal cells to neighboring cells. We demonstrated the uptake of EVs by neuronal cells and the efficacy of miRNAs to lower target genes upon transfer to recipient cell.

To finalize, **chapter 6** is a general discussion of the main findings of this thesis in the context of HD field and miRNA-based gene therapies for neurodegenerative diseases. We further discuss the needs and future perspectives for a successful gene therapy to treat HD as well as other neurodegenerative diseases.



Nederlandse Samenvatting

De Ziekte van Huntington (HD/ZvH) is een fatale neurodegeneratieve ziekte die veroorzaakt wordt door een CAG-repeat-expansie in exon 1 van het huntingtin-gen (HTT). Deze mutatie veroorzaakt een verlengde polyglutaminestring in het mutant HTT eiwit, wat leidt tot eiwit gerelateerde toxiciteit door eiwit aggregatie en wat uiteindelijk in celdood resulteert. Vanwege de genetische monogene achtergrond en onmiskenbaar polyglutamine afhankelijke toxiciteit is mutant HTT-eiwit het ideale doelwit voor veel therapieën in ontwikkeling.

Een van de meest geavanceerde HTT exon 1 verlagende benaderingen is gebaseerd op een microRNA (miRNA) gerelateerde gentherapie, bestaande uit een gemanipuleerde miRNA gericht op HTT (miHTT) en word afgeleverd door adeno-geassocieerd virus (AAV) die vanaf nu aangeduid zal worden als "AAV-miHTT". De directe toediening van AAV-miHTT in het striatum van diermodellen heeft de werkzaamheid aangetoond door het verlagen van het mutante HTT eiwit, het redden van ZvH-fenotypen en de veiligheid in toxicologische onderzoeken bij niet-menselijke primaten. Gedurende de laatste jaren hebben relevante studies in het veld aangetoond dat de ZvH-pathologie erg complex is waarbij er wordt gediscussieerd over nieuwe hypothesen zoals de oorzaak en de progressie van de ziekte. De eerste klinische onderzoeken suggereren het gebrek aan effectiviteit in naar mutante HTT verlaging en dat de verlaging van het mutant HTT eiwit mogelijk niet voldoende is om de progressie van de ziekte te vertragen.

Dit proefschrift beschrijft nieuwe mechanistische inzichten met betrekking tot miRNA gebaseerde gentherapieën, waaronder het behandelen van verschillende HTT eiwit types, de therapeutische verspreiding tussen neuronale cellen en de ontwikkeling van translationele biomarkers om het effect ervan in de aangetaste hersengebieden te volgen.

Hoofdstuk 1 is een algemene inleiding op het gebied van de ZvH en bevat een actuele uitgebreide analyse van de meest relevante vragen en uitdagingen die nodig zijn voor de ontwikkeling van succesvolle therapieën. We beschrijven wat, hoe en waar de ziekte zich tot moet richten/behandelen en de belangrijkste resultaten om de werkzaamheid (hoe goed) en toxiciteit (hoe slecht) te beoordelen om een optimale vertaling naar patiënten te garanderen.

Toenemend bewijs geeft aan dat naast het mutante HTT-eiwit van volledige lengte er exon 1 HTT (HTTex1) fragmenten gegenereerd worden door een afwijkende splicing activiteit die zeer vatbaar zijn voor aggregatie en extensief bijdragen aan de ZvH-pathologie. Het genereren van pathogene HTTex1 correleert sterk met CAG-herhalingsexpansie en somatische instabiliteit. De langzame maar gestage accumulatie van HTTex1 eiwit in de loop van de tijd zou kunnen verklaren waarom ZvH-patiënten neurodegeneratie en symptomen

ontwikkelen in het volwassen leven. Deze bevinding suggereert ook dat het verminderen van de expressie van HTT_{ex1} transcripten een groter therapeutisch voordeel zou kunnen opleveren dan het alleen richten op de mutante HTT van volledige lengte en omgekeerd. Strategieën die zich uitsluitend richten op HTT van volledige lengte zouden de pathogenese van de ZvH niet kunnen voorkomen. In **hoofdstuk 2** evalueerden we het vermogen van AAV5-miHTT om de niveaus van afwijkend gesplitst HTT_{ex1} in de hersenen van twee muismodellen van de ZvH te verminderen. Intrastriatale toediening van AAV5-miHTT resulteerde in een dosisafhankelijke significante verlaging van zowel de mutant HTT als HTT_{ex1} van de volledige lengte in het striatum en de cortex van Q175 knock-in en gehumaniseerde Hu128/21-muizen na respectievelijk twee en vier maanden. Deze resultaten tonen aan dat AAV5-miHTT-getherapie een efficiënte benadering is om zowel HTT van volledige lengte als de zeer pathogene HTT_{ex1}-niveaus te verlagen, en het toegevoegde therapeutische voordeel van HTT_{ex1} gerichte therapieën voor de ZvH te ondersteunen.

Een van de grootste uitdagingen bij de behandeling van hersenziekten is het bereiken van een adequate biodistributie en dekking van alle aangetaste hersengebieden evenals een duurzaam effect in de tijd. Hiervoor zijn preklinische studies bij grote dieren belangrijk voor een succesvolle vertaling naar patiënten. In **hoofdstuk 3** onderzochten we de vertaling en lange termijn werkzaamheid van AAV5-miHTT toegediend in het striatum bij transgene ZvH minivarkens. We hebben aangetoond dat directe intrastriatale toediening van AAV-miHTT-therapie resulteert in wijdverbreide en aanhoudende HTT eiwitverlaging in alle hersengebieden. Mogelijke betrouwbare biomarkers om expressie en therapeutische werkzaamheid te volgen werden ook onderzocht. Deze studie, samen met afzonderlijke toxicologische studies, was essentieel om de klinische ontwikkeling van AAV5-miHTT in de kliniek te ondersteunen.

Met betrekking tot het werkingsmechanisme van AAV-miHTT hebben we een nieuw mechanisme voorgesteld voor de uitscheiding en verspreiding van getherapieën die worden gemedieerd door extracellulaire vesicles (EV). In **hoofdstuk 4** hebben we de secretie van gemanipuleerde miRNA's onderzocht en het mogelijke gebruik ervan als geschikte markers om de expressie en duurzaamheid van getherapieën in de hersenen te volgen. Bovendien werden meetbare gemanipuleerde miRNA niveaus verrijkt in EV's gedetecteerd in het CSF van niet menselijke primaten tot 2 jaar na intrastriatale infusie. Deze resultaten ondersteunen het gebruik van EV geassocieerde miRNA's als nieuwe translationele farmacokinetische markers in de huidige klinische onderzoeken naar getherapieën voor neurodegeneratieve ziekten.

Mechanismen die therapieën verspreiden buiten de aanvankelijk getransduceerde cellen, kunnen bijdragen aan de eliminatie van intracellulaire ziekteverwekkende eiwitten

in alle aangetaste hersencellen en regio's en uiteindelijk ziekteprogressie voorkomen. In **hoofdstuk 5** hebben we de EV-gemedieerde functionele overdracht van AAV geleverde therapeutische microRNA moleculen van AAV-miRNA gecorrigeerde neuronale cellen naar naburige cellen onderzocht. We hebben de opname van EV's door neuronale cellen aangetoond en de werkzaamheid van miRNA's om doelgenen te verlagen bij overdracht naar de ontvangende cel.

Hoofdstuk 6 een algemene bespreking van de belangrijkste bevindingen van dit proefschrift in de context van ZvH veld- en miRNA gebaseerde gentherapieën voor neurodegeneratieve ziekten. We bespreken verder de behoeften en toekomstperspectieven voor een succesvolle gentherapie voor de behandeling van de ZvH en andere neurodegeneratieve ziekten.



Resumen en Español

La enfermedad de Huntington (EH), también conocida como corea de Huntington, es una grave enfermedad neurodegenerativa y hereditaria causada por una mutación en el exón 1 del gen de la huntingtina (*HTT*). Esta mutación genética da lugar a una proteína huntingtina mutante (mHTT) que contiene una cadena de poliglutamina y que induce procesos tóxicos como la agregación de proteínas y la muerte celular de neuronas. Debido a su causa monogénica y su toxicidad innegablemente asociada a la proteína mutante, la reducción de mHTT se ha convertido en la diana terapéutica de muchas terapias en desarrollo.

Una de las terapias de reducción de mHTT más avanzadas es una terapia génica basada en microARN (miARN), que consiste en un miARN sintético que se une a la secuencia de la HTT (miHTT) e inhibe la expresión de la proteína mHTT tóxica. El miARN sintético es administrado por un virus adenoasociado (AAV), y se conoce como "AAV-miHTT". La administración directa de AAV-miHTT en el cerebro de modelos animales ha demostrado eficacia para reducir la proteína mHTT y rescatar síntomas motores de la enfermedad de Huntington. También se ha demostrado estudios de toxicología en primates que la terapia es segura. Sin embargo, durante los últimos años, estudios relevantes en el campo han demostrado que la patología de la Huntington es más compleja y se están debatiendo nuevas hipótesis sobre la causa de la aparición y progresión de la enfermedad. Además, la falta de eficacia en los primeros ensayos clínicos sugiere que la reducción de la proteína mHTT podría no ser suficiente para retrasar la progresión de la enfermedad.

Esta tesis describe nuevos conocimientos sobre el mecanismo de acción de las terapias génicas basadas en miARN, incluida el ataque de diferentes especies tóxicas de HTT, la propagación terapéutica de miARN entre las células neuronales y el desarrollo de biomarcadores traslacionales para supervisar su efecto en las regiones cerebrales afectadas.

El **Capítulo 1** es una introducción general al campo de la enfermedad de Huntington e incluye un análisis actualizado de las preguntas y desafíos más relevantes para el desarrollo de terapias exitosas. Describimos el *qué*, el *cómo* y *dónde* atacar y tratar la enfermedad y los principales métodos para evaluar la eficacia (*qué tan bueno*) y la toxicidad (*qué tan malo*) para garantizar una traslación óptima de modelos de animales a pacientes.

Cada vez más evidencia indica que, además de la proteína HTT mutante de longitud completa, fragmentos de la huntingtina, como el fragmento del exón 1 (HTTex1) generado por splicing alternativo, son más propensos a agregarse y contribuir a la patología de Huntington. La producción del fragmento HTTex1 tóxico se correlaciona altamente con la expansión de repeticiones CAG, la inestabilidad somática, y su acumulación lenta pero



constante en el tiempo que podría explicar por qué los pacientes con EH desarrollan neurodegeneración y síntomas en la vida adulta. Este hallazgo también sugiere que la reducción de la expresión de HTTex1 podría lograr un mayor beneficio terapéutico que atacando sólo la HTT mutante de longitud completa y, por el contrario, las estrategias que se dirigen exclusivamente a la HTT de longitud completa podrían no prevenir la aparición de la EH. En el **capítulo 2**, evaluamos la capacidad de AAV5-miHTT para reducir los niveles de los fragmentos de HTTex1 en el cerebro de dos modelos de ratones con EH. La administración intra-cerebral de AAV5-miHTT resultó en una reducción significativa tanto de HTT mutante de longitud completa como del fragmento tóxico de HTTex1 en el cerebro (cuerpo estriado y corteza cerebral) de ratones Q175 knock-in y humanizados Hu128/21 a los dos y cuatro meses, respectivamente. Estos resultados demuestran que la terapia génica AAV-miHTT es un tratamiento eficaz para reducir los niveles de HTT de longitud completa y los niveles altamente tóxicos del fragmento HTTex1, y apoya el beneficio terapéutico adicional de los tratamientos dirigidos a la secuencia del exón 1 para la EH.

Uno de los mayores retos en el tratamiento de las enfermedades cerebrales es conseguir una adecuada distribución y cobertura de todas las áreas cerebrales afectadas, así como un efecto sostenido en el tiempo. Para esto, los estudios preclínicos en animales de gran tamaño son importantes para una traslación óptima a los pacientes. En el **capítulo 3**, investigamos la eficacia a largo plazo de AAV-miHTT administrado en el cerebro (cuerpo estriado) en cerdos transgénicos con EH. Demostramos que la administración intra-cerebral de la terapia AAV-miHTT resulta en una reducción generalizada y persistente (hasta 1 año) de la proteína HTT en todas las áreas del cerebro afectadas en EH. También se investigaron posibles biomarcadores para evaluar la expresión y la eficacia terapéutica. Este estudio, junto con estudios de toxicología que demostraron la seguridad de esta terapia, fue esencial para respaldar la aplicación clínica de AAV5-miHTT en pacientes de EH en Mayo de 2021.

En cuanto al mecanismo de acción de AAV-miHTT, en esta tesis presentamos un novedoso mecanismo de secreción y diseminación de terapias génicas facilitadas por vesículas extracelulares (EV). En el **capítulo 4**, investigamos la secreción de miRNA sintéticos y su uso como marcadores terapéuticos para evaluar la expresión y la durabilidad de las terapias génicas en el cerebro. Niveles detectables de miARN sintéticos se midieron en vesículas extracelulares en el líquido cefalorraquídeo de primates hasta 2 años después de la inyección intra-cerebral. Estos resultados respaldan el uso de vesículas extracelulares como marcadores farmacocinéticos en ensayos clínicos de terapias génicas con miRNA sintéticos para enfermedades neurodegenerativas.

La diseminación de terapias más allá de las células tratadas inicialmente podría contribuir a la eliminación de proteínas tóxicas en todas las regiones y células cerebrales afectadas y, finalmente, prevenir la progresión de la enfermedad. En el **capítulo 5**,



investigamos la transferencia funcional por vesículas extracelulares de moléculas de miRNA sintéticos desde células neuronales corregidas por AAV-miARN a células vecinas. Este estudio demuestra la internalización de vesículas extracelulares por parte de las células neuronales y la eficacia de los miRNA sintéticos para reducir los genes diana tras la transferencia a la célula receptora.

Para finalizar, el **capítulo 6** es una revisión de los principales hallazgos de esta tesis en el contexto del campo de la EH y las terapias génicas basadas en miARN para enfermedades neurodegenerativas. Además, debatimos las necesidades y las perspectivas futuras para el desarrollo de una terapia exitosa para la cura de EH y otras enfermedades neurodegenerativas.

List of abbreviations

3'UTR	3' untranslated region
AAV	adeno-associated virus
AGO	argonaute protein
ASO	antisense oligonucleotide
ATXN	ataxin gene
BBB	blood brain barrier
CAG	cytomegalovirus immediate-early enhancer fused to chicken β -actin promoter
cDNA	complementary DNA
CED	convection-enhanced delivery
CMV	cytomegalovirus
CNS	central nervous system
CRISPR	clustered regularly interspaced short palindromic repeats
CSF	cerebrospinal fluid
CT	computed tomography
dsDNase	double-strand DNase
EV	extracellular vesicle
FDA	food and drug administration
FL-HTT	full length HTT
GAPDH	glyceraldehyde 3-phosphate dehydrogenase gene
gc	genome copies
gDNA	genomic DNA
GFAP	glial fibrillary acidic protein
GFP	green fluorescent protein
HD	Huntington disease
HTT	huntingtin
HTTex1	exon 1 HTT
iPSC	induced pluripotent stem cells
ITR	inverted terminal repeat



Appendix

MAP2	microtubule-associated protein 2
miATXN3	<i>ATXN3</i> targeting microRNA
MRI	magnetic resonance imaging
mHTT	mutant huntingtin protein
miHTT	<i>HTT</i> targeting microRNA
miRNA	microRNA
NFL	neurofilament light chain
NHP	nonhuman primate
PK	pharmacokinetic
PolyA	polyalanine
PolyQ	polyglutamine
Pre-miRNA	precursor miRNA
Pri-miRNA	primary miRNA
qPCR	quantitative real-time polymerase chain reaction
rAAV	recombinant AAV
RISC	RNA-induced silencing complex
RNAi	RNA interference
RT-qPCR	reverse transcription quantitative real-time PCR
SCA	spinocerebellar ataxia
SEC	size exclusion chromatography
shRNA	short hairpin RNA
siRNA	small interference RNA
SNP	single nucleotide polymorphism
tgHD	transgenic minipig model for HD
vDNA	vector DNA
VG	vector genome
wtHTT	wild-type HTT
ZFP	zinc finger protein

Curriculum vitae

Marina Sogorb Gonzalez was born on 7th July 1992 in Burgos, Spain, where she graduated at high school IES Comuneros de Castilla in 2010. After her graduation, she moved to Salamanca to initiate her bachelor studies in Biotechnology at University of Salamanca, Spain. In 2012-2013, she participated in the “Erasmus Program” as an exchange student in Comenius University, Bratislava, Slovakia. Her final thesis was under the supervision of Dr. Marina Holgado Madruga, where she performed a literature review titled “Optogenetics and its application”. It was during this time that she discovered her passion for the brain and translational research.

In 2014, Marina moved to the Netherlands, to study the master’s degree in Neuroscience at the Vrije Universiteit (VU) in Amsterdam, where she specialized in Clinical Neurosciences. Following her interest in the field of applied sciences, in 2016, she performed a one-year internship at the Research Department of uniQure B.V, Amsterdam, under the daily supervision of Dr. Jana Miniarikova and Dr. Pavlina Konstantinova. During this time, she was introduced to the field of Huntington disease and contributed to investigating miRNA-based gene therapies. In October 2017, Marina received her Master of Science degree with *Cum Laude* distinction.

With the goal to further contribute to the development of gene therapies for neurodegenerative diseases, in January 2018, she enrolled in a PhD position at Leiden University Medical Center (LUMC) under the supervision of Prof. Dr. Sander van Deventer, and funded by uniQure B.V. The experimental work presented in this thesis was performed at uniQure, Amsterdam, under the daily supervision of Dr. Melvin Evers. From 2018 to 2020, Marina investigated novel mechanisms of action of microRNA-based gene therapies relevant for the treatment of Huntington disease. She presented at numerous scientific conferences and contributed as a co-inventor in two patent applications regarding her work at uniQure.

In February 2021, while finalizing her doctoral studies, Marina started working as a Scientist Translational Biology at VectorY B.V, a recent gene therapy start-up based in Amsterdam. With the supervision of Dr. Pavlina Konstantinova, CSO at VectorY, and her promotor Prof. Dr. Sander van Deventer, she finalized writing this thesis and interpreting the results. At VectorY, Marina contributes to the *in vivo* studies and preclinical development of novel therapeutics with vectorized antibodies, applying her knowledge in the field while learning new challenges.

Marina is a creative, enthusiastic and proactive scientist with a great interest in neuroscience. She aims to contribute to the development of curative therapies for brain diseases.



List of first-author presentations

- 2018** HD Dutch Meeting, Amsterdam, The Netherlands. Poster presentation
- 2019** RNA & Oligonucleotide Therapeutics, Cold Spring, NY, USA. Oral presentation
- 2019** ASGCT, Washington, DC, USA. Poster presentation
- 2019** HD Dutch Meeting, Groningen, The Netherlands. Poster Presentation
- 2020** CHDI, Palm Springs, LA, USA. Poster presentation
- 2020** AAN, Virtual, Poster presentation
- 2020** ASGCT, Virtual, Poster presentation



List of publications

Morais R*, **Sogorb-Gonzalez M***, Bar C, Timmer NC, van der Bent ML, Wartel M, Vallès V. Functional intercellular transmission of miHTT via extracellular vesicles: an in vitro proof-of-mechanism study. *Cells* (2022); 11(17):2748. *These authors contributed equally to this work.

Sogorb-Gonzalez M, Vendrell-Tornero C, Snapper J, Stam A, Keskin S, Miniarikova J, Spronck EA, de Haan M, Nieuwland R, Konstantinova P, van Deventer SJ, Evers MM, Vallès A. Secreted therapeutics: monitoring durability of microRNA-based gene therapies in the central nervous system. *Brain Communications* (2021); 3(2): fcb054.

Valles A*, Evers MM*, Stam A, **Sogorb-Gonzalez M**, Brouwers CC, Vendrell-Tornero C, Acar-Broekmans S, Paerels L, Klima J, Bohuslavova B, Pintauro R, Fodale V, Bresciani A, Liscak R, Urgosik D, Starek Z, Crha M, Blits, B, Petry H, Ellederova Z, Motlik J, van Deventer SJ, Konstantinova P. Widespread and sustained target engagement in Huntington s disease minipigs upon intrastriatal microRNA-based gene therapy. *Science Translational Medicine* (2021); 13(588). *These authors contributed equally to this work.

Depla JA, **Sogorb-Gonzalez M**, Mulder LA, Heine VM, Konstantinova P, van Deventer SJ, Wolthers KC, Pajkrt D, Sridhar A, Evers MM. Cerebral organoids: a human model for AAV capsid selection and therapeutic transgene efficacy in the brain. *Molecular Therapeutics - Methods & Clinical Development* (2020); 18: 167-175

Martier R, **Sogorb-Gonzalez M**, Stricker-Shaver J, Hübener-Schmid J, Keskin S, Klima J, Toonen LJ, Juhas S, Juhasova J, Ellederova Z, Motlik J, Haas E, van Deventer SJ, Konstantinova P, Nguyen HP, Evers MM. Development of an AAV-Based MicroRNA Gene Therapy to Treat Machado-Joseph Disease. *Molecular Therapeutics - Methods & Clinical Development* (2019); 15: 343–58.

Keskin S, Brouwers CC, **Sogorb-Gonzalez M**, Martier R, Depla JA, Vallès A, van Deventer SJ, Konstantinova P, Evers MM. AAV5-miHTT lowers huntingtin mRNA and protein without off-target effects in patient-derived neuronal cultures and astrocytes. *Molecular Therapeutics - Methods & Clinical Development* (2019); 15: 275-284.

Patent applications

Valles-Sanchez, A, Konstantinova PS, van Deventer SJH, **Sogorb-Gonzalez M**. Methods and means to deliver mirna to target cells. WO-2020104469-A1. Patent filed by UniQure IP BV on November 19th, 2019.

Van Deventer SJH, Evers MM, **Sogorb-Gonzalez M**, Konstantinova PS, Valles-Sanchez A. Targeting mis-spliced transcripts in genetic disorders. WO-2021053018-A1. Patent filed by UniQure IP BV on September 16th, 2020.



Acknowledgements

Ok, it's time to close this chapter. This PhD journey has been definitely challenging but above all, worthy. When I look back, I could have never imagined how much I would learn and grow in these years. It is indeed a character-building experience. After the first three years of excitement playing in the lab, hard work and falling in love with science, I took the decision to keep growing in my professional career and I embarked myself in a new project. It wasn't an easy decision to make and it added extra challenges to the final stages of this PhD journey. Nevertheless, here I am. And luckily, I didn't have to do it all alone. I would like to thank all the people who have accompanied me during this journey, contributing to my work, helping me grow or sharing fun moments together.

Dear **Sander**, thank you for always supporting my work and giving me the opportunity to share it with others, for your patience reminding me that I would one day finish and for standing up for me when I needed. Your knowledge is endless and your curiosity truly motivating. Most of the content in this thesis is thanks to your creative ideas which taught me to broaden my knowledge and think outside of the box. Also, thank you for organizing the best trip ever to Burgos.

Dear **Pavlina**, you have always challenged me, you made me GROW in capital letters. Thank you for always making time to critically review my work and giving me the most valuable feedback. I also appreciate that you also helped me making Amsterdam a home and trusted me with cute Cuppie. I wouldn't be here without your support and I am very grateful to keep sharing my scientific career with you.

Dear **Melvin**, I started this journey with you and I will always be grateful for your support. Thank you for your guidance, supporting my work and keeping up with my enthusiastic ideas. As a good team player, you were always looking for ways to enable collaborations and bring the projects further. Dear **Astrid**, thank you for your substantial contribution to this thesis. I am very grateful we got to work together in so many projects. Thank you for your advises and sharing your knowledge with me. I learned so much from you, both professionally and personally.

Dear **Carlos**, you were the most important person of this journey, my little brother. For sure I wouldn't be here without you. Your energy, your curiosity and your friendship made this journey much, much better. I learned a lot from you and I really enjoyed our brainstorm sessions together (Bamboooo forever). I have no doubt that you will do a great job in your PhD adventure and I hope to be part of it as well. And together with **Pablo**, thank you for bringing so much joy in my life, for taking care of me with the best meals and always making me laugh. Dear **Fanny**, my student and also my friend, I admired your motivation



and patience to learn. I had a lot of fun working with you and growing together. Thank you for your contribution to this thesis.

Dear **Jana**, my mentor, my flatmate, my friend, my “not-only love”. I started this journey with you even before I knew that one day I would get here, when we were searching for exosomes in the exosomes! Thank you for building a strong scientific basis in me and for showing me that science is more fun when approached with lots of curiosity and also humor. I learned from you to have a global vision and the importance of creating a solid story, even with just few graphs of data. Thank you very much for helping me grow in all aspects of my life and for sharing so many moments together. And together with **Rudy** and **Kasia**, thank you for the sport sessions, fun moments and for always taking care of me when I needed.

Dear **Loreto**, so many years together and I feel so lucky to keep growing close to you. Thank you for always being there and for reminding me who I am when I get lost. Who would have told us that two biotech students would have gotten this far and survived in Dutch lands. Dear **Sanne** thank you for our fun Manguito&Mangon adventures, and for always being there as my friend. Thank you for your positive energy, your humor and for helping me make The Netherlands my home during these years. You became my family here and I will always be grateful for that. Dear **Gio**, also good things happened during covid times, thank you for your friendship and for the best advises during our sport sessions. Dear **Alessia**, friends at first sight. Thank you for your friendship, sweet hugs and best Italian recipes. I miss you. Dear **Carmen**, I am so happy you came into my life, and that it feels like we grew up together. Thank you for supporting me during the end of this journey, also as my paranymp and best organizer! Can’t wait to share more moments together.

Dear **Sonay**, thank you for your positive energy, for teaching me the best tricks in the lab and for making the best shakshuka. Thank you for always being there, in the good and challenging times. I miss working with you. Dear **Cynthia**, thank you for your kindness and always being willing to help me and others. Thank you for your support as a colleague and as a friend during these years. Dear **Raygene**, thank you for your input and advises. I always learned a lot from your experience and our discussions together. I am happy that we keep working closely together. Dear **Kimberly**, I truly admire your perseverance and solid work. Thank you for your scientific input and helpful advises. Dear **Lisa**, we are so lucky to have you to support the research team with positive energy and dedication. Thank you for being always keen to help me. I admired you as a person and I am very thankful to have you as a friend. Dear **Giorgia, Furkan, Hendrina, Morgane, Anouk, Lieke, Roberto, Tom, Bas, Lodewijk, Vanessa, Ying Poi, Paula, Sumiati, Jolanda L., Lisa S., Anna, Iolanda, Ellen, Alise, Monique, Laura, Marsha, Kostas, IT dept, IP dept, uniQure runners**, and many more! You made my days in the lab and in the office much more fun. Moreover, it was very special for



me that most of you came to visit my hometown Burgos in Spain. Thank you for your infinite support and for keeping up with my enthusiasm all those years. I will always look back with fondness to those moments. To all **uniQurians**, I admire the work you do and your vision to develop therapies for patients. I am very proud of having being part of your achievements.

Dear **VectorYans**, your creativity and teamwork to build a start-up from scratch gave me a big push to finish this journey. Thank you for your trust, support and motivation. Thank you (not thank you) for keeping asking me about my thesis and becoming part of this adventure as well. Special thanks to **Wouter, Menno, Martino, Christina, Marco, Lisette, Barbara, Alies, Tony, Etsuko, Jolanda, Svetlana, Roland, Andreia, Linda, Farangis, Shilpita, Charlotte, Ruud, Sofia, Kwankwan, Melanie, Giulia, Rob, Saskia, Alexander**, and many more people that joined us on the way. I look forward to achieving great successes together and to deliver therapies for devastating neurodegenerative diseases.

I also would like to thank the scientific collaborators I had the opportunity to work with for their input and time. Special thanks to **Rienk Nieuwland** and his team for their technical input regarding isolation of extracellular vesicles; **Zdenka, Jan, Jiri, Helena** and **Stefan** from PIGMOD Centre (Libechov, Czech Republic) for being very welcoming hosts during my visits; **Sabine** and **Eric Reits** from Amsterdam UMC for opening their doors to me; **Nicholas Caron** from UBC (Vancouver, Canada), **Gillian Bates** and **Christian Landles** from UCL (London, UK) for performing experiments to detect HTT exon 1 protein.

My dear **friends from Spain**, thank you for showing me that friendship is not measured in km away, or months without seeing each other. Thank you for waiting for me with your arms open every time I come back, no matter how express my visits are. To my dear **salsa friends**, life is definitely much better dancing and I am very lucky I got to meet you during these years. Thank you for all the dances, hard trainings and fun trips. Recharging batteries is better with you.

Dear **Tiago**, I am so grateful you walked next to me during the last two years. Thank you for transforming difficulties into growth in such a peaceful manner. Your calmness, trust and love it's what help me to keep going with "one rabbit at a time". I truly admire your infinite curiosity and creativity, it's very unique and also contagious! We are definitely the coolest team and I can't wait to keep growing together.

A **mis padres, mi hermano, mi hermana, cuñados, sobrinos, tíos y abuelos**, gracias por educarme, por enseñarme vuestros valores humildes, por demostrarme que las cosas sólo se consiguen con esfuerzo. Sois y siempre seréis mi mayor admiración. Gracias por apoyarme en mis decisiones, por celebrar mis logros, y por esperarme con una comilona y miles de abrazos cuando vuelvo para veros. No es fácil teneros lejos tantos años pero siempre siento vuestro cariño muy muy cerca. Os quiero.



